TECHNICAL REPORT ECOM-03733-12 OCTOBER 1965

A STUDY OF RANDOM ACCESS DISCRETE ADDRESS COMMUNICATIONS SYSTEMS

VOLUME I: STUDY AND ANALYSIS

TECHNICAL REPORT 167

Contract No. DA-36-039 AMC-03733(E)
Signal Corps, Department of the Army
Department of the Army Project No. 1P021101A042

By:

C. CRAIG FERRIS

For

U. S. ARMY ELECTRONICS COMMAND, FORT MONMOUTH, N. J.

October 1965

ACKNOWLEDGEMENTS

The author wishes to thank the members of his doctoral committee for their council and technical guidance. Particular appreciation is expressed to Professor Gunnar Hok for his encouragement and technical support.

Further, the author wishes to thank Mr. Donald R. Rothschild and Professor Ben F. Barton for their suggestions and helpful criticism. The author also acknowledges helpful discussions with Messrs. Alan L. Cohn and Victor L. Wallace on particular aspects of the work.

Finally, special gratitude is owed Miss Ann M. Rentschler for her skilled and intensive effort with several drafts of this dissertation, and to Messrs. Thomas E. Jennett and Ronald H. Kilgren for their careful preparation of the final draft.

The research reported in this dissertation was supported by the U. S. Army Electronics Command on Contract DA-36-039-AMC-03733(E).

TABLE OF CONTENTS

TABLE OF CONTENTS (Cont.)

TABLE OF CONTENTS (Cont.)

TABLE OF CONTENTS (Cont.)

LIST OF ILLUSTRATIONS

LIST OF ILLUSTRATIONS (Cont.)

LIST OF ILLUSTRATIONS (Cont.)

LIST OF SYMBOLS

		Page
A	area of a communication net	47
a	a randomly occurring event	57
a	upper limit of integration	121
B	nominal bandwidth of a pulse	168
B_g	guardband width employed in a RADA system	172
b	a constant	168
$Ch_t(\xi)$	characteristic function of a random variable, t	95
c	propagation constant for a net area	44
c_p	center of the pulse envelope p(t)	168
E	operator denoting averaging over an ensemble of random variables	51
$E(P_i)$	expected value of the mutual interference power at the target receiver input terminals	52
E_p	energy of the pulse envelope p(t)	167
$e(t)$	waveform of a pulse	166
$F(a, b, c ---)$	the joint probability of events a, b, c, ---	107
$F(a, b, c --- \mid u, v, w ---)$	the joint probability of events a, b, c --- given events u, v, w ---	107
$F_e(f)$	Fourier transform of the waveform, e(t), of a pulse	167
$\mathcal{F}(P)$	a particular function of P	147

LIST OF SYMBOLS (Cont.)

		Page
$F_p(f)$	Fourier transform of the envelope, p(t), of a pulse	166
$F(\lambda_f)$	general expression denoting functional dependence on λ_f	176
f_o	carrier frequency of a pulse	166
f_1, f_2, f_3	the three carrier frequencies employed in an example RADA transmitter	7
H(j)	for a system employing clocked binary modulation, the entropy of the receiver output states is a particular clock interval	145
H(j|i)	for a system employing clocked binary modulation, the entropy of the receiver output state, given the transmitter state	145
H(t)	probability distribution function of the duration of an error pulse	82
i	an integer index of the receiver AND gate input connections	107
i	when clocked binary modulation is employed, an index of the state of the RADA system transmitter output in a particular clock period (i = 0, 1)	145
(i)	the event a turn-on pulse occurs at AND gate input i	107
i, j	integer indices of the active transmitters in the net area A	62, 63
j	when clocked binary modulation is employed, j is an index of the state of the receiver post gate or sampler output in a particular clock period (j = 0, 1)	145

		Page
K	number of error pulse processes, each of τ seconds duration, contained in an ensemble of such processes	124
k	in a system using clocked binary modulation, k is the fraction of on-modulated pulses	35
k	an integer	110
k	an integer index of members of an error process ensemble containing error processes of duration τ seconds	124
ℓ	an integer index	138
M	number of transceivers which could be placed in a net area, A, with at least a distance r_0 separating them	49
m	number of wideband RADA transmitters which interfere with a particular RADA receiver at a given time	35
$\bar{N}$	expected number of error pulses per second	84
$N^{(k)}(\tau)$	number of error pulses in the kth ensemble member	124
n	number of successive overlapping pulses in a "composite," "n-pulse"	92
n	a dummy integer variable in the expression for the nth term of a sum	141
$n^{(k)}$	enumerator of the nth error pulse in the kth ensemble member	124

		Page
P	for a receiver at the center of an annular area, the interference power from a single transmitter placed randomly, with a uniform probability distribution, in an annular area	44 (footnote)
P	a dummy variable	147
$P(a)$	probability of a	46
$P_e(\tau)$	probability distribution function of τ	85
$\tilde{P}_e(\tau)$	approximation for $P_e(\tau)$	86
$\tilde{\tilde{P}}_e(\tau)$	lower bound for $P_e(\tau)$	86
P_i	available mutual interference power at the target receiver input terminals	51
$P(i)$	probability of transmitter state i	145
$P(j)$	probability of receiver output state j	145
$P(j\|i)$	probability of receiver output state j, given transmitter state i	145
P_m	receiver AND gate output error pulse duty factor	81
P_{max}	maximum value of the interference power, P	44 (footnote)
P_{min}	minimum value of the interference power, P	44 (footnote)
$P_m^{(k)}$	duty factor of the error process of the kth ensemble member	125
$P_m(min)$	the value of P_m minimized with respect to the product $\lambda_f\lambda_t$	212

		Page
$P_m(\tau)$	probability distribution function of the time τ to the epoch of an error pulse, measured from any time instant in the OFF state	85
$\tilde{P}_m(\tau)$	approximation for $P_m(\tau)$	85
P_s	available signal power which is produced by the given transmitter at the target receiver input terminals	51
P_t	output power of a RADA transmitter	44
$P_{1FA}(T_p)$	probability of a type one false alarm	138
$P_{2FA}(T_p)$	probability of a type two false alarm	143
$P_3(n)$	conditional probability of an n pulse, given a composite pulse	98
P_4	probability of pulse overlap	98
$P_5(t_5)$	probability distribution function of t_5	104
$P_7(t_7)$	probability distribution function of t_7	106
$P_{FA} = P_{FA}(\gamma\Delta_t, \lambda_f\lambda_t)$	a general measure of RADA system performance	175
P_{SFA}	probability of false alarm, for a sampling receiver	87
$P_{SFA}(Mq_1, m)$	the value of P_{SFA} minimized with respect to the product $\lambda_f\lambda_t$ for Mq_1 subscribers, when m subscribers are using the system	202

LIST OF SYMBOLS (Cont.)

		Page
$P_{SFA}(\min)$	the value of P_{SFA} minimized with respect to the product $\lambda_f \lambda_t$	192
p(P)	probability density of the interference power, P	44 (footnote)
p(t)	probability density function of a random variable t	95
p(t)	envelope waveform of a pulse	166
$p_e(\tau_e)$	probability density function of τ_e	132
$\tilde{p}_e(\tau_e)$	approximation for $p_e(\tau_e)$	132
$p_r(\tau_r)$	probability density function of τ_r	137
$p_1(t_1)$	probability density function of t_1	95
$p_2(t_2)$	probability density function of t_2	98
$p_2(t_2 \mid n)$	conditional probability density function of t_2, given an n pulse	97
$p_5(t_5)$	probability density function of t_5	104
$p_7(t_7$	probability density function of t_7	105
q_1	an area packing density for net transceivers	51
q_2	instantaneous fraction of the transceivers in the net area, A, which are active	51
R	rate of information transmission in bits per clock period, T_c, for a RADA system employing clocked binary modulation. $R = H(j) - H(j \mid i)$	147

		Page
$R(Mq_1, m)$	for a system employing clocked binary modulation and sampling receivers, the information rate, R, in bits per clock period, T_c, which corresponds to $P_{SFA}(Mq_1, m)$	213
R_{max}	for a system employing clocked binary modulation and sampling receivers, the information rate, R, in bits per clock period, T_c, which corresponds to $P_{SFA}(min)$	212
R_{SFA}	false alarm rate, for a sampling receiver	144
$R_{1FA}(T_p)$	type one false alarm rate	142
$R_{2FA}(T_p)$	type two false alarm rate	143
r	an integer index of error pulses	124
r_i, r_j	distance separating the target receiver from particular interfering transmitters which are indexed by values of the subscripts i and j	62, 63
r_o	minimum distance separating transceivers, specified for a net	43
r_1	radius of a circular net area	58
r_2	distance separating the given transmitter and target receiver within a net	43
r_{2max}	maximum separation of the given transmitter and target receiver in a communications net	49
$(S/N)_{IN}$	input signal-to-noise ratio of a receiver of a bandspreading communications system	20

		Page
$(S/N)_{OUT}$	output signal-to-noise ratio of a receiver of a bandspreading communications system	20
s	integer value of $\lambda_f \lambda_t$ which corresponds to a minimal value of P_{FA}	181
s	complex variable of the Laplace transform. $s = -i\xi$	102
T	effective integrating time of the output of a receiver of a bandspreading communications system	20
T	nominal width of a pulse	168
$\bar{T}$	average time interval between successive transmitted frames	35
T_c	clock period, for a system using clocked binary modulation	35
T_d	duration of a frame	31
T_p	the gate interval of a gated receiver	36
$T_{.50}$	width of a pulse, measured between the half voltage points of the pulse envelope	170
t	the (random) duration of an error pulse	82
t	a dummy random variable	95
t	time	166
$\bar{t}$	mean duration of an error pulse	84
$\tilde{t}$	approximation for the mean duration, $\bar{t}$, of an error pulse	84
$\approx$ t	another approximation for the mean duration, $\bar{t}$, of an error pulse	84

		Page
$t_n^{(k)}$	duration of the nth error pulse of the kth member of an error process ensemble containing error processes of duration τ seconds	124
t(i)	the event that the duration of a pulse at the ith AND gate input connection is greater than t	107
t_r	duration of the error pulse which corresponds to the index value r	124
t_o	a reference time	91
t_o	a number	110
t_1	the time interval between epochs of successive pulses of a composite pulse	95
t_1, t_2, t_3	the three time delays of pulses in a frame, for an example RADA transmitter	7
t_2	time from the epoch of the first pulse to the epoch of the last pulse of a composite pulse	97
t_5	total duration of a composite pulse. $t_5 = t_2 + \Delta_t$	100
t_6	time to the (negative) epoch of the first pulse in a composite pulse which occurs in the time interval $[-\Delta_t, 0]$	101
t_7	with respect to the epoch-time of an AND gate output error pulse, t_7 is the (random) time to the termination of each of those pulses present at the $(\lambda_f \lambda_t - 1)$ AND gate inputs at the epoch-time of the error pulse (whtn the epoch of the "turn-on pulse" occurs at the remaining AND gate input). $t_7 = t_5 + t_6$	101

LIST OF SYMBOLS (Cont.)

		Page
$u(t)$	a unit step function at the time origin	104
W	input bandwidth of a receiver of a bandspreading communications system	20
W	bandwidth of a RADA system	172
$W_e(f)$	energy spectrum of the pulse e(t)	167
W_m	measured bandwidth of a particular prototype RADA system	174
W_n	bandwidth of a RADA system employing Gaussian transmitted pulse envelopes	173
$W_p(f)$	energy spectrum of the pulse envelope p(t)	167
x	used in receiver block diagrams to indicate the receiver AND gate output	36
x	reciprocal of the numerical value, y, of receiver dynamic range. $x = 1/y$	56
x	a dummy variable	105
y	numerical value of receiver dynamic range	42
γ	average number of interfering pulses per second on each of the Λ_f frequency channels	31
γ'	reciprocal of the mean time from the beginning of the OFF state to the epoch of the first error pulse	130
Δ_t	width of rectangular pulses transmitted by a modeled RADA system. Also, the equivalent rectangular width of non-rectangular transmitted pulses	38

LIST OF SYMBOLS (Cont.)

		Page
$\Delta\tau_r$	an increment in τ_r	137
$\delta(t)$	a unit impulse function at the time origin	104
θ	phase of the carrier frequency of an RF pulse	166
Λ_f	total number of frequency channels used by a RADA system	31
Λ_t	number of time slots in a frame	31
λ	a parameter	56
λ_f	for any transmitter, the number of frequencies on which pulses are transmitted	31
λ_f'	an upper bound on λ_f which is determined by practical constraints	196
λ_t	for any transmitter, the number of pulses transmitted per frame on each of λ_f frequency channels	31
λ_t'	an upper bound on λ_t which is determined by practical constraints	196
ξ	argument of a characteristic function	95
ρ	for systems employing clocked binary modulation; $\rho = P_e(T_p)$ for a gated receiver, $\rho = P_m$ for a sampling receiver	146
$\sigma(P_i)$	standard deviation of the mutual interference power at the target receiver input terminals	52
σ_1	standard deviation of the pulse envelope voltage p(t), for a Gaussian pulse envelope	169

		Page
σ_2	standard deviation of the amplitude of the complex spectrum for a pulse with a Gaussian envelope voltage, p(t)	169
τ	time duration of each member of an ensemble of error pulse processes	124
τ	a dummy variable	85
τ_e	time from the opening of the post gate to the first occurrence of an error pulse	132
τ_r	time of the epoch of a message pulse	137
$\overline{\tau_r^n}$	nth moment of the probability density of τ_r	141
$\omega_1, \omega_2 \text{---} \omega_n$	events	137
$[\omega_1, \omega_2, \text{--} \omega_n]$	the joint event; ω_1 occurs and ω_2 occurs --- and ω_n occurs	137

ABSTRACT

A net communications system frequently has many users, for each of whom only a low-duty-factor need exists. Random access discrete address (RADA) communications systems are particularly suited to this type of communications environment. A RADA system is a co-channel pulse communication system, in which each transmitter, by proper coding of its radiated pulse groups, may address a target receiver. Mutual interference and cross talk among various transceivers in the net are undesirable consequences of this co-channel operation.

This dissertation is an overall analytical study of RADA (random access discrete address) communications systems. In this study, the factors influencing system performance are embodied in mathematical models which in turn are used to determine, analytically, the quantitative effects of these factors on system performance. In pursuing this approach, several different aspects of the systems have been investigated. The investigations include the following. An analytical study of the mutual-interference-power density at a receiver in a general co-channel RADA net environment is carried out. This study is used to determine a lower bound for the probability that a "useful signal" is available at the input terminals of a particular receiver in the net. Mutual interference among the co-channel RADA transceivers produces an error process at the

receiver output. An approximate model of the mutual interference process is used to obtain theoretical expressions for the pertinent statistics of this error process. The effects of the error process on two generic types of modulations are evaluated analytically. This analysis is performed for three receiver types, the simplest of which utilizes delay devices and an AND gate in the video processing. The second and third receiver types are characterized by gating and sampling, respectively, of the AND gate output. A method of choosing system parameters to minimize the receiver output error probability when the system bandwidth is specified is determined. An expression is derived for the information rate of a RADA transmission in terms of the statistics of the error process. Finally, a particular type of RADA receiver, a sampling RADA receiver, is proposed for use with clocked binary modulation. A theoretical expression is determined for the error probability at the receiver output. And, the error probability minimization technique is used to specify an optimum choice of parameters for systems using this type of receiver. Also, analytic expressions are derived for the information rate for both the case in which parameters are chosen freely, and for the case in which parameters are constrained by the error minimization process.

General considerations in the design of RADA systems are given. Examples are worked out which illustrate the use of the analytical results

obtained in this report. Also, some of the existing prototypes of RADA systems are described in an appendix.

FOREWARD

This report is in two volumes, which are bound separately. In Volume I, "Study and Analysis," some of the fundamental aspects of RADA system design are investigated. Volume I, which is unclassified, is essentially the same as the dissertation "A Study of RADA (Random Access Discrete Address) Communications Systems" submitted in partial fulfillment of the degree Doctor of Philosophy at The University of Michigan. Volume II, "Vulnerability Considerations," is a study of countermeasures aspects of RADA systems, and it has a Confidential security classification.

Volume I of this report takes a theoretical approach in evaluating RADA system performance. Along with the advantages of such an approach in indicating the basic dependence on certain parameters, there are disadvantages. In particular, the assumptions required to develop a tractable theoretical system model are somewhat idealized, and tend to yield an upper bound of system performance. The most important of these assumptions are described briefly here.

In modeling the placement of transceivers in the net area (Chapter II), an inequality is given for the probability of a "useful" received signal in terms of the receiver dynamic range, and the ratio of the distance between the transceivers, and the minimum transceiver separation for the net. This inequality is based upon the assumption of a uniform distribution of transceivers in the net area. The results can readily be extended to the case where clustering occurs, as discussed in Chapter II (p. 45).

In modeling the interference pulse process (Chapter III), it is assumed that the received pulses are rectangular (pulses of other shape are assigned an "effective rectangular width"--Chapter V) and of equal width. The amplitude of the received pulses vary widely, and when these pulses are clipped at a low level, their widths vary considerably. Pulse stretching due to multipath and receiver recovery from large pulses also produce pulses of unequal width. Further, in modeling the receiver, it was assumed on intuitive grounds that pulse cancellation does not occur when the clipping level is low. Recent experimental results indicate that roughly 10 percent of the transmitted pulses are cancelled, leading to two counteracting effects; the number of message pulses is reduced, as well as the number of interference pulses. It is expected that the former result will more than counterbalance the latter, so that the model tends to provide an upper bound of system performance.

Finally, some of the illustrative problems were worked before complete information was available concerning source coding characteristics and military system requirements. The results of these problems are therefore optimistic. The assumed value of the maximum error rate of 10 percent (page 78) is higher than that which is actually permissible with PPM. Five percent is more typical. The assumed maximum error rate of 20-30 percent (page 79) for delta modulation is also high. Five percent is again more realistic. With regard to the parameters assumed for an example

net environment, distances of as little as 3 to 5 feet are characteristic of an actual military net environment, whereas a value of 100 feet is used (Chapter II).

CHAPTER I

INTRODUCTORY DISCUSSION

1.1 Objectives and Organization

This dissertation is an overall, analytical study of RADA (random access discrete address) communications systems. In this study, the factors influencing system performance are embodied in mathematical models which in turn are used to determine, analytically, the quantative effects of these factors on system performance. In pursuing this approach, several different aspects of the systems have been investigated. The overall study as well as these particular investigations are the original contributions of this dissertation. The investigations include the following. An analytical study of the mutual-interference-power density at a receiver in a general co-channel RADA net environment is carried out. This study is used to determine a lower bound for the probability that a "useful signal" is available at the input terminals of a particular receiver in the net. Assuming that a useful signal is present, mutual interference among the co-channel RADA transceivers produces an error process at the receiver output. An approximate model of the mutual interference process is used to obtain theoretical expressions for the pertinent statistics of this error process. The effects of the error process on two generic types of modulation, pulse position modulation

and clocked binary modulation, are evaluated analytically. In pulse position modulation, the information is modulated in the shifts of the pulses of a clocked binary pulse train from their clocked positions. In clocked binary modulation, information pulses gate the occurrence of pulses of a clocked binary pulse train. The choice of system parameter values to minimize the receiver output error rate is also studied. The effects of the error process on several generic types of modulation and receivers are evaluated. An expression is derived for the information rate of a RADA transmission in terms of the statistics of the error process. General considerations in the design of RADA systems are described. Several examples are worked out, illustrating the use of the analytical results obtained in this report. Finally, some of the existing prototypes of RADA systems are described in an appendix.

The work of these studies is original work. The analytical work was completed before any other corresponding work was published. However, prior to the publication of this dissertation, a paper containing some material similar to that contained here was published by other authors. In particular, the work of Ref. 16 makes use of the same general method, although it employs slightly differing analytical tools, in determining some of the same statistics of the error process. Studies of the same problems have been undertaken by others, using differing approaches; much of this work has been described in Section 1.5 (Review of the Literature), and the corresponding publications are listed in the

Lists of References.*

The organization of this dissertation is as follows. Chapter I introduces RADA net communications systems. In particular, a generalized RADA system is described, and the terms used in this work are defined. In Chapter II, the assumptions and theoretical results of the chapter, concerning the mutual-interference power density at a RADA receiver in a net environment, are first summarized and then presented in detail. More specifically, the mean and variance of the interference power density at a receiver in a RADA net are determined analytically as a function of the significant parameters. Chebyshev-type inequalities, which contain the mean and variance, delimit the fraction of the time that a "useful signal" is available at a target receiver within the net. The significant statistics of errors caused by mutual interference among RADA systems are summarized at the beginning of Chapter III; analytical details supporting the conclusions therein are then presented. Example calculations for several sets of system parameter values are given in Chapter IV using results of Chapter III. In particular, some current prototype RADA systems, of which the appendix is descriptive, are evaluated.

---

*For the purpose of giving appropriate credit to all available sources, an "Auxiliary List of References" has been included in this dissertation for material which is pertinent to RADA systems, and which has not been published in the open literature. Publications contained in the List of References are simply enumerated, whereas those in the Auxiliary List of References are enumerated with the prefix 1.

Specific considerations in the design of RADA systems are treated in Chapter V. The influences on system performance of differences in power levels of received signals, and of receiver synchronization are described, as are the effects of variations of such parameters as bandwidth and mutual interference. A method of determining the number of RADA frequencies, and the number of pulses on each frequency, which minimizes the system bandwidth at a specified error rate, or minimizes the error rate at a specified bandwidth is also described.

In Chapter VI, the results of Chapter III and Chapter V are used to determine an optimum choice of parameters for a RADA system using a sampling receiver. Expressions for information transmission rates are determined for the optimum system and for a practical suboptimum system.

Conclusions and recommendations for the direction of future efforts are presented in Chapter VII.

1.2 Description of RADA (Random Access Discrete Address) Coding

A communications net, as defined in this dissertation, is a group of fixed or mobile individuals, within line-of-sight range, equipped with radio transceivers. Each net member can communicate directly to each other net member, without using intervening switching apparatus, by transmitting a radio signal which is properly addressed or coded. A common frequency band, or channel, is utilized for these transmissions.

This study is concerned with the performance characteristics of a communications net in which a particular type of (transmission) coding, referred to as RADA coding, is used throughout. The block diagram of a typical system for use with pulse information is shown in Fig. 1. 1. When analog information is transmitted, it must first be source-encoded by using some form of pulse modulation.[1] Pulse modulated analog voice signals are of primary concern in this dissertation. In Fig. 1. 1, RADA encoding of a signal for multiplex transmission over a wireless channel is illustrated. The same techniques may be used in a wire channel.

When applying the RADA principle, all information signals are first converted to a pulse signal form. Each "information pulse" is then coded into a group of pulses (a "time-frequency code frame," or "frame") which is "matched" to the receiver addressed. The coding scheme is chosen so that the RADA decoder in a particular receiver produces an output "message" pulse when a properly addressed frame is received, and (ideally) produces no output pulse when an improperly addressed frame is received.

Mutual interference among transceivers produces "error pulses" at the output of the RADA decoder because the frames from several transmitters can combine randomly to produce frames which are coded

---

[1]Source encoding will be referred to herein as "modulating", permitting its clear distinction from the subsequent (RADA) transmission "coding."

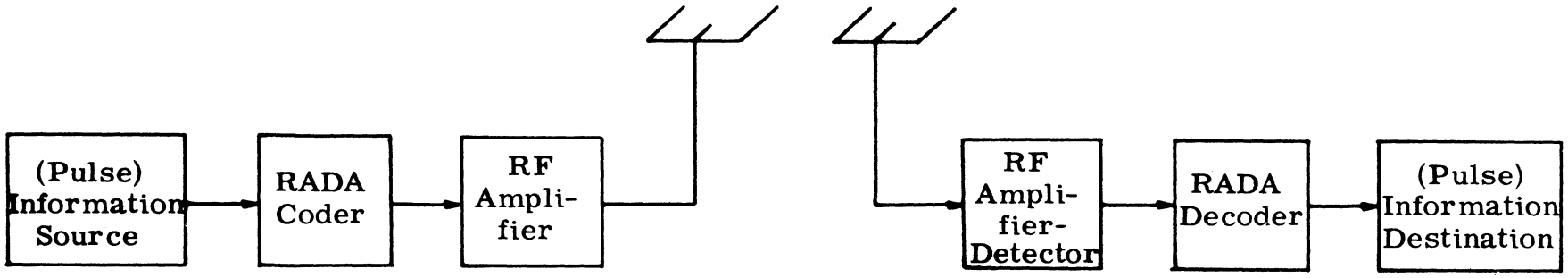

Fig. 1. 1. Block diagram of a RADA system for transmission of pulse information.

for a particular receiver, even though the frames of the individual transmitters are not so coded.

RADA coding can be used with delta modulation, pulse-position modulation (PPM), pulse code modulation (PCM) (in which case the receiver must be time-synchronized with the transmitter), and with other types of pulse modulation.

An example of RADA coding of an information pulse train is shown in Fig. 1.2. Figure 1.2(a) shows a (binary) pulse train fed to the RADA coder of a transmitter. Figure 1.2(b) illustrates how each binary pulse is coded in a "time-frequency code frame." The delays, t_1, t_2, t_3, of pulses of carrier signals at frequencies f_1, f_2, f_3, respectively, constitute the address of a net user. The maximum delay in a frame is generally chosen to be less than, or equal to, the minimum time between information pulses. In general, the number of system frequencies and the number of pulses per frame on each frequency are parameters of a RADA system.

A representative implementation of a RADA system for transmitting (analog) voice information is shown in Fig. 1.3. A voice signal produces the information train of position-modulated pulses shown in Fig. 1.2(a) at the transmitter modulator output. Each information pulse is addressed in the RADA coder in the manner described above.

At the receiver to which the frame is addressed, the pulses of carrier signals at frequencies f_1, f_2, f_3 are delayed by $(32 - t_1)$, $(32 - t_2)$,

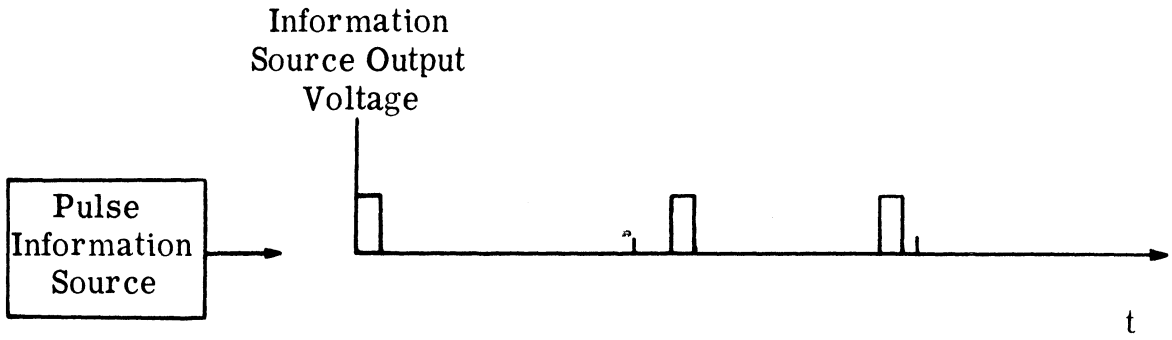

Fig. 1.2a. Transmitter information source output voltage.

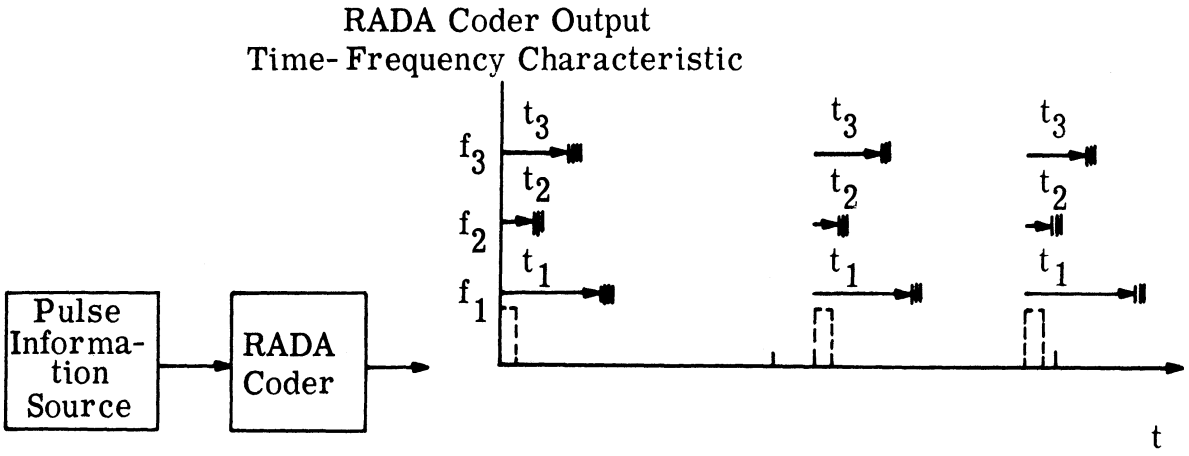

Fig. 1.2b. RADA coder output voltage.

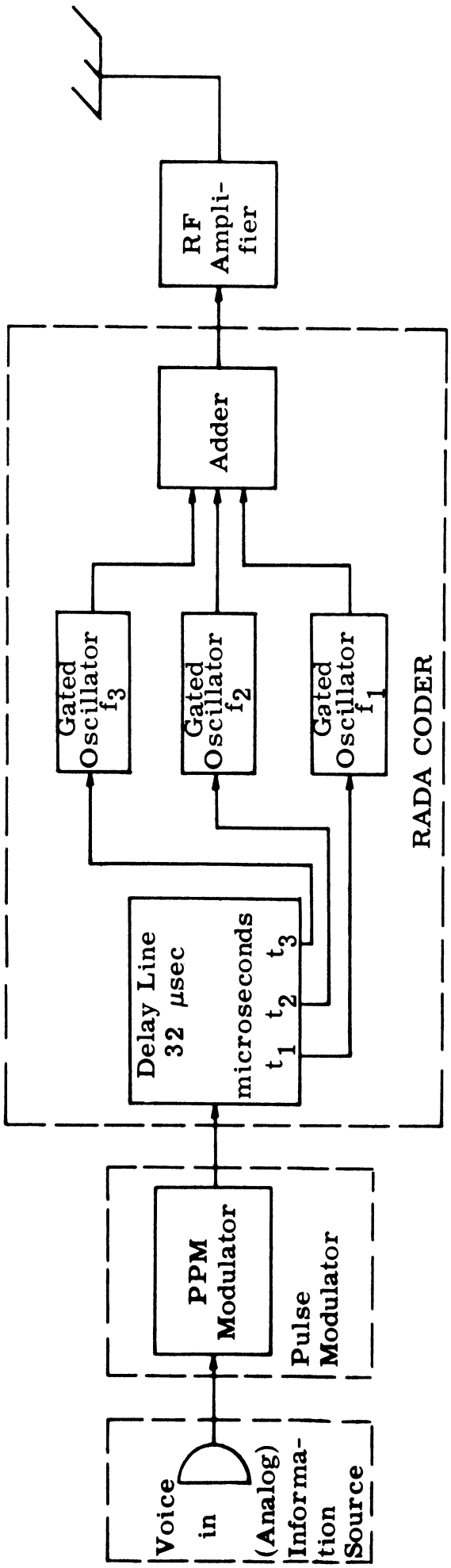

Fig. 1.3(a). Block diagram of a typical RADA transmitter.

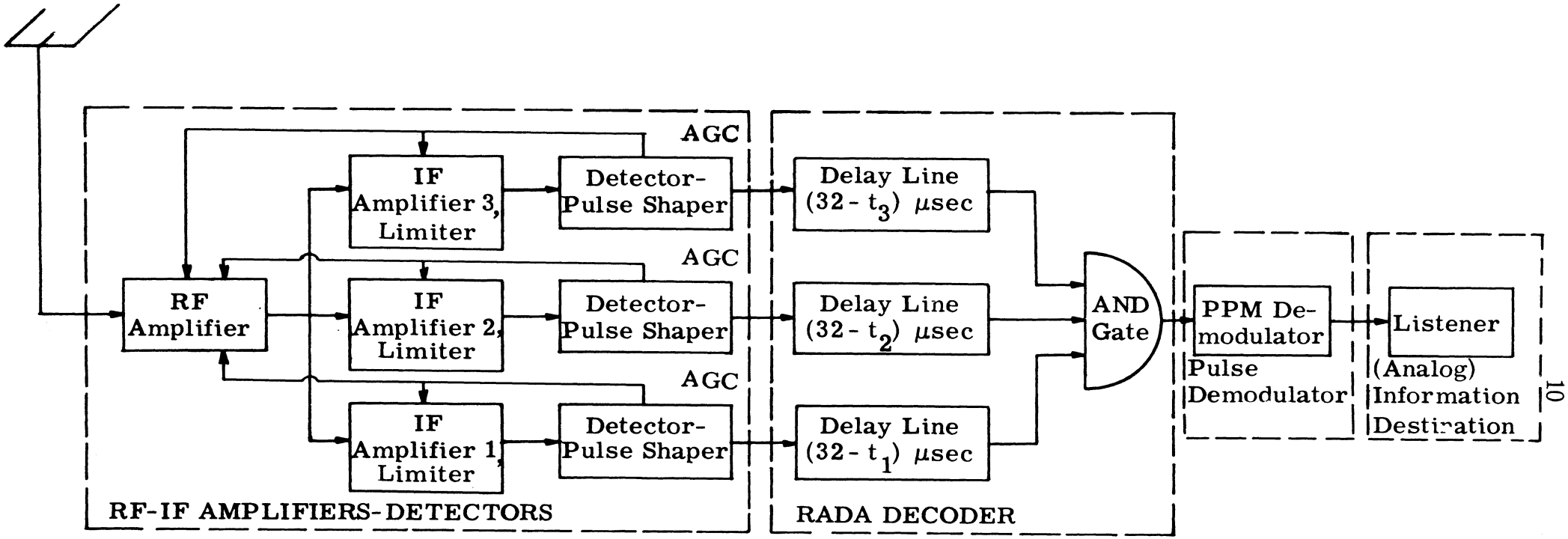

Fig. 1.3b. Block diagram of a typical RADA receiver.

(32 - t_3) microseconds, respectively, as shown in Fig. 1.3(b). These delay values are complements of the delays used in the transmitter to address each information pulse. Each frame coded for the receiver produces three coincident input pulses at the AND gate, causing an AND gate output message pulse. Demodulation of the AND gate output message pulse train reconstitutes the coded voice signal, i.e., the train of position-modulated pulses. A common RF stage for all frequency channels is shown in Fig. 1.3(b); alternately, separate RF stages [Fig. 1.4(c)] tend to minimize interference effects among frequency channels. Automatic gain control (AGC) and limiting are employed in processing the received signals to accommodate the wide range of the amplitude levels of these signals (Section 1.4.5).

Thus, the RADA coder encodes an information-bearing pulse train for multiplex transmission over the channel; the RADA decoder recovers the information-bearing pulse train. The use of a common frequency band by the RADA transmitters means that there is mutual interference among net users. The interference results in spurious, or error, pulses at the output of the AND gate of the receiver decoder. As discussed in Section 1.4.3, the effect of these error pulses on the receiver output depends upon the type of demodulation employed.

1.3 Applications of RADA Coding

RADA (random access discrete address) coding was devised for use in a radio pulse communication system to provide net communications

characterized by a large number of net-user addresses, immediate, non-synchronous user access to the channel (random access), and relatively efficient use of bandwidth when the net communications system use factor is small. RADA coding principles are applicable to various modes of communication including: multiplexed signals in wire communications systems, multiplexed signals through active and passive earth satellite repeaters, multiplexed transmissions from air-to-air and ground-to-ground, as well as multiplexed communications between air and ground. The problems involved in multiplexing depend upon the communications mode considered. The primary concern in this study is with line-of-sight propagation over the ground. The use of transponders in this application is projected in several studies (Refs. 1.19, 1.24 and 1.28), although their use has not been investigated in this dissertation.

The U. S. Army Electronics Command has supported studies of the applicability of RADA techniques to communications within an Army division.

It is worthwhile to compare multiplexing using RADA and using alternative principles. Previously, addressing within the net was usually accomplished by assignment of fixed frequency slots to net users in a frequency-division multiplex (FDM) scheme. An alternative method of addressing is by assignment of fixed time slots in a time-division multiplex (TDM) system, although this method is not normally employed in net applications because the transmitter synchronization which is

necessary is not always feasible. For FDM and TDM systems, which employ a fixed assignment of addresses to frequency and time slots, respectively, the total number of addresses determines the system bandwidth requirement, even though the system use factor is small. Thus, a low use factor of the frequency or time slot addresses results in inefficient utilization of system bandwidth.

In contrast to FDM and TDM signals, RADA signals are transmitted over a common frequency channel, i.e., RADA systems are "co-channel" systems. RADA techniques permit specification of addresses for a large number of subscribers, or potential users. However, the bandwidth of a RADA system is determined by the average quality specified for the received signal and, in contradistinction to FDM and TDM systems, by the number of active system users.[2] However, with a specified quality and system bandwidth, a greater number of active users can be accommodated by using a channel assignment scheme in conjunction with FDM or TDM than by using RADA. (These factors suggest the use of RADA techniques for addressing and channel assignment in conjunction with FDM to achieve efficiency in certain information transmission systems.[3] However, this approach has merit only when

---

[2] The bandwidth is influenced by the number of system addresses, or potential users, when this number is unusually large.

[3] For example, recent prototypes of the Martin Company "RADA" System (Refs. 1.19 - 1.23).

the bandwidth needed for addressing and assignment operations is a small fraction of the overall bandwidth requirement).

In RADA systems, transmissions are not synchronized. Such systems are frequently called "asynchronous," or "nonsynchronous" systems. Performance of a target RADA receiver can usually be improved by time synchronization with the transmitter addressing it, and this technique has been exploited in extant systems.

1.4 Problems in RADA System Design

Many parameters must be specified in the design of communications systems using RADA encoding. Among these parameters are the system subscriber address capacity and use factor; the associated quality or error rate; modulation parameters such as basic modulation clock rate and modulator-output-pulse duty factor; and code frame parameters such as the number of system frequencies and the number of pulses per frame on each frequency. Some systematic procedure is needed for determining an optimal choice of parameters for a particular application.

Considerations in the design of RADA systems can usefully be classified in two areas--factors associated with modulation and RADA coding, and factors associated with the physical environment during a communication. These factors are listed separately in this section although they are in fact interrelated, which complicates the design of an optimum RADA system. A near-optimal design can be found by considering aspects of the problem separately and by compromising judiciously for overall system design.

1.4.1 Modulation (Source Coding) Problems. The information signals handled by RADA systems may be continuous or discrete in level and may be continuous or quantized in time. For a given number of users, the quality of a RADA receiver output depends on the modulation-demodulation methods employed. Therefore, modulation (source coding) methods should be employed which minimize the effect of errors on over-all system performance. Efficient modulation schemes tend to be characterized by a low (binary) pulse rate, so that mutual interference and therefore, the number of errors at the demodulator input is small. These modulation schemes should also tend to minimize the receiver output distortion caused by a demodulator input error.

1.4.2 RADA Coding Problems. RADA code sets are needed which produce, for a particular modulation scheme and parameters, the "highest quality" signals at the receiver demodulator output. Two extremes in choosing code sets are their generation by a systematic procedure and their generation randomly, with provision for discarding codes which have undesirable properties. In either case, the digital computer is a useful tool. Since RADA transmissions are asynchronous, the codes chosen should have "good properties" at all relative timings among transmissions.

1.4.3 Mutual Interference. The mutual interference problem is related in a complicated way to problems discussed previously. A description of the error rate at the output of the RADA decoder is

required for specific choices of modulation parameters and RADA code sets. Such a description involves a characterization of the statistics of the error process at the receiver decoder output.

Various measures can be used for evaluating RADA system performance. Error rate and information transmission rate are conventional measures of digital system performance, and are useful for evaluation of RADA links driven by digital information sources. Such evaluations usually can be based directly on the statistics of the RADA decoder output errors.

Demodulator output signal-to-noise ratio is a conventional measure of analog system performance. It is useful for evaluation of RADA links driven by analog information sources. The demodulator output signal usually contains one noise component because of quantization, and another which arises because of errors at the demodulator input.

Some measure of the subjective property "quality" of the demodulated signal is needed for RADA links driven by voice sources. The quality of the demodulated signal is closely related to the error rate at the demodulator input. The relationship between error statistics and quality must be studied through listening tests.

For any of these types of information source, mutual interference effects can be evaluated experimentally by observing the demodulator output in the presence of either actual interference, or in a simulated error process with the appropriate statistics. It is apparent that the

error rate at the RADA decoder output is a useful specific measure of RADA system performance.

1.4.4 RADA Receiver Time-Synchronization. Error pulses at the output of the receiver AND gate sometimes occur between message pulses. These may be partially gated out based on estimates of timing between message pulses. A gate placed at the AND gate output for this purpose is called a "post gate" in this dissertation. Receivers with and without post gates will be referred to as gated and ungated receivers, respectively. In a given communication, a gated RADA receiver operates in time (clock) synchronization with a particular transmitter.

1.4.5 Environmental Problems. A significant parameter of a RADA net is the ratio of range extremes, r_{2max}/r_o--the ratio of the maximum to the minimum distance separating RADA transceivers in the net. Since line-of-sight paths in a ground based net exhibit approximately an inverse fourth power attenuation characteristic (Ref. 1); the ratio of the attenuation of transmissions (signals as well as mutual interference), traveling the shortest and longest paths $(r_{2max}/r_o)^4$, increases rapidly with this distance ratio. As a result, when this ratio is large, both the signal power density and the total interference power density vary over extremely wide limits. Because of these wide limits, and because the signal power density may fall anywhere within these limits, it follows that the dynamic range of the receiver must be extremely large so that the receiver will be able to detect and process received RF pulses even in the presence of pulses of much larger amplitude.

In addition to the extreme level of variation of the target and the direct mutual interference signals which result from the inverse fourth power attenuation characteristic of the ground based net environment, this environment also imposes other problems. Line-of-sight propagation over the ground at VHF and UHF is subject to multipath and scatter effects. RF energy arrives at a given receiver along a direct path from a transmitter, as well as after single and multiple reflections from hills, trees, shrubs, personnel, vehicles, and other objects. Reflected pulses delayed, with respect to the direct pulse, by a small fraction of a pulsewidth tend to distort the pulse envelope. When the reflected pulse delay is of the order of a pulsewidth, the reflected pulse tends to stretch the direct pulse. When the reflected pulse delay exceeds the pulsewidth, two distinct pulses are received. In a typical situation involving line-of-sight propagation over the ground there are many reflections; a received pulse exhibits all three types of multipath effects, particularly when short pulses are transmitted. "Residual interference" is another class of interference which does not originate within the environment, but which has the same effect as the multipath interference. The short pulses typically used in RADA systems tend to produce crosstalk among frequency channels in the RADA receiver. In particular, decreases of pulse duration tend to increase both capacitive and inductive coupling among RF frequency channels, as well as increasing radiation within the receiver. As a result, such practical problems as coupling

through ground loops, pick-up of interfering signals radiated within the receiver itself, and construction of RF and IF filters with sufficiently large skirt rejection, are enhanced. These problems are especially severe in small portable units. Thus, in addition to direct mutual interference, a RADA receiver is also subject to multipath and residual interference. Further, the extreme variation in the levels of the receiver input signals causes variation of the widths of the detected pulses, particularly as a result of the limiting which is employed in processing received signals.

1.4.6 Problems in Military Applications of RADA. Desirable attributes of a division-level military communications system are reliability, mobility, random-access capability, and efficiency of the bandwidth utilization in a high-signal-density environment. The mobility attribute implies a small, light, wireless system. The use of a switching center, an "Achilles' heel" exposed to direct enemy action, is undesirable.

Because of the wide amplitude range of received signals resulting from geometric and propagation characteristics, a RADA receiver must be highly insensitive to signal amplitude. Therefore, RADA coding should not be used with amplitude modulation. When other types of modulation are used, separation of the desired signal from undesired signals at the receiver is feasible even though the power of the desired signal may be much smaller than that of the interfering signals. An advantage of RADA

systems for division communications is that their receivers can be made both sensitive to the timing of received pulses and relatively insensitive to their amplitude.

In the communications system sought, the receiver output signal-to-mutual-interference power ratio should be highly independent of receiver input signal-to-mutual-interference power ratio. Thus, those "bandspreading" systems, proposed for use in a co-channel environment (Ref. 2), which exchange bandwidth of the transmitted signal for signal-to-noise ratio enhancement should not be considered for this application. For such systems, the receiver input and output signal-to-noise ratios are related by (1. 1).

$$(S/N)_{OUT} = 2WT(S/N)_{IN} \qquad (1.1)$$

where W is the receiver input bandwidth and T is the effective receiver output integration time. Because of the extremely small signal-to-mutual-interference power ratios typically encountered in a ground based net environment, it follows from (1. 1) that the bandwidth expansion factor TW required to produce a usable value of $(S/N)_{OUT}$ is excessive. In addition to this inefficiency in the use of bandwidth, the required bandwidth expansion factor, 2TW, is well beyond the "state-of-the-art."

1.5 Review of the Literature

1.5.1 Co-Channel Systems, General. The possibility of co-channel operation of communications systems is implicit in Shannon's epochal work on information theory (Ref. 3).

Various coding and modulation techniques for co-channel communications were proposed and studied before 1958. In 1958, Taylor studied the problems of multiplexing information over a common wideband channel, for both continuous and binary signals (Ref. 1.1). Employing information theory concepts, he obtained channel-capacity expressions for an asynchronous co-channel system which uses a noise-like waveform for receiver "coding"; and, for a general class of systems called "channel-synchronized-asynchronous" systems.

Using a "coding theory" approach, he also investigated two specific multiplexing schemes: one based on recognition of binary signals chosen for their correlation properties, and the other based on recognition of randomly generated binary signals.

The merits of co-channel systems were becoming apparent when, in 1959, Costas pointed out the fallacy of the traditional instinctive approach of reducing bandwidth and data rate to reduce the error rate of a received signal. Costas indicated some of the advantages of co-channel systems over an FDM system with fixed-address frequency channels and the advantages over a system in which the total bandwidth is used randomly by unsupervised narrowband channels (Ref. 2).

In 1960, Hamsher described some aspects of applications of RADA methods to a net communication system, including the extension of range coverage by using single and multiple transponders (Ref. 4).

Spogen, Reading, and Latorre suggested the use of an adaptive, channelized system, and also the use of two RADA type systems in low-use-factor communications applications which require a large number of addresses (Ref. 1.2). One of these RADA systems uses a two-pulse address on a single frequency, and the other system uses a k-pulse address with one pulse on each of k frequencies. The RADA systems described employ amplitude modulation of the transmitted pulses. Spogen, Reading, and Latorre also presented analyses for error-pulse generation, system bandwidth, and subscriber capacity.

In 1961, Fulton, Jr. applied concepts of information theory to show that when the use factor of a net communication system is sufficiently small, it is possible to transmit information more efficiently on a co-channel basis than by either time-division multiplexing (TDM) or frequency division multiplexing (FDM) (Ref. 1.3). More explicitly, he assumed a bandlimited channel with additive Gaussian noise and showed that it is possible to select a set of nonorthogonal waveforms to code an arbitrary number of signals for co-channel transmission with an arbitrarily small error. The maximum number of active transmissions the channel can accommodate is equal to the number of channels of an FDM system of equal bandwidth. The powers of any subset of transmitters

using the channel must be appropriate for the transmitted information rate. The increase in power over that required for FDM or TDM is moderate, so that a reasonable power-bandwidth trade-off is possible.

In 1961, Harris discussed the greater channel capacity of a wideband co-channel system. He compared it with an unsupervised FDM system of equal bandwidth, when the system use factor is small (Refs. 1. 4 and 5). He suggested that advances in coding techniques would be needed before the required trade-off between bandwidth and signal-to-noise ratio could be achieved in co-channel systems. He determined channel capacity for wideband systems with transmitters of equal power, assuming the received signal power from randomly placed transmitters varies inversely with the square of distance.

Chesler proposes (Ref. 30) an m-ary RADA system in which each receiver is addressed by any one of a set of m coded groups of k pulses. These groups are selected from N time and frequency cells. The relation among the system parameter values which minimizes the probability of a false k-fold coincidence of at least one of the m receiver addresses is determined, and is used to define an optimal m-ary RADA system. The probability of a false coincidence of at least one address for an optimal m=2 system is compared with the probability of a false alarm for a binary RADA system in which the two signaling symbols are a coded pulse group. In addition, the "channel utilization" of an m-ary RADA system is compared with that of an m-ary co-channel multiplexing

system which employs pseudo-noise addressing sequences.

Einarsson (Ref. 33) also compared the probability of false coincidence for an m=2, m-ary, RADA system with that of a binary RADA system.

Recently, the applicability of RADA techniques to satellite communications has been investigated (for example, see Refs. 1.34 and 1.35).

Various multiplexing methods have been proposed and studied (for example, see Refs. 6, 7 and 8). Dawson gives a good general discussion of co-channel systems, and includes an annotated bibliography describing the work done in this area (Ref. 9). Included in Refs. 1.19 through 1.33 is a thorough description of the theoretical and experimental aspects of design of particular systems.

1.5.2 RADA Systems. One of the first applications of the RADA concept was in the work of Pierce and Hopper of the Bell Telephone Laboratories (Ref. 10). In this work, a RADA-like system using a code of two pulses per frame on a single frequency, one positive and one negative in phase, was constructed and analyzed. Random samples of voice were transmitted by amplitude-modulating the pulses of the frame.

The Bendix Radio Division of the Bendix Corporation proposed the CAPRI (coded-address, private radio intercom) system, a RADA system in which the amplitude of periodic information samples is used

to frequency-modulate the pulses of a frame (See appendix and Ref. 1. 5)

The Martin Company, Orlando Division, has developed RADA systems using the acronyms RACEP (random access and correlation for extended performance) and "RADA." Initial prototype RACEP systems employed RADA coding in conjunction with pulse position modulation (See appendix and Refs. 11 - 13 and 1. 6 - 1. 8). RADA coding was also employed in conjunction with modifications of delta modulation (Ref. 14).

Most recently, the acronym "RADA" has been applied to a Martin net communications system in which the information is modulated in pulse-position modulation and transmitted in adaptive frequency-division multiplex after a search for a vacant frequency channel (Refs. 1. 19 - 1. 23). RADA techniques are employed for both the vacant channel search and for other supervisory functions. The system, not described in this dissertation, is a complex one which is characterized by many special functions.

The Motorola Corporation developed the RADEM (random access-delta modulation) system (See appendix and Refs. 11 - 13, 15, 1. 9, 1. 10 and 1. 28 - 1. 33) which uses delta modulation.

The extent of U. S. Army Electronics Command's interest in RADA techniques, including foreseen applications, is indicated by the scope of the RADA work which they have sponsored. In 1963, USAEC supported three concurrent studies of the feasibility of using RADA systems for Army divisional communications (Ref. 11). Some early

aspects of this work (Refs. 14, 16 - 19) were summarized in papers presented at the 1964 International Convention of the Institute of Electrical and Electronics Engineers. More recent and complete results of these extensive studies are presented in Refs. 1. 19 through 1. 33.

1. 5. 2. 1 Modulation Methods. Studies of optimum modulation methods applicable to RADA systems have concentrated on two techniques for sampling voice: namely, DATEC (digital adaptive technique for efficient communications) (Ref. 14), and "extremal sampling" (Refs. 20, 21 and 1. 11 through 1. 18). Both modulation methods have been used with RADA techniques because the required transmission rate of samples is lower than the Nyquist rate. Initial results obtained for extremal sampling indicate that because of the low level of information redundancy, the received signal is quite sensitive to the occurrence of false samples. This factor may reduce the utility of this modulation technique in RADA systems (Ref. 1. 15).

1. 5. 2. 2 Coding. Selection of RADA vocabularies and characterization of the mutual interference characteristics of RADA code vocabularies are an important aspect of the study of RADA systems. Gilbert (Ref. 32) investigates the coding of pulses on a single frequency channel. He shows how to construct lists of N digit ($N = \Lambda_t$) code words so that the weight (number of "ones", or pulses) of each word is less than a specified upper limit. The lists are also constructed so that the Hamming distance of any given word from all N shifts of all other words

is greater than a specified minimum value. Einarsson (Ref. 33) defines a RADA system in which a frame consists of M pulses placed in a frame of K frequency channels and A time cells, with at least one pulse in the first time cell. For such a code frame, he specifies the size of the code vocabulary as the number of ways of placing the M pulses in the KA cells conditional on a pulse being in the first time cell. A study of a code using a frame consisting of a single pulse on each of three frequencies is reported in Ref. 1.8. Several coding methods for RADA systems are described in Ref. 1.23.

1.5.2.3 Mutual Interference. The statistics of the RADA decoder output error process, their suitable approximation, and their use in evaluating RADA system performance have been a primary concern of several studies. Spogen and associates (in Ref. 1.15) use a particular model and set of assumptions to investigate the error process in RADA systems. They also make comparisons of the error rates of RADA systems using pulse position modulation with those of systems using extremal sampling (Refs. 1.11 - 1.18, 20 and 21).

Sommer (Ref. 31) and Einarsson (Ref. 33) defined RADA systems in which the code frames consist of n pulses randomly distributed among p frequencies and in j time cells. Employing slightly differing analyses, both authors determined the probability of a false receiver output signal at a given time instant (equivalent to the duty factor determined in this dissertation). They also determined the relationship among

the parameter values which minimizes the probability of a false receiver output signal.

Einarsson also investigated and compared the effects of false receiver output signals on pulse position modulation, pulse code modulation, and delta modulation. A model of a RADA system is developed by Dawson and Sklar (Ref. 16) and independently in this study which is based on the assumption that the times of occurrence of mutual interference pulses at the different receiver AND gate inputs are independent Poisson processes. The work of Dawson and Sklar, and that of this author, employ similar methods in determining a duty factor of the error process, the distribution function of the duration of an error pulse, and the average error pulse rate. Other statistics, including the autocorrelation function of the error process are also obtained in Ref. 16.

Evaluation of the effect of the error pulse process on the intelligibility of a demodulated signal has been the subject of several studies. Psycho-acoustic testing was undertaken by Diaz and Norvell, who determined, for three kinds of pulse modulation, the effect of commissive and omissive modulator input pulse errors on the intelligibility of the demodulated voice (Ref. 17). The effects of errors on demodulated PPM and "DATEC" signals is investigated experimentally and theoretically in Ref. 1.23. We also note the investigation by Spogen and associates of the effect of omissive and commissive errors on extremal amplitude sampling (Ref. 1.16).

1.5.2.4 RADA Receiver Time Synchronization. RADA receiver time synchronization has essentially been considered in various other contexts, for example, in studies of synchronization of the early and late range-tracking gates in radar. In addition, some effort has been directed specifically at the problem of receiver synchronization in RADA systems which use pulse position modulation (Ref. 22).

1.5.2.5 Environmental Problems. An experimental study was made to determine the effects of propagation (over the ground) phenomena on RADA systems (Ref. 18). Path attenuation, variation in the level of pulses in a frame, and pulse stretching because of multipath were measured. For a ground-based net in which transmitters are randomly distributed with a fixed probability per unit area, Einarsson (Ref. 33) theoretically determined the distribution of the number of interfering signals which exceeds a threshold within the target receiver. Using both this result and an analysis of the probability of error at the output of a RADA receiver in the presence of a given number of interfering signals, he determined the net reliability (i.e., the probability that the number of interfering signals which exceeds the receiver threshold is less than the number for which the RADA system is designed).

Heffner used a theoretical backscatter model to predict pulse-stretch effects in a pulse communication system using line-of-sight propagation over the ground (Ref. 19).

In a study conducted by the Martin Corporation (Ref. 1.23), a

computer simulation is used to determine the probability distribution of the envelope of the mutual interference for a particular net configuration. This distribution, in turn, is used to determine the probability that a signal from a transmitter at a particular range is not within the dynamic range of the receiver.

Similarly, in this dissertation, the probability of a "useful" receiver signal at a target receiver imbedded within a RADA net is defined as the probability that the signal-to-mutual-interference power ratio at the target receiver terminals exceeds the reciprocal of the receiver dynamic range. A lower bound is determined for the probability distribution of the signal-to-mutual-interference power ratio as a function of the distance separating the given transmitter, target receiver, and the basic net parameters.

There are no known theoretical results which account for the effects on the RADA receiver output of the fluctuation of detected pulsewidths resulting from the wide range of variation in power level of received pulses described in Section 1.4.5. However, a computer simulation of RADA systems has included the effects of variation of the widths of detected pulses (Ref. 23).

1.6 The Basic RADA System

The following definition of a "basic RADA system," having certain essential features, unifies subsequent discussion and analysis. These essential features are common to current prototype RADA

systems (described in the appendix) which differ considerably, however, in implementation details.

The transmitter, transmitted waveform, and receiver of this "basic RADA system" are shown in Figs. 1.4(a), 1.4(b), and 1.4(c). In the transmitter of Fig. 1.4(a), the information is subject to some type of pulse modulation (source-encoding). Subsequently, each modulator output pulse causes the transmission, through RADA encoding, of a group of pulses (termed a "frame") coded within a "matrix of time-frequency cells" (or simply matrix) which occupy a time interval T_d seconds long and a frequency band W cycles per second wide centered at the nominal RADA system center frequency. Further, the matrix contains Λ_t equal "time slots" within the time interval of length T_d and Λ_f equal "frequency channels" within the frequency band (of width W). In each frame, pulses are transmitted in λ_t out of the Λ_t "time slots" within λ_f out of the Λ_f "frequency channels." Addressing to particular receivers is accomplished by the choice of time-frequency cells in which pulses are transmitted. A representative frame has the form indicated in Fig. 1.4(c).

To prevent overlapping of successive frames, a frame duration T_d is chosen which is less than or equal to the minimum interval between modulator output pulses. To minimize system bandwidth, the frame duration is usually chosen to equal the minimum interval between modulator output pulses. The average number γ of interfering

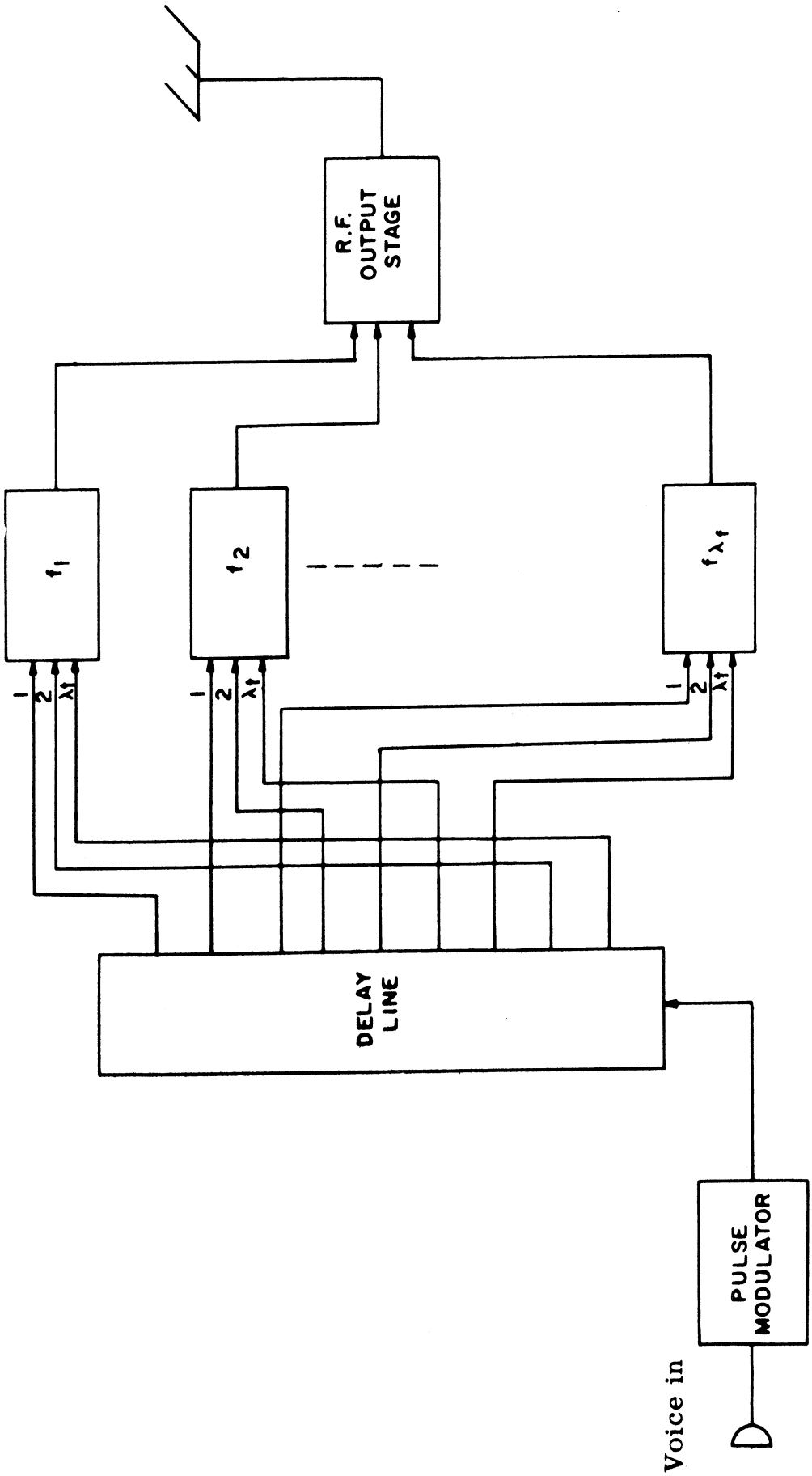

Fig. 1. 4(a). Basic RADA system transmitter.

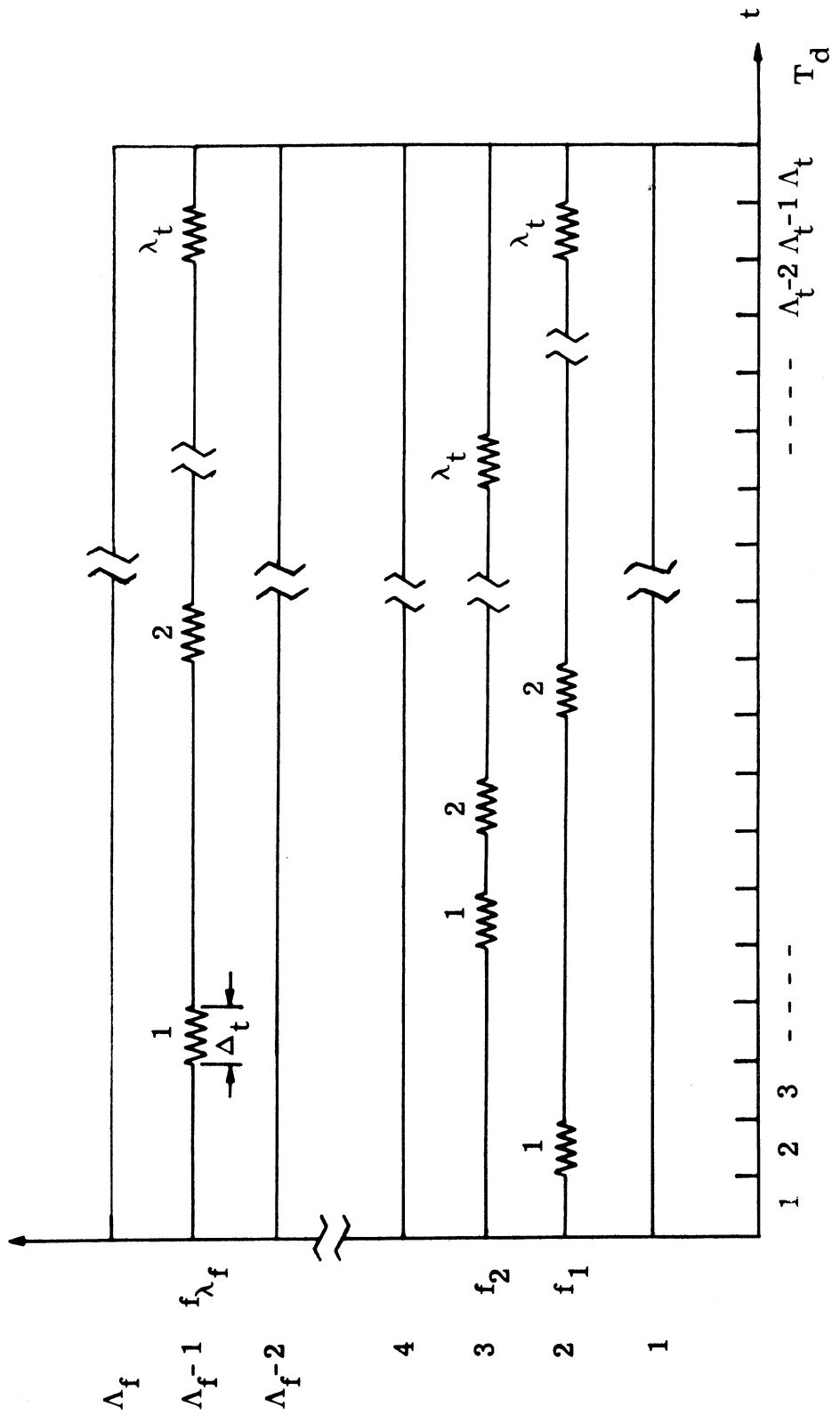

Fig. 1.4(b). Basic RADA system transmitted signal (1 code frame).

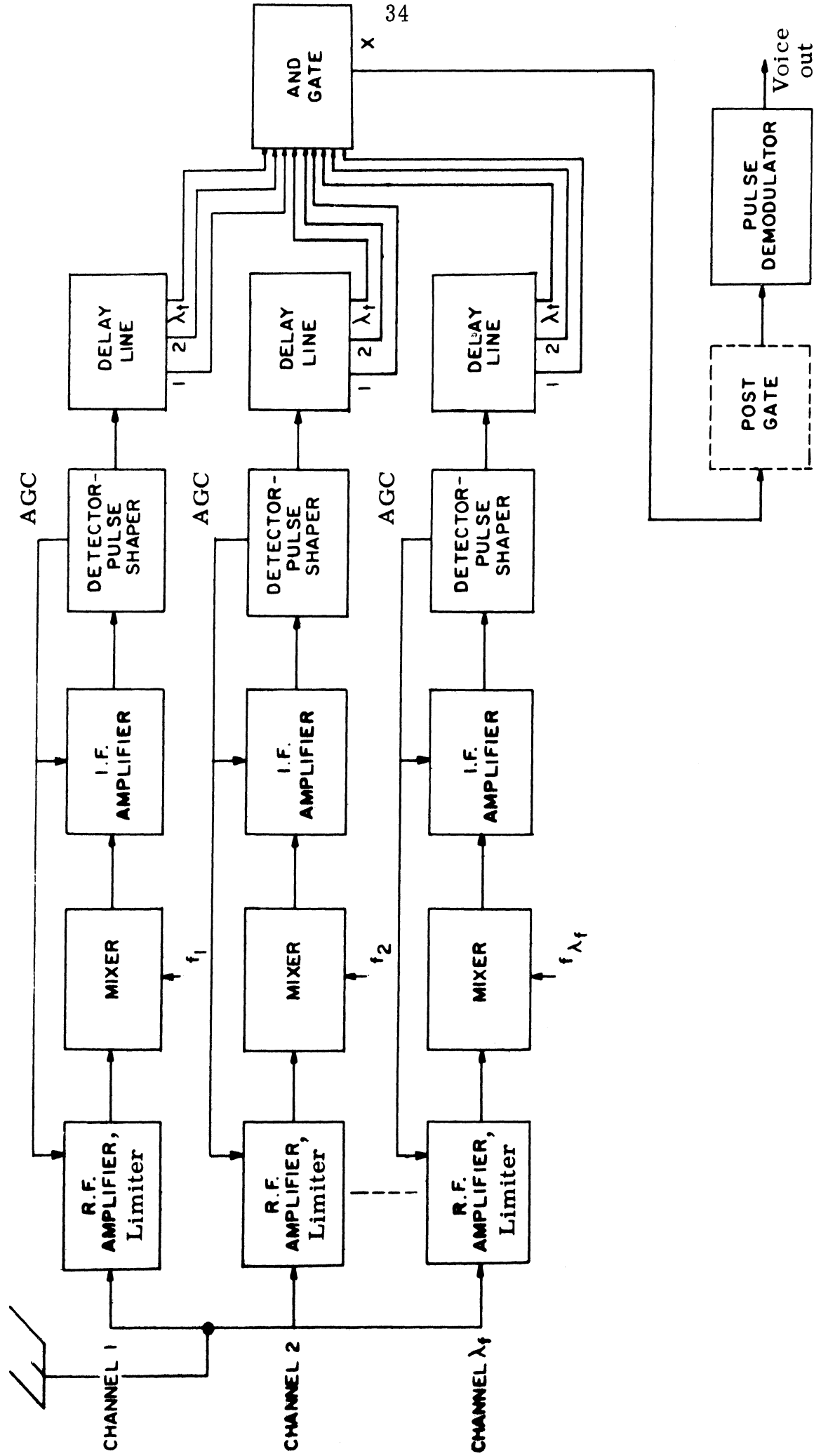

Fig. 1.4(c). Basic RADA system receiver.

pulses which occur per second on each frequency channel is an important parameter for the description of RADA system performance. In (1.2), γ is expressed in terms of Λ_f, λ_f, λ_t; in terms of m, the number of active transmitters; and, $\bar{T}$, the average time interval between successive transmitted frames.

$$\gamma = \frac{m \lambda_f \lambda_t}{\Lambda_f \bar{T}} \quad . \tag{1.2}$$

In a RADA system which uses clocked binary modulation, information pulses gate the occurrence of pulses of a clocked binary pulse train. For such a system, the frame duration T_d is usually chosen to equal the clock period T_c. When the average fraction of on-modulated pulses is k, the mean number of frames which occurs per second is,

$$\frac{1}{\bar{T}} = \frac{k}{T_c} \tag{1.3}$$

Substituting Eq. 1.3 into Eq. 1.2, γ is determined for clocked binary modulations with clock period T_c and parameter k,

$$\gamma = \frac{m k \lambda_f \lambda_t}{\Lambda_f T_c} \quad . \tag{1.4}$$

Whenever a group of pulses with the proper timing occurs at a receiver input, the receiver AND gate produces an output pulse. The major effect of mutual interference in this type of system is the

production of error pulses at the output of the receiver AND gate. This gate output has been indicated by an x in Fig. 1.4(c). When the times at which the AND gate might be triggered by a message pulse can be predicted from the reception of previous message pulses, a receiver "post gate" may be used to gate some of the interference from the AND gate output. The post gate is characterized by the time interval T_p (the "gate interval") that it remains open. The use of a post gate implies receiver time synchronization, since the gate interval must be synchronized with the times at which there are AND gate output message pulses. Post gates will be further considered in Section 1.6.2.

1.6.1 Definitions and Parameters. The following list of terms will facilitate future discussion.

Definition of Terms

Frame - Abbreviation for time-frequency code frame. A group of pulses within a matrix of time frequency cells.

Epoch - The epoch of a pulse is the leading edge of the pulse.

Message Frame - A received signal frame [Fig. 1.4(b)] at the antenna terminals of a particular receiver which has been properly coded for that receiver by a given transmitter.

Error Frame - A received signal frame present at the receiver antenna terminals which causes an AND gate output as a result of a chance correct phase relationship of frames of signals coded for other receivers.

Message Pulse - A pulse at the AND gate output which is caused by a message frame. The corresponding pulse at the post gate output when the post gate is specified.

Error Pulse - An AND gate output pulse caused by an error frame. The corresponding pulse (if any) at the post gate output, when the post gate is specified.

Gated Receiver - A RADA receiver with a post gate is referred to as a gated receiver.

Ungated Receiver - A RADA receiver with no post gate.

Synchronism - A gated target receiver is time synchronized with its given transmitter when the receiver post gate intervals are centered on message pulses from the given transmitter.

Definition of Parameters

T_d Frame Duration. The time interval measured between the beginning of the first time cell of a frame and the end of the last time cell.

$\bar{T}$ Frame Interval. The average time interval between successive transmitted frames.

T_c Clock Period. For a system using clocked binary modulation, T_c is the modulator clock period.

Λ_t The number of time slots in a frame.

λ_t For any transmitter, the number of pulses transmitted per frame on each frequency channel. $\lambda_t \leq \Lambda_t$.

Λ_f The total number of frequency channels used by a RADA system.

λ_f For any transmitter, the number of frequencies on which pulses are transmitted. $\lambda_f \leq \Lambda_f$.

Δ_t Width of rectangular pulses transmitted by a modeled RADA system. Also, the equivalent rectangular width of non-rectangular transmitted pulses, as defined in Section 5.3.

k In a system using clocked binary modulation, k is the average fraction of on-modulated clock pulses.

m The number of wideband RADA transmitters which interfere with a particular RADA receiver at a particular time. Numerical results are obtained in terms of m.

γ The average number of interfering pulses per second on each of the λ_f frequency channels. In general, $\gamma = \frac{m \lambda_f \lambda_t}{\Lambda_f \overline{T}}$. For systems using clocked binary modulation, γ can also be expressed as $\gamma = \frac{m k \lambda_f \lambda_t}{\Lambda_f T_c}$.

T_p Gate Interval. For a gated receiver, the period of time when the post gate is open.

1.6.2 The Post Gate. RADA receiver performance can usually be improved by gating interference from the AND gate output by means of a post gate. Different types of post gates will be described in this section.

When frames are transmitted with random intervals, the position of a message pulse cannot be used to predict the position of the following message pulse. No interference gating method is effective. For example, in the Pierce-Hopper system (Ref. 10) a voice waveform is sampled randomly at a sufficient rate to convey the voice intelligence. Each sample is coded into a frame and transmitted. Because of the random sampling process, there is no clocking rate associated with the transmitted waveform. The position of a sample cannot be predicted from the position of the preceding sample, and, therefore, a post gate cannot be used with this system.

When it is possible to predict a range of possible positions of the next message pulse from a given message pulse, a post gate can

be used to gate out some of the error pulses which occur between message pulses. The post gate is synchronized as long as the post gate timing is based on message pulses. If error pulses occur in the interval between the opening of the post gate and the epoch of the message pulse in several successive frames, the post gate may lose synchronization and gate out runs of message pulses. The average length of runs will depend on the amount of interference, the gate parameters, and the signal parameters. A post gate of the type just described uses a pulse-to-pulse type of post gate synchronization, which is somewhat unreliable in moderate or heavy interference.

If a message pulse train is derived from a clocked waveform, as in pulse position and delta modulation, a more reliable type of post gate synchronization can be used. For example, by use of gating circuitry analogous to the early and late range tracking gates used in RADAR, the clock rate and phase of a message pulse train may be determined even in moderate or heavy interference. A clocked gating waveform derived from the early and late gating circuitry can then be used to gate the AND gate output. In future discussion of gated receivers, receiver synchronization will be assumed. That is, it will be assumed that the post gate uses a clocked gating waveform with a gate interval T_p which is centered on the expected positions of message pulses.

The types of post gate errors which are significant depend on

the kind of modulation which is used. In the case of a position-modulated signal, it is assumed that the message pulse is the first pulse which occurs in the gate interval in that frame (the other pulses are gated out). If the first pulse is a message pulse, the frame information is correct; if the first pulse is an error pulse, the frame information is erroneous. This error event is referred to as a "type one false alarm."

In a system using clocked binary modulation (e.g., PCM, Δ modulation), it is assumed that the gate interval is centered at the times when a message pulse might occur. Errors ("type two false alarms") occur when at least one error pulse occurs in a gate interval T_p in which there is no message pulse. Errors of both types will be investigated in Chapter III.

CHAPTER II

ENVIRONMENTAL CONSIDERATIONS

2.1 Introduction

In a ground based RADA net with transceivers within line-of-sight range, the power density of the field associated with a transmission falls off approximately as the inverse fourth power of distance from the transmitter. Since the ratio of the maximum to minimum separation of receivers from transmitters may be as large as 1000, both the receiver signal power and the mutual interference power at a given instant may differ greatly (± 150 db) among the receivers. To enable signal detection of these highly variable signal levels in an interference background, the RADA receiver is typically constructed with a large dynamic range. The dynamic range is defined here as the maximum value of the ratio of interference power to the power of a detectable receiver input signal. The dynamic range is thus defined in an average sense which depends upon both the number of interfering signals and upon their power. There are multipath and residual interference effects, described in Section 1.4.5, that limit the maximum value of dynamic range which can be used to advantage. A receiver with this maximum value y of dynamic range, can detect signals which cause a receiver input signal power which is greater than the mutual interference

power divided by y. Given a receiver with dynamic range y, it follows, approximately, that the probability of a "useful" received signal equals the probability that the receiver input signal to mutual interference power ratio exceeds 1/y. The probability of a useful signal depends, then, upon the probability distribution of the receiver input signal to mutual interference power ratio. In this chapter, the probability distribution function is defined with respect to an ensemble of equally likely sets of m transceivers which are "uniformly distributed" in the net area. The use of this ensemble distribution function has the advantage that analytical results can be obtained in terms of a small number of basic parameters which characterize the net. From a practical point of view, the ensemble distribution of the signal-to-mutual interference power ratio is the fraction of random nets, constructed according to a particular set of rules and assumptions, for which the signal-to-mutual interference power ratio exceeds a given value. The assumptions upon which the results are derived are presented in Section 2.2. They include the assumption that there are m interfering transmitters in the net; that all transceivers are separated at least by a distance r_o; and that a distance r_2 separates the given transmitter and target receiver. If the probability of a useful signal is small, it can be concluded that the other net constraints are too severe for the particular values of m, r_o, and r_2 which are used, and that they must be relaxed.

Theoretical determination of the ensemble probability

distribution of the mutual interference power is difficult.[1] However, a theoretical lower bound of the distribution is determined in this chapter which in turn gives a lower bound of the probability of a useful signal. It turns out that because the primary source of interference power is from transmitters which are relatively close to the

---

[1] For example, a good approximation to the distribution results from determining the total interference power as the sum of the interference power from all of the m interfering transmitters, as follows. Each of the transmitters is assumed situated at a point which is randomly positioned within an annular area centered at the target receiver. The radius, r_o, of the inner boundary of the annulus is the minimum distance separating transceivers in the net area. As a first order approximation, the outer boundary is assumed at a radius $r_1 = 2r_o$, as subsequent results (Section 2.3.4) indicate that the major contribution to the interference power is from transmitters within this radius. The probability that each transmitter is positioned at any point within the annular area is assumed constant throughout the area. With these assumptions, it can be shown that the probability density p(P) of the interference power P from a single transmitter is

$$p(P) = \begin{cases} \dfrac{c}{P^{1.5}} ; & P_{min} \leq P \leq P_{max} \\ 0 ; & \text{otherwise} \end{cases}$$

where

$$P_{min} = \frac{c\,P_t}{r_1^4} ; \qquad P_{max} = \frac{c\,P_t}{r_o^4} ,$$

and where c is the propagation constant, and P_t is the transmitted power (Section 2.3). The probability density of the total interference power is then assumed to equal the sum of the power received from m transmitters, the power from each being distributed as p(P). This assumption does neglect the statistical dependence of the power from the various transmitters. The dependence exists because, when a number of transmitters are distributed within the net area, the remaining transmitters cannot be independently placed within the area; but must be placed in such a way that the transmitters are separated by a distance greater than r_o from those which are already within the area. The assumption of independent transceiver locations, and independent distributions of power from each interfering transmitter yields accurate results with the typically small density of packing of transmitters within the net area.

The probability density of the total interference power P_i from the m transmitters is the m fold convolution of the density p(P). The evaluation of this convolution either directly, or by utilizing characteristic functions is difficult, and the results are in an unwieldy series form.

target receiver, the lower bound of the probability distribution is essentially independent of the position of the target receiver in the net area, and independent of the shape of the net area. The bound depends only upon the density of "packing" of transmitters in the net area, and the ratio of the transmitter-receiver distance r_2 to the minimum allowable distance r_o between the transceivers.[1] The objective of this chapter then, is to obtain a theoretical lower bound for the probability of a useful signal at a target receiver within a RADA net. In Chapter III, the interaction of the message process and the error process at the receiver output is investigated theoretically, under the assumption that there is a useful receiver input signal.

There is intuitive justification for considering that the probability distribution, defined for an ensemble containing nets with m transceivers, is equivalent to other probability distributions. The ensemble probability distribution also approximately equals the fraction of receivers in a given net, at a given time, which receive useful signals.

---

[1] The lower bound for the probability of a useful received signal is based upon the assumption of a (random) uniform placement of transceivers in the net area. When clustering occurs, the inequality for the probability of a "useful" received signal at a transceiver within a cluster is determined by the active transceiver "packing density," q_1q_2, for the cluster area (with no clustering, q_1q_2 is specified as the average for the net area). This simple extension of results to the clustered situations is possible because nearby transmitters (within the cluster area) are the primary source of interference power in all practical situations.

When the transceivers are mobile, but in such a way that the assumptions are always satisfied, the probability distribution can be given both of the preceding interpretations, and can also be interpreted as the probability distribution of signal-to-mutual interference power, in time, at a particular target receiver.

For the readers' convenience, the results of this chapter are summarized in Section 2.2, and then derived in Section 2.3. The definitions and assumptions which apply to the most general model developed in Section 2.3 are given in Section 2.2.

2.2 Problem Characterization and Results for Mutual Interference Power Analysis

In the previous section, it was indicated that for a given packing density of transmitters in the net area, a given receiver dynamic range y, and a given ratio of transmitter-receiver separation to minimum specified distance between transceivers, and for other prescribed conditions; a lower bound is determined for the probability that the signal-to-mutual interference power ratio exceeds 1/y. This lower bound is also a lower bound on the probability that a given transmitter radiates a signal which is useful at its target receiver.

The objectives in this section are to characterize a model for estimating the distribution of the ratio of signal-to-interference power in a RADA net, and to summarize the results of its analysis detailed in Section 2.3. The idealized net geometry assumed for this analysis

is depicted in Fig. 2.1. The m transmitters which interfere with a target receiver, the given transmitter, and the target receiver itself are contained in the "simply connected" net area A. Within the area, the given transmitter and the target receiver are at particular positions, and the interfering transmitters are positioned randomly under the conditions imposed below. The minimum distance separating transceivers is r_o so that each transceiver can be thought of as occupying a circle of radius $r_o/2$ which does not overlap the circle corresponding to any other transceiver. The a-priori probability that any interfering transmitter is placed at any position in the net (which does not overlap the given transmitter or target receiver) is the same throughout the net area. When a fraction of the m transceivers have already been placed in the area, the conditional probability that any one of the remaining receivers is placed at any point in the remaining area is the same throughout the remaining area. The previous constraints define interfering transmitters which are "uniformly distributed" over the net area.

The following definitions and assumptions further define the model and delimit the applicability of results:

1. The transceivers of a net are uniformly distributed over an arbitrary area A.

2. All antennas are omnidirectional in a horizontal plane.

3. Equal power is radiated by each transmitter of the net.

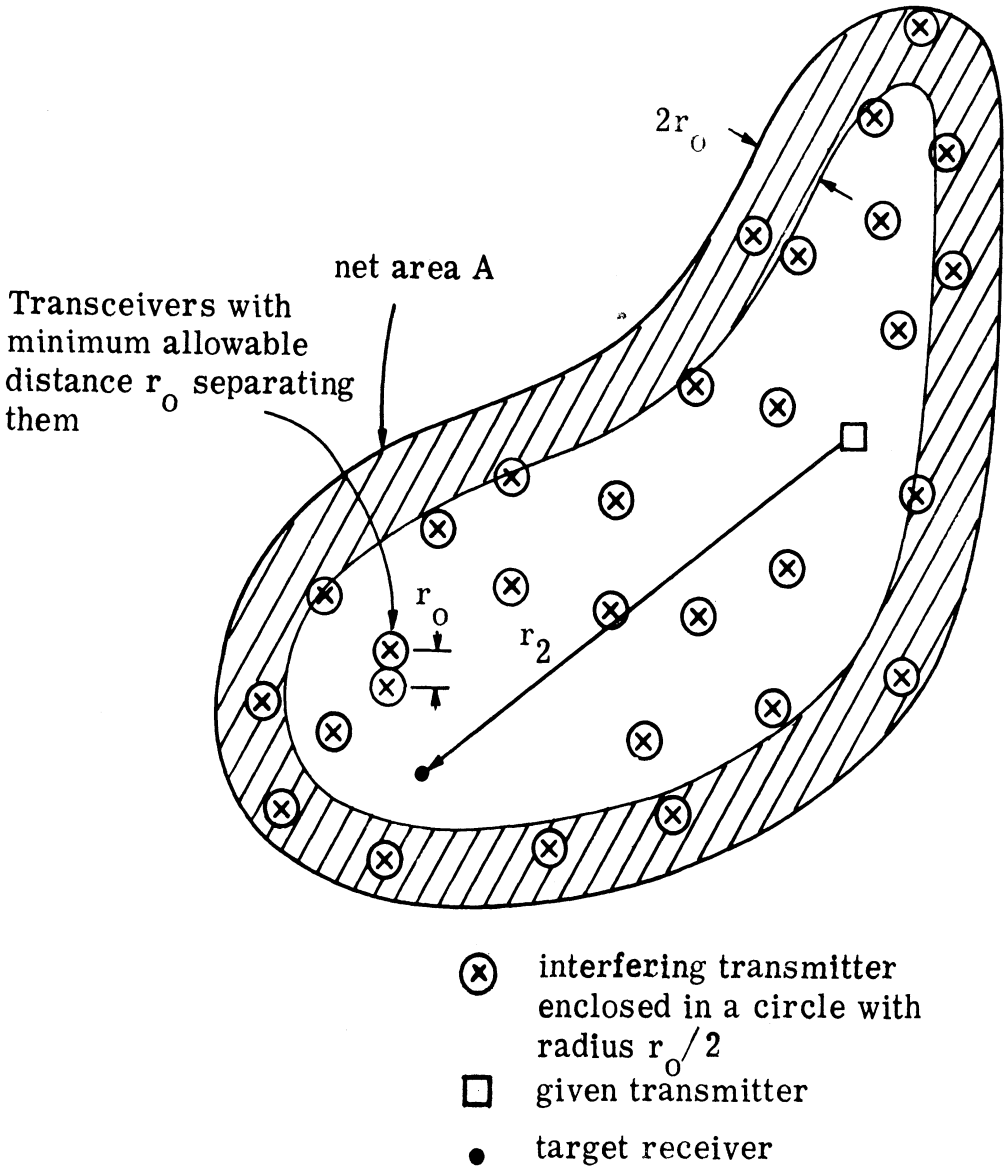

1. The target receiver is a distance r_2 from the given transmitter

2. The target receiver is within the area A, and further than a distance $2r_o$ from the boundary of A (i. e., the target receiver cannot be within the crosshatched area).

3. The minimum distance between transceivers is r_o.

Fig. 2.1. Geometry for determination of the ratio $P_s/E(P_i)$ of signal power to mutual interference power at a receiver within the net environment.

4. The interference power at any given receiver in the net is the sum of the powers received from all active interfering transmitters (co-channel operation).

5. r_2 is the distance between a particular transmitter and a particular receiver of the net, these being a given transmitter and a target receiver. Radiations from m other active transmitters of the net interfere with communication between the given transmitter and its target receiver.

6. r_o is the minimum separation of transceivers.

7. M is the number of transceivers which could be placed in the area A at this minimum separation r_o, excluding the given transmitter and its target receiver, which is given by (2.15).

$$M = .3612\left(\frac{A}{\pi r_o^2} - 2\right) \qquad (2.15)$$

8. For the results to apply, the target receiver must be at least a distance $2r_o$ from the boundary of the area A.

9. Let r_{2max} be defined as the greatest separation of transceivers in the net so that the results of Section 2.3 apply for a transmitter and receiver separated by at most a distance $r_{2max} - 2r_o$ (see Fig. 2.2). Then the minimum value of signal-to-mean-mutual interference power ratio for which the results apply occurs for $r_2 = r_{2max} - 2r_o$. When $r_{2max} >> 2r_o$, this minimum value approximately equals

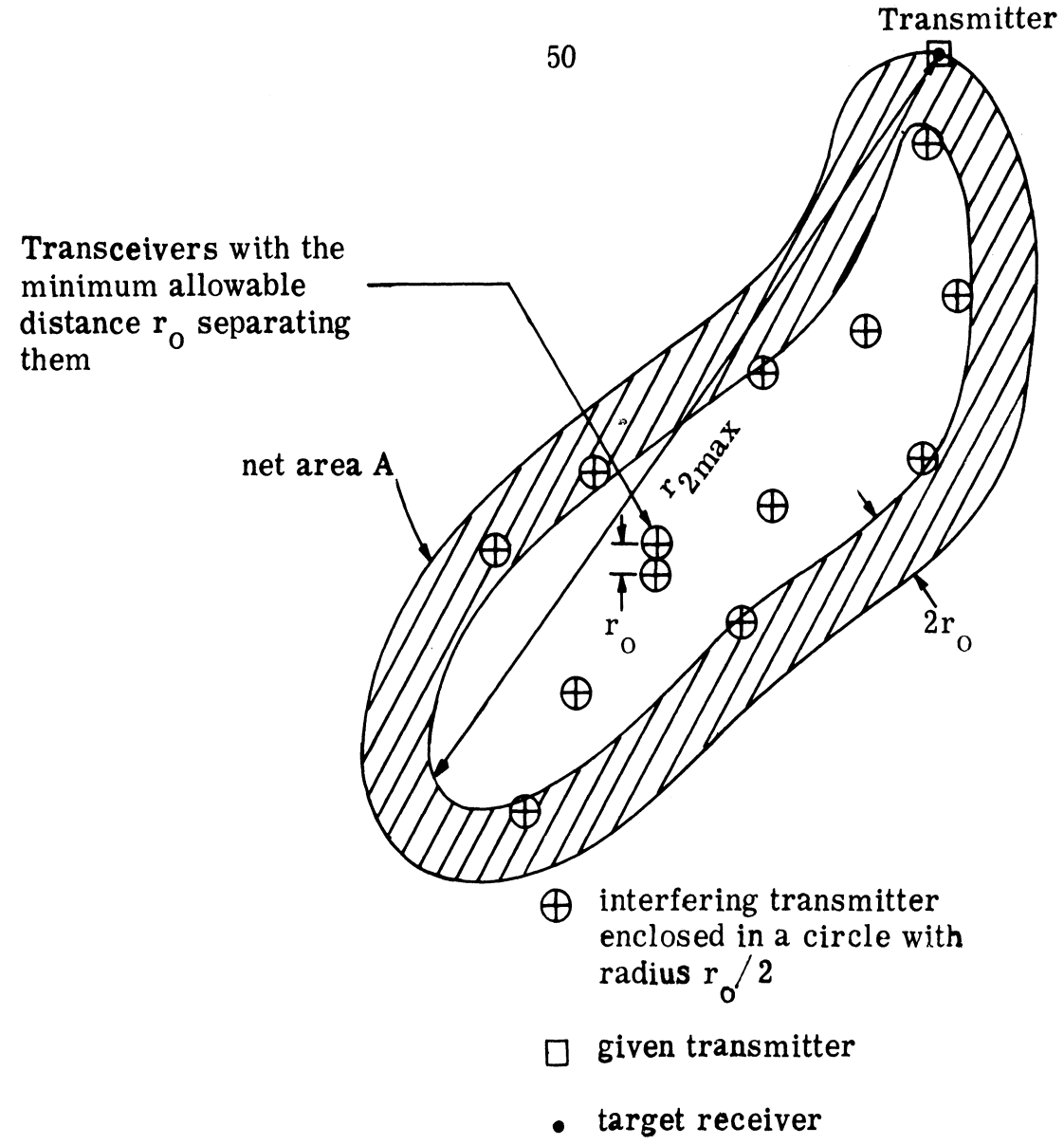

1. The target receiver a distance $r_2 = (r_{2max} - 2r_o)$ from the given transmitter.

2. The target receiver is within the area A, and further than a distance $2r_o$ from the boundary of A (i. e., the target receiver cannot be within the crosshatched area.

3. The minimum distance separating transceivers is r_o.

Fig. 2.2 Geometry for determination of the minimum value, $P_s/E(P_i)\Big|_{min}$ of the ratio of signal power to mutual interference power at a receiver within a net environment.

the value of the ratio calculated for $r_2 = r_{2max}$. This value of the ratio is used in "worst case" calculations of the distribution of the signal-to-mean-mutual interference power ratio.

10. $q_1 (q_1 \leq 1)$ is an (area) packing density for net transceivers. The quantity q_1 is the ratio of the actual number of transceivers in an area A to the maximum number M of transceivers which can be placed in the area A at the minimum separation r_o.

11. $q_2 (q_2 \leq 1)$ is the instantaneous fraction of the number Mq_1 of transceivers which are transmitting and contributing to the interference power.

12. m is the number of active transceivers which are interfering with communications between the given transmitter and the target receiver, so that

$$m = q_1 q_2 M \tag{2.1}$$

13. The randomness of the interference power is due to the probabilistic character of the positioning of the sets of m interfering transmitters in the area A.

14. P_s is the signal power density at the target receiver which is produced by the given transmitter.

15. P_i is the mutual interference power density at the target receiver.

16. E is an operator denoting ensemble average. The

members of the ensemble of interest are sets of m transceivers. Each different set corresponds to a different, equally likely placement of the m transceivers in the area A.

17. $E(P_i)$ is the expected value of the mutual interference power at the target receiver input terminals, under an ensemble average.

18. $\sigma(P_i)$ is the standard deviation of the distribution of P_i resulting from an ensemble average.

To reiterate, the objective of this section is to characterize a model for determining a lower bound of the distribution of the signal-to-mutual interference power ratio, and to summarize this primary result which is detailed in Section 2.3. The major steps in obtaining the result are as follows. The ratio $P_s/E(P_i)$ of received signal power P_s to average interference power $E(P_i)$ is determined analytically as a function of the known packing density q_1q_2 of receivers in the net area, and as a function of the known ratio r_2/r_o of transmitter-receiver separation r_2 to minimum permissible separation r_o. The quantity $\frac{P_s}{E(P_i)}$ indicates the signal-to-interference power ratio to be expected at a receiver as a function of the use factor of the communication system; $\frac{P_s}{E(P_i)}$ is plotted in Fig. 2.3. The ratio $\sigma(P_i)/E(P_i)$ of standard deviation $\sigma(P_i)$ of the received interference power to the mean $E(P_i)$ of the interference power is determined as a function of the known packing factor q_1q_2. The quantity $\frac{\sigma(P_i)}{E(P_i)}$ indicates the relative

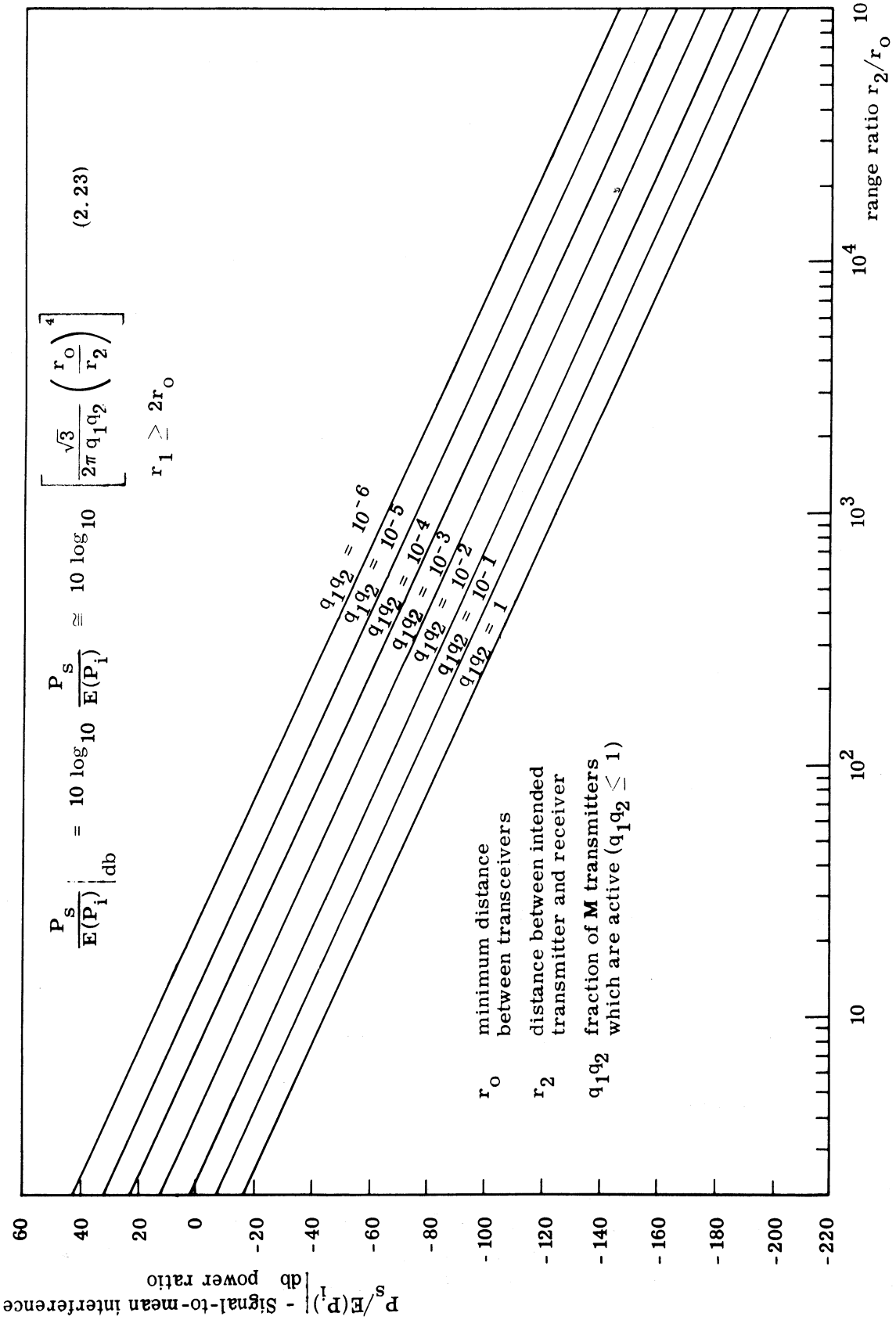

Fig. 2.3. Signal-to-mean interference power ratio, $\frac{P_s}{E(P_i)}\Big|_{db}$ vs. range ratio r_2/r_o.

fluctuation which can be expected in the signal-to-interference power ratio because of random placement of a given number of transceivers in a prescribed area, as a function of the ratio of the transmitter-receiver distance and the minimum distance r_o between transceivers; $\frac{\sigma(P_i)}{E(P_i)}$ is plotted in Fig. 2.4 as a function of the system use factor, $q_1 q_2$.

Using Chebychev-type inequalities (specifically here, the Chebychev and Markov inequalities (Ref. 24),[2] lower bounds for the probability distribution function $P\left(\frac{P_s}{P_i} > x\right)$ of the signal-to-mutual interference power ratio can be expressed analytically in terms of $P_s/E(P_i)$ and $\sigma(P_i)/E(P_i)$. It is noted that for values of $P(P_s/P_i > x)$ in the range of interest, .50 to .90, the inequalities are usually close enough to the true distribution so that they may be employed as first order approximations for design purposes. Their use is realistic in view of the approximations which must be made in developing any tractable analytical model. The errors in approximations using the normal distribution, which are justified for sufficiently large m by the central limit theorem, are not known. Results obtained using a normal approximation typically indicate a significant probability of negative mutual interference power P_i so that this distribution appears to be a poor approximation to the true one.

---

[2] There are stronger inequalities which are also applicable here, in particular, for example, those due to Guttman (Ref. 35, p. 935) and Bernstein (Ref. 35, p. 936). However, the use of these inequalities is not as convenient as the use of the Chebychev and Markov inequalities.

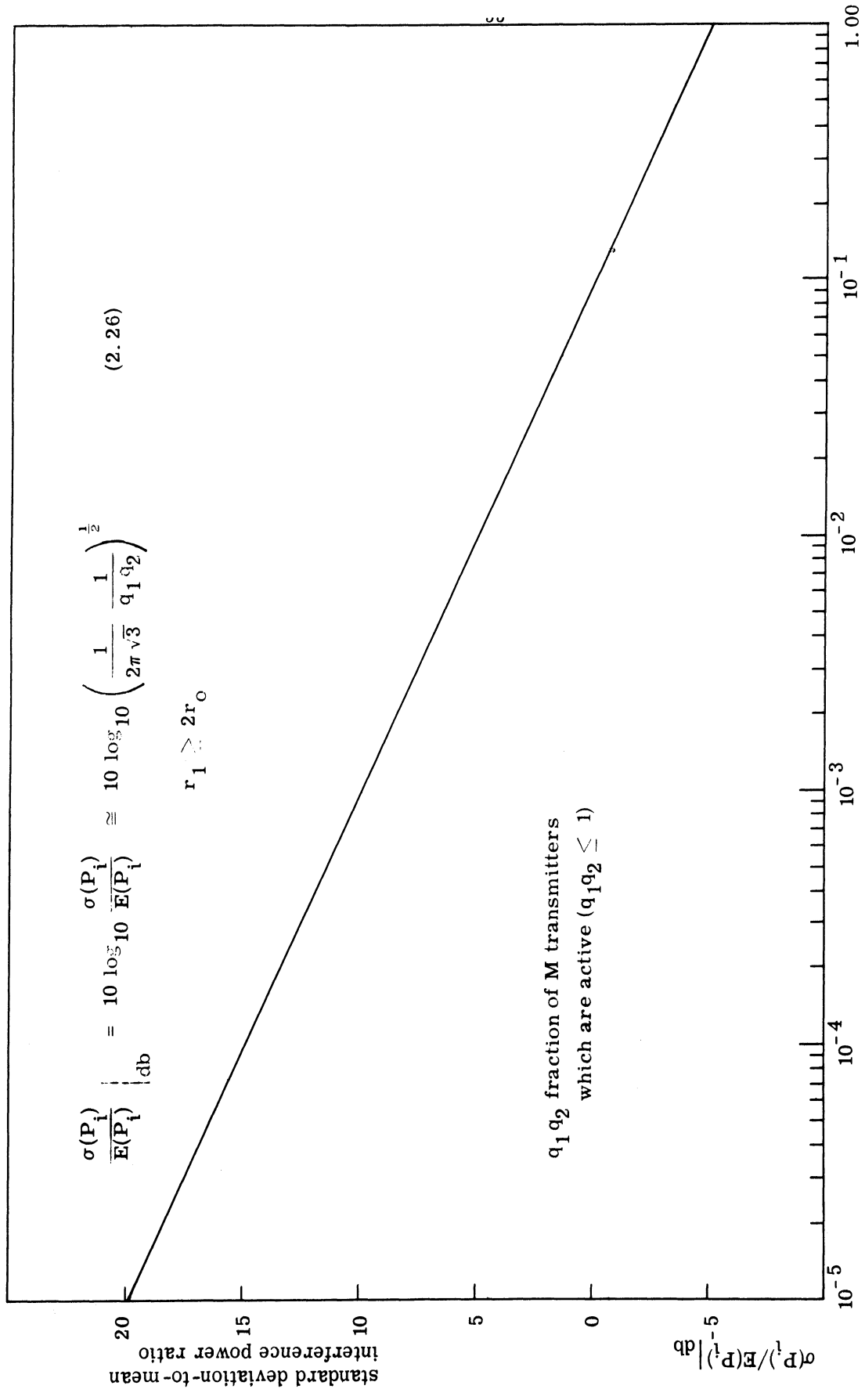

Fig. 2.4. Approximate ratio of standard deviation-to-mean interference power $\sigma(P_i)/E(P_i)|_{db}$ vs. fraction of active transmitters $q_1 q_2$.

When the receiver dynamic range is y, then the probability of a useful received signal is given by (2.2), where P(a) is the probability of the event a.

$$P\left(\frac{P_s}{P_i} > \frac{1}{y}\right) \tag{2.2}$$

In Section 2.3.5, when the fraction of active transmitters, $q_1 q_2$, satisfies the inequality $q_1 q_2 < .1$, the Chebychev inequality is expressed as[3]

$$P\left(\frac{P_s}{P_i} > x\right) \begin{cases} \geq 1 - \dfrac{x^2}{\lambda^2\left[1 - \dfrac{x}{\lambda}\dfrac{E(P_i)}{\sigma(P_i)}\right]^2} ; & \dfrac{x^2}{\lambda^2\left[1 - \dfrac{x\,E(P_i)}{\lambda\,\sigma(P_i)}\right]^2} \leq 1 \\ \geq 0 ; & \text{otherwise} \end{cases} \tag{2.32}$$

where the parameter λ is defined by (2.29).

$$\lambda = \frac{P_s}{E(P_i)}\frac{E(P_i)}{\sigma(P_i)} \tag{2.29}$$

The Markov inequality is given by

$$P\left(\frac{P_s}{P_i} > x\right) \begin{cases} > 1 - x\dfrac{E(P_i)}{P_s} ; & x\dfrac{E(P_i)}{P_s} \leq 1 \\ \geq 0 ; & \text{otherwise} \end{cases} \tag{2.34}$$

---

[3] Alternately, higher order moments than the second can be employed in a generalized form of Chebychev's inequality (Ref. 36).

A numerical example of the application of these results is given in Section 2.3.7, the results of which are presented here. In this example,[1] $Mq_1 = 2000$ transceivers are distributed nearly uniformly over an area A = 100 square miles; $m = Mq_1q_2 = 200$ of them are active. The maximum distance, between transceivers in the area A is $r_{2max} = 15$ miles. The minimum distance is $r_o = 100$ feet. The receiver dynamic range is 60 db.

Using Figs. 2.3 and 2.4 for a transmitter receiver pair with the maximum range separation, r_{2max},

$$\left.\frac{P_s}{E(P_i)}\right|_{db} = -96 \text{ db}$$

$$\left.\frac{\sigma(P_i)}{E(P_i)}\right|_{db} = 7 \text{ db}$$

Chebychev's and Markov's inequalities specify lower bounds of the probabilities. In this case, the lower bound is zero so that the inequalities provide no information; this particular result does not assure that a useful received signal is available in a net with the given parameters. More precisely, the result indicates that either the signal-to-mutual interference power ratio is seldom more positive than -60 db, or that the inequalities are too weak to provide useful information in this case.

---

[1] This example merely illustrates the use of the derived results and is not necessarily typical of an actual ground-based communication net.

For the same net, using Markov's inequality, it was found that when r_2 = 8000 feet, the signal-to-mutual interference power ratio exceeds -60 db at least 50 percent of the time. Thus, the received signals in at least 50 percent of the nets constructed with the parameters specified above will be useful, and these parameters would be a good starting point for initial specification of the net parameters.

2.3 Derivation of Results for Mutual Interference Power Analysis

In the remainder of this chapter, approximate analytical expressions will be obtained for the ratio of standard deviation-to-mean of interference power, for the signal-to-mean-interference power ratio at a target receiver, and for related quantities. Both of these ratios will be used to evaluate Chebychev-type inequalities which provide a lower bound for the probability distribution function of the ratio of signal power to interference power at a target receiver, when a given number of transmitters are interfering. As a starting point of the following development, assume a circular net area A of radius r_1 (refer to Fig. 2.5). In addition to the definitions and assumptions previously given in Section 2.2, the following definitions and assumptions also apply:

r_1 The radius of the circle which includes all transceivers. The target receiver is at the center of the circle.

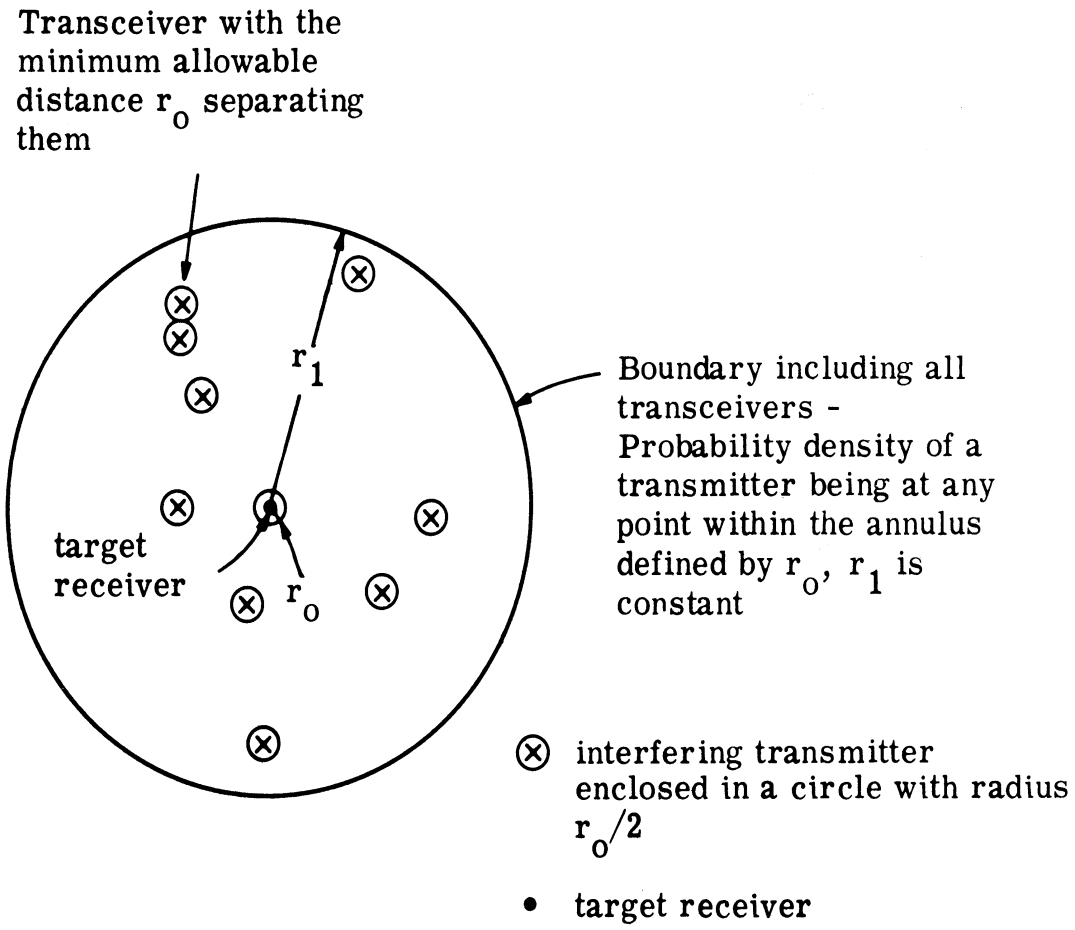

Fig. 2. 5. Initial geometric model of transceiver placement in the net area.

P_t The transmitter power. P_t is assumed to be the same for all active transmitters.

c A propagation constant which depends on the terrain, on the antenna polarization, and on the antenna height.

The restriction to circular geometry is the least realistic of these assumptions. It will be seen that, with small error, this assumption can be relaxed considerably so that the results apply to general and realistic situations. In the preceding definitions, M, q_1, q_2 are defined with respect to sets of transceivers which exclude the given transmitter and its target receiver. As a result, $q_1 q_2$ has a direct interpretation as the fraction of the M transceivers which are interfering with the target receiver.

2.3.1 Maximum Transmitter "Packing", Circular Boundary.

Since the target receiver is at the center of the circular area, M is the maximum number of interfering transmitters which can be placed in the annular area of Fig. 2.5 with at least a distance r_o separating them. The type of packing which allows this maximum number is shown in Fig. 2.6. Boundary effects at the perimeter of the circle are ignored. The efficiency of packing transceivers in the circle with radius r_1 can be determined by dividing the area in the three sectors in any equilateral triangle in Fig. 2.6 by the total area of the triangle. It is

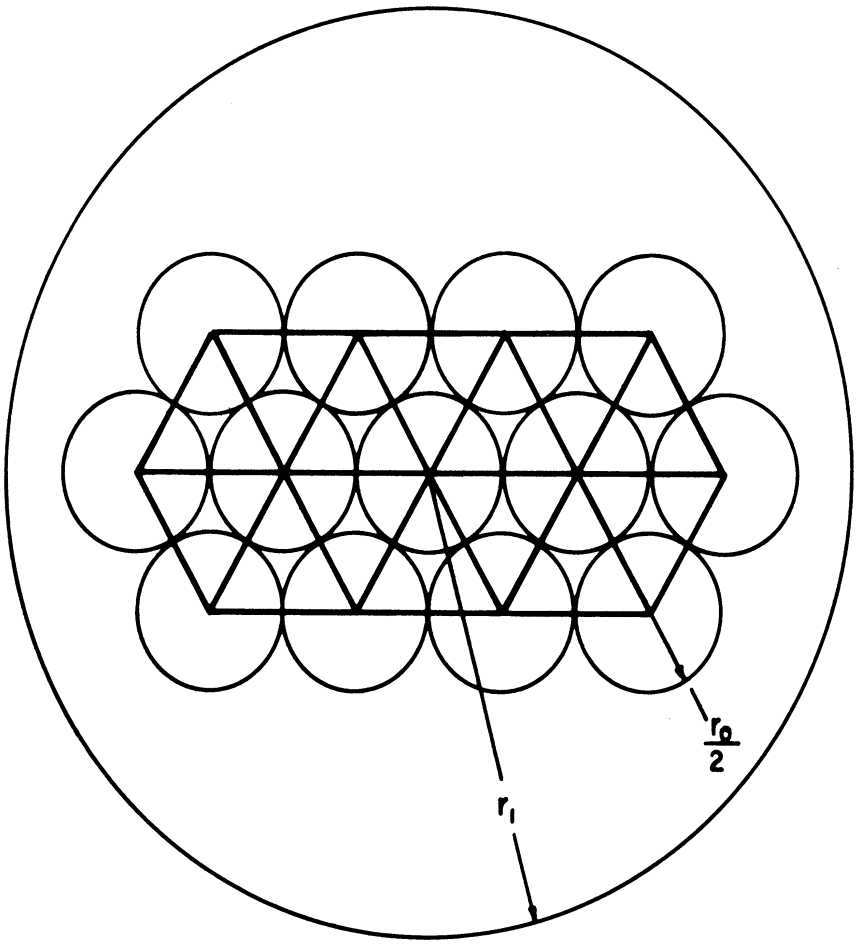

Fig. 2.6. Circles of radius $r_0/2$ arranged for maximum packing in circle of radius r_1.

$$3 \times \frac{1}{6} \pi \left(\frac{r_o}{2}\right)^2 \Big/ \frac{1}{2} r_o \times \frac{\sqrt{3}}{2} r_o = \frac{\pi}{2\sqrt{3}} \qquad (2.3)$$

Hence, for a circular area A,

$$M = \frac{2\pi}{\sqrt{3}} \frac{(r_1^2 - 2r_o^2)}{r_o^2} \qquad (2.4)$$

2.3.2 Mean Interference Power, Annular Boundary. The interfering power P_i at the receiver terminals for the geometry of Fig. 2.5 is given by (2.5).

$$P_i = P_t \sum_{i=1}^{m} \frac{c}{r_i^4} \qquad (2.5)$$

Neglecting the slight tendency of the given transmitter to reduce the probability of interfering transmitters at radius r_2, the mean interfering power is given by (2.6),

$$E(P_i) = c P_t \sum_{i=1}^{m} E(1/r_i^4) = c P_t m E(1/r^4) \qquad (2.6)$$

where $E(1/r^4)$ is given by (2.7).

$$E(1/r^4) = \int_{r_o}^{r_1} \frac{2\pi r}{\pi(r_1^2 - r_o^2)} (1/r^4)\, dr = \frac{1}{r_o^2 r_1^2} \qquad (2.7)$$

Substituting (2. 4) into (2. 1), (2. 1) into (2. 6), and using (2. 7); $E(P_i)$ is determined by (2. 8) as

$$E(P_i) \cong \frac{c\, P_t\, q_1 q_2}{r_o^2\, r_1^2} \times \frac{2\pi}{\sqrt{3}} \frac{(r_1^2 - 2r_o^2)}{r_o^2} \qquad (2.8)$$

2.3.3 Approximation to the Variance of the Interference Power, Annular Boundary. Using the same method as was used in Section 2. 3. 2 to obtain the second moment,

$$E(P_i^2) = E\left[c\, P_t \sum_{i=1}^{m} \frac{1}{r_i^4}\right]^2 = P_t^2\, c^2\, E\left[\sum_{i=1}^{m} \frac{1}{r_i^4}\right]^2$$

$$= P_t^2\, c^2 \sum_{i=1}^{m} \sum_{j=1}^{m} E\left(\frac{1}{r_i^4} \frac{1}{r_j^4}\right) \qquad (2.9)$$

Now it is noted that $1/r_i^4$ is not statistically independent of $1/r_j^4$. That is, if transmitter i is at a position at radius r_i, the total number of transmitters allowable at this radius is reduced. Hence, the probability of other transmitters at radius $r_j = r_i$ is reduced, which makes the dependence of the two probabilities clear. For low values of $q_1 q_2$, that is, a low-packing density in the annulus, conditions of statistical independence are approached. Hence, an approximate expression for $E(P_i^2)$ based on the assumption of statistical independence can be used. In many practical situations, the packing density will be low.

The variance of the interference power is approximated below, but no information is given concerning the size of errors resulting from assumptions of statistical independence. From (2.9)

$$E(P_i^2) \cong P_t^2 c^2 \left\{ m E\left(\frac{1}{r^8}\right) + m(m-1) \left[E\left(\frac{1}{r^4}\right)\right]^2 \right\} \qquad (2.10)$$

Also,

$$\sigma^2(P_i) = E(P_i^2) - [E(P_i)]^2 \qquad (2.11)$$

Substituting (2.1) and (2.4) into (2.10) and (2.8), and (2.10 into (2.11),

$$\sigma^2(P_i) \cong P_t^2 c^2 \left\{ q_1 q_2 M E\left(\frac{1}{r^8}\right) + q_1 q_2 M(q_1 q_2 M - 1) \left[E\left(\frac{1}{r^4}\right)\right]^2 \right\}$$

$$- c^2 P_t^2 q_1^2 q_2^2 M^2 \left[E\left(\frac{1}{r^4}\right)\right]^2$$

$$= \frac{2\pi P_t^2 c^2 q_1 q_2 (r_1^2 - 2r_o^2)}{\sqrt{3}\, r_o^2} \left\{ E\left(\frac{1}{r^8}\right) - \left[E\left(\frac{1}{r^4}\right)\right]^2 \right\} \qquad (2.12)$$

Neglecting the presence of the given transmitter at radius $r_2 \leq r_1$,

$$E\left(\frac{1}{r^8}\right) = \int_{r_o}^{r_1} \frac{2\pi r}{\pi(r_1^2 - r_o^2)} \frac{1}{r^8}\, dr = \frac{r_1^6 - r_o^6}{3 r_1^6 r_o^6 (r_1^2 - r_o^2)} \qquad (2.13)$$

Substituting (2. 7) and (2. 13) into (2. 12) gives (2. 14).

$$\sigma^2(P_i) \cong \frac{2\pi P_t^2 c^2 q_1 q_2}{3\sqrt{3}\, r_o^8} \left\{\frac{r_1^2 - 2r_o^2}{r_1^2 - r_o^2}\right\}$$

$$\times \left\{1 - \left(\frac{r_o}{r_1}\right)^6 - 3\left(\frac{r_o}{r_1}\right)^2 \left[1 - \left(\frac{r_o}{r_1}\right)^2\right]\right\} \qquad (2.14)$$

for $q_1 q_2$ small. The variance results from the different possible distributions of a given number of transmitting transceivers within the circular area.

2. 3. 4 Extension of Results to General Net Areas. In this section, it is shown that the expressions previously obtained for $E(P_i)$ and $\sigma(P_i)$, obtained by assuming circular geometry, can be extended to apply within a general, simply connected net of area A. Approximate expressions will also be obtained for $P_s/E(P_i)$, for $\sigma(P_i)/E(P_i)$, and for $P_i\left[\frac{P_s}{P_i} > x\right]$ at a target receiver within the general net area A. In addition to the other assumptions upon which these expressions were obtained, the following assumption also applies. The target receiver is within the area A, and is farther than a distance $2r_o$ from all points of the boundary of A. The target transmitter may be at any point within the area A, subject to the following restriction. All transceivers must be separated by at least a distance r_o, as initially indicated in the assumptions of Section 2. 2. The maximum number M of transceivers,

excluding the given transmitter and target receiver, which can be placed in the general area A with at least a distance r_o separating them is given by (2. 15).

$$M = .3612\left(\frac{A}{\pi r_o^2} - 2\right) \qquad (2.15)$$

Expression 2. 15 is obtained in the same way as (2. 4).

Assume, then, that a target receiver within the net area A which is farther than a distance $2r_o$ from all points of the boundary of A, as indicated in Fig. 2. 7. A circular net area of radius $r_1 = 2r_o$ centered at the target receiver is completely enclosed within the net area A, and a circular net area with radius $r_1 = \infty$ completely encloses the net area. It follows that the number of transceivers which contribute to the mutual interference at a target receiver in the actual net area A is intermediate between the number which contribute in a circular net area with radius $r_1 = 2r_o$ and in a circular net area with radius $r_1 = \infty$. Since the expected value of interference power is a monotonically increasing function of the number of interfering transmitters, it follows that the expected value of interference power $E(P_i)$ for the area A is bounded below by the expected value of interference power in a circular net area with radius $r_1 = 2r_o$, and is bounded above by the expected value of interference power in a circular area with radius $r_1 = \infty$. That is, using (2. 8), the expected value $E(P_i)$ of

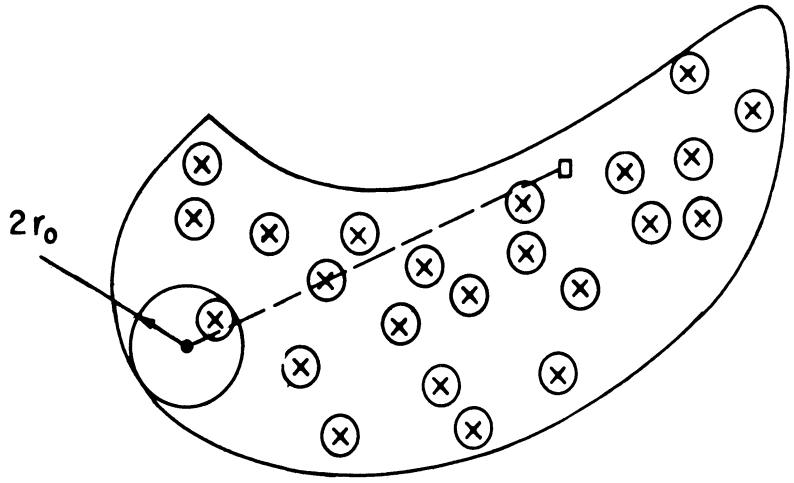

□ given transmitter

• target receiver

⊗ interfering transmitter enclosed in a circle with radius $r_o/2$.

Fig. 2.7. Distribution of transmitters and receiver within a particular boundary.

interference power in a general net area A satisfies inequality (2. 16).

$$\frac{1}{2}\left(\frac{2\pi}{\sqrt{3}}\ \frac{c\,P_t\,q_1q_2}{r_o^{\,4}}\right)\ \leq\ E(P_i)\ \leq\ \left(\frac{2\pi}{\sqrt{3}}\ \frac{c\,P_t\,q_1q_2}{r_o^{\,4}}\right) \qquad (2.16)$$

An approximation for $E(P_i)$ which is within +3 db of the correct value is given by (2. 17).

$$E(P_i)\ \cong\ \frac{2\pi}{\sqrt{3}}\ \frac{c\,P_t\,q_1q_2}{r_o^{\,4}} \qquad (2.17)$$

An argument similar to the preceding one applies for $\sigma(P_i)$, and using (2. 14) it can be shown in the same way that for any simply connected area A, $\sigma(P_i)$ satisfies (2. 18).

$$\sqrt{\frac{9}{32}}\ \sqrt{\frac{2\pi\,c^2\,P_t^{\,2}\,q_1q_2}{3\sqrt{3}\,r_o^{\,8}}}\ \leq\ \sigma(P_i)\ \leq\sqrt{\frac{2\pi\,c^2\,P_t^{\,2}\,q_1q_2}{3\sqrt{3}\,r_o^{\,8}}} \qquad (2.18)$$

Equation 2. 19 is an approximation for $\sigma(P_i)$ which is within +3 db of the correct value

$$\sigma(P_i)\ \cong\ \sqrt{\frac{2\pi\,c^2\,P_t^{\,2}\,q_1q_2}{3\sqrt{3}\,r_o^{\,8}}} \qquad (2.19)$$

The inequalities (2. 16) and (2. 18) for $E(P_i)$ and $\sigma(P_i)$ will now be used to obtain bounds and approximations for $P_s/E(P_i)$ and for $\sigma(P_i)/E(P_i)$. The signal power P_s at the target receiver input terminals produced by the given transmitter is given by (2. 20).

$$P_s = \frac{c\,P_t}{r_2^4} \tag{2.20}$$

The inequality (2. 21) for $P_s/E(P_i)$ follows from (2. 16) and (2. 20).

$$\frac{\sqrt{3}}{2\pi\, q_1 q_2}\left(\frac{r_o}{r_2}\right)^4 \leq \frac{P_s}{E(P_i)} \leq \frac{2\sqrt{3}}{2\pi\, q_1 q_2}\left(\frac{r_o}{r_2}\right)^4 \tag{2.21}$$

It also follows that within -3 db of the correct value,

$$\frac{P_s}{E(P_i)} \cong \frac{\sqrt{3}}{2\pi\, q_1 q_2}\left(\frac{r_o}{r_2}\right)^4 \tag{2.22}$$

Also,

$$\left.\frac{P_s}{E(P_i)}\right|_{db} \cong 10 \log_{10} \frac{\sqrt{3}}{2\pi\, q_1 q_2}\left(\frac{r_o}{r_2}\right)^4 \tag{2.23}$$

Similarly, from (2. 16) and (2. 18), $\sigma(P_i)/E(P_i)$ satisfies (2. 24) and (2. 25).

$$\sqrt{\frac{9}{32}}\sqrt{\frac{1}{2\pi\sqrt{3}\, q_1 q_2}} \leq \frac{\sigma(P_i)}{E(P_i)} \leq 2\sqrt{\frac{1}{2\pi\sqrt{3}\, q_1 q_2}} \tag{2.24}$$

Within ±3 db,

$$\frac{\sigma(P_i)}{E(P_i)} \cong \sqrt{\frac{1}{2\pi\sqrt{3}\, q_1 q_2}} \tag{2.25}$$

Also,

$$\left.\frac{\sigma(P_i)}{E(P_i)}\right|_{db} \cong 10 \log_{10} \left(\frac{1}{2\pi\sqrt{3}\, q_1 q_2}\right)^{\frac{1}{2}} \tag{2.26}$$

The quantities $P_s/E(P_i)\Big|_{db}$ and $\sigma(P_i)/E(P_i)\Big|_{db}$ given by (2.23) and (2.26) are plotted in Fig. 2.3 and Fig. 2.4.

A case of particular interest occurs when the distance separating the given transmitter and target receiver is the longest chord, r_{2max}, which spans the net area A. On the average, the smallest value of signal-to-mutual-interference power occurs for this particular link, and it follows that if the net parameters are chosen to provide, for this link, a useful received signal with an acceptable probability, then the probability of a useful received signal is acceptable for all other links. Because the assumptions require that the target receiver be within the area A, and farther than a distance $2r_o$ from the boundary of A, the longest value of r_2 for which the assumptions apply is actually given by

$$r_2 = r_{2max} - 2r_o \tag{2.27}$$

However in typical cases, $r_{2max} >> 2r_o$ so that a negligible error results from using $r_2 = r_{2max}$ in the calculations.

2.3.5 Chebychev Type Inequalities. It was indicated in Section 2.1 that it is difficult to analytically determine the probability distribution function $P\left(\frac{P_s}{P_i} > x\right)$ in a particular situation. For this reason, Chebychev-type inequalities are used to bound the probability distribution function (Ref. 24). The two inequalities which are used are the Chebychev and Markov inequalities. The interest here is in the determination of lower bounds for the probability distribution function of the signal-to-interference power ratio at the terminals of the target receiver. The distance r_2 separating the intended transmitter is a parameter of the result (i.e., intended transmitter range is not a random variable). The transmitters which produce the mutual interference are uniformly distributed over the area A in accordance with the assumptions of Section 2.2. Inequalities for the distribution function of signal-to-interference power ratio are developed as follows.

$$P\left(\frac{P_s}{P_i} > x\right) = P\left(P_i < \frac{P_s}{x}\right)$$

$$= P\left\{P_i < \left[\frac{1}{x}\,\frac{P_s}{E(P_i)}\,\frac{E(P_i)}{\sigma(P_i)}\right]\sigma(P_i)\right\} \qquad (2.28)$$

Define:

$$\lambda = \frac{P_s}{E(P_i)} \frac{E(P_i)}{\sigma(P_i)} \tag{2.29}$$

Then from (2.28) and (2.29),

$$\begin{aligned} P\left(\frac{P_s}{P_i} > x\right) &= P\left[P_i - E(P_i) < \frac{\lambda}{x}\,\sigma(P_i) - E(P_i)\right] \\ &= P\left\{P_i - E(P_i) < \sigma(P_i)\frac{\lambda}{x}\left[1 - \frac{x}{\lambda}\frac{E(P_i)}{\sigma(P_i)}\right]\right\} \end{aligned} \tag{2.30}$$

In many typical net situations, the fraction of active transceivers, $q_1 q_2$, satisfies the inequality $q_1 q_2 < .1$; and it follows from Fig. 2.4 that $E(P_i)$ is less than $\sigma(P_i)$ in these situations. When $E(P_i)$ is less than $\sigma(P_i)$, and when in addition $\frac{\lambda}{x}\left(1 - \frac{x}{\lambda}\frac{E(P_i)}{\sigma(P_i)}\right) \geq 1$, it follows from (2.30) that

$$P\left(\frac{P_s}{P_i} > x\right) = P\left\{|P_i - E(P_i)| < \sigma(P_i)\frac{\lambda}{x}\left[1 - \frac{x}{\lambda}\frac{E(P_i)}{\sigma(P_i)}\right]\right\} \tag{2.31}$$

Application of Chebychev's inequality (Ref. 24) to the right hand side of (2.31) yields,

$$P\left(\frac{P_s}{P_i} > x\right) \begin{cases} \geq 1 - \dfrac{x^2}{\lambda^2\left[1 - \frac{x}{\lambda}\frac{E(P_i)}{\sigma(P_i)}\right]^2} & ; \quad \dfrac{x^2}{\lambda^2\left[1 - \frac{x}{\lambda}\frac{E(P_i)}{\sigma(P_i)}\right]^2} \leq 1 \\ \geq 0 & ; \quad \text{otherwise} \end{cases} \tag{2.32}$$

A good approximation to $P_s/E(P_i)$, expressed in decibels, is given by (2.23), which is plotted in Fig. 2.3. A good approximation to $\sigma(P_i)/E(P_i)$, expressed in decibels, is given by (2.26), which is plotted in Fig. 2.4. By using

Fig. 2.3, Fig. 2.4, (2.29), and (2.32), a Chebyshev inequality for $P\left(\frac{P_s}{P_i} > x\right)$ is obtained.

Application of Markov's inequality (Ref. 24) to the right side of (2.30) gives,

$$P\left[P_i < \frac{\lambda}{x}\,\sigma(P_i)\right] \begin{cases} \geq 1 - \frac{x}{\lambda}\,\frac{E(P_i)}{\sigma(P_i)} ; & \frac{x}{\lambda}\,\frac{E(P_i)}{\sigma(P_i)} \leq 1 \\ \geq 0 ; & \text{otherwise} \end{cases} \tag{2.33}$$

Substituting (2.29) and (2.30) into (2.33),

$$P\left(\frac{P_s}{P_i} > x\right) \begin{cases} \geq 1 - \frac{x}{\lambda}\,\frac{E(P_i)}{P_s} ; & x\,\frac{E(P_i)}{P_s} \leq 1 \\ \geq 0 ; & \text{otherwise} \end{cases} \tag{2.34}$$

By using Fig. 2.3 and (2.34), a Markov inequality for $P\left(\frac{P_s}{P_i} > x\right)$ is obtained. The stronger of the equalities of (2.32) and (2.34) for a given choice of parameters is the one which has the larger right hand side.

2.3.6 Effect of Changes in Geometry. A change in geometry by a constant scale factor results in a new geometry for which the same Chebychev and Markov inequalities apply as in the original geometry. Therefore, the same lower bound for the probability distribution of P_s/P_i applies to all sets of geometry which are related by a constant scale factor. The change in scale factor is defined so that

r_o, r_2 and $\sqrt{A}$ are increased by a constant factor, and m remains constant. This definition implies that $q_1 q_2$ remains constant when the scale factor is changed. These relations may readily be shown as follows. For $A >> \pi r_o^2$, a constant scale factor increase in $\sqrt{A}/r_o$ results, according to (2. 15) in the same value of M. Allowing the number m of transmitters in the expanded area to remain the same as in the original area, it follows from (2. 1) that $q_1 q_2$ remains constant through the expansion. It follows directly from (2. 25) that $\sigma(P_i)/E(P_i)$ remains constant in the expansion. Since r_o/r_2 remains constant in the expansion, it follows from (2. 22) that $P_s/E(P_i)$ also remains constant. Since $\sigma(P_i)/E(P_i)$ and $P_s/E(P_i)$ remain constant in the expansion, it follows from (2. 29), (2. 32), and (2. 34) that the same Chebychev and Markov inequalities apply after the expansion as before it.

2. 3. 7 Application of Results. As an example of the use of the foregoing results, consider the following situation. $Mq_1 = 2000$ transceivers are distributed nearly uniformly over an area A = 100 square miles. A number $Mq_1 q_2 = 200$ of them are interfering with the target receiver. The maximum distance separating transceivers in the area A is $r_{2max} = 15$ miles. The minimum distance $r_o = 100$ feet. The receiver dynamic range is 60 db, that is, the receiver can detect signals for which the signal-to-mutual-interference power ratio is more positive than -60 db. Using Chebychev's and Markov's inequalities,

the following will be determined:

1. Whether it is likely that the signal-to-mutual-interference power ratio at a receiver operating at maximum range from a transmitter in the net (r_{2max} = 15 miles) will exceed the -60 db level.

2. The range r_2 between transmitter and receiver corresponding to a signal-to-interference power level which is greater than -60 db with a probability of greater than .50.

For the first situation, using (2.15)

$$M = .3612 \left(\frac{A}{\pi r_o^2} - 2 \right) = 3.22 \times 10^4$$

From (2.1),

$$q_1 q_2 = \frac{200}{M} = 6.21 \times 10^{-3}$$

$$\frac{r_{2max}}{r_o} = \frac{(15)(5280)}{100} = 793$$

From Fig. 2.3,

$$P_s/E(P_i)\Big|_{\substack{min \\ db}} = -96 \text{ db}$$

From Fig. 2.4,

$$\sigma(P_i)/E(P_i)\Big|_{db} \cong 7 \text{ db}$$

From (2.29),

$$\lambda = 10^{-10.3} = 5 \times 10^{-11}$$

Using Chebychev's inequality, (2.32), with $x = 10^{-6}$,

$$\frac{x^2}{\lambda^2 \left[1 - \frac{x}{\lambda} \frac{E(P_i)}{\sigma(P_i)}\right]^2}$$

is greater than one, and therefore $P\left(\frac{P_s}{P_i} > x\right) \geq 0$. Using Markov's inequality, (2.34),

$$x \frac{E(P_i)}{P_s}$$

is greater than one, and therefore again, $P\left(\frac{P_s}{P_i} > x\right) \geq 0$. These results indicate that either the inequalities are too weak to provide useful information in this case, or that the signal-to-mutual-interference power ratio is seldom more positive than -60 db. For the second situation, again,

$$M = 3.22 \times 10^4$$

$$q_1 q_2 = 6.21 \times 10^{-3}$$

$$\left.\frac{\sigma(P_i)}{E(P_i)}\right|_{db} \cong 7 \text{ db} .$$

Using Chebychev's inequality in the form of (2.32), it is required that

$$1 - \frac{x^2}{\lambda^2 \left[1 - \frac{x}{\lambda} \frac{E(P_i)}{\sigma(P_i)}\right]^2} = .50$$

or that

$$\frac{x^2}{\lambda^2 \left[1 - \frac{x}{\lambda} \frac{E(P_i)}{\sigma(P_i)}\right]^2} = .50$$

Rearranging, and substituting $\sigma(P_i)/E(P_i)$ and the value of x,

$$\lambda = 1.61 \times 10^{-6}$$

Substituting λ, and, $\sigma(P_i)/E(P_i)$ into (2.29) and rearranging

$$\frac{P_s}{E(P_i)} = (1.61)(10^{-6})(5) = 8.05 \times 10^{-6} = -50.94 \text{ db}$$

From Fig. 2.3

$$r_2/r_o = 60$$

hence $r_2 \cong 6000$ feet. Therefore, using Chebychev's inequality when $r_2 = 6000$ feet, P_s/P_i exceeds -60 db at least 50 percent of the time.

Using Markov's inequality in the form of (2.34), it is required that

$$P\left(\frac{P_s}{P_i} > 10^{-6}\right) > 1 - 10^{-6}\,\frac{E(P_i)}{P_s} = .50$$

Thus,

$$\frac{P_s}{E(P_i)} = 2 \times 10^{-6} = -57 \text{ db} .$$

From Fig. 2.3

$$r_2/r_o = 80$$

$$r_2 = (80)(100) = 8000 \text{ feet} .$$

Therefore, using Markov's inequality with $r_2 = 8000$ feet, P_s/P_i exceeds -60 db at least 50 percent of the time. It is seen that in this case, Markov's inequality is stronger than Chebychev's. The results of Section 2.3.6 can, of course, be used to extend the applicability of this result.

CHAPTER III

ANALYSIS OF A RADA SYSTEM MODEL

3.1 Introduction

In Chapter I, the principles of RADA systems were described, and in particular, a "basic RADA system" was characterized in Section 1.6. The terms and definitions of Section 1.6 constitute the background for this chapter. A lower bound of the probability of a "useful signal" at the input terminals of a target receiver within a RADA net was determined analytically in Chapter II, as a function of the net parameters. In this chapter, a model of a RADA system is presented and analyzed. It is assumed that in modeling the system, at the input terminals of the target receiver, an RF pulse from one transmitter is never canceled by an RF pulse from another. It is further assumed that the individual detected and delayed RF pulses, the AND gate video input pulses, are all rectangular pulses of equal amplitude and of the same duration Δ_t as a transmitted pulse; except when the overlapping of several video pulses on a particular frequency results in a composite rectangular video pulse of duration longer than Δ_t. These assumptions are explained in greater detail, and additional ones are presented in Section 3.2.

In the process of evaluating the performance of a target RADA

receiver, consider the case where both message frames and mutual interference constitute the receiver input. Because of the AND operation, and because pulse cancellation does not occur, the receiver AND gate output voltage at any instant is the logical union of the voltage which would be produced by the signal alone and that which would be produced by the mutual interference alone. That is, the receiver AND gate output voltage waveform is the binary waveform obtained by superimposing the error process on the message process. It is, therefore, convenient to use a two-step procedure in evaluating RADA system performance. First the statistics of the error process are determined theoretically (Section 3.3). Then, assuming a useful signal is present at the target receiver input terminals, measures of system performance are evaluated by considering the interaction of the error process with the message process (Section 3.4). These measures apply to systems which use pulse position modulation and clocked binary modulation, respectively, and to systems which employ ungated and gated receivers, respectively. Performance measures are also developed which apply to systems using clocked binary modulation and a "sampling" receiver.

The basic concern of this dissertation is with voice communications systems. At best, the measures which result from analysis are error rates and information rates for samples of received information. "Quality" and "intelligibility ", which are preferable measures

for voice, can be related to the error rates and information rates by listening tests. The work of this dissertation is restricted to the determination of error rates, information rates, and similar analytically determined measures; no subjective tests have been performed. For purposes of discussion, it is considered that a maximum error rate of about .1 error pulse per frame causes the maximum permissible distortion for a system which codes each sample into pulse position or frequency (assuming the sampling rate equals the Nyquist rate--about 8000 samples per second for voice). For an integrating system, such as delta modulation, it is considered that the maximum permissible distortion occurs at a higher error rate--perhaps .2-.3 error pulses per frame. These values will be used in numerical calculations in Chapter IV which require specification of maximum permissible error rates. Data relating error rates of a pulse modulated waveform to the quality and intelligibility of the demodulated waveform, have recently become available (Refs. 14, 17, 1.16,and 1.23).

A more detailed summary of the content of the remainder of this chapter is presented now. In particular, a description of the useful results is stressed. In Section 3.2, the model of a RADA system is presented, and the differences between the modeled system and an actual system are discussed. The statistics of the error process are determined theoretically in Section 3.3; the following results are included. The duty factor, P_m, of the error process is determined in

Section 3.3.1, and is plotted in Fig. 3.1 as a function of the "mutual interference parameter," $\gamma\Delta_t$, with $\lambda_f\lambda_t$ as a parameter. The quantity $\gamma\Delta_t$ is the average number of detected mutual interference pulses which occur at each AND gate input in a time interval Δ_t corresponding to the duration of a transmitted pulse; the quantity $\lambda_f\lambda_t$ equals the number of receiver AND gate input connections from the delay devices. Physically, the duty factor P_m of the error process is the fraction of the time that the AND gate output produces an error pulse (or, equivalently, is in the "one" state) when only mutual interference is present at the receiver input terminals. The quantity P_m increases monotonically with $\gamma\Delta_t$, and with fixed system parameters (λ_f, λ_t, Δ_t, Λ_f, $\bar{T}$); $\gamma\Delta_t$ increases linearly with the number of interfering transmitters, m; it follows that, as would be expected, the duty factor of the error process increases as the number of interfering transmitters increases.

Although it is an important statistic of the error process, P_m is an incomplete statistic; it determines what fraction of the time error pulses are present, but gives no idea of the duration of these pulses. The probability distribution function H(t) of the duration, t, of an error pulse is determined in Section 3.3.2. The normalized distribution is specified by (3.29), (3.33), and (3.39), and is plotted in Fig. 3.5a through Fig. 3.5i as a function of the normalized argument t/Δ_t. In each figure, $\gamma\Delta_t$ is a parameter; different figures (figures having a different alphabetic index in the set a through i) correspond to systems

having a differing number $\lambda_f\lambda_t$ of receiver AND gate inputs. The distributions follow trends which would be expected intuitively. In a given figure (for a given value of $\lambda_f\lambda_t$), the error pulse duration tends to increase as the mutual interference parameter $\gamma\Delta_t$ increases. This tendency results because, with a higher mutual interference pulse rate at the AND gate input, more interference pulses are available to sustain the duration of an error pulse. A trend of the distribution of the duration of an error pulse is that as the number $\lambda_f\lambda_t$ of AND gate inputs increases, with other parameters remaining constant, the duration of the error pulses tends to decrease. This effect would also be expected intuitively since, given an error pulse, this pulse terminates as soon as one of the AND gate input pulses terminates. The probability that at least one AND gate input pulse terminates before any specified time increases as the number of AND gate inputs, and hence input pulses, increases. The distributions of Fig. 3.5a through Fig. 3.5i have a discontinuity at $t = \Delta_t$ which can be explained as follows. A discontinuity in the distribution function corresponds to an impulse in the probability density function, which in turn implies that there is a finite probability that the error pulse will end at time $t = \Delta_t$. To complete the explanation, it must be shown why there is a finite probability that the error pulse will terminate at time $t = \Delta_t$. An error pulse starts at time zero, if mutual interference pulses are present at all but one of the AND gate inputs at time 0_-, and if a mutual

interference pulse (the "turn-on pulse") occurs at the remaining input at time zero. The error pulse ends when any one of the interference pulses (including the turn-on pulse) terminates. There is a finite probability that all pulses except the turn-on pulse are extended past Δ_t by overlapping interference pulses and that the turn-on pulse terminates at time Δ_t. This finite probability accounts for the discontinuity in the distributions of the error pulse duration. It is noted that for a given value of $\lambda_f\lambda_t$, the amplitude of the discontinuity decreases as $\gamma\Delta_t$ increases. This trend occurs because the probability that another pulse overlaps the turn-on pulse increases as $\gamma\Delta_t$ increases, which decreases the probability that the turn-on pulse terminates at time Δ_t, which in turn reduces the amplitude of the discontinuity in the distribution H(t). The mean value, $\bar{t}$, of the duration of an error pulse is expressed in terms of H(t) in (3.41) of Section 3.3.2. Two approximations, $\tilde{t}$ and $\tilde{\tilde{t}}$, for $\bar{t}$ are presented in (3.43) and (3.52) of Section 3.3.3.

The average error pulse rate is an important statistic of the error process. This average rate, $\bar{N}$, is shown in (3.55) of Section 3.3.4 to equal to quotient of P_m and $\bar{t}$. A normalized plot of $\bar{N}\,\Delta_t$, the average number of error pulses which occur in a time duration Δ_t, is presented in Fig. 3.6 as a function of $\gamma\Delta_t$, with $\lambda_f\lambda_t$ as a parameter. For a fixed value of $\lambda_f\lambda_t$, and for increasing $\gamma\Delta_t$, the error rate at first increases, reflecting the tendency of an increased interference

pulse rate to increase the error rate. With further increases of $\gamma\Delta_t$, the error rate levels off, then decreases. Values of $\gamma\Delta_t$ in the region to the right of the peak appear to be of little practical interest. In this region, the error pulses tend to become longer and fewer in number, until in the limit, $\gamma\Delta_t \to \infty$, and there is a single error pulse of infinite duration, corresponding to an error rate of zero, and no reception is possible. Another point of view is that the region to the left of the peak is the region where P_m increases more rapidly with $\gamma\Delta_t$ than does $\bar{t}$. However, as $\gamma\Delta_t$ increases, P_m is bounded above by unity and $\bar{t}$ is bounded above by infinity. It follows that for some value of $\gamma\Delta_t$, the quotient, $\bar{N}$, of P_m and $\bar{t}$ will first level off, then decrease. Typically the system parameters will always be chosen so that with the mutual interference levels anticipated, P_m will be less than 0.1, and the receiver operation will be to the left of the peak of the appropriate curve of $\bar{N}\Delta_t$ vs. $\gamma\Delta_t$.

Finally, using the previously determined error process statistics, P_m, $\bar{t}$, and $\bar{N}$, two additional statistics, $P_m(\tau)$ and $P_e(\tau)$ are investigated in Section 3.3.5 and Section 3.3.6, respectively. The quantity $P_m(\tau)$ is the probability that an error pulse starts in a time interval τ. An approximation $\tilde{P}_m(\tau)$ for $P_m(\tau)$ is given by (3.58) and (3.60). The quantity $P_e(\tau)$, which is determined by using $P_m(\tau)$, is the probability that an error pulse, or part of an error pulse, is contained in the interval τ. This probability is a crucial one in

evaluating the performance of RADA systems which use gated receivers. An approximation $\tilde{P}_e(\tau_e)$ and a lower bound $\tilde{\tilde{P}}_e(\tau_e)$ for $P_e(\tau_e)$ are given by (3.62) and (3.65). This completes the discussion of the investigation of the statistics of the error pulse process.

Measures of system performance are presented in Section 3.4. The measures which are reasonable in a particular case depend upon both the modulation process and the receiver type which are being considered. For ungated receivers using either pulse position modulation or clocked binary modulation, the duty factor P_m and the error rate $\bar{N}$ are suitable measures of system performance. That is, it is expected that the intelligibility and quality of signals observed in listening tests are correlated with the duty factor, and even more highly correlated with the error pulse rate $\bar{N}$. When gated receivers are considered, the gate is assumed to be synchronized with the message pulses. The measure of performance of a system using pulse position modulation and a gated receiver is taken as the probability that at least one error pulse precedes the message pulse in a gate interval (Section 3.4.3). The occurrence of an error pulse within the gate and prior to the message pulse is defined as a type one false alarm, and the corresponding probability is denoted by P_{1FA}. The measure of performance of systems which use clocked binary modulation and a gated receiver is the probability that at least one error pulse occurs in a gate interval in which there is no message pulse (Section 3.4.4). This event is

called a type two false alarm, and its probability is designated by P_{2FA}. Analogously, the measure of the performance of systems using clocked binary modulation and a sampling receiver is the probability that an error sample occurs at a sampling time when there is no message sample (Section 3.4.5). The corresponding event is called a sample false alarm, and its probability is denoted by P_{SFA}. In addition to these measures, the information transmission rate is determined for systems which use clocked binary modulation, and either a gated or a sampling receiver (Section 3.4.6).

3.2 Model of a RADA System

In this section, a model of a RADA system is presented which embodies the essential features of the system, and which allows tractable analytical results. The model, and the error process statistics P_m, $H(t)$, and $\bar{N}$ obtained by analyzing it are essentially the same as those of Ref. 16, although the results herein were obtained independently using slightly different mathematical techniques prior to publication of the reference. The definition of a "basic RADA system" which was given in Section 1.6 is a required background for this section. The model of a RADA system will be obtained by making the following assumptions. First, only direct transmissions from RADA transmitters which are addressing other RADA receivers cause mutual interference at the target receiver. Second, at the target receiver input terminals, the mutual interference from a given transmitter causes

spurious receiver input pulses; it does not cause cancellation of the message pulses, or of the spurious pulses from any other interfering transmitter. Third, all received RF pulses produce (rectangular) video AND gate input pulses of equal amplitude and of duration Δ_t seconds. The overlapping of several video pulses results in a composite pulse which has the same amplitude as the video pulse, and which is of longer duration than Δ_t seconds. Fourth, defining the epoch of a pulse as the leading edge of the pulse, it is assumed that the time of occurrence of the epochs of the mutual interference pulses at the different AND gate inputs are independent Poisson processes. Fifth, when gated receivers are considered, it is assumed that the target receiver is synchronized with its given transmitter.

The assumption that the primary source of degradation of receiver performance results from direct mutual interference neglects the effects of multipath and residual interference as discussed in Section 1.4.5. This assumption, therefore, tends to produce a model which gives an upper bound of system performance.

The extreme variations in the level of received RADA signals was pointed out in Section 1.4.5. Because of this variation, there is only a small probability that the timing, phase, and amplitude relationships of a group of received RF pulses will result in sufficient cancellation among pulses so that some of them will not be detected. Although the probability of pulse cancellation is small, degradation of

receiver performance will occur in those cases in which a message pulse is cancelled. For this reason, results obtained which neglect pulse cancellation tend to give an upper bound of RADA system performance.

In Section 1.4.5, it was shown that the widths of the RF pulses, and therefore of the video AND gate input pulses, vary with the nearer transmitters tending to produce wider pulses. The wider video pulses tend to be more effective in producing error pulses than the pulses having the nominal system pulse width, Δ_t. The assumption of rectangular video pulses of width Δ_t equal to the nominal RADA system transmitted pulse width tends to give analytical results which are an upper bound of RADA system performance.

For systems in which only a single pulse is transmitted on each frequency of a frame ($\lambda_t = 1$), the assumption that the pulse epoch process on each channel is a Poisson process is a valid assumption. For systems with $\lambda_t > 1$ which transmit more than one pulse on each frequency in a frame, the pulse process on each frequency channel is no longer strictly Poisson. For systems using $\lambda_f > 1$, the pulse epoch process on each frequency channel is not strictly independent of the pulse epoch process on each other frequency channel. The assumed condition of independent Poisson processes on each frequency channel is approached as the number of system users, m, is increased.

Since a receiver which is maintained in synchronization will always open the post gate, or sample, at the correct time instant, receiver performance calculations predicted on a synchronized post gate provide an upper bound of RADA system performance.

In summary, performance measures calculated for the modeled system tend to be an upper bound of the actual receiver performance (e.g., the modeled system has a smaller duty factor P_m, and a smaller error rate $\bar{N}$ than an actual system).

3.3 Mutual Interference Statistics of the Basic RADA Receiver Output

In this section, theoretical expressions are obtained for the statistics of the error process at the RADA receiver AND gate output. In deriving these statistics, it is assumed that the probability of a pulse epoch at a particular AND gate input in an incremental time interval dt equals γdt. This probability is assumed to be independent of the epochs of the pulses at the other $(\lambda_f \lambda_t - 1)$ AND gate inputs.

In Section 3.3.1, a duty factor P_m of the RADA receiver AND gate output is determined. In Section 3.3.2 the probability distribution function H(t) of the duration of a RADA receiver AND gate output error pulse is determined. An expression is also determined for the mean duration $\bar{t}$ of an error pulse in terms of the distribution function H(t). Approximations $\tilde{t}$ and $\tilde{\tilde{t}}$ for $\bar{t}$ are determined in Section 3.3.3. The quantities $\bar{t}$ and P_m are used to determine $\bar{N}$, which is the average

number of error pulses per second at the RADA receiver AND gate output in Section 3.3.4. An approximate expression $\tilde{P}_e(\tau)$, and a lower bound $\tilde{\tilde{P}}_e(\tau)$ are determined for $P_e(\tau)$, which is the probability that there is at least one receiver AND gate output error pulse in time τ, in Section 3.3.6.

Using the results of Sections 3.3.1 - 3.3.6, various measures of RADA system performance are specified in Section 3.4. For RADA systems using PPM or clocked binary modulation, and an ungated receiver, the duty factor P_m and the average number $\bar{N}$ of receiver AND gate output error pulses are used as measures of system performance. Probability of a false alarm is used as a measure of performance of RADA systems using gated and sampling receivers, respectively. Information transmission rate is used as a measure of performance of RADA systems using clocked binary modulation and a gated or sampling receiver.

3.3.1 Receiver AND Gate Output Error Pulse Duty Factor. When no message pulses are received, P_m is the duty factor of the error pulse process at the RADA receiver AND gate output. The quantity P_m equals the fraction of the time that an error pulse is present at the AND gate output. Equivalently, P_m is the fraction of the time that the AND gate output is a binary ONE, when mutual interference is the only receiver input. The probability that a ONE occurs at a particular AND gate input at a time t_o equals the probability that at least

one input pulse epoch occurs in the interval $[t_o - \Delta_t, t_o]$. The probability of this occurrence is $\left(1 - e^{-\gamma\Delta_t}\right)$. The probability of a ONE at all $\lambda_f\lambda_t$ AND gate inputs at time t_o is, therefore, given by (3.1).

$$P_m = \left(1 - e^{-\gamma\Delta_t}\right)^{\lambda_f\lambda_t} \qquad (3.1)$$

The quantity P_m is plotted in Fig. 3.1 as a function of γ and the parameter $\lambda_f\lambda_t$.

3.3.2 Relating to the Distribution of the Duration of an Error Pulse. In this section, the characteristic function of the duration of the pulses at each AND gate input will be determined. The characteristic function will be used to obtain the probability density function and the probability distribution function of the duration of pulses at the AND gate input. This distribution function, and a closely related distribution function will then be used to determine the distribution function of the duration of error pulses. The mean error pulse duration will then be determined.

The method by which pulses are generated at the output of each delay line tap by overlapping is shown in Fig. 3.2. Pulses of width Δ_t overlap to produce wider "composite" pulses as shown. A composite pulse of n pulses is referred to as an n-pulse. For an n-pulse to occur, given the first pulse (i.e., given there is a composite pulse), n-1 successive pulses must overlap, and the following pulse

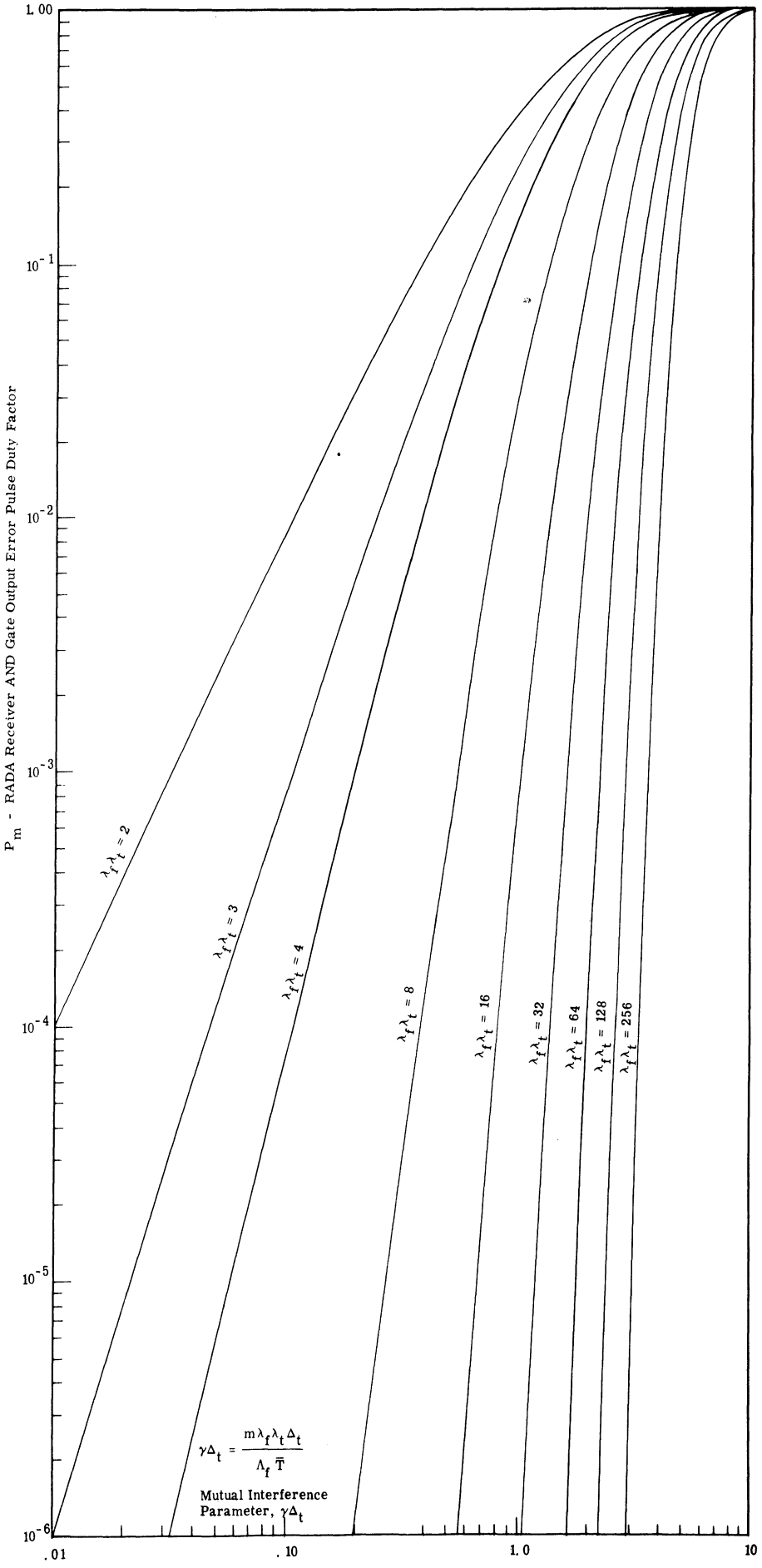

Fig. 3.1. RADA receiver AND gate output error pulse duty factor P_m vs. mutual interference parameter, $\gamma\Delta_t$.

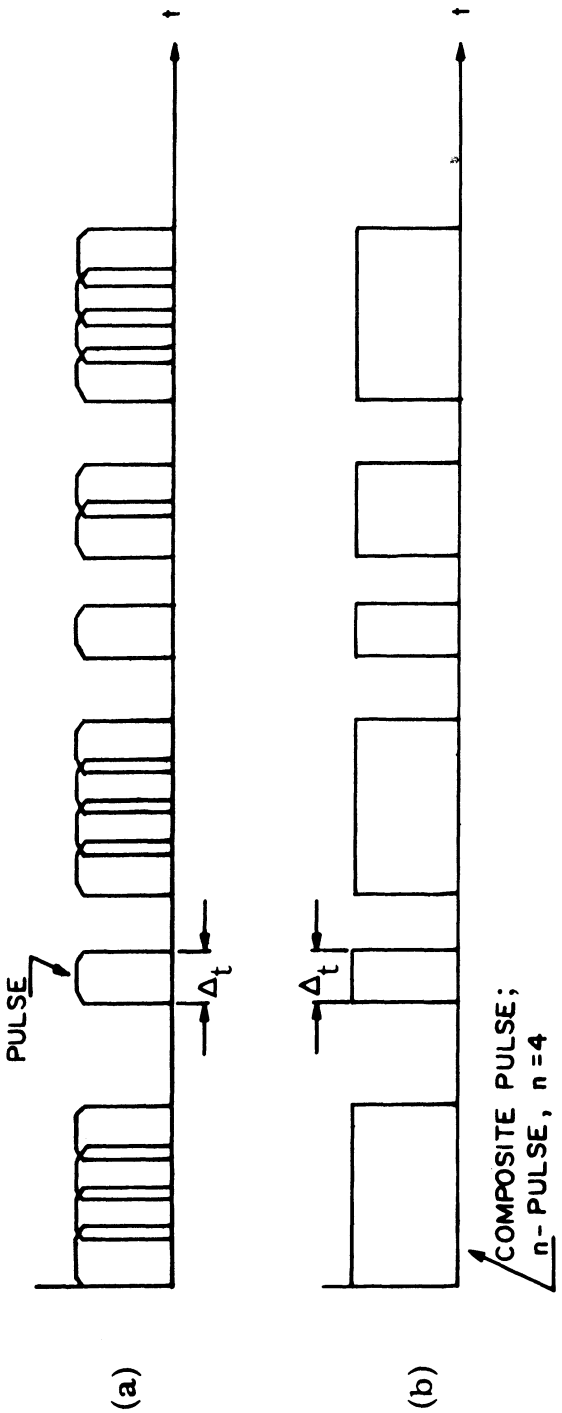

(a) Pulse overlapping at each AND gate input.

(b) Composite pulses resulting from pulse overlapping in (a).

Fig. 3.2. Illustration of the formation of composite pulses.

must not overlap. A number of probability functions will be defined now and will be used to determine the probability distribution function of the duration of a composite pulse. In much of the development which follows, it will be convenient to make use of characteristic functions. The characteristic function $Ch_t(\xi)$ of a random variable t having a probability density function p(t) is given by (3.2).

$$Ch_t(\xi) = \int_{-\infty}^{\infty} p(t)\, e^{i\xi t}\, dt \tag{3.2}$$

Conversely, when the characteristic function $Ch_t(\xi)$ is known, the probability density function p(t) of the random variable t is given by

$$p(t) = \frac{1}{2\pi} \int_{-\infty}^{\infty} Ch_t(\xi)\, e^{-i\xi t}\, d\xi \tag{3.3}$$

Let t_1 be defined as the time between epochs of successive pulses of a composite pulse, as shown in Fig. 3.3a. The probability density function $p_1(t_1)$ of t_1 is given by the truncated exponential function in (3.4).

$$\begin{aligned} p_1(t_1) &= \frac{\gamma\, e^{-\gamma t_1}}{1 - e^{-\gamma \Delta_t}} \quad ; \quad 0 \leq t_1 \leq \Delta_t \\ p_1(t_1) &= 0 \quad ; \quad t_1 < 0 \\ & \qquad\quad t_1 > \Delta_t \end{aligned} \tag{3.4}$$

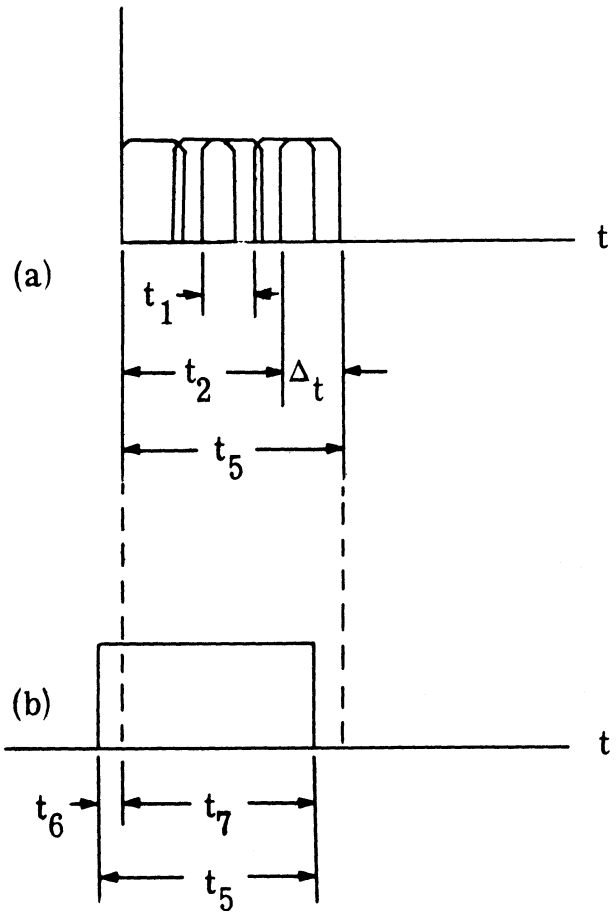

(a) Relationship between t_1, t_2, t_5 and Δ_t.

(b) Relationship between t_5, t_6 and t_7.

Fig. 3.3. Illustration of the time relationships within a composite pulse.

The characteristic function of t_1 is given by (3.5).

$$Ch_{t_1}(\xi) = \frac{\gamma}{1-e^{-\gamma\Delta_t}} \int_0^{\Delta_t} e^{(i\xi-\gamma)t_1}\, dt_1 = \frac{\gamma}{1-e^{-\gamma\Delta_t}} \left[\frac{e^{(i\xi-\gamma)\Delta_t}-1}{i\xi-\gamma}\right] \tag{3.5}$$

Given an n pulse, the time t_2 from the epoch of the first pulse to the epoch of the last pulse of the n-pulse is the sum of the (n-1) independent time intervals t_1 between epochs of successive pulses as shown in Fig. 3.3a. Therefore, the characteristic function $Ch_{t_2|n}(\xi)$ of the time t_2, given an n-pulse is the (n-1) fold product of the characteristic function of t_1, as given in (3.6).

$$Ch_{t_2|n}(\xi) = \left[Ch_{t_1}(\xi)\right]^{n-1} \tag{3.6}$$

Substituting (3.5) into (3.6) yields (3.7).

$$Ch_{t_2|n}(\xi) = \left(\frac{\gamma}{1-e^{-\gamma\Delta_t}}\right)^{n-1} \left[\frac{e^{(i\xi-\gamma)\Delta_t}-1}{i\xi-\gamma}\right]^{n-1} \tag{3.7}$$

It follows from (3.3) that the conditional probability density $p_2(t_2|n)$ of the time t_2, given an n-pulse, is given by (3.8).

$$p_2(t_2|n) = \frac{1}{2\pi} \int_{-\infty}^{\infty} Ch_{t_2|n}(\xi)\, e^{-i\xi t_2}\, d\xi \tag{3.8}$$

Let $P_3(n)$ be the conditional probability of an n-pulse, given that there is a composite pulse. The probability density function $p_2(t_2)$ of the time t_2 between the epochs of the first and last pulses of an n-pulse is obtained by averaging $p_2(t_2 \mid n)$ over n as in (3.9).

$$p_2(t_2) = \sum_{n=1}^{\infty} P_3(n)\, p_2(t_2 \mid n) \tag{3.9}$$

The characteristic function of t_2 is obtained by substituting (3.9) into (3.3), and is given by (3.10).

$$Ch_{t_2}(\xi) = \sum_{n=1}^{\infty} P_3(n)\, Ch_{t_2 \mid n}(\xi) \tag{3.10}$$

To determine $Ch_{t_2}(\xi)$, it is only necessary to determine $P_3(n)$, since $Ch_{t_2 \mid n}(\xi)$ has already been determined in (3.7). For an n-pulse to occur, given the first pulse, each of (n-1) successive pulses must overlap the previous pulse, and the nth pulse must not overlap the (n-1)st pulse. The probability of a pulse overlapping the previous pulse equals the probability of a new pulse epoch within Δ_t seconds after the previous pulse epoch. This probability, P_4, is given in (3.11).

$$P_4 = \int_0^{\Delta_t} \gamma\, e^{-\gamma \Delta_t}\, dt = \left(1 - e^{-\gamma \Delta_t}\right) \tag{3.11}$$

The probability $P_3(n)$ is the probability that (n-1) pulses start before the preceding pulses end, and that no pulse starts before the (n-1)th

pulse ends.

$$P_3(n) = P_4^{n-1} e^{-\gamma\Delta_t} \tag{3.12}$$

Substituting (3.11) into (3.12) yields (3.13).

$$P_3(n) = \left(1 - e^{-\gamma\Delta_t}\right)^{n-1} e^{-\gamma\Delta_t} \tag{3.13}$$

Now, substituting (3.7) and (3.13) into (3.10), we obtain $Ch_{t_2}(\xi)$ in (3.14).

$$Ch_{t_2}(\xi) = \sum_{n=1}^{\infty} e^{-\gamma\Delta_t}\left(1 - e^{-\gamma\Delta_t}\right)^{n-1}\left(\frac{\gamma}{1 - e^{-\gamma\Delta_t}}\right)^{n-1}\left[\frac{e^{(i\xi-\gamma)\Delta_t} - 1}{i\xi - \gamma}\right]^{n-1}$$

$$= e^{-\gamma\Delta_t} \sum_{n=1}^{\infty} \left\{\frac{\gamma}{i\xi - \gamma}\left[e^{(i\xi-\gamma)\Delta_t} - 1\right]\right\}^{n-1}$$

$$= e^{-\gamma\Delta_t} \sum_{n=0}^{\infty} \left\{\frac{\gamma}{i\xi - \gamma}\left[e^{(i\xi-\gamma)\Delta_t} - 1\right]\right\}^{n} \tag{3.14}$$

$$= \frac{e^{-\gamma\Delta_t}}{1 - \frac{\gamma}{i\xi-\gamma}\left[e^{(i\xi-\gamma)\Delta_t} - 1\right]}$$

$$= \frac{(i\xi - \gamma)\, e^{-\gamma\Delta_t}}{i\xi - \gamma\, e^{(i\xi-\gamma)\Delta_t}}$$

In Fig. 3.3a, it is seen that the total duration, t_5, of a composite pulse is given by (3.15).

$$t_5 = t_2 + \Delta_t \tag{3.15}$$

The characteristic function of t_5 is thus given by (3.16),

$$Ch_{t_5}(\xi) = e^{i\xi\Delta_t} Ch_{t_2}(\xi) = \frac{e^{(i\xi-\gamma)\Delta_t}(i\xi-\gamma)}{(i\xi-\gamma)\Delta_t} \tag{3.16}$$

and from (3.4), the density function of the duration t_5 of a composite pulse is given by (3.17).

$$p_5(t_5) = \frac{1}{2\pi} \int_{-\infty}^{\infty} Ch_{t_5}(\xi)\, e^{-i\xi t}\, d\xi \tag{3.17}$$

A closed form expression for $p_5(t_5)$ does not exist. The density $p_5(t_5)$ must be represented as a series of singularity functions.

In review, composite pulses are generated randomly by the overlapping of pulses at each AND gate input. An AND gate output voltage results whenever there is a composite pulse at all $\lambda_f\lambda_t$ AND gate inputs.

Information about the distribution of the AND gate error pulse duration will now be found. Consider that there is an AND gate output error pulse epoch. The error pulse epoch occurs when there are composite pulses at $(\lambda_f\lambda_t - 1)$ AND gate inputs and a composite pulse (the "turn-on pulse") epoch occurs at the $(\lambda_f\lambda_t)$th AND gate input.

The AND gate output ceases when any one of the $\lambda_f\lambda_t$ composite pulses turns off.

The probability density of the duration of the turn-on pulse is known. It is just the density $p_5(t_5)$ of the duration of a composite pulse. The turn-on pulse epoch occurs at $t=0$, and defines the reference time origin. As shown in Fig. 3.3b, for each of the $(\lambda_f\lambda_t - 1)$ composite pulses, let t_6 denote the time to the (negative) epoch of the first pulse in the composite pulse which occurs in the time interval $-\Delta_t \leq t_6 \leq 0$. Given that there is a composite pulse, the density function $p_6(t_6)$ is a truncated exponential density function with time origin at $-\Delta_t$.

$$p_6(t_6) = \begin{cases} \dfrac{\gamma\, e^{-\gamma(t_6+\Delta_t)}}{1-e^{-\gamma\Delta_t}} & ; \quad -\Delta_t \leq t_6 \leq 0 \\ 0 & ; \quad t < -\Delta_t \\ & \quad t > 0 \end{cases} \tag{3.18}$$

The characteristic function of $p_6(t_6)$ is,

$$Ch_{t_6}(\xi) = \frac{\gamma}{1-e^{-\gamma\Delta_t}} \frac{1}{i\xi - \gamma} \left\{ e^{-\gamma\Delta_t} - e^{-i\xi\Delta_t} \right\} \tag{3.19}$$

From Fig. 3.3b, it is seen that the time t_7 to the end of each of the $\lambda_f\lambda_t - 1$ pulses is given by (3.20).

$$t_7 = t_5 + t_6 \tag{3.20}$$

The probability density function $p_7(t_7)$ of the duration t_7 of each of the $(\lambda_f \lambda_t - 1)$ pulses is the convolution of the density functions $p_5(t_5)$ and $p_6(t_6)$. In terms of characteristic functions,

$$Ch_{t_7}(\xi) = Ch_{t_5}(\xi)\, Ch_{t_6}(\xi) \tag{3.21}$$

From (3.16), (3.19), and (3.21)

$$Ch_{t_7}(\xi) = \frac{\gamma}{e^{\gamma \Delta_t} - 1} \; \frac{\left[e^{(i\xi - \gamma)\Delta_t} - 1\right]}{(i\xi - \gamma)\, e^{(i\xi - \gamma)\Delta_t}} \tag{3.22}$$

The probability density functions of $p_5(t_5)$ and $p_7(t_7)$ can be determined by inverting the transforms $Ch_{t_5}(\xi)$, $Ch_{t_7}(\xi)$. To put the transforms in a more familiar form, the characteristic function will be changed to a one sided Laplace transform [both density functions $p_5(t_5)$, $p_7(t_7)$ are zero for negative time] by making the change of variable

$$s = -i\xi \tag{3.23}$$

Substituting (3.23) into (3.16) there results,

$$Ch_{t_5}(s) = \frac{(s+\gamma)\, e^{-(s+\gamma)\Delta_t}}{s+\gamma\, e^{-(s+\gamma)\Delta_t}}$$

$$= (1+\frac{\gamma}{s})\, e^{-(\gamma+s)\Delta_t}\, \frac{1}{1+\left(\gamma\, e^{-\gamma\Delta_t}\right)\frac{e^{-s\Delta_t}}{s}} \qquad (3.24)$$

$$= e^{-(\gamma+s)\Delta_t} \sum_{n=0}^{\infty} (-\gamma)^n\, e^{-\gamma n\Delta_t}\, (1+\frac{\gamma}{s})\, \frac{e^{-sn\Delta_t}}{s^n}$$

$$= \sum_{n=0}^{\infty} (-\gamma)^n\, e^{-\gamma(n+1)\Delta_t} \left(\frac{e^{-s(n+1)\Delta_t}}{s^n} + \frac{\gamma\, e^{-s(n+1)\Delta_t}}{s^{n+1}} \right)$$

Substituting (3.23) into (3.22),

$$Ch_{t_7}(s) = \frac{\gamma}{e^{\gamma\Delta_t}-1}\, \frac{\left[1-e^{-(s+\gamma)\Delta_t}\right]}{s+\gamma\, e^{-(s+\gamma)\Delta_t}}$$

$$= \frac{\gamma}{e^{\gamma\Delta_t}-1}\, \frac{1-e^{-(s+\gamma)\Delta_t}}{s\left[1+\gamma\, e^{-\gamma\Delta_t}\, \frac{e^{-s\Delta_t}}{s}\right]} \qquad (3.25)$$

$$= \frac{\gamma}{e^{\gamma\Delta_t}-1} \sum_{n=0}^{\infty} (-\gamma)^n\, e^{-\gamma n\Delta_t} \left[1-e^{-(s+\gamma)\Delta_t}\right] \frac{e^{-sn\Delta_t}}{s^n}$$

Denoting an impulse function, and a unit step function at the origin by $\delta(t)$, $u(t)$, respectively, and taking the inverse transform of $Ch_{t_5}(s)$, there results,

$$p_5(t_5) = 0 ; \qquad t_5 < 0$$

$$p_5(t_5) = e^{-\gamma\Delta_t}\left[\delta(t_5 - \Delta_t) + \gamma\, u(t_5 - \Delta_t)\right] + \gamma \sum_{n=1}^{\infty} (-1)^n e^{-\gamma(n+1)\Delta_t}$$

$$\left\{\frac{\left\{\gamma\left[t_5 - (n+1)\Delta_t\right]\right\}^{n-1}}{(n-1)!} + \frac{\left\{\gamma\left[t_5 - (n+1)\Delta_t\right]\right\}^{n}}{n!}\right\} \qquad (3.26)$$

$$u\left[t_5 - (n+1)\Delta_t\right] ; \qquad t_5 \geq 0 .$$

The distribution function $P_5(t_5)$ is determined by

$$P_5(t_5) = \int_0^{t_5} p_5(t)\, dt \qquad (3.27)$$

Substituting (3.26) into (3.27),

$$P_5(t_5) = 0 ; \qquad t_5 < \Delta_t$$

$$P_5(t_5) = \sum_{n=0}^{\infty} (-1)^n e^{-\gamma(n+1)\Delta_t} \left\{\frac{\left\{\gamma\left[t_5 - (n+1)\Delta_t\right]\right\}^{n}}{n!}\right. \qquad (3.28)$$

$$\left. + \frac{\left\{\gamma\left[t_5 - (n+1)\Delta_t\right]\right\}^{n+1}}{(n+1)!}\right\} u\left[t_5 - (n+1)\Delta_t\right] ; \quad t_5 \geq \Delta_t$$

Equation(3.28)can be expressed more compactly by expressing the argument in normalized form and eliminating the unit step function by restricting the range of the sum index. Denoting the "largest integer in x" by $\lfloor x \rfloor$, $P_5(t_5)$ is given by (3.29).

$$P_5(t_5) = 0 ; \qquad t_5 < \Delta_t$$

$$P_5(t_5) = \sum_{n=0}^{\left\lfloor \frac{t_5}{\Delta_t} \right\rfloor - 1} (-\gamma\Delta_t)^n e^{-\gamma(n+1)\Delta_t} \left\{ \frac{\left[\frac{t_5}{\Delta_t} - (n+1) \right]^n}{n!} + \frac{\gamma\Delta_t \left[\frac{t_5}{\Delta_t} - (n+1) \right]^{n+1}}{(n+1)!} \right\} ; \quad t_5 \geq \Delta_t \tag{3.29}$$

Similarly, inverting (3.25),

$$p_7(t_7) = 0 ; \qquad t_7 < 0$$

$$p_7(t_7) = \frac{\gamma e^{-\gamma\Delta_t}}{1 - e^{-\gamma\Delta_t}} + \frac{\gamma e^{-\gamma\Delta_t}}{1 - e^{-\gamma\Delta_t}} \sum_{n=1}^{\infty} (-1)^n e^{-\gamma n\Delta_t} \left\{ \frac{[\gamma(t_7 - n\Delta_t)]^n}{n!} + \frac{[\gamma(t_7 - n\Delta_t)]^{n-1}}{(n-1)!} \right\} u(t_7 - n\Delta_t) ; \quad t_7 \geq 0 \tag{3.30}$$

The distribution function $P_7(t_7)$ is determined by

$$P_7(t_7) = \int_0^{t_7} p_7(t)\, dt \ . \tag{3.31}$$

Substituting (3.30) into (3.31),

$$P_7(t_7) = 0 ; \qquad t_7 < 0$$

$$P_7(t_7) = \frac{\gamma t_7 e^{-\gamma\Delta_t}}{1 - e^{-\gamma\Delta_t}} + \frac{e^{-\gamma\Delta_t}}{1 - e^{-\gamma\Delta_t}} \sum_{n=1}^{\infty} (-1)^n e^{-\gamma n\Delta_t}$$

$$\left\{ \frac{[\gamma(t_7 - n\Delta_t)]^n}{n!} + \frac{[\gamma(t_7 - n\Delta_t)]^{n+1}}{(n+1)!} \right\} u(t_7 - n\Delta_t); \quad t_7 \geq 0 \tag{3.32}$$

Normalizing the argument of (3.32), restricting the range of summation, and rearranging the terms of the sum,

$$P_7(t_7) = 0 ; \qquad t_7 < 0$$

$$P_7(t_7) = \frac{-e^{-\gamma\Delta_t}}{1 - e^{-\gamma\Delta_t}} + \frac{e^{-\gamma\Delta_t}}{1 - e^{-\gamma\Delta_t}} \sum_{n=0}^{\left[\frac{t_7}{\Delta_t}\right]} (-\gamma\Delta_t)^n e^{-\gamma n\Delta_t}$$

$$\left\{ \frac{\left(\frac{t_7}{\Delta_t} - n\right)^n}{n!} + \frac{\gamma\Delta_t\left(\frac{t_7}{\Delta_t} - n\right)^{n+1}}{(n+1)!} \right\} ; \quad t_7 \geq 0 \tag{3.33}$$

Using $P_5(t_5)$ and $P_7(t_7)$, the probability distribution function H(t) of the duration of an error pulse will now be determined. The time reference used is the epoch of the turn-on pulse which corresponds to the error pulse.

Define:

(i) - the event a turn-on pulse occurs at AND gate input i.

t(i) - the event the duration of a pulse at the ith AND gate input is greater than t.

F(a, b, c---) - the joint probability of events a, b, c, --- .

F(a, b, c--- | u, v, w---) - the joint probability of events a, b, c --- given events u, v, w --- .

Then

$$1 - H(t) = \sum_{i=1}^{\lambda_f\lambda_t} F[(i),\ t(1),\ t(2),\ --\ t(i),\ --t(\lambda_f\lambda_t)]$$

$$= \sum_{i=1}^{\lambda_f\lambda_t} F[t(i),(i)]\ F[t(1),t(2),--t(i-1),t(i+1)--t(\lambda_f\lambda_t)\,|\,t(i),(i)]$$

$$= \sum_{i=1}^{\lambda_f\lambda_t} F(i)\quad F[t(i)\,|\,(i)]\ F[t(1),t(2)---t(i-1),t(i+1),--t(\lambda_f\lambda_t)\,|\,t(i),(i)]. \tag{3.34}$$

Since a turn-on pulse is as likely to occur at any AND gate input,

$$F(i) = 1/\lambda_f\lambda_t \tag{3.35}$$

By definition

$$F[t(i)\,|\,(i)] = 1 - P_5(t) \tag{3.36}$$

Since the processes at the AND gate inputs are assumed to be independent processes,

$$F[t(1), t(2)---t(\lambda_f\lambda_t)\,|\,t(i), (i)] = F[t(1), t(2), --t(\lambda_f\lambda_t)]$$

$$= [1 - P_7(t)]^{\lambda_f\lambda_t - 1} \tag{3.37}$$

Substituting (3.35), (3.36), and (3.37) into (3.34)

$$1 - H(t) = \sum_{i=1}^{\lambda_f\lambda_t} \frac{1}{\lambda_f\lambda_t} [1 - P_5(t)]\,[1 - P_7(t)]^{\lambda_f\lambda_t - 1}$$

$$= [1 - P_5(t)]\,[1 - P_7(t)]^{\lambda_f\lambda_t - 1} \tag{3.38}$$

Rearranging,

$$H(t) = 1 - \left\{ [1 - P_5(t)][1 - P_7(t)]^{\lambda_f\lambda_t - 1} \right\} \tag{3.39}$$

The function H(t) is the probability distribution of the duration of error pulses at the RADA receiver AND gate output.

The fractions $P_5(t)$, $P_7(t)$, H(t) are plotted in Fig. 3.4 to illustrate their form and relationship. Parameter values are:

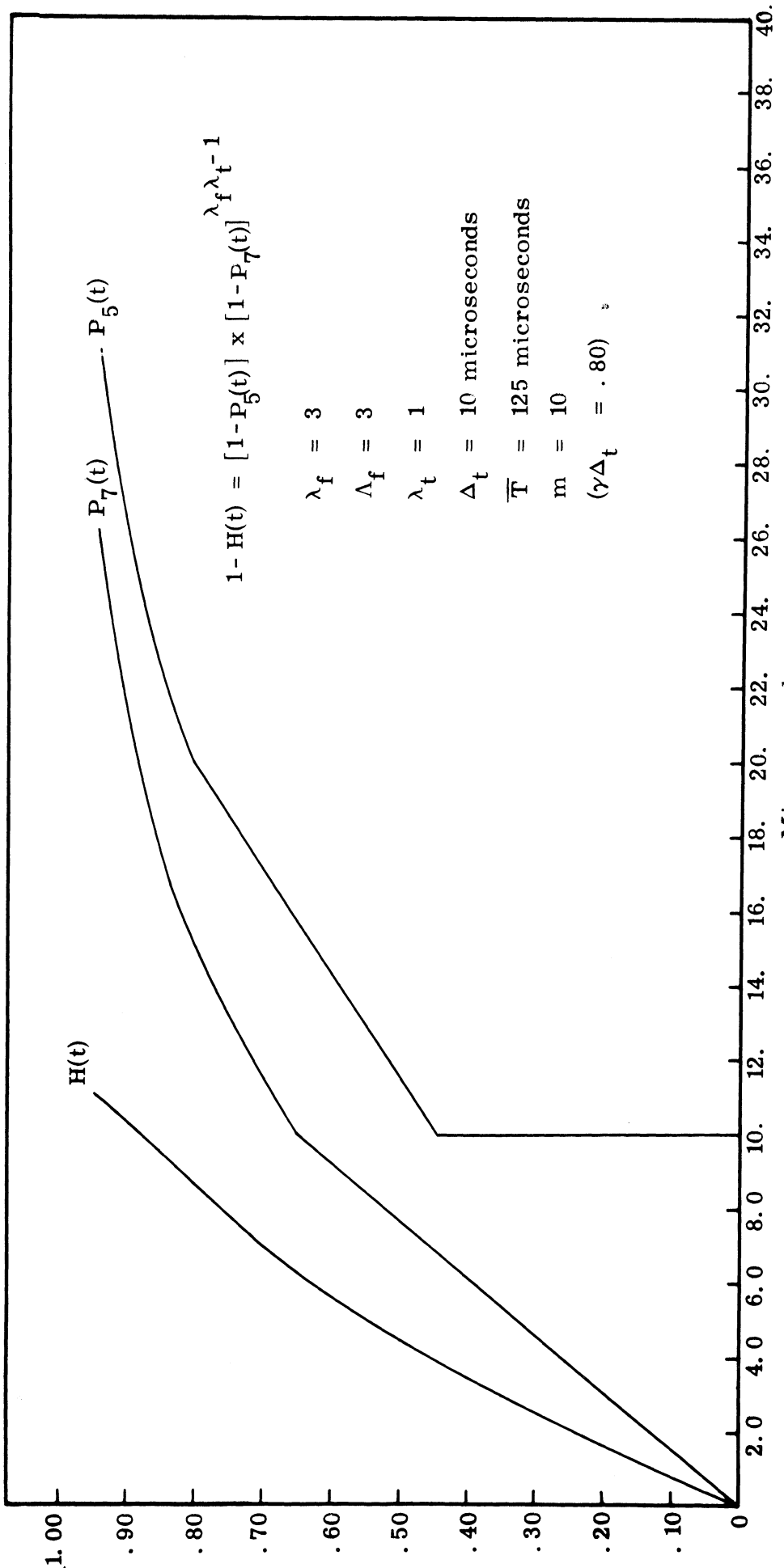

Fig. 3.4. Representative distribution function H(t) of the duration t of an error pulse, and associated functions $P_5(t)$, $P_7(t)$, vs. t.

$\lambda_f = 3$ $\qquad\qquad$ $\bar{T} = 125$ microseconds

$\Lambda_f = 3$ $\qquad\qquad$ $m = 10$

$\lambda_t = 1$

$\Delta_t = 10$ microseconds

The function H(t) is plotted in terms of t/Δ_t with $\gamma\Delta_t$ and $\lambda_f\lambda_t$ as parameters in Fig. 3.5a through Fig. 3.5i.

The mean, $\bar{t}$ corresponding to the distribution function H(t) will be required for future results; $\bar{t}$ is determined by the following theorem.

Theorem: Let t be a real random variable with distribution function H(t) such that t is "one sided." [H(t) exists only for $t \geq 0$ here.] Then if

$$E(t^k) \text{ exists} ,$$

for every t_o such that $H(t_o) = 0$

$$\int_{t_o}^{\infty} k\, t^{k-1} [1 - H(t)]\, dt = E(t^k) - t_o^{\,k} \qquad (3.40)$$

This theorem can readily be proved by using integration by parts (see Ref. 25). It follows from the theorem that, with $t_o = 0$, and with the one-sided distribution of H(t) that

$$\bar{t} = E(t) = \int_0^{\infty} [1 - H(t)]\, dt . \qquad (3.41)$$

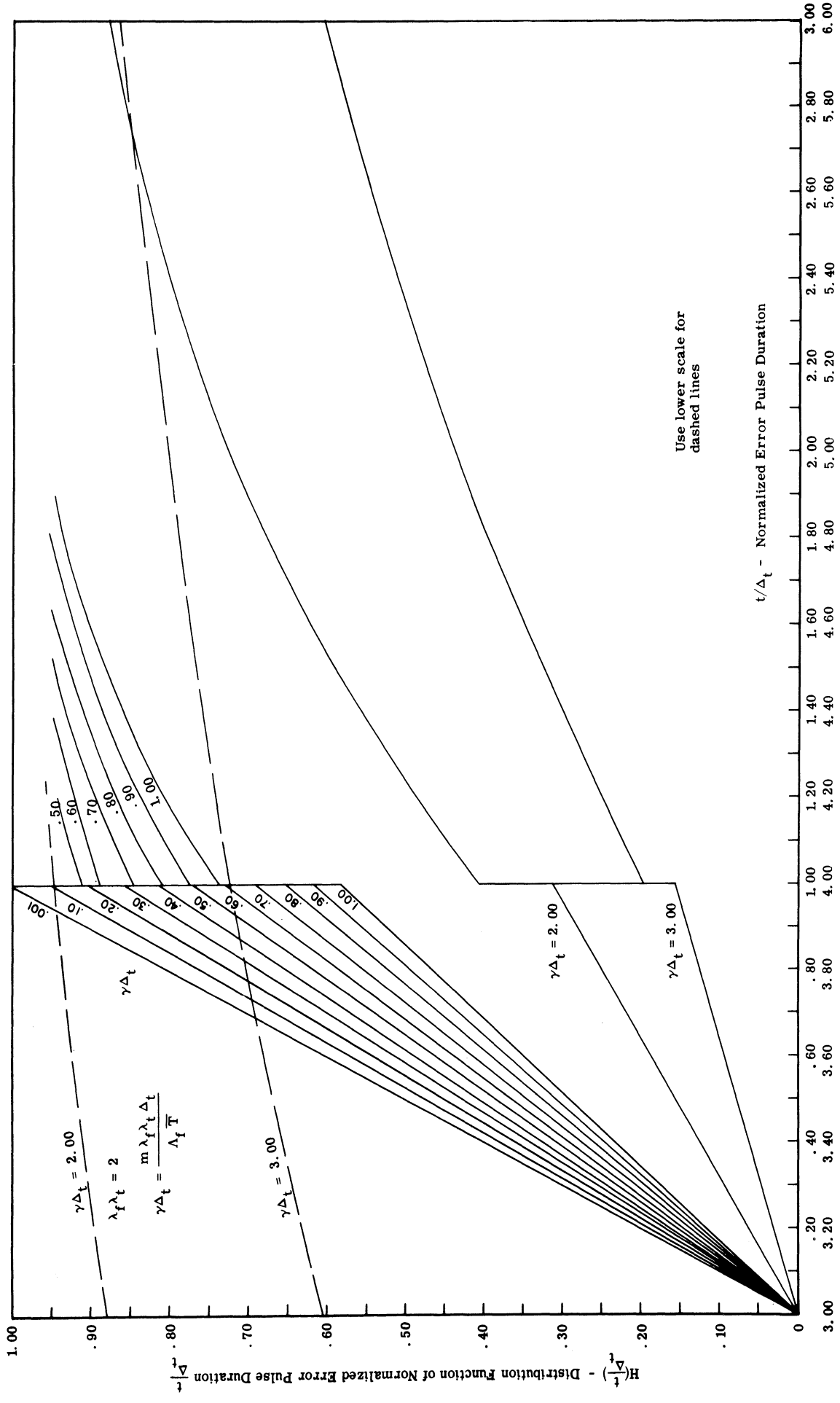

Fig. 3.5(a). Distribution function $H(t/\Delta_t)$ of normalized error pulse duration vs. normalized error pulse duration t/Δ_t. $\lambda_f\lambda_t = 2$.

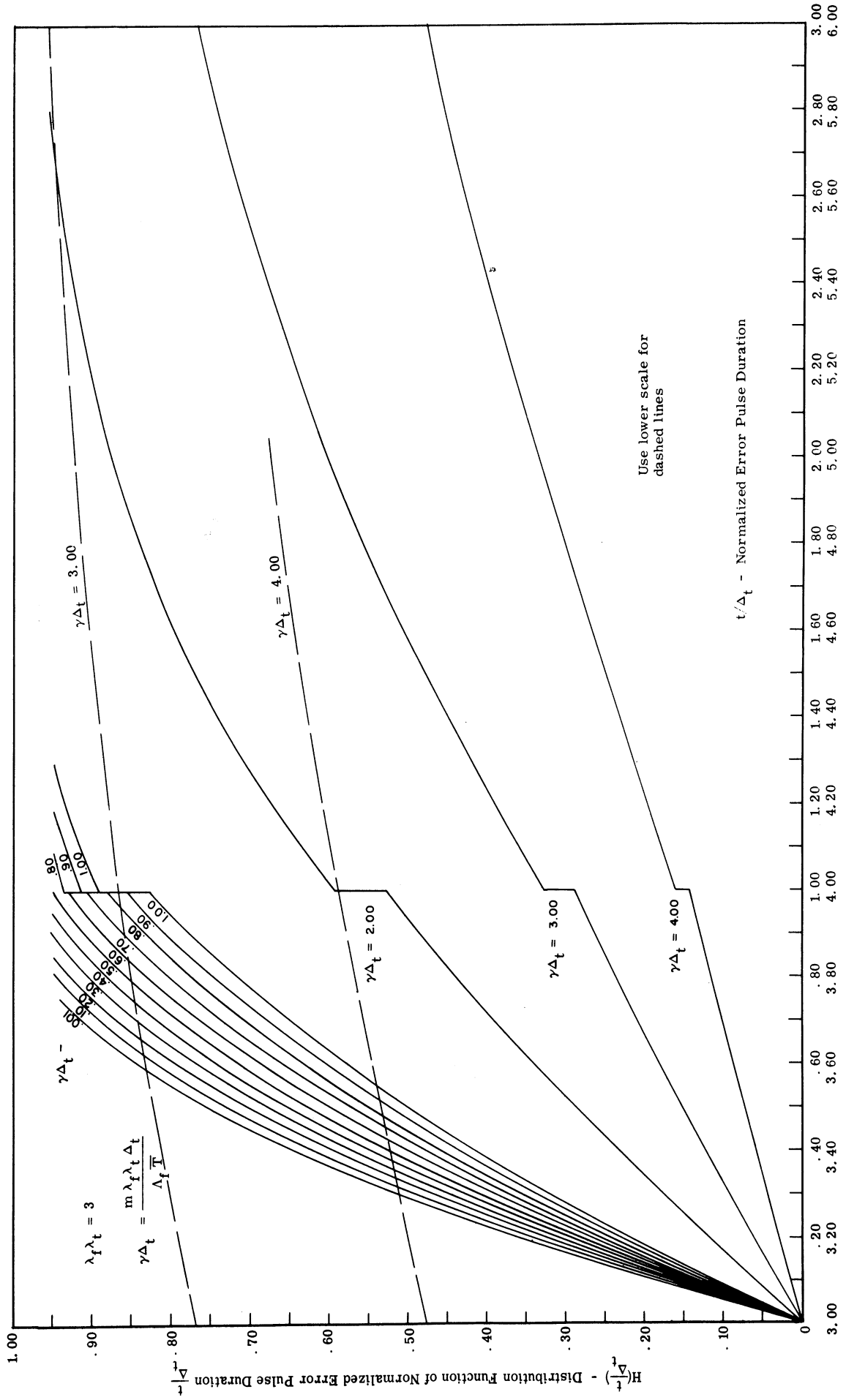

Fig. 3.5(b). Distribution function $H(t/\Delta_t)$ of normalized error pulse duration vs. normalized error pulse duration t/Δ_t. $\lambda_f\lambda_t = 3$.

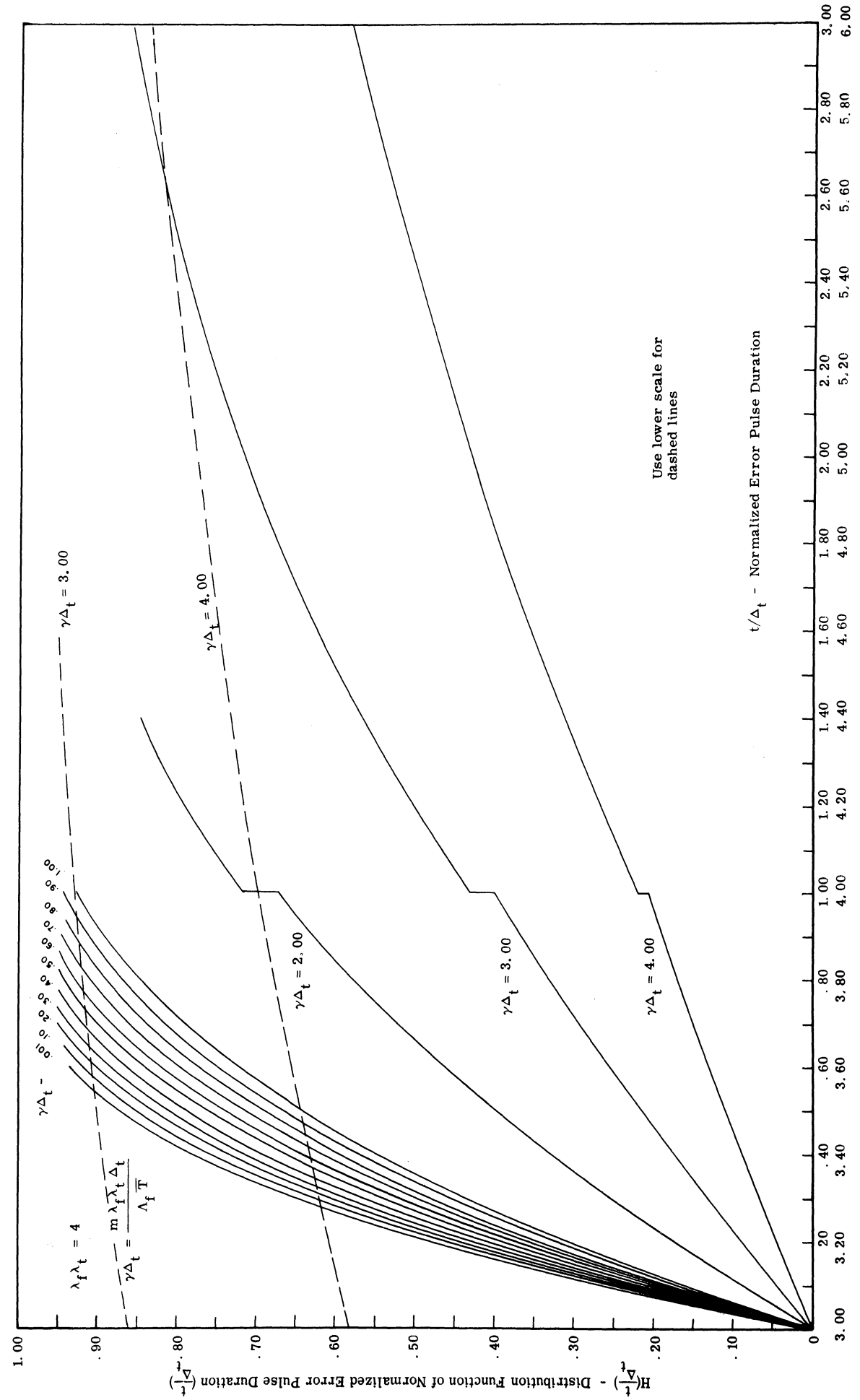

Fig. 3.5(c). Distribution function $H(t/\Delta_t)$ of normalized error pulse duration vs. normalized error pulse duration t/Δ_t; $\lambda_f\lambda_t = 4$.

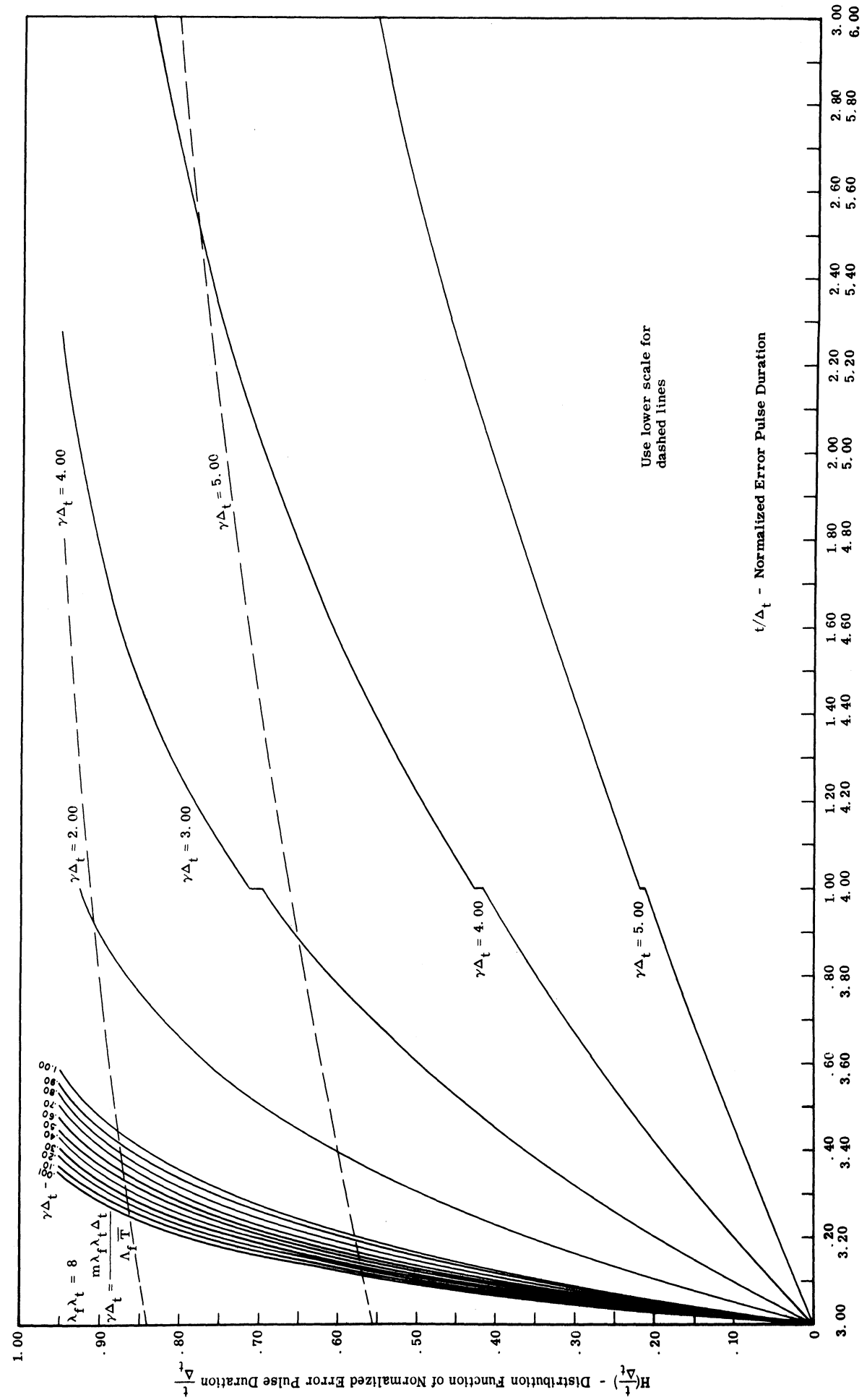

Fig. 3.5(d). Distribution function $H(t/\Delta_t)$ of normalized error pulse duration vs. normalized error pulse duration t/Δ_t. $\lambda_f\lambda_t = 8$.

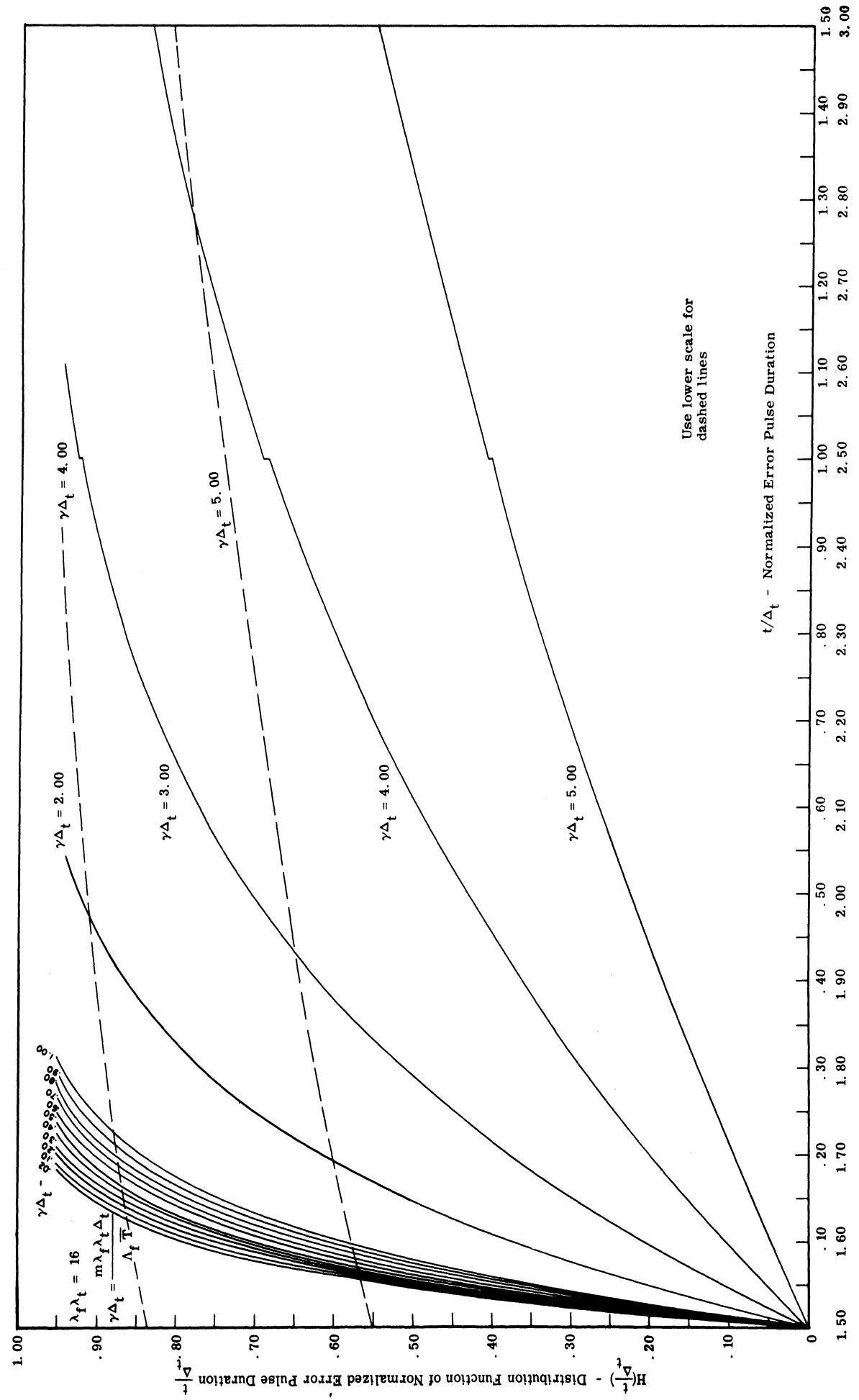

Fig. 3.5(e). Distribution function $H(t/\Delta_t)$ of normalized error pulse duration vs. normalized error pulse duration t/Δ_t. $\lambda_f\lambda_t = 16$.

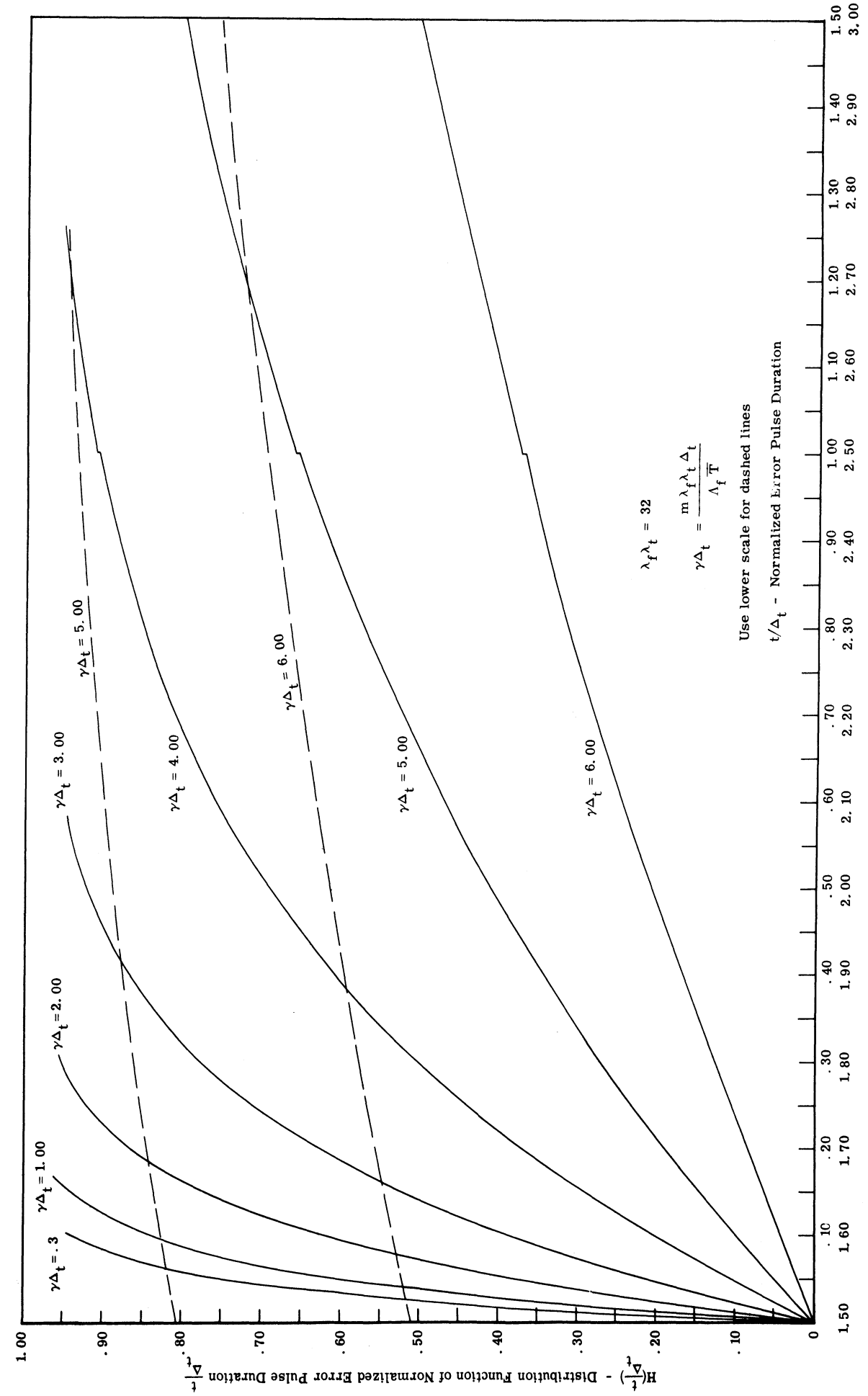

Fig. 3.5(f). Distribution function $H(t/\Delta_t)$ of normalized error pulse duration vs. normalized error pulse duration t/Δ_t. $\lambda_f\lambda_t = 32$.

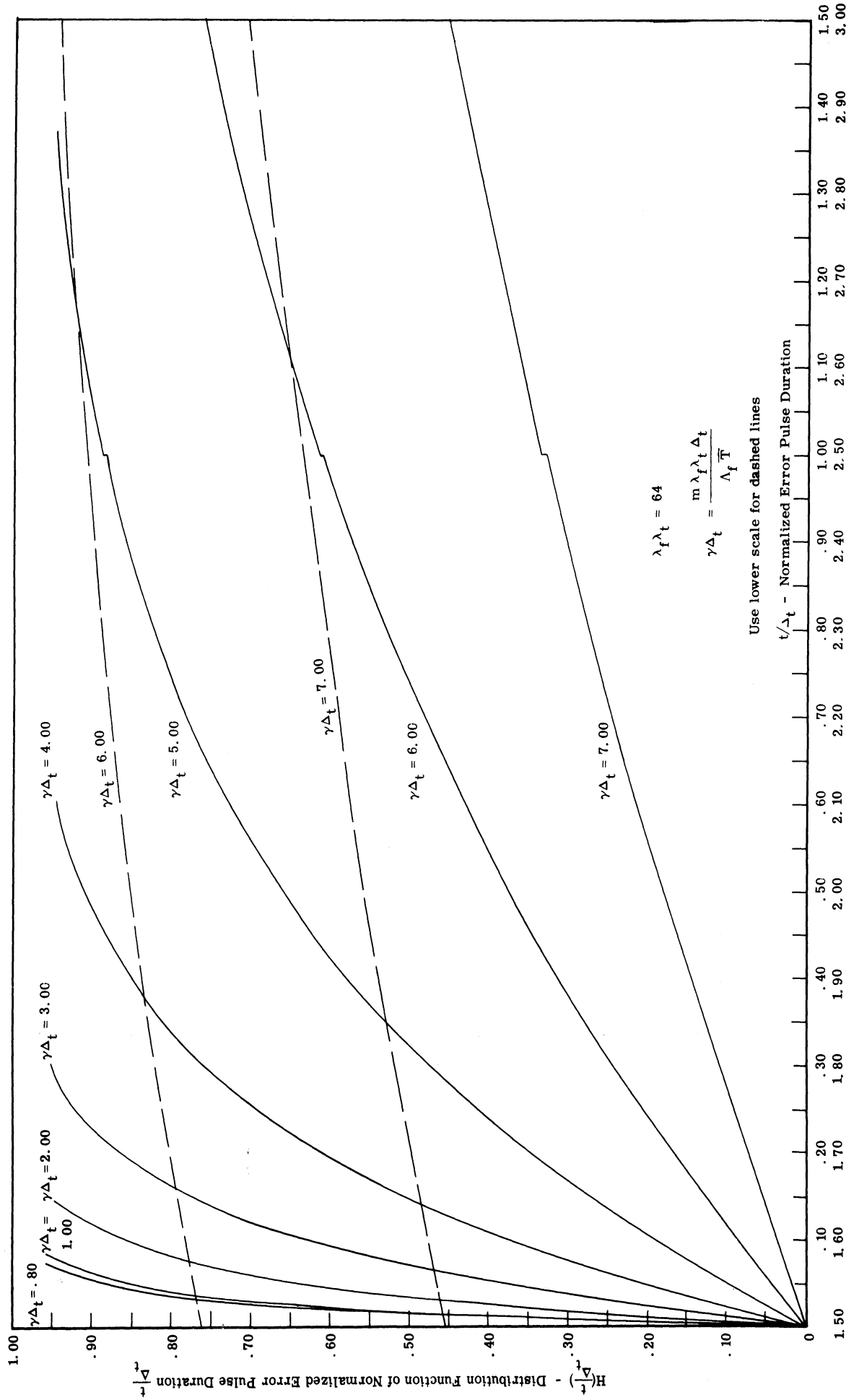

Fig. 3.5(g). Distribution function $H(t/\Delta_t)$ of normalized error pulse duration vs. normalized error pulse duration t/Δ_t. $\lambda_f\lambda_t = 64$.

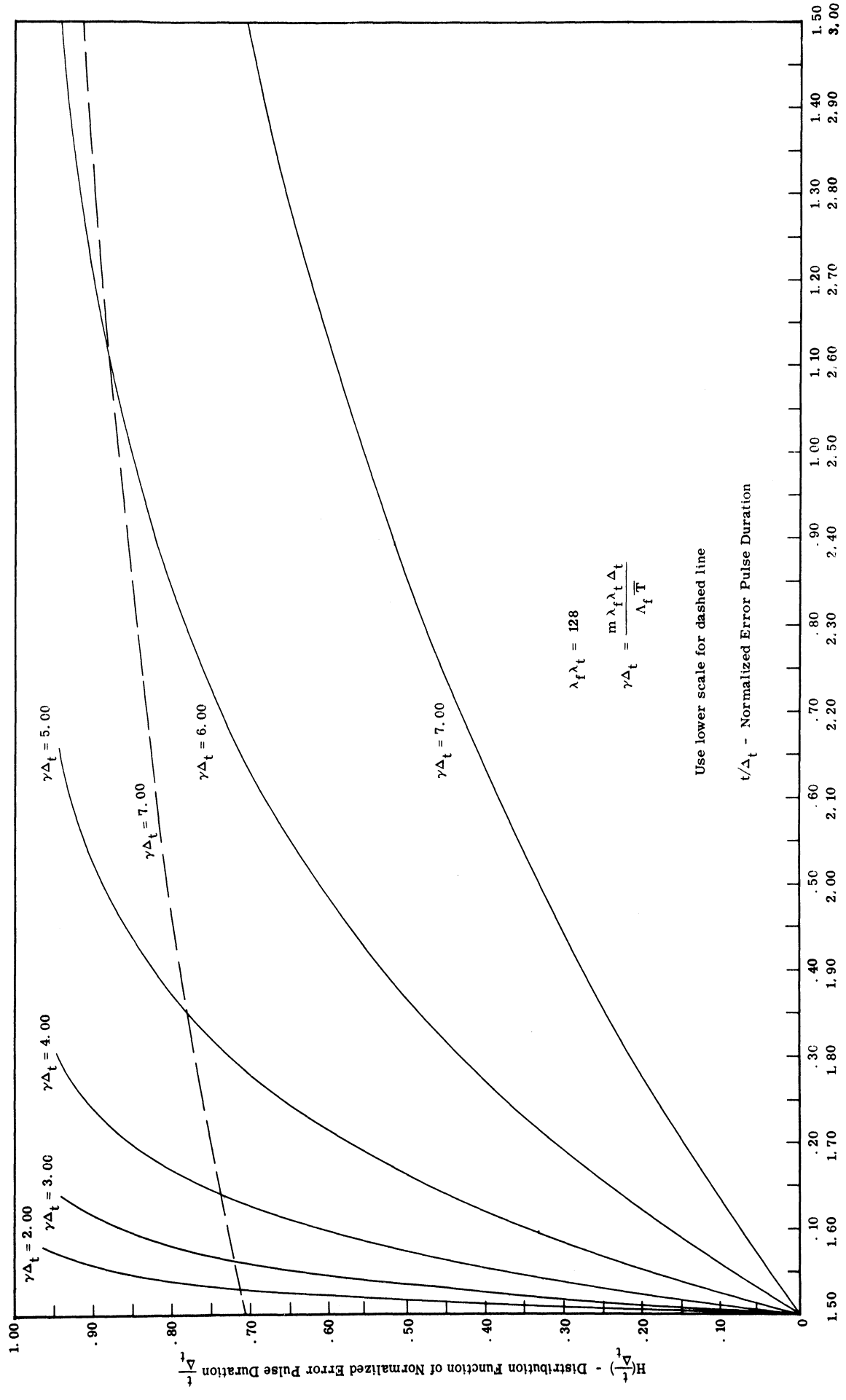

Fig. 3.5(h). Distribution function $H(t/\Delta_t)$ of normalized error pulse duration vs. normalized error pulse duration t/Δ_t. $\lambda_f\lambda_t = 128$.

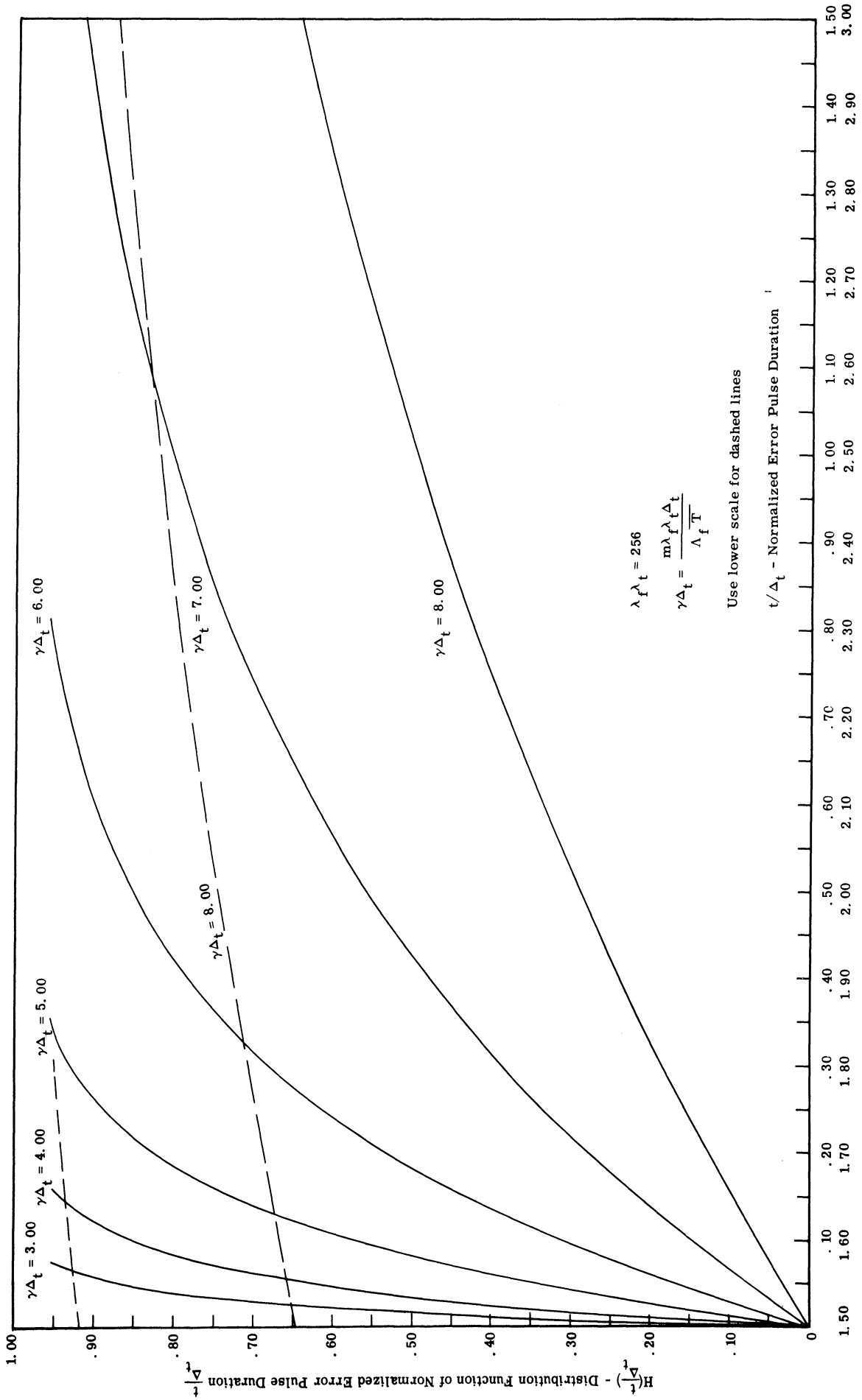

Fig. 3.5(i). Distribution function $H(t/\Delta_t)$ of normalized error pulse duration vs. normalized error pulse duration (t/Δ_t). $\lambda_f\lambda_t = 256$.

Or, substituting (3.38) into (3.41)

$$\bar{t} = \int_0^\infty [1 - P_5(t)]\,[1 - P_7(t)]^{\lambda_f \lambda_t - 1}\, dt \qquad (3.42)$$

Let the t axis be partitioned in successive intervals of duration Δ_t. For t in any interval, $P_5(t)$, $P_7(t)$ can be described by a finite series of functions using (3.29) and (3.35). In any interval, $[1 - P_7(t)]^{\lambda_f \lambda_t - 1}$ can be expressed by a multinomial expansion, and the terms in the product $[1 - P_5(t)]\,[1 - P_7(t)]^{\lambda_f \lambda_t - 1}$ can be determined. If (3.42) is evaluated by integrating the terms in the product $[1 - P_5(t)]\,[1 - P_7(t)]^{\lambda_f \lambda_t - 1}$ in successive intervals of duration Δ_t, practical difficulties are encountered because for $t \to \infty$ the number of terms becomes infinite. These difficulties are bypassed in the approximations for $\bar{t}$ which are given in Section 3.3.3.

3.3.3 Approximations for the Mean Duration, $\bar{t}$, of an Error Pulse. Although, as was pointed out in Section 3.3.2, an infinite number of terms is required to determine $\bar{t}$ exactly, only a finite number of terms is required to approximate $\bar{t}$ to any desired degree of accuracy. Two approximations, $\tilde{t}$ and $\tilde{\tilde{t}}$, for $\bar{t}$ will be given in this section.

A practical method of approximating $\bar{t}$ of (3.42), using machine computation, is to evaluate $\tilde{t}$, which is defined by

$$\bar{t} \cong \tilde{t} = \int_0^a [1 - P_5(t)]\,[1 - P_7(t)]^{\lambda_f \lambda_t - 1}\, dt \qquad (3.43)$$

Using (3.43), numerical values of $\tilde{t}$ have been determined with an IBM 7090 computer; these numerical computations are used in Section 3.3.4. The value of a used is such that $1 - H(a) = .02$; it is expected that the error in $\tilde{t}$ resulting from this approximation is of the order of one percent for all values of the parameters.

A second approximation for $\bar{t}$ is determined now.[1] Approximate but quite accurate results can be obtained for $\bar{t}$ for $\lambda_f \lambda_t \geq 4$ and for $\gamma \Delta_t \leq 1.0$. Note in Figs. 3.5a through 3.5i that for $\lambda_f \lambda_t \geq 4$ and $\gamma \Delta_t \leq 1.0$, $H(t) \cong 1$ for $t \geq \Delta_t$. It follows that

$$1 - H(t) \cong 0\,; \qquad t \geq \Delta_t \qquad (3.44)$$
$$\lambda_f \lambda_t \geq 4$$
$$\gamma \Delta_t \leq 1.0$$

Therefore from (3.41),

$$\bar{t} = \int_0^\infty [1 - H(t)]\, dt = \int_0^{\Delta_t} [1 - H(t)]\, dt + \int_{\Delta_t}^\infty [1 - H(t)]\, dt\,. \qquad (3.45)$$

---

[1] This method of approximation is taken from Ref. 16.

Define

$$\tilde{\tilde{t}} = \int_0^{\Delta_t} [1 - H(t)]\, dt \quad . \tag{3.46}$$

Substituting (3.46) into (3.45),

$$\bar{t} = \tilde{\tilde{t}} + \int_{\Delta_t}^{\infty} [1 - H(t)]\, dt \tag{3.47}$$

Substituting (3.44) into (3.47)

$$\bar{t} \cong \tilde{\tilde{t}} = \int_0^{\Delta_t} [1 - H(t)]\, dt \; ; \qquad \lambda_f \lambda_t \geq 4 \qquad \gamma \Delta_t \leq 1.0 \tag{3.48}$$

From (3.38)

$$1 - H(t) = [1 - P_5(t)]\, [1 - P_7(t)]^{\lambda_f \lambda_t - 1} \tag{3.38}$$

For t in the range $0 \leq t \leq \Delta_t$, (3.29) can be written as (3.49).

$$1 - P_5(t) = 1 \; ; \qquad t \leq \Delta_t \tag{3.49}$$

Similarly, (3.33) can be written as (3.50).

$$1 - P_7(t) = 1 \; ; \qquad t < 0$$

$$1 - P_7(t) = 1 - \frac{e^{-\gamma\Delta_t}}{1 - e^{-\gamma\Delta_t}} (\gamma t) ; \qquad 0 \leq t < \Delta_t \qquad (3.50)$$

Substituting (3.49) and (3.50) in (3.38)

$$1 - H(t) = 1 ; \qquad t < 0$$

$$1 - H(t) = \left[1 - \frac{e^{-\gamma\Delta_t}}{1 - e^{-\gamma\Delta_t}} (\gamma t) \right]^{\lambda_f\lambda_t - 1} ; \qquad 0 \leq t < \Delta_t \qquad (3.51)$$

From (3.44),

$$1 - H(t) \cong 0 ; \qquad t \geq \Delta_t$$

Substituting (3.51) into (3.48), and integrating,

$$\tilde{\tilde{t}} = \frac{1 - e^{-\gamma\Delta_t}}{\gamma \lambda_f\lambda_t e^{-\gamma\Delta_t}} \left\{ 1 - \left[1 - \frac{(\gamma\Delta_t) e^{-\gamma\Delta_t}}{1 - e^{-\gamma\Delta_t}} \right]^{\lambda_f\lambda_t} \right\} ; \qquad \begin{matrix} \lambda_f\lambda_t \geq 4 \\ \gamma\Delta_t \leq 1.0 \end{matrix} \qquad (3.52)$$

3.3.4 Determination of the Error Rate at the AND Gate Output.

In this section, an expression will be determined for the average number of error pulses per second at the output of a RADA receiver AND gate.

Consider the ensemble of AND gate error pulse trains of

duration τ produced by m interfering RADA transmitters; τ is chosen sufficiently large that truncation of error pulses at the extremes of the interval does not significantly affect the average duration of error pulses in the interval. Let there be $K(K \to \infty)$ ensemble members of duration τ, each denoted by the index k. Different ensemble members are generated by different groups of $\lambda_f \lambda_t$ statistically independent Poisson pulse epoch processes at the $\lambda_f \lambda_t$ AND gate inputs.

Define:

$t_n^{(k)}$ the duration of the nth error pulse of the kth ensemble member.

$n^{(k)}$ enumerator of the nth error pulse in the kth ensemble member.

$N^{(k)}(\tau)$ number of error pulses in the kth ensemble member.

$\bar{N}$ the expected number of error pulses per second.

r let a single error pulse process be formed by placing successive ensemble members "end to end" so that the end of the τ second duration of the kth ensemble member corresponds to the beginning of the τ second duration of the (k+1)st ensemble member. The quantity r is the index of successive error pulses of this error pulse process.

t_r the duration of the error pulse which corresponds to the index value r.

$\bar{t}$ the mean of $t_n^{(k)}$.

The duty factor $P_m^{(k)}$ of the kth ensemble member is,

$$P_m^{(k)} = \frac{1}{\tau} \sum_{n^{(k)}=1}^{N^{(k)}(\tau)} t_n^{(k)} \qquad (3.53)$$

The expected duty factor is,

$$P_m = E\left[P_m^{(k)}\right] = \lim_{K\to\infty} \frac{1}{K} \sum_{k=1}^{K} P_m^{(k)}$$

$$= \lim_{K\to\infty} \frac{1}{K} \left(\sum_{k=1}^{K} \frac{1}{\tau} \sum_{n^{(k)}}^{N^{(k)}(\tau)} t_n^{(k)} \right) \qquad (3.54)$$

$$= \lim_{K\to\infty} \frac{1}{K} \left(\frac{1}{\tau} \sum_{r=1}^{\left[\sum_{k=1}^{K} N^k(\tau)\right]} t_r \right) = \lim_{K\to\infty} \frac{1}{K\tau} \sum_{r=1}^{K\tau\bar{N}} t_r$$

$$= \lim_{K\to\infty} \bar{N} \left(\frac{1}{K\tau\bar{N}} \sum_{r=1}^{K\tau\bar{N}} t_r \right) = \bar{N}\bar{t}$$

Thus,

$$\bar{N} = \frac{P_m}{\bar{t}} \qquad (3.55)$$

The average number of AND gate output pulses in a frame period is $\bar{N}\,\bar{T}$. The average number of AND gate output pulses per second is $\bar{N}$.

An approximate computer solution for $\bar{N}$ has been obtained by substituting $\tilde{t}$ of (3.43) into (3.53). The approximation $\tilde{t}$ for $\bar{t}$ is determined using a value of a determined by $1 - H(a) = .02$. It is expected that the error in $\tilde{t}$, corresponding to this value of a, is of the order of one percent, for all values of the parameters. In Ref. 16, an approximate solution for $\bar{N}$ is obtained by substituting $\tilde{\tilde{t}}$ of (3.52) into (3.55); this solution gives an accurate approximation for $\bar{N}$ for $\lambda_f\lambda_t \geq 4$ and $\gamma\Delta_t \leq 1.0$.

The quantity $\bar{N}\,\Delta_t$ is plotted in Fig. 3.6 as a function of $\gamma\Delta_t$ with $\lambda_f\lambda_t$ as parameter. $\bar{N}\,\bar{T}$ is plotted in Fig. 3.7 as a function of $m\frac{\lambda_f}{\Lambda_f}$ with Δ_t as parameter, and with $\lambda_f = 3$, $\lambda_t = 1$, $\bar{T} = 125$ microseconds; these parameter values correspond to those of prototype RACEP systems (Appendix A). The quantity $\bar{N}\,T_c$ is plotted in Fig. 3.8 as a function of $mk\frac{\lambda_f}{\Lambda_f}$ with Δ_t as parameter, and with $\lambda_f = 3$, $\lambda_t = 1$, $T_c = 26$ microseconds; these parameter values correspond to those of prototype RADEM systems.

3.3.5 Properties of the Error Pulse Process at the Receiver AND Gate Output. In this section, a new approximation will be obtained for the probability distribution function of the time to the epoch of an error pulse, given that no error pulse is present initially. This result will be used in Section 3.3.6 to determine the probability that at least

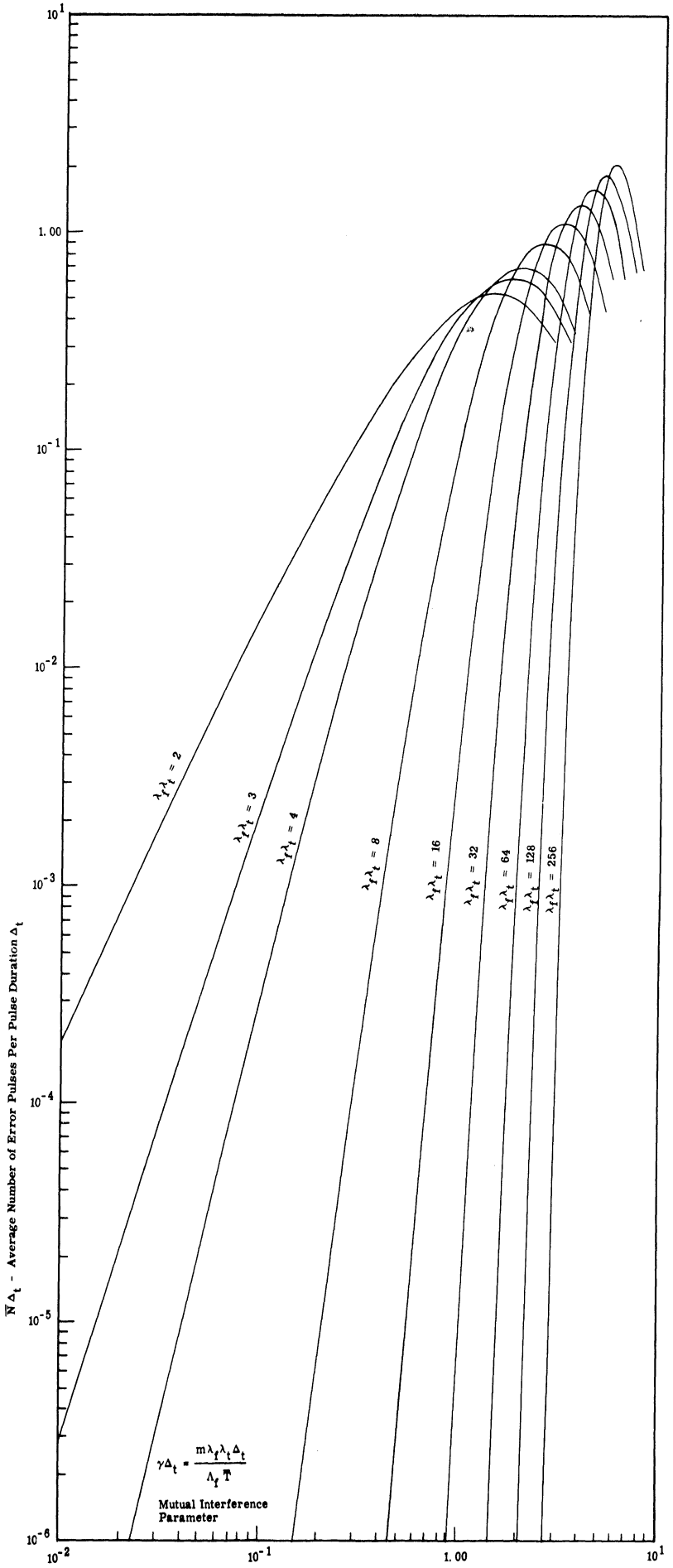

Fig. 3.6. Average number of error pulses per pulse duration $\overline{N}\Delta_t$ vs. mutual interference parameter, $\gamma\Delta_t$.

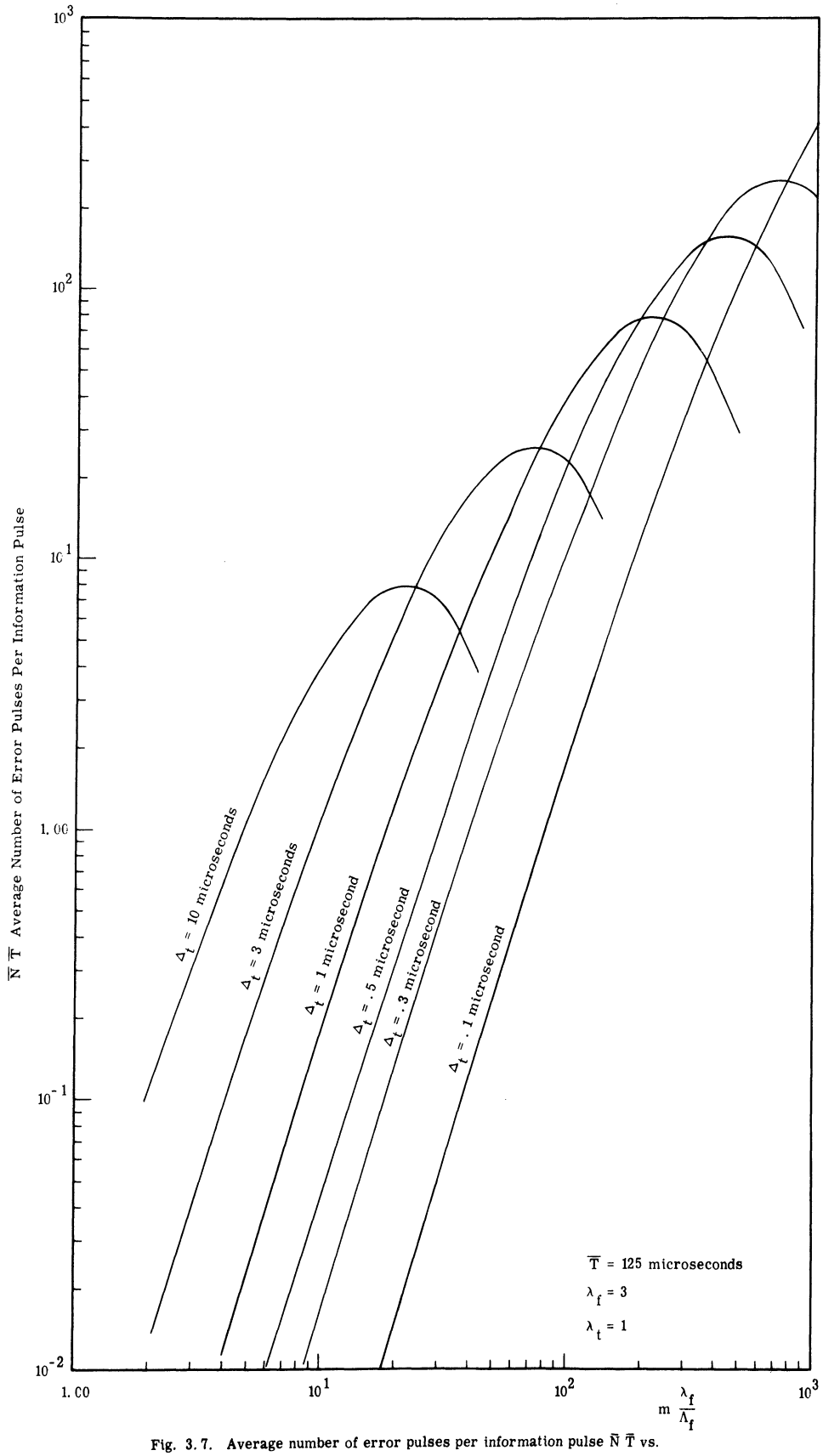

Fig. 3.7. Average number of error pulses per information pulse $\overline{N}\ \overline{T}$ vs. $m \frac{\lambda_f}{\Lambda_f}$. $\overline{T}$ = 125 microseconds, λ_f = 3, λ_t = 1.

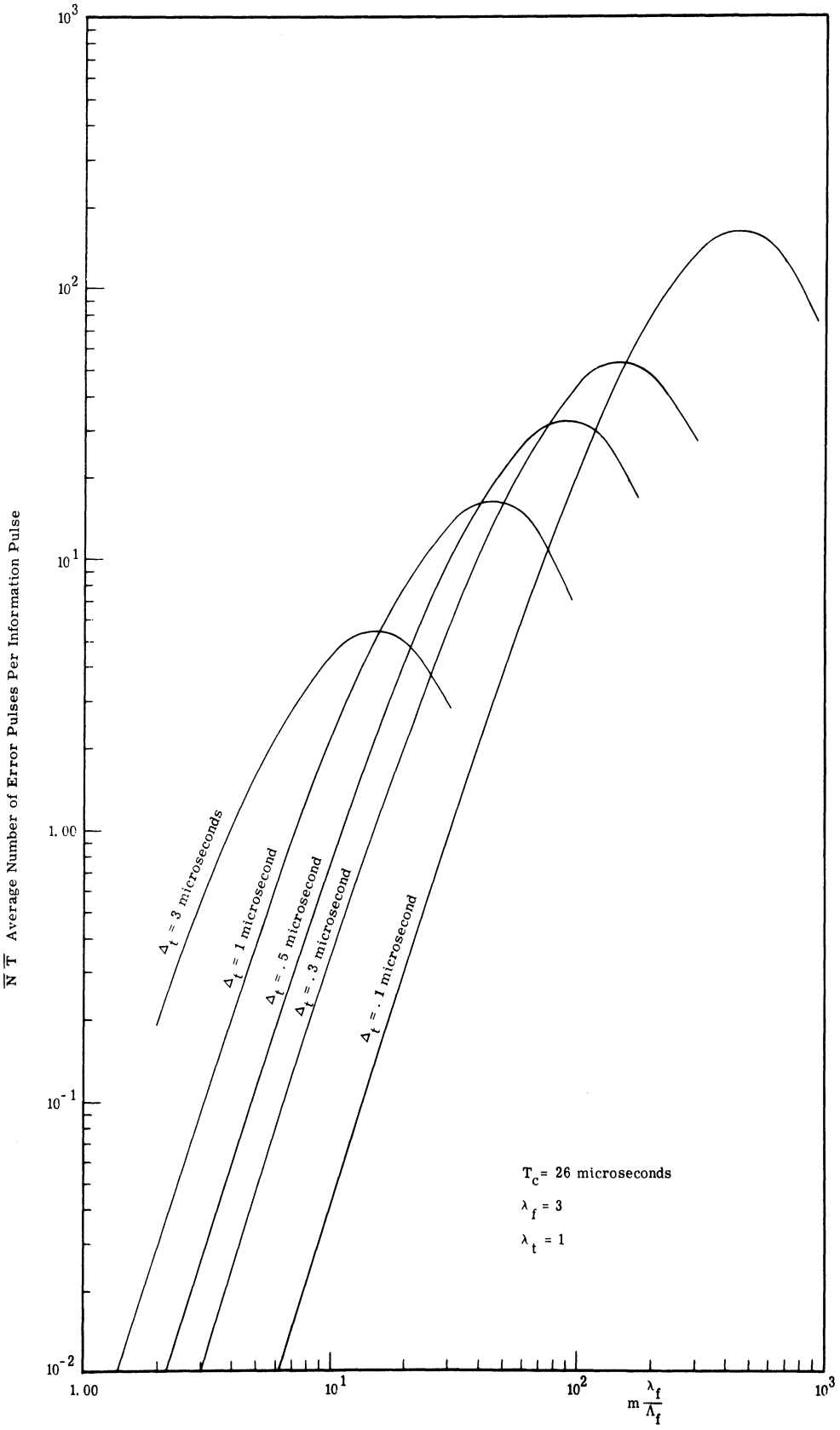

Fig. 3.8. Average number of error pulses per information pulse $\overline{N}\,\overline{T}$ vs. $m\frac{\lambda_f}{\Lambda_f}$. T_c = 26 microseconds, λ_f = 3, λ_t = 1.

one error pulse occurs in a given time interval.

The quantities H(t) and $\bar{t}$ provide a fairly complete description of the error process at the AND gate output. The process has three distinct states, an ON state, a transition state, and an OFF state. After an error pulse epoch, the process is in the ON state and is described by the distribution function H(t). The transition state begins when the error pulse output stops, and ends when either an error pulse appears or Δ_t seconds elapse, whichever occurs first. If Δ_t seconds elapse first, the process is in the OFF state and is described, approximately, by Poisson statistics and the parameter $\bar{N}$.

The significance of the transition state is that within Δ_t seconds of the last occurrence of an error pulse, the probability of the epoch of an error pulse in a time interval Δ_t is dependent upon the fact that an error pulse occurred within the last Δ_t seconds. Assuming that the transition state ends after Δ_t seconds (there is no error pulse epoch in the Δ_t second transition period) the process goes to the OFF state. In the OFF state, the probability of occurrence of an error pulse epoch in any small time interval of Δ_t seconds duration is constant. The distribution of the time to the epoch of an error pulse, measured from any time instant in the OFF state is, therefore, exponential.

As an approximation, assume that the OFF state begins when the error pulse ceases, and that there is no transition state. With this assumption, the mean time $1/\gamma'$ from the beginning of the OFF state to

the epoch of the next error pulse is equal to the difference in the mean interval, $1/\bar{N}$ between error pulse epochs and the mean error pulse duration $\bar{t}$. That is

$$\frac{1}{\gamma'} = \frac{1}{\bar{N}} - \bar{t} \tag{3.56}$$

or

$$\gamma' = \frac{\bar{N}}{1 - \bar{N}\bar{t}} \tag{3.57}$$

Substituting (3.55) into (3.57),

$$\gamma' = \frac{\bar{N}}{1 - P_m} \quad . \tag{3.58}$$

When the duty factor P_m is much smaller than unity, as will frequently be true,

$$\gamma' \cong \bar{N}; \qquad P_m << 1 \tag{3.59}$$

Let $P_m(\tau)$ be the probability distribution of the time, τ, to the epoch of an error pulse, measured from any time instant in the OFF state. Then

$$\begin{aligned} P_m(\tau) &= 0 && ; \quad \tau < 0 \\ P_m(\tau) &\cong \tilde{P}_m(\tau) = 1 - e^{-\gamma'\tau} && ; \quad \tau \geq 0 \end{aligned} \tag{3.60}$$

By definition, $P_m(\tau)$ is also the probability that there is at least one error pulse epoch in the time interval τ. The probability distribution function $\tilde{P}_m(\tau)$ is used in Section 3.3.6.

3.3.6 Approximation and Lower Bound for the Probability of an Error Pulse in a Time Interval. In this section, the approximate distribution of the duration of the AND gate output OFF-state process described in Section 3.3.5 is used to determine approximations, $\tilde{p}_e(\tau_e)$ and $\tilde{P}_e(\tau_e)$, for the probability density and distribution functions $p_e(\tau_e)$, $P_e(\tau_e)$ which will be employed in Section 3.4 to evaluate the performance of gated receivers.

Let τ_e be the time from the opening of the post gate to the first occurrence of an error pulse; $\tau_e = 0$ if there is an error pulse at the AND gate output when the post gate opens; otherwise τ_e is the time from the opening of the post gate to the epoch of the first error pulse.

The probability distribution function of τ_e equals the probability that either there is an error pulse at the AND gate output when the post gate opens, or there is no error pulse then, and at least one error pulse epoch occurs within τ_e seconds of the opening of the post gate.

The probability distribution of τ_e is,

$$P_e(\tau_e) = 0; \qquad \tau_e < 0$$

$$P_e(\tau_e) = P_m + (1 - P_m) P_m(\tau_e); \qquad \tau_e \geq 0 \tag{3.61}$$

Substituting the approximation $\tilde{P}_m(\tau_e)$ for $P_m(\tau_e)$ in (3.61) gives an approximation $\tilde{P}_e(\tau_e)$ for $P_e(\tau_e)$.

$$\begin{aligned} \tilde{P}_e(\tau_e) &= 0 \qquad\qquad ; \quad \tau_e < 0 \\ \tilde{P}_e(\tau_e) &= P_m + (1 - P_m)\,\tilde{P}_m(\tau_e) \; ; \quad \tau_e \geq 0 \end{aligned} \tag{3.62}$$

Substituting (3.60) into (3.62) and differentiating, an approximation $\tilde{p}_e(\tau_e)$ is determined for the density function $p_e(\tau_e)$ of τ_e.

$$\begin{aligned} p_e(\tau_e) &\cong \tilde{p}_e(\tau_e) = 0 \; ; \quad \tau_e < 0 \\ p_e(\tau_e) &\cong \tilde{p}_e(\tau_e) = P_m\,\delta(\tau_e) + (1 - P_m)\,\gamma'\,e^{-\gamma'\tau_e} \end{aligned} \tag{3.63}$$

A lower bound $\tilde{\tilde{P}}_e(\tau_e)$ for $P_e(\tau_e)$ will be determined now which applies when Δ_t divides τ_e. Let the AND gate output be sampled once every Δ_t seconds in the closed τ_e second interval. There are $\frac{\tau_e + \Delta_t}{\Delta_t}$ samples in the interval. The quantity $\tilde{\tilde{P}}_e(\tau_e)$ is the probability that at least one sample is an error pulse sample.

$$\tilde{\tilde{P}}_e(\tau_e) = 1 - (1 - P_m)^{\frac{\tau + \Delta_t}{\Delta_t}} \tag{3.64}$$

Substituting (3.1) into (3.63)

$$\tilde{\tilde{P}}_e(\tau_e) = 1 - \left[1 - \left(1 - e^{-\gamma\Delta_t}\right)^{\lambda_f\lambda_t}\right]^{\frac{\tau_e + \Delta_t}{\Delta_t}} \qquad (3.65)$$

If at least one of the samples is an error pulse sample, then there must be at least one error pulse in the interval τ_e, whereas the converse is not true. It follows that

$$\tilde{\tilde{P}}_e(\tau_e) < P_e(\tau_e) \ . \qquad (3.66)$$

Future results will indicate that, in the range of m for which mutual interference is not excessive, the average width of error pulses will be somewhat less than Δ_t, so that error pulses will frequently occur between samples. It follows that $\tilde{\tilde{P}}_e(\tau)$ is not a close lower bound for $P_e(\tau)$.

It follows from (3.62), that P_m is also a lower bound for $P_e(\tau_e)$. It follows from (3.64) that $P_m \leq \tilde{\tilde{P}}_e(\tau_e)$ and, hence, that P_m is a lower bound of $P_e(\tau_e)$ than is $\tilde{P}_e(\tau_e)$. Summarizing,

$$P_m < \tilde{\tilde{P}}_e(\tau_e) < P_e(\tau_e) \cong \tilde{P}_e(\tau_e) \qquad (3.67)$$

The lower bounds for $P_e(\tau_e)$ are useful in making quick, coarse approximations for $P_e(\tau_e)$.

3.4 Measures of RADA System Performance

Several different measures of RADA system performance will be described in this section. Different measures will be required depending on the type of modulation and the type of receiver to be used in the system. Pulse position modulation and clocked binary modulation; ungated and synchronized gated and sampling receivers will be considered.

3.4.1 Duty Factor of Error Pulses at the AND Gate Output of an Ungated Receiver.

In a RADA system using PPM or clocked binary modulation, and in ungated receivers, the duty factor P_m of the error pulses at the output of the receiver AND gate is a measure of the severity of the mutual interference.

$$P_m = \left(1 - e^{-\gamma\Delta_t}\right)^{\lambda_f\lambda_t} \tag{3.1}$$

Because the effect of error pulse interference depends on the duration and number of error pulses as well as on the duty factor, P_m is not a precise measure of the mutual interference.

At the present time, data are not available which relate the quality and intelligibility of voice directly to the duty factor of error pulses for various types of modulation.

The quantity P_m is plotted as a function of $\gamma\Delta_t$ with $\lambda_f\lambda_t$ as a parameter in Fig. 3.1.

3.4.2 Number of Error Pulses at the Output of an Ungated Receiver. The average number $\bar{N}\,\bar{T}$ of error pulses per message pulse, or $\bar{N}$ per second, is a measure of performance for RADA systems using either pulse position or clocked binary modulation and an ungated receiver. For $\bar{N}\,\bar{T}$ to have a concrete meaning it is necessary to convert the error pulse rate into some measure of intelligibility of the demodulated information signal as discussed in Section 3.1.

An expression for $\bar{N}$ is given by (3.55), along with (3.1) and (3.43) or (3.52). $\bar{N}\,\Delta_t$ is plotted as a function of $\gamma\Delta_t$ and parameters $\lambda_f\lambda_t$ in Fig. 3.6.

3.4.3 False Alarm Probability and Rate for a RADA System Using Pulse Position Modulation with a Synchronized Gated Receiver. Assume a RADA system using pulse position modulation. The receiver is synchronized and uses a gate of width T_p. A type one false alarm occurs when there is at least one error pulse in the interval between the opening of the post gate and the epoch of the message pulse (see Section 3.1). Let the expected epoch of a message pulse be used as the time reference and assume the gate interval is centered on the expected center position of a message pulse. With respect to this time reference, a particular gate interval begins at time $\frac{-T_p+\Delta_t}{2}$ and ends at time $\frac{T_p+\Delta_t}{2}$. For a message pulse to be completely within the gate interval, the epoch of the message pulse must be within the closed interval $\left[\frac{-T_p+\Delta_t}{2}, \frac{T_p-\Delta_t}{2}\right]$.

Let τ_r be the time of the epoch of the message pulse. Let the probability density of τ_r be $p_r(\tau_r)$.

Let τ_e be the time from the opening of the post gate to the first occurrence of an error pulse; $\tau_e = 0$ if there is an error pulse at the AND gate output when the post gate opens, otherwise τ_e is the time from the opening of the post gate to the epoch of the first error pulse. The probability density and distribution functions of τ_e are $p_e(\tau_e)$ and $P_e(\tau_e)$.

Let $[\omega_1, \omega_2, \text{--- } \omega_n]$ be the joint event ω_1 occurs and ω_2 occurs---and ω_n occurs. (Although the same notation is used for a closed interval, the application of the notation will be clear in each case.)

The event a type one false alarm is the union of events, as $\Delta\tau_r \to 0$;

$$\left[\frac{-T_p+\Delta_t}{2} \leq \tau_r < \frac{-T_p+\Delta_t}{2} + \Delta\tau_r,\ \frac{-T_p+\Delta_t}{2} \leq \tau_e \leq \tau_r\right] \cup$$

$$\left[\frac{-T_p+\Delta_t}{2} + \Delta\tau_r \leq \tau_r < \frac{-T_p+\Delta_t}{2} + 2\Delta\tau_r,\ \frac{-T_p+\Delta_t}{2} \leq \tau_e \leq \tau_r\right] \text{----}$$

$$\left[\frac{T_p-\Delta_t}{2} - \Delta\tau_r \leq \tau_r \leq \frac{T_p-\Delta_t}{2},\ \frac{-T_p+\Delta_t}{2} \leq \tau_e \leq \tau_r\right] . \tag{3.68}$$

The bracketed events are mutually exclusive since the epoch τ_r of the position modulated message pulse will occur in just one of the intervals.

$$\left[\frac{-T_p+\Delta_t}{2}\ ,\ \frac{-T_p+\Delta_t}{2}+\Delta\tau_r\right]$$

$$\left[\frac{-T_p+\Delta_t}{2}+\Delta\tau_r\ ,\ \frac{-T_p+\Delta_t}{2}+2\Delta\tau_r\right]\text{----} \qquad (3.69)$$

$$\left[\frac{T_p-\Delta_t}{2}-\Delta\tau_r\ ,\ \frac{T_p-\Delta_t}{2}\right] \quad .$$

It follows that the probability of a type one false alarm is the sum of the probabilities of the bracketed events in expression (3.68)

$$P_{1FA}(T_p) = \lim_{\Delta\tau_r\to 0} \sum_{\ell=0}^{\frac{T_p-\Delta_t}{\Delta\tau_r}} P\left[\frac{-T_p+\Delta_t}{2}+\ell\Delta\tau_r \le \tau_r < \frac{-T_p+\Delta_t}{2}\right.$$

$$\left. +(\ell+1)\Delta\tau_r,\ \frac{-T_p+\Delta_t}{2} \le \tau_e \le \tau_r\right] \qquad (3.70)$$

Since

$$P\left[\frac{-T_p+\Delta_t}{2}+\ell\Delta\tau_r \le \tau_r < \frac{-T_p+\Delta_t}{2}+(\ell+1)\Delta\tau_r\ ,\right.$$

$$\left.\frac{-T_p+\Delta_t}{2} \le \tau_e \le \tau_r\right]$$

is the joint probability of two independent events, it can be written as the product of the probabilities of the individual events.

$$P\left[\frac{-T_p+\Delta_t}{2} + \ell\Delta\tau_r \leq \tau_r < \frac{-T_p+\Delta_t}{2} + (\ell+1)\,\Delta\tau_r\,,\ \frac{-T_p+\Delta_t}{2} \leq \tau_e \leq \tau_r\right]$$

$$= P\left[\frac{-T_p+\Delta_t}{2} + \ell\Delta\tau_r \leq \tau_r < \frac{-T_p+\Delta_t}{2} + (\ell+1)\,\Delta\tau_r\right]$$

$$P\left[\frac{-T_p+\Delta_t}{2} \leq \tau_e \leq \tau_r\right] \quad . \tag{3.71}$$

Substituting (3.71) into (3.70) and evaluating the limit there results,

$$P_{1FA}(T_p) = \lim_{\Delta\tau_r \to 0} \sum_{\ell=0}^{\frac{T_p-\Delta_t}{\Delta\tau_r}} P\left[\frac{-T_p+\Delta_t}{2} + \ell\Delta\tau_r \leq \tau_r < \frac{-T_p+\Delta_t}{2}\right.$$

$$\left. + (\ell+1)\,\Delta\tau_r\right] \ P\left[\frac{-T_p+\Delta_t}{2} \leq \tau_e \leq \tau_r\right]$$

$$= \lim_{\Delta\tau_r \to 0} \sum_{\ell=0}^{\frac{T_p-\Delta_t}{\Delta\tau_r}} p_r\left(\frac{-T_p+\Delta_t}{2} + \ell\Delta\tau_r\right)\Delta\tau_r \int_0^{\tau_r - \left(\frac{-T_p+\Delta_t}{2}\right)}$$

$$p_e(\tau_e)\,d\tau_e$$

$$= \int_{\frac{-T_p+\Delta_t}{2}}^{\frac{T_p-\Delta_t}{2}} p_r(\tau_r)\,d\tau_r \int_0^{\tau_r - \left(\frac{-T_p+\Delta_t}{2}\right)} p_e(\tau_e)\,d\tau_e \tag{3.72}$$

From (3.72), it is apparent that both $p_e(\tau_e)$, the density function of the time to the epoch of an error pulse and $p_r(\tau_r)$ the density function of the epoch of the position modulated message pulses must be known.

Subject to the assumptions of (3.63)

$$p_e(\tau_e) \cong \tilde{p}_e(\tau_e) = P_m \delta(\tau_e) + (1 - P_m) \gamma' e^{-\gamma' \tau_e} \tag{3.63}$$

where

$$\gamma' = \frac{\bar{N}}{1 - P_m} \quad . \tag{3.58}$$

Substituting (3.63) into the second integral on the right hand side of (3.72)

$$\int_0^{\tau_r - \left(\frac{-T_p + \Delta_t}{2}\right)} p_e(\tau_e)\, d\tau_e \cong \int_0^{\tau_r - \left(\frac{-T_p + \Delta_t}{2}\right)} \left[P_m \delta(\tau_e) + (1 - P_m) \gamma' e^{-\gamma' \tau_e} \right] d\tau_e \tag{3.73}$$

$$= P_m + (1 - P_m) \left[1 - e^{-\gamma' \left(\tau_r + \frac{T_p - \Delta_t}{2} \right)} \right]$$

Substituting (3.73) into (3.72)

$$P_{1FA}(T_p) \cong \int_{\frac{-T_p+\Delta_t}{2}}^{\frac{T_p-\Delta_t}{2}} p_r(\tau_r) \left\{ P_m + (1 - P_m) \left[1 - e^{-\gamma' \left(\tau_r + \frac{T_p - \Delta_t}{2} \right)} \right] \right\} d\tau_r \qquad (3.74)$$

Since it is assumed that the position-modulated message pulse will always fall in the gate interval,

$$P_{1FA}(T_p) \cong 1 - (1 - P_m)\, e^{-\gamma' \left(\frac{T_p - \Delta_t}{2} \right)} \int_{\frac{-T_p+\Delta_t}{2}}^{\frac{T_p-\Delta_t}{2}} e^{-\gamma' \tau_r} p_r(\tau_r)\, d\tau_r \qquad (3.75)$$

When $p_r(\tau_r)$ is known exactly, (3.75) can be used to determine P_{1FA}. If $p_r(\tau_r)$ is not known, but some moments are known, or if the integral cannot be evaluated in a convenient form, an approximate expression for (3.75) may be used which is obtained by expanding the exponential in the integral.

$$P_{1FA}(T_p) \cong 1 - (1 - P_m)\, e^{-\gamma' \left(\frac{T_p - \Delta_t}{2} \right)} \left[1 - \gamma' \bar{\tau}_r + \frac{(\gamma')^2}{2!} \overline{\tau_r^2} - \frac{(\gamma')^3}{3!} \overline{\tau_r^3} - \cdots - + (-1)^n \frac{(\gamma')^n}{n!} \overline{\tau_r^n} \right] \qquad (3.76)$$

where $\overline{\tau_r^n}$ is the nth moment of the density of τ_r. Above, $\overline{\tau_r} = 0$ because of the way in which the time origin for τ_r has been defined.

Thus,

$$P_{1FA}(T_p) \cong \left[1-(1-P_m)\, e^{-\gamma'\left(\frac{T_p-\Delta_t}{2}\right)}\right] - \left[(1-P_m)\, e^{-\gamma'\left(\frac{T_p-\Delta_t}{2}\right)}\right] x \left[\sum_{n=2}^{\infty} \frac{(\gamma')^n}{n!}\, \overline{\tau_r^n}\right] \tag{3.77}$$

Alternately, from (3.72)

$$P_{1FA}(T_p) = \int_{\frac{-T_p+\Delta_t}{2}}^{\frac{T_p-\Delta_t}{2}} p_r(\tau_r)\, P_e\left(\tau_r + \frac{T_p-\Delta_t}{2}\right) d\tau_r \tag{3.78}$$

The type one false alarm rate is given by

$$R_{1FA}(T_p) = \frac{P_{1FA}(T_p)}{\overline{T}} \tag{3.79}$$

3.4.4 False Alarm Probability and Rate for a RADA System Using Clocked Binary Modulation, with a Synchronized, Gated Receiver.

Assume a RADA system using clocked, binary (pulse or no pulse) modulation. Let k be the average fraction of on-modulated pulses. The

receiver uses a post gate with a gate interval T_p seconds, which is synchronized. If there is at least one post gate output pulse in the interval T_p, the receiver demodulator will assume a message pulse was present in that interval. The only type of error which this receiver can commit is a "type two false alarm" which occurs when there is no message pulse in the gate interval and when there is at least one error pulse in the gate interval.

Let $P_e(T_p)$ be the probability that there is at least one error pulse in the post gate interval. Then the probability $P_{2FA}(T_p)$ of a type two false alarm is,

$$P_{2FA}(T_p) = (1-k)\, P_e(T_p) \ . \tag{3.80}$$

The type two false alarm rate $R_{2FA}(T_p)$ is defined by

$$R_{2FA}(T_p) = P_{2FA}(T_p)/T_c \ . \tag{3.81}$$

3.4.5 False Alarm Probability and Rate of a Synchronized Sampling RADA Receiver, Clocked Binary Modulation. Assume for a RADA system using clocked binary modulation that a message is received and interference is present. The receiver is synchronized to the message pulse train by some method, perhaps as suggested in Section 1.6.2. A new type of receiver is proposed which samples the AND gate output synchronously with the times at which message pulses might occur. The quantity k is the fraction of on-modulated pulses in the

clocked binary pulse train. Since the probability of pulse cancellation is assumed negligible and the receiver is assumed synchronized, false alarms are the only kind of errors which can occur in reception.

The probability of a false alarm, P_{SFA} is

$$P_{SFA} = (1-k)\, P_m \tag{3.82}$$

and the false alarm rate is

$$R_{SFA} = \frac{P_{SFA}}{T_c} = \frac{1-k}{T_c}\, P_m \tag{3.83}$$

The sampling receiver is a practical type of receiver. The false alarm probability of this receiver is a lower bound of the false alarm rate of the clocked binary modulation RADA system using a synchronized gated receiver. This is apparent heuristically since the sampling procedure can be interpreted as using a gate interval $T_p \to 0$, and since a small gate interval is the most effective in gating interference. It is also apparent from (3.62), (3.67), and (3.80) and since

$$\lim_{T_p \to 0} P_e(T_p) = P_m \tag{3.84}$$

3.4.6 Information Rate of a RADA System Using Clocked Binary Modulation and a Gated or Sampling Receiver. In this section, the rate of transmission of information will be determined for a RADA

system using clocked binary modulation and a gated or sampling receiver.

Let i be an index for the state of the RADA system transmitter output in a particular clock period. If no frame is transmitted in that clock period i = 0. If a frame is transmitted i = 1. Let j be an index of the state of the receiver post gate or sampler output corresponding to the same clock period. If the post gate or sampler output is zero volts in the frame period, j = 0. If the post gate or sampler output is a received pulse or pulse sample, or an error pulse or pulse sample, j = 1. The quantities

$$P(i),\ P(j),\ P(j|i)$$

are respectively the probability of: transmitter state i; receiver state j; receiver state j given transmitter state i. These probabilities will also be designated more specifically as $P(i=0)$, $P(i=1)$, and so forth.

The expressions for the entropies which will be required are:

$$H(j) = -\sum_{j=0,1} P(j) \log_2 P(j) \tag{3.85}$$

$$H(j|i) = -\sum_{i=0,1} P(i) \sum_{j=0,1} P(j|i) \log_2 P(j|i) \tag{3.86}$$

Since

$$P(j) = \sum_{i=0,1} P(j|i)\, P(i) \tag{3.87}$$

$$H(j) = -\left\{ \sum_{j=0,1} \left[\sum_{i=0,1} P(j|i)\, P(i) \right] \log_2 \left[\sum_{i=0,1} P(j|i)\, P(i) \right] \right\}$$

$$= -\Big\{ [P(j=0|i=0)\, P(i=0) + P(j=0|i=1)\, P(i=1)] \log_2$$

$$[P(j=0|i=0)\, P(i=0) + P(j=0|i=1)\, P(i=1)]$$

$$+ [P(j=1|i=0)\, P(i=0) + P(j=1|i=1)] \log_2 [P(j=1|i=0)\, P(i=0)$$

$$+ P(j=1|i=1)\, P(i=1)] \Big\} \qquad (3.88)$$

$$H(j|i) = -\sum_{i=0,1} P(i) \sum_{j=0,1} P(j|i) \log_2 P(j|i)$$

$$= -\Big\{ P(i=0)\, [P(j=0|i=0) \log_2 P(j=0|i=0) + P(j=1|i=0) \log_2$$

$$P(j=1|i=0)] + P(i=1)\, [P(j=0|i=1) \log_2 P(j=0|i=1)$$

$$+ P(j=1|i=1) \log_2 P(j=1|i=1)] \Big\} \qquad (3.89)$$

Let $\rho = P_e(T_p)$ for the gated receiver. Let $\rho = P_m$ for the sampling receiver. The probabilities are explicitly:

$$P(i=0) = (1-k) \qquad (3.90)$$

$$P(i=1) = k \qquad (3.91)$$

$$P(j=0|i=0) = (1-\rho) \qquad (3.92)$$

$$P(j=1|i=0) = \rho \qquad (3.93)$$

$$P(j=0|i=1) = 0 \qquad (3.94)$$

$$P(j=1|i=1) = 1 \qquad (3.95)$$

The expression for the rate R, per clock period, at which information is transmitted by the system is given by Ref. 3.

$$R = H(j) - H(j|i) \text{ bits per clock period} \quad . \tag{3.96}$$

Substituting the probabilities (3.90) through (3.95) into the entropy expressions (3.88) and (3.89) and the entropy expressions into (3.96)

$$R = -\Big\{[(1-\rho)(1-k)] \log_2 [(1-\rho)(1-k)] + [\rho(1-k)+k] \log_2 [\rho(1-k)+k]\Big\} + (1-k)[(1-\rho)\log_2(1-\rho) + \rho \log_2 \rho] \text{ bits per clock period.} \tag{3.97}$$

In terms of the function

$$\mathcal{F}(P) = -[P \log_2 P + (1-P) \log_2 (1-P)] \tag{3.98}$$

$$R = \mathcal{F}[(1-\rho)(1-k)] - (1-k)\,\mathcal{F}(\rho) \text{ bits per clock period} \tag{3.99}$$

Equations (3.97) and (3.99) are expressions for the rate at which information is transmitted by a RADA system using clocked binary modulation and a gated or sampling receiver; in general, when $k = .5$, and when there is little mutual interference, the rate approaches its maximum value of .5 bit per clock period. The rate R is not referred to as the channel capacity of a RADA system since it is assumed here that the source is not necessarily matched to the channel. This assumption is thus consistent with the usual practice of using the direct transmitter

modulator output (without first coding it to maximize the information rate) to drive the transmitter RADA coder. Matching of the source and channel can be achieved either by properly coding the modulated signal prior to RADA coding, or by employing optimal modulations. It appears that coding of the modulator output, prior to RADA coding, would defeat the current simplicity of RADA equipment. Numerical values for the information rate of a RADA system employing clocked binary modulation and a sampling receiver are obtained in Section 6. 6.

CHAPTER IV

EXAMPLES OF RADA SYSTEM PERFORMANCE

4.1 Examples

In this chapter, the results given in Chapter III will be applied to the evaluation of the performance of three specific RADA systems. The three systems will be designated System One, System Two, and System Three. System One employs pulse position modulation, while System Two and System Three employ clocked binary modulation. Ungated and gated receivers, respectively, are assumed for System One and System Two. System Three employs a sampling receiver.

System One--A system using pulse position modulation

An ungated receiver is assumed in Examples 1(a) through 1(e). Then a gated receiver is assumed in Example 1(f).

System One Parameter Values

$\lambda_f = 3$ $\qquad$ $\Delta_t = 1.5$ microseconds

$\Lambda_f = 3$ $\qquad$ $\overline{T} = 125$ microseconds

$\lambda_t = 1$

Ungated Receiver in Examples 1(a) Through 1(e)

Example 1(a). Determine the number m of transmitting transceivers which produce an average error pulse rate of .1 error pulse per frame interval, i.e., given the parameter values above, determine m when $\bar{N}\,\bar{T} = .1$.

Solution 1(a). From the data given for Example 1(a)

$$\bar{N}\,\bar{T} = \bar{N}\,\Delta_t\,\frac{\bar{T}}{\Delta_t} = .10$$

Hence

$$\bar{N}\,\Delta_t = .10\,\frac{\Delta_t}{\bar{T}} = 1.20 \times 10^{-3}$$

Using the $\lambda_f\lambda_t = 3$ curve in Fig. 3.7, the abscissa corresponding to the ordinate $\bar{N}\,\bar{T} = .1$ is $m\lambda_f/\Lambda_f = m = 6.50 \cong 7$.

$$\gamma\Delta_t = \frac{m\lambda_f\lambda_t\Delta_t}{\Lambda_f\,\bar{T}} = 7.80 \times 10^{-2}$$

Alternately, using the normalized curves of Fig. 3.6, for $\lambda_f\lambda_t = 3$, the abscissa corresponding to the ordinate $\bar{N}\,\Delta_t = 1.20 \times 10^{-3}$ is $\gamma\Delta_t = 7.80 \times 10^{-2}$. Hence $m = 6.50 \cong 7$.

Example 1(b). Determine the receiver output error pulse duty factor P_m when there are m transmitting transceivers, m given by Solution 1(a).

Solution 1(b). From Solution 1(a), $\gamma\Delta_t = 7.80 \times 10^{-2}$. The curve in Fig. 3.1 for $\lambda_f\lambda_t = 3$ is used. The ordinate of this curve corresponding to the abscissa $\gamma\Delta_t = 7.80 \times 10^{-2}$ is $P_m = 4.20 \times 10^{-4}$, which is the duty factor of the error pulses at the RADA receiver AND gate output.

Example 1(c). Determine the probability distribution function of the width of error pulses at the receiver output for m given in Solution 1(a).

Solution 1(c). Interpolate a curve for $\gamma\Delta_t = 7.80 \times 10^{-2}$ between the $\gamma\Delta_t = 10^{-1}$ and $\gamma\Delta_t = 10^{-3}$ curves of Fig. 3.5(b). The interpolated curve is approximately the same as the curve for $\gamma\Delta_t = 10^{-3}$, and is the desired probability distribution function in normalized form.

Example 1(d). Assume that a receiver output network prevents error pulses of width less than $.3\Delta_t$ from entering the receiver demodulator. Using the probability distribution function found in Solution 1(c), determine the average number of error pulses which enter the receiver demodulator in a frame interval [m is given by Solution 1(a)].

Solution 1(d). Using the curve determined in 1(c), the ordinate corresponding to $t/\Delta_t = .3$ is $H(.3\Delta_t) = .51$. Since 51 percent of the error pulses are of a width less than $.3\Delta_t$, the number of error pulses which enter the receiver demodulator per frame interval is

$$[1 - H(t)]\,\bar{N}\,\bar{T} = (.49)(.1) = .049$$

Example 1(e). Determine the mean width of error pulses at the AND gate output for m given by Solution 1(a).

Solution 1(e). From (3.55), $\bar{t} = \frac{P_m}{\bar{N}\,\bar{T}}\,\bar{T}$. From Solution 1(b), $P_m = 4.20 \times 10^{-4}$, hence $\bar{t} = .525$ microsecond.

Gated Receiver (e.g., RACEP)

Example 1(f). Consider now a RADA system which has the same parameter values as System One, and which uses gated receivers. Assume that the gate interval T_p is 60 microseconds, and that the probability density function $p_r(\tau_r)$ of message pulse positions with respect to the expected positions of message pulses is normal with a standard deviation of 10 microseconds. Determine, approximately, the probability of a type one false alarm $P_{1FA}(T_p)$ and the false alarm rate $R_{1FA}(T_p)$ when m = 15.

Solution 1(f).

$$\gamma\Delta_t = \frac{m\lambda_f\lambda_t\Delta_t}{\Lambda_f\,\bar{T}} = 1.5\,\frac{\Delta_t}{\bar{T}} = 1.80 \times 10^{-1}$$

From Fig. 3.1,

$$P_m = 4.40 \times 10^{-3}$$

From Fig. 3.6,

$$\bar{N}\,\Delta_t = 1.20 \times 10^{-2}$$

Hence,

$$\bar{\bar{N}} = 8.34 \times 10^3$$

From (3.58),

$$\gamma' = \frac{\bar{\bar{N}}}{1 - P_m} \tag{3.58}$$

$$\gamma' = \frac{8.35 \times 10^3}{1 - 4.40 \times 10^3} \cong 8.35 \times 10^3$$

The nth (even) moment of $p_r(\tau_r)$ when τ_r is normally distributed is

$$\overline{\tau_r^n} = 1 \cdot 3 \cdots (n-1) \left(\overline{\tau_r^2}\right)^{n/2} .$$

Substituting the moment expression into (3.77)

$$P_{1FA}(T_p) = \left[1 - (1 - P_m)\, e^{-\gamma'\left(\frac{T_p - \Delta_t}{2}\right)}\right] - \left[(1 - P_m)\, e^{-\gamma'\left(\frac{T_p - \Delta_t}{2}\right)}\right] \left\{ \sum_{n=2}^{\infty} \frac{1}{(\frac{n}{2})!} \left[\frac{(\gamma')^2 \tau_r^2}{2}\right]^{n/2} \right\} \tag{3.77}$$

$$\overline{\tau_r^2} = (10^{-5})^2 = 10^{-10}$$

$$P_{1FA}(T_p) \cong (1 - e^{-.246}) - e^{-.246} \sum_{n=2}^{\infty} \frac{1}{(\frac{n}{2})!} (3.5 \times 10^{-3})^{\frac{n}{2}}$$

The sum converges rapidly to a small value so that

$$P_{1FA}(T_p) \cong (1 - e^{-.246}) \cong .22$$

The false alarm rate $R_{1FA}(T_p)$ given by Eq. 3.79 is

$$R_{1FA}(T_p) = \frac{P_{1FA}(T_p)}{\bar{T}} = 1760 \text{ false alarms/second} ,$$

which is 22 percent of the 8,000 pulse per second message pulse rate.

System Two--A system using clocked binary modulation

An ungated receiver is assumed in Examples 2(a) through 2(e). A gated receiver is assumed in Example 2(f).

System Two Parameters:

$k = .5$	$\lambda_t = 1$
$\lambda_f = 3$	$\Delta_t = .5$ microsecond
$\Lambda_f = 5$	$T_c = 26$ microseconds

Ungated Receiver in Examples 2(a) Through 2(e)

Give corresponding solutions to 1(a) through 1(e) above for the parameter values of System Two when the average error pulse rate is

.2 error pulse per frame interval, i.e., when $\bar{N}\,\bar{T} = \frac{\bar{N}\,T_c}{k} = .2$

Solution 2(a).

$$\bar{N}\,T_c = \bar{N}\,\Delta_t\,\frac{T_c}{\Delta_t} = .1$$

Hence $\bar{N}\,\Delta_t = .1\,\frac{\Delta_t}{T_c} = 1.925 \times 10^{-3}$.

Using the normalized curve of Fig. 3.6, the abscissa on the $\lambda_f\lambda_t = 3$ curve corresponding to the ordinate $\bar{N}\,\Delta_t = 1.925 \times 10^{-3}$ is $\gamma\Delta_t = 9.2 \times 10^{-2}$. Hence $m = 15.9 \cong 16$. Alternately, using the $\Delta_t = .5$ curve in Fig. 3.8, the abscissa corresponding to the ordinate $\bar{N}\,\bar{T} = .1$ is $mk\lambda_f/\Lambda_f = 4.77$ and $m = 15.9$.

Solution 2(b). From Solution 2(a), $\gamma\Delta_t = 9.2 \times 10^{-2}$. From the curve for $\lambda_f\lambda_t = 3$ in Fig. 3.1 the ordinate corresponding to the abscissa $\gamma\Delta_t = 9.2 \times 10^{-2}$ is $P_m = 6.6 \times 10^{-4}$ which is the duty factor of the error pulses at the RADA receiver AND gate output.

Solution 2(c). Interpolate a curve for $\gamma\Delta_t = 9.2 \times 10^{-2}$ between the curves of Fig. 3.5(b) for $\gamma\Delta_t = .001$ and $\gamma\Delta_t = .10$. The interpolated curve is approximately the same as the curve for $\gamma\Delta_t = .10$, and is the desired distribution function in normalized form.

Solution 2(d). From the curve determined in Solution 2(c), $H(.3\Delta_t) = .490$. The number of error pulses which enter the receiver demodulator per frame interval is

$$[1 - H(t)] \frac{\bar{N} T_c}{k} = (.51)(.2) = .102$$

Solution 2(e). From (3.55),

$$\bar{t} = \frac{P_m}{\bar{N}}$$

Hence $\bar{t} = .171$ microsecond.

Example 2(f). Gated Receiver (e.g., RADEM). Consider a RADA system with the parameters given for System Two, using a gated receiver. Assume that the gate interval T_p is 1 microsecond. Determine the approximate probability of a type two false alarm $P_{2FA}(T_p)$, and the type two false alarm rate $R_{2FA}(T_p)$ when m = 80.

Solution 2(f).

$$P_{2FA}(T_p) = (1-k) P_e(T_p) \tag{3.80}$$

$$R_{2FA}(T_p) = \frac{P_{2FA}(T_p)}{T_c} \tag{3.81}$$

where

$$P_e(T_p) \cong P_m + (1-P_m)\left(1 - e^{-\gamma' T_p}\right) \tag{3.58}$$
$$\tag{3.60}$$
$$\tag{3.62}$$

$$\gamma' = \frac{\bar{N}}{1 - P_m}$$

From Fig. 3.6

$$\tilde{N}\,\Delta_t = 1.20 \times 10^{-1}; \qquad \tilde{N} = 2.4 \times 10^{5}$$

From Fig. 3.1

$$P_m = 5.0 \times 10^{-2}$$

$$\gamma' = 2.4 \times 10^{5}; \qquad \gamma' T_p = 2.4 \times 10^{-1}$$

$$1 - e^{-\gamma' T_p} = 1 - e^{-.24} = .214$$

From (3.58), (3.60), and (3.62),

$$P_e(T_p) \cong .253$$

$$P_{2FA}(T_p) \cong .126$$

$R_{2FA}(T_p) \cong 4.85 \times 10^{3}$, which is 25.3 percent of the 19.2×10^{3} pps message pulse rate.

System Three--A system using clocked binary modulation.

The system uses a sampling RADA receiver.

System Three Parameters

$k = .125$	$\lambda_t = 1$
$\lambda_f = 3$	$\Delta_t = .5\ \mu\text{sec}$
$\Lambda_f = 5$	$T_c = 26\ \mu\text{sec}$

Example 3(a). Determine the system three false alarm probability P_{SFA} and false alarm rate R_{SFA} when m = 80.

Solution 3(a).

$$P_{SFA} = (1-k)\, P_m \tag{3.82}$$

$$R_{SFA} = \frac{P_{SFA}}{T_c} \tag{3.83}$$

$$\gamma\Delta_t = \frac{m k \lambda_f \lambda_t \Delta_t}{\Lambda_f T_c} = 1.15 \times 10^{-1}$$

From (3.1),

$$P_m = 1.30 \times 10^{-3}$$

From (3.82) and (3.83),

$$P_{SFA} = 1.14 \times 10^{-3}$$

R_{SFA} = 43.9 false alarms per second, which is .912 percent of the 4813 pps message pulse rate of System Three.

4.2 Conclusions

The performance characteristics of the three systems described in Section 4.1, as well as those of two other systems, which employ sampling receivers, are presented in Table 4.1. Included in the table

Parameter Values	SYSTEM ONE		SYSTEM TWO		SAMPLING SYSTEM ONE	SAMPLING SYSTEM TWO	SAMPLING SYSTEM THREE (SYSTEM THREE)
	$\Lambda_f = 3$ $\Delta_t = 1.5$ μsec $\lambda_f = 3$ $\lambda_t = 1$ $\bar{T} = 125$ μsec		k = .5 $\Lambda_f = 5$ $\Delta_t = .5$ μsec $\lambda_f = 3$ $\lambda_t = 1$ $T_c = 26$ μsec		k = .5 $\Lambda_f = 3$ $\Delta_t = 1.5$ μsec $\lambda_f = 3$ $\lambda_t = 1$ $T_c = 125$ μsec	k = .5 $\Lambda_f = 5$ $\Delta_t = .5$ μsec $\lambda_f = 3$ $\lambda_t = 1$ $T_c = 26$ μsec	k = .125 $\Lambda_f = 5$ $\Delta_t = .5$ μsec $\lambda_f = 3$ $\lambda_t = 1$ $T_c = 26$ μsec
	UNGATED	GATED $T_p = 60$ μsec	UNGATED	GATED $T_p = 1$ μsec			
Modulation	PPM	PPM	DELTA	DELTA	---	DELTA	e.g., DATEC, Ref. 14
$W_n = 2\Lambda_f/\Delta_t$	2.56 Mc	2.56 Mc	12.8 Mc	12.8 Mc	2.56 Mc	12.8 Mc	12.8 Mc
Data Sampling Rate $1/\bar{T}$ or $1/T_c$	8×10^3/sec	8×10^3/sec	3.85×10^4/sec	3.85×10^4/sec	8×10^3/sec	3.85×10^4/sec	3.85×10^4/sec
Message Pulse Rate, $k/\bar{T}$ or k/T_c	8×10^3/sec	8×10^3/sec	1.925×10^4/sec	1.925×10^4/sec	4×10^3/sec	1.925×10^4/sec	4.813×10^3/sec
m	7	15	16	80	80	80	80
$\gamma\Delta_t$		1.80×10^{-1}	9.2×10^{-2}	4.62×10^{-1}	4.80×10^{-1}	4.62×10^{-1}	1.15×10^{-1}
$\bar{N}\,\bar{T}$	10^{-1}	1.00	2×10^{-1}	6.24	---	---	---
P_m	4.20×10^{-4}	4.40×10^{-3}	6.6×10^{-4}	5.0×10^{-2}	5.50×10^{-2}	5.00×10^{-2}	1.30×10^{-3}
$\bar{t}$	.525 μsec	.551 μsec	.171 μsec	.208 μsec	---	---	---
False Alarm Probability	---	2.2×10^{-1}/sample	---	1.26×10^{-1}/sample	2.75×10^{-2}/sample	2.50×10^{-2}/sample	1.14×10^{-3}/sample
False Alarm Rate	---	$R_{1FA} = 1.76 \times 10^3$/sec	---	$R_{2FA} = 4.85 \times 10^3$/sec	$R_{SFA} = 220$/sec	$R_{SFA} = 9.61 \times 10^2$/sec	$R_{SFA} = 4.39 \times 10^1$
$\frac{\text{False Alarm Rate}}{\text{Message Pulse Rate}}$	---	2.2×10^{-1}	---	2.53×10^{-1}	5.50×10^{-2}	5.00×10^{-2}	9.12×10^{-3}

Table 4.1. Comparison of Systems One, Two, Three.

are values of Δ_t, the width of the rectangular pulses, and W_n, the system bandwidth. The nominal width of pulses of arbitrary shape is defined, and related to the "equivalent rectangular width," Δ_t, of a pulse in Section 5.3. In particular, it is shown in that section, that the "equivalent rectangular width" of a Gaussian pulse approximately equals the width of the pulse measured between the half voltage points of the pulse envelope. The system bandwidth W_n is related to the equivalent rectangular pulsewidth Δ_t in Section 5.4 by

$$W_n = 1.28\, \Lambda_f/\Delta_t \ . \qquad (5.22)$$

This expression for bandwidth is based upon the assumption of Gaussian transmitted pulses, and upon other assumptions as discussed in Section 5.4.

System One uses pulse position modulation; clocked 8 kc Nyquist samples of the voice waveform position-modulate the pulses of an 8 kc pulse train. The system bandwidth is $W_n = 2.56$ Mc. With m = 7 transmitters interfering, $\bar{N}\,\bar{T} = .1$, so that on the average one error pulse occurs for every ten message pulses. Thus, the system provides fair receiver output voice quality (see Section 3.1) with as many as 7 interfering transmitters.

Let System One now be modified to include a post gate which gates an interval of ± 30 microseconds on either side of the expected position of a message pulse. The standard deviation of the positions of

the message pulses about their expected positions in 10 microseconds --the message pulses almost always occur within the post gate interval. With fifteen interfering transmitters (m = 15), $P_{1FA} = .22$ for the gated receiver, so that there is approximately one false alarm, on the average, for every five post gate output message pulses. Thus, this system can accommodate 16 transmitters (including the target transmitter), but with poor quality receiver output voice signals.

Within the transmitter of System Two, delta modulation characterizes the voice information as a clocked 38.5 kc digit stream with a duty factor k = .5 (an average of 19.25×10^4 pulses per second). System Two requires five times as much bandwidth ($W_n = 12.8$ Mc) as System One. With m = 16 interfering transmitters, and when ungated receivers are considered $\bar{N}\,\bar{T} = .20$ for System Two. Although with ungated receivers, the value of $\bar{N}\,\bar{T}$ is larger for System Two ($\bar{N}\,\bar{T} = .20$) with m = 16 than for System One ($\bar{N}\,\bar{T} = .10$) with m = 7, the receiver output signal quality will be approximately the same in both cases as a result of the integration of message samples in the System Two receiver. Thus, System Two can accommodate more than twice as many subscribers (m = 16) as System One (m = 7) with roughly equivalent quality, when ungated receivers are used in both cases.

Use of gated receivers with System Two considerably improves the system performance. With gated receivers five times as many transmitters (m = 80) can be accommodated as with ungated receivers,

in the same bandwidth (W_n = 12.8 Mc), and with approximately the same ratio of error pulses to message pulses in both cases (ungated, $\bar{N}\,\bar{T}$ = .20; gated, $\frac{\text{false alarm rate}}{\text{message pulse rate}}$ = .253). The greater effectiveness of the post gate in improving system performance in this case relative to its effectiveness in improving the performance of System One results from the shorter post gate interval used with System Two.

The parameter values of the first system in Table 4.1 which employs clocked binary modulation and a sampling receiver, Sampling System One, are tabulated in column five. The parameter values of this system (T_c = 125 microseconds, k = .5) would result in excessive quantization noise if applied to the representation of voice by any of the clocked binary modulations; for example, these values would apply to the characterization of voice by 8 kc samples of clipped voice, a characterization with excessive distortion caused by the coarse quantization. The parameter values of Sampling System One were chosen to allow a direct comparison with System One. The sampling system samples the information at the same rate (8 kc) as System One (although System One is not constrained to transmit clocked samples) and requires the same bandwidth (W_n = 2.56 Mc). With more than five times as many users (m = 80) as System One (m = 15), and when both systems employ sampling receivers, the sampling system has a smaller ratio of error pulses to message pulses (5.5×10^{-2}) than System One (2.2×10^{-1}). Despite this smaller ratio quality of the sampling system, the receiver voice

signals will be poor as a result of the distortion introduced by coarse quantization.

The parameters of a second system using clocked binary modulation and a sampling receiver, Sampling System Two, are tabulated in column 6. This system employs the same data sampling rate (3. 85 x 10^4 samples/second) and the same bandwidth (W_n = 12. 8 Mc) as System Two using a gated receiver and accommodates the same number of active users (m = 80). However, the ratio of error pulses to message pulses of this system is smaller (5. 00 x 10^{-2}) than that of System Two (2. 53 x 10^{-1}). The superior performance of Sampling System Two in comparison to System Two is a manifestation of the fact that it is less probable that an error pulse will be sampled than it is that the pulse will occur within the post gate interval T_p.

The parameters of Sampling System Three, which uses clocked binary modulation and a sampling receiver are tabulated in Table 4. 1, column seven. This system is System Three of Section 4. 1. With the exception of the value of k, the parameter values of System Three are the same as those of System Two and those of the Sampling System Two; the data sampling rate (3. 85 x 10^4 samples per second), the system bandwidth (W_n = 12. 8 Mc), and the number of system users (m = 80) are also the same. The duty factor k = . 125 of the transmitter modulator output information pulse train corresponds to an average of 4813 information pulses per second. This pulse rate, which is smaller than that

used in System Two and in Sampling System Two, is consistent with the rates which have been achieved with the most recent modulation methods (Ref. 14). As a result of this reduced pulse rate, the ratio of error pulses to message pulses (9.12×10^{-3}) is smaller than the ratios for both System Two (2.53×10^{-1}) and for Sampling System Two (5.00×10^{-2}).

Four fundamental points are illustrated by the preceding examples. First, clocked binary modulation is preferable to position modulation because it permits the use of post gates with short gate intervals, which results usually in superior performance.

Second, the performance of the sampling receiver is superior to that of the gated receiver for detecting signals with clocked binary modulation, provided the gated receiver doesn't employ pulse width discrimination or filtering and thresholding (Section 5.6).

Third, for good RADA system performance in heavy mutual interference situations, it is best to transmit samples of the information at the lowest rate $1/\overline{T}$ which provides a suitable quality demodulated signal. A given increase in $1/\overline{T}$ typically increases the false alarm rate of the receiver samples more than enough to offset the decrease in signal-to-noise ratio which results from integrating the message samples.

Fourth, RADA system performance generally improves with bandwidth.

CHAPTER V

FURTHER CONSIDERATIONS

5.1 Introduction

In Chapter III, an idealized model of a RADA communications system was developed and analyzed. The detected RF pulses were assumed to be rectangular in the model. In this chapter, the results of Chapter III are extended to apply to general pulse shapes. In addition, several considerations in the application and design of RADA systems are investigated. First, the duration and bandwidth of a pulse are defined, and the relation between them is presented. Next, using these results, the "effective rectangular width" of a pulse is defined for pulses of general shape; this definition allows application of the results of Chapter III when general pulse shapes are studied. The factors which influence system bandwidth are examined, and the system bandwidth is defined. Then the effects of variation of system parameters, and the choice of parameter values to optimize system performance are studied. Finally, practical problems, including reduction of the error pulse rate at the RADA receiver output terminals and synchronization of target RADA receivers to their given transmitters, are investigated.

5.2 Relations Between Duration and Bandwidth of a Pulse

The "nominal bandwidth" B and "nominal duration" T of a single transmitted pulse will now be defined and related. The RADA system bandwidth will then be expressed in terms of the nominal pulse bandwidth. The synonymous terms "width" and "duration" of a pulse were defined in Chapter III for rectangular pulses. To permit a clear distinction of the definitions of the width and duration of a pulse as defined in Chapter III from the definitions used in this chapter, the terms "nominal width" and "nominal duration" of a pulse are defined here. The term "nominal bandwidth" of a pulse is also employed in this chapter in the interests of consistency. The basic concepts involved in the definitions of the nominal duration and nominal bandwidth of a pulse are described in detail in Ref. 26. In defining these terms, some preliminary definitions are required first. Assume an RF pulse with an envelope p(t), a carrier frequency f_o, and a phase θ. The voltage waveform of the pulse is specified by (5.1).

$$e(t) = p(t) \cos(2\pi f_o t + \theta) \tag{5.1}$$

The Fourier transform $F_p(f)$ of the envelope p(t) is given by (5.2)

$$F_p(f) = \int_{-\infty}^{\infty} p(t)\, e^{-j2\pi ft}\, dt \tag{5.2}$$

and that of e(t) by (5.3).

$$F_e(f) = \int_{-\infty}^{\infty} e(t)\, e^{-j2\pi ft}\, dt \qquad (5.3)$$

The energy spectra $W_p(f)$ and $W_e(f)$ of p(t) and e(t), respectively, are presented in (5.4) and (5.5), in which ψ^* of a complex function ψ denotes the complex conjugate of the function ψ, and where $|y|$ of a function y denotes the absolute value of y.

$$W_p(f) = F_p(f)\, F_p^*(f) = |F_p(f)|^2 \qquad (5.4)$$

$$W_e(f) = F_e(f)\, F_e^*(f) = |F_e(f)|^2 \qquad (5.5)$$

Except for an amplitude scale factor, the energy spectrum $W_e(f)$ is just a translation of the spectrum $W_p(f)$ from a symmetric spectrum centered at zero frequency to a symmetric spectrum centered at frequency f_o; it is emphasized that the spectrum $W_p(f)$ which is translated is the two sided or symmetric spectrum centered at zero frequency. Thus, it is only necessary to determine the nominal bandwidth of this symmetric spectrum of the pulse envelope p(t) to define the bandwidth of the pulse e(t). The total energy E_p of the pulse envelope p(t) [which is twice the energy of the actual RF pulse e(t)] is used to normalize the instantaneous pulse envelope energy and the pulse envelope energy spectrum.

$$E_p = \int_{-\infty}^{\infty} p^2(t)\, dt = \int_{-\infty}^{\infty} |F_p(f)|^2\, df = \int_{-\infty}^{\infty} W_p(f)\, df \qquad (5.6)$$

The center c_p of the pulse p(t) is defined by (5.7).

$$c_p = \int_{-\infty}^{\infty} t \frac{p^2(t)}{E_p} dt \tag{5.7}$$

The nominal pulse width T, in seconds, is defined as

$$T = 2 \sqrt{\int_{-\infty}^{\infty} (t - c_p)^2 \frac{p^2(t)}{E_p} dt} \tag{5.8}$$

and the nominal bandwidth B of the pulse, in cycles per second, is defined by (5.9).

$$B = 2 \sqrt{\int_{-\infty}^{\infty} f^2 \frac{|F_p(f)|^2}{E_p} df} \tag{5.9}$$

For any particular pulse envelope p(t), the nominal pulse width T and the nominal bandwidth B are related by (5.10)

$$B = \frac{b}{T}; \qquad b \geq \frac{1}{\pi} \tag{5.10}$$

where the constant b is a function of the envelope shape p(t) which is determined by substituting (5.8) and (5.9) into (5.10). It is emphasized here that the pulsewidth and bandwidth are defined in terms of the standard deviation of the pulse envelope p(t) squared and the magnitude of the complex spectrum $|F(f)|$ squared.

Equation (5.10) is satisfied by $b = 1/\pi$, if and only if, the pulse envelope is Gaussian. Thus, the nominal bandwidth B of a

Gaussian pulse of nominal width T is less than the nominal bandwidth of a pulse of any other shape which is also of nominal width T. Since the bandwidth of a RADA system decreases as the bandwidth of the transmitted pulses decreases, it follows that where there is interest in minimal system bandwidth, RF pulses with Gaussian-shaped envelopes will usually be employed. The utility of Gaussian pulses in the design of minimal bandwidth RADA systems warrants a further description of their characteristics. In terms of the standard deviation σ_1 of the Gaussian pulse envelope voltage p(t), the nominal pulse width T is given by (5. 11).

$$T = \sqrt{2}\,\sigma_1 \tag{5.11}$$

Similarly, in terms of the standard deviation, σ_2, of the amplitude of the complex spectrum, the nominal bandwidth is given by

$$B = \sqrt{2}\,\sigma_2 \quad . \tag{5.12}$$

It follows from (5. 11) and (5. 12) that the nominal pulse duration T of a Gaussian pulse is measured between the positions of the pulse which are .776 of the peak pulse amplitude; the nominal bandwidth is measured between points on the complex spectrum $F_p(f)$ which are .776 of the peak of the spectrum, or between points of the energy spectrum $W_p(f)$ which are .607 of the peak of the energy spectrum. Since pulse widths are frequently measured between points on the envelope of the

pulse which are 50 percent of the envelope peak, the pulse width $T_{.50}$ measured between these points is, here, related to the nominal width of the pulse. For a Gaussian pulse

$$T_{.50} = 1.665\ T \tag{5.13}$$

5.3 Equivalent Rectangular Width of a Pulse

To apply the results of Chapter III, which were derived for the special case of rectangular transmitted pulses, to the general case in which pulse shapes are chosen freely; it is assumed that all pulses of nominal duration T have the same effect on RADA system performance as rectangular pulses, of nominal duration T. This assumption is reasonable in an average sense, since most of the receiver input pulses are from distant transmitters (transmitters separated from the receiver by distances of from 25 percent to 100 percent of the maximum receiver range). The average width of these pulses is typically of the order of the equivalent rectangular width of the transmitted pulses. The nominal duration T of a rectangular pulse of width Δ_t is, using (5.8), $T = \Delta_t/\sqrt{3}$. It follows, then, from these assumptions, that all pulses of nominal duration T are equivalent in their effect on RADA systems to rectangular pulses of width

$$\Delta_t = \sqrt{3}\ T\ . \tag{5.14}$$

From (5. 13) and (5. 14), the equivalent rectangular width of a Gaussian pulse is related to the width $T_{.50}$ by (5. 15).

$$\Delta_t = 1.04\ T_{.50} \tag{5.15}$$

Thus, the equivalent rectangular width of a Gaussian pulse approximately equals the width of the pulse measured between the half-voltage points of the pulse envelope.

5. 4 Bandwidth of a RADA System

A basic requirement of RADA receivers is that a target receiver detects signal pulses from a distant given transmitter even in the presence of strong interference from local interfering transmitters. In such a situation, as discussed in Section 1. 4. 5, the large interference pulses on a particular system frequency will enter the target receiver RF stage at that frequency and also, through the skirts of the RF filters, the RF stages at adjacent frequencies. Further, the interference effects of the large pulses will tend to be enhanced by the stretching of these pulses caused by receiver sensitivity, and their blocking effect caused by receiver recovery characteristics. These undesirable effects are reduced by properly shaping the transmitted pulses and the receiver RF and IF filters, and by allocating sufficient guardband width between the system frequencies to provide adequate RF and IF filter skirt rejection. Since the net parameters determine the guardband

width, they also influence the total system bandwidth requirement. Thus, the net parameters, transmitted pulse shape, and receiver filter characteristics are among the factors which determine the system bandwidth. Because the system bandwidth does depend upon a variety of factors, it is best determined empirically. To facilitate this, an analytic definition of bandwidth, in which the effects of the net characteristics are isolated, will be presented in this section. In the definition, it is assumed that the shape of the individual transmitted pulses determines the bandwidth of the pulse transmissions on each frequency. This assumption is correct for systems which radiate at most a single pulse on each frequency of a frame (systems for which $\lambda_t = 1$); although the assumption is not strictly correct for RADA systems which radiate more than one pulse, ($\lambda_t > 1$), it will also be used to obtain approximations for the bandwidth of these systems.

The nominal bandwidth of the individual transmitted pulses was defined in Section 5.2. This bandwidth will be used now in defining the bandwidth of a RADA system. To reduce the mutual interference between pulses which occur in the same time slot and on adjacent system frequencies, a guardband B_g is allowed between the system frequencies. The guardband width is determined by the net parameters. The total RADA system bandwidth is given by (5.16).

$$W = \Lambda_f(B + B_g) \tag{5.16}$$

or, substituting (5.10) into (5.16), by (5.17).

$$W = \Lambda_f \left(\frac{b}{T} + B_g \right) ; \qquad b \geq \frac{1}{\pi} \tag{5.17}$$

For use with the results of Chapter III, it is more convenient to express (5.17) in terms of the equivalent rectangular pulsewidth which provides a specified level of performance, by substituting (5.14) into (5.17)

$$W = \Lambda_f \left(\sqrt{3} \, \frac{b}{\Delta_t} + B_g \right) ; \qquad b \geq \frac{1}{\pi} \tag{5.18}$$

When Gaussian pulses are used, an estimate of the system bandwidth $W = W_n$ can be determined as follows. Assuming that the power spectrum of a pulse on a given system frequency is 60 db down at the adjacent system frequencies, then

$$B_g = 1.33 \; B \; . \tag{5.19}$$

Substituting $b = \frac{1}{\pi}$ and (5.19) into (5.16),

$$W_n = .741 \, \frac{\Lambda_f}{T} \; . \tag{5.20}$$

In terms of the pulse duration between 50 percent points on the pulse voltage envelope,

$$W_n = 1.24 \, \frac{\Lambda_f}{T_{.50}} \tag{5.21}$$

or in terms of the equivalent rectangular pulsewidth,

$$W_n = 1.28 \frac{\Lambda_f}{\Delta_t} \tag{5.22}$$

Equation(5.22) relates the system bandwidth to the parameters of the model of Chapter III. The bandwidth W_n is the bandwidth of the system spectrum between points which are 60 db below the peak of the spectrum. Equation(5.22) will be used in the bandwidth calculations of Chapter VI.

The bandwidth W_m of one of the prototype systems (Ref. 1.8, p. 50), measured between 6 db points of the power spectrum, is given by

$$W_m = 1.5 \frac{\Lambda_f}{T_{.50}} ; \qquad \Lambda_f = 3 ,$$

$$T_{.50} = 1.5 \times 10^{-6} \text{ second} \tag{5.23}$$

The wider bandwidth of this system compared with a system using Gaussian pulses appeared to result directly from the (non-Gaussian) shape of the transmitted pulses.

5.5 The Effects of Parameter Variations on System Performance, and the Optimization of RADA System Performance

In this section, the effect on RADA system performance of differential variations of the values of the system parameters is investigated. This investigation leads to methods of optimizing the

performance of RADA systems; these methods, in general, necessitate complicating the system or increasing the system bandwidth. Although some of the parameters can only assume discrete values, useful information is nevertheless obtained about the system by investigating the effects of differential changes of the parameter values. Consider that the measure of system performance is P_{FA}, which may be $P_{1FA}(T_p)$, or $P_{2FA}(T_p)$ for gated receivers, P_{SFA} for sampling receivers, and P_m or $\bar{N}\Delta_t$ for ungated receivers. When $\bar{N}\Delta_t$ is the measure, the region of the positive slope of the plot of $\bar{N}\Delta_t$ vs. $\gamma\Delta_t$ is of interest. Typically, these measures, P_{FA}, of system performance are functions of both $\gamma\Delta_t$ and $\lambda_f\lambda_t$ so that

$$P_{FA} = P_{FA}(\gamma\Delta_t, \lambda_f\lambda_t) \quad . \tag{5.24}$$

System performance is improved by differential changes in parameter values when these changes cause a negative differential dP_{FA} (reduce P_{FA}). In the following paragraphs, the requirements for a negative differential are investigated. Because it is already known that in the case of gated receivers, a decrease of gate width T_p decreases P_{FA}, the effects of differential variations of T_p are not studied. Similarly, since it can readily be shown that a decrease in the number m of interfering transmitters always decreases P_{FA}, and since in addition m is a parameter which is not subject to control in normal RADA system operation, it is assumed that m is constant when

the effect of differential parameter variations is studied. Again, because m is not normally subject to control, it is also assumed constant when parameter values are selected to optimize system performance. In writing equations for systems which use clocked binary modulation, $\overline{T}$ can be replaced by T_c/k [see (1.4)] wherever it appears; in this section, $\overline{T}$ is employed in the equations for clocked binary modulation as well as in those for pulse position modulation to avoid duplication of the equations. When Λ_f is specified, differential increments of λ_f are only meaningful when λ_f is not a function of $\Lambda_f [\lambda_f \neq F(\Lambda_f)]$. A similar problem does not normally arise with respect to λ_t and Λ_t since in the cases which are typically considered, λ_t is not constrained by Λ_t, except that $\lambda_t < \Lambda_t$.

The total differential of P_{FA} is expressed in terms of differential changes of $(\gamma\Delta_t)$ and $(\lambda_f\lambda_t)$ in (5.25)

$$dP_{FA} = \frac{\partial P_{FA}}{\partial(\gamma\Delta_t)}\, d(\gamma\Delta_t) + \frac{\partial P_{FA}}{\partial(\lambda_f\lambda_t)}\, d(\lambda_f\lambda_t) \qquad (5.25)$$

In a particular situation, the partials of P_{FA} with respect to $\gamma\Delta_t$ and with respect to $\lambda_f\lambda_t$ can be determined from the graph of the appropriate measure P_{FA}, which is plotted in Chapter III. This is the reason for expressing P_{FA} in the particular form of (5.24). The differential $d(\gamma\Delta_t)$ is a function of the differential $d(\lambda_f\lambda_t)$; it is therefore preferable to rewrite (5.25), including the functional dependence of

$d(\gamma\Delta_t)$ on $d(\lambda_f\lambda_t)$. Using (1.2),

$$d(\gamma\Delta_t) = \frac{m\Delta_t}{\Lambda_f \bar{T}}\, d(\lambda_f\lambda_t) + m\lambda_f\lambda_t\, d\left(\frac{\Delta_t}{\Lambda_f \bar{T}}\right) \tag{5.26}$$

Substituting (5.26) into (5.25),

$$dP_{FA} = \left[\left(\frac{m\Delta_t}{\Lambda_f \bar{T}}\right)\frac{\partial P_{FA}}{\partial(\gamma\Delta_t)} + \frac{\partial P_{FA}}{\partial(\lambda_f\lambda_t)}\right] d(\lambda_f\lambda_t) + \left[m\lambda_f\lambda_t \frac{\partial P_{FA}}{\partial(\gamma\Delta_t)}\right] d\left(\frac{\Delta_t}{\Lambda_f \bar{T}}\right) \tag{5.27}$$

For all of the measures P_{FA}, including the measure $\bar{N}\Delta_t$ when only the region of positive slope of the curve of $\bar{N}\Delta_t$ vs. $\gamma\Delta_t$ is of interest,

$$\frac{\partial P_{FA}}{\partial(\lambda_f\lambda_t)} \leq 0 \tag{5.28}$$

$$\frac{\partial P_{FA}}{\partial(\gamma\Delta_t)} \geq 0 \tag{5.29}$$

Equations (5.27), (5.28), and (5.29) are useful in deducing the effects of parameter variations.

5.5.1 The Effect of Differential Changes of Bandwidth, Modulation Efficiency, and of the Number of AND Gate Inputs on the Measure P_{FA}; $\lambda_f \neq F(\Lambda_f)$. The effect of the various parameters on system performance can be determined by examining (5.27) with

cognizance of (5.28) and (5.29). In preference to using the terms positive and negative differential in discussing changes in the parameter values and in the value of P_{FA}, the terms increase and decrease are primarily used. An increase in $\lambda_f\lambda_t$ has two opposite effects which are indicated by the two terms in the bracketed coefficient of $d(\lambda_f\lambda_t)$ in (5.27). First, increasing the number, λ_t, of pulses transmitted on the frequencies of a frame or increasing the number, λ_f, of frequencies on which pulses are transmitted both tend to increase the mutual interference and, thereby, to increase P_{FA}. Second, increasing the number $\lambda_f\lambda_t$ of AND gate inputs tends to decrease dP_{FA}. Whether or not an increase in $\lambda_f\lambda_t$ tends to increase or decrease P_{FA} depends upon the relative size of the two terms of the bracketed coefficient of $d(\lambda_f\lambda_t)$. It also follows from (5.27) that a decrease in $(\Delta_t/\Lambda_f\,\bar{T})$ always tends to decrease P_{FA}; that is, increasing the bandwidth (Λ_f/Δ_t) or increasing the modulation efficiency $\bar{T}$ always tend to improve system performance. The net change in dP_{FA} which results from changes in both $(\lambda_f\lambda_t)$ and $(\Delta_t/\Lambda_f\,\bar{T})$ depends upon the relative sizes of the bracketed terms in (5.26), and upon the size of the changes.

5.5.2 The Effect of Differential Changes of System Bandwidth and Modulation Efficiency on the False Alarm Probability P_{FA}, for a Fixed Number, $\lambda_f\lambda_t$, of AND Gate Inputs; $\lambda_f \neq F(\Lambda_f)$. The effect on the measure P_{FA} of differential changes in the product $\Delta_t/\Lambda_t\,\bar{T}$, of bandwidth and modulation efficiency, when $\lambda_f\lambda_t$ is constant, is

expressed by the partial differential of P_{FA} with respect to $\Delta_t/\Lambda_f \bar{T}$, which is obtained by equating $d(\lambda_f\lambda_t)$ to zero in (5.26).

$$d_{(\Delta_t/\Lambda_f \bar{T})} P_{FA} = m\lambda_f\lambda_t \frac{\partial P_{FA}}{\partial(\gamma\Delta_t)} d\left(\frac{\Delta_t}{\Lambda_f \bar{T}}\right) \qquad (5.30)$$

Equation (5.30) shows that when $(\lambda_f\lambda_t)$ is constant, P_{FA} can only be decreased by increasing bandwidth (Λ_f/Δ_t) or increasing modulation efficiency $\bar{T}$.

5.5.3 Determination of the Number $\lambda_f\lambda_t$ of AND Gate Inputs which Minimizes P_{FA}, when the Product $(\Delta_t/\Lambda_f \bar{T})$ of Bandwidth and Modulation Efficiency is Fixed; $\lambda_f \neq F(\Lambda_f)$. When $(\Delta_t/\Lambda_f \bar{T})$ is constant, (the product of system bandwidth and modulation efficiency is fixed), the effect of differential changes in $(\lambda_f\lambda_t)$ is expressed by the partial differential of P_{FA} with respect to $(\lambda_f\lambda_t)$.

$$d_{(\lambda_f\lambda_t)} P_{FA} = \left[\left(\frac{m\Delta_t}{\Lambda_f \bar{T}}\right) \frac{\partial P_{FA}}{\partial(\gamma\Delta_t)} + \frac{\partial P_{FA}}{\partial(\lambda_f\lambda_t)}\right] d(\lambda_f\lambda_t) \qquad (5.31)$$

The right hand side of (5.31) is identical with the first bracketed term of (5.27), and the comments concerning that term also apply to (5.31). Namely, an increase in $\lambda_f\lambda_t$ tends to increase P_{FA} as a result of the increased number λ_t of interference pulses transmitted on each frequency of a frame, or the increased number, λ_f, of frequencies on which these pulses are transmitted; both changes tend to increase the number of interfering pulses radiated by each transmitter. An increase

in the number $\lambda_f\lambda_t$ of AND gate inputs tends to decrease P_{FA}. The net result is that increases in $\lambda_f\lambda_t$ decrease P_{FA} when

$$-\frac{\partial P_{FA}}{\partial(\lambda_f\lambda_t)} > \left(\frac{m\Delta_t}{\Lambda_f \bar{T}}\right) \frac{\partial P_{FA}}{\partial(\gamma\Delta_t)} \qquad (5.32)$$

When the left hand side of (5.32) is larger than the right, P_{FA} can usually be decreased by increasing $(\lambda_f\lambda_t)$, assuming all other parameters remain constant. As $\lambda_f\lambda_t$ is increased, $\gamma\Delta_t$ increases; typically, as $\gamma\Delta_t$ increases, $-[\partial P_{FA}/\partial(\lambda_f\lambda_t)]$ tends to decrease monotonically and $\partial P_{FA}/\partial(\gamma\Delta_t)$ tends to increase monotonically. When $(\lambda_f\lambda_t)$ is increased beyond a particular value, (5.32) is no longer satisfied and P_{FA} tends to increase. That is, when $\lambda_f\lambda_t$ is increased beyond a certain value, the degradation in system performance which results from increasing the number of interfering pulses radiated on each frequency of a frame or from increasing the number of frequencies on which these interference pulses occur exceeds the enhancement of system performance which results from increasing the number of AND gate inputs. Thus, there is an optimum value of $\lambda_f\lambda_t$ which minimizes P_{FA} when all system parameters except $\lambda_f\lambda_t$ are fixed. Equivalently, since the product $\lambda_f\lambda_t$ does not influence system bandwidth, for a given bandwidth, and number m of users, there is a value of $(\lambda_f\lambda_t)$ which minimizes P_{FA}. One method of determining this minimum value is simply to fix all system parameters and increase $\lambda_f\lambda_t$ until

the minimum is found. Another method is to determine the generally nonrealizable, noninteger value of $\lambda_f\lambda_t$ which satisfies (5.32) with an equality [assuming all system parameter values except $(\lambda_f\lambda_t)$ are fixed].

$$- \frac{\partial P_{FA}}{\partial(\lambda_f\lambda_t)} = \left(\frac{m\Delta_t}{\Lambda_f \bar{T}}\right) \frac{\partial P_{FA}}{\partial(\gamma\Delta_t)} \tag{5.33}$$

Then, of the two integer values of $\lambda_f\lambda_t$ which are adjacent to the noninteger value, the integer value $(\lambda_f\lambda_t) = s$ which corresponds to the smaller value of P_{FA} optimizes system performance. The values of λ_f and λ_t are then selected, subject only to (5.34).

$$\lambda_f\lambda_t = s \; ; \qquad \lambda_f \leq \Lambda_f \tag{5.34}$$

In some cases, rather than choose an optimum value $\lambda_f\lambda_t$, a near optimal value provides nearly equivalent performance and allows a more convenient choice of the values of λ_f and λ_t.

5.5.4 The Effect of Differential Changes of System Parameters on the Measure P_{FA}; $\lambda_f = \Lambda_f$. Depending upon how the RADA system is defined, increments in λ_f and Λ_f may be functionally related. When this is the case, it is preferable to define the total differential of P_{FA} by (5.35).

$$dP_{FA} = \left(\frac{m\Delta_t}{\bar{T}}\right) \frac{\partial P_{FA}}{\partial(\gamma\Delta_t)}\, d\left(\frac{\lambda_f\lambda_t}{\Lambda_f}\right) + \frac{\partial P_{FA}}{\partial(\lambda_f\lambda_t)}\, d(\lambda_f\lambda_t)$$

$$+ \left(m\,\frac{\lambda_f\lambda_t}{\Lambda_f}\right) \frac{\partial P_{FA}}{\partial(\gamma\Delta_t)}\, d\left(\frac{\Delta_t}{\bar{T}}\right) ; \qquad \lambda_f \leq \Lambda_f \tag{5.35}$$

As an example of the application of (5.35), consider a system which is defined with $\lambda_f = \Lambda_f$; that is, each transmitter radiates pulses on all of the system frequencies. For such a system, the total differential of P_{FA} is given by (5.36).

$$dP_{FA} = \left(\frac{m\Delta_t}{\bar{T}}\right) \frac{\partial P_{FA}}{\partial(\gamma\Delta_t)}\, d\lambda_t + \frac{\partial P_{FA}}{\partial(\lambda_f\lambda_t)}\, d(\lambda_f\lambda_t)$$

$$+ (m\lambda_t) \frac{\partial P_{FA}}{\partial(\gamma\Delta_t)}\, d\left(\frac{\Delta_t}{\bar{T}}\right) ; \qquad \lambda_f = \Lambda_f \tag{5.36}$$

Interpreted in conjunction with (5.28) and (5.29), (5.36) can be explained as follows. The first term of (5.36) shows that when the number λ_t of pulses on the frequencies of a frame increases, P_{FA} tends to increase. The second term illustrates the tendency of an increase in the number $(\lambda_f\lambda_t)$ of AND gate inputs to decrease P_{FA}. Finally, the last term of (5.36) shows that increased pulse width and increased modulation efficiency $\bar{T}$ tend to decrease P_{FA}. If is apparent from the first two terms of (5.36) that an increase in λ_f is more effective in decreasing dP_{FA} than a corresponding increase $d\lambda_t$. (Strictly, "corresponding" increases of λ_f and λ_t must satisfy

$\lambda_f \, d\lambda_t = \lambda_t \, d\lambda_f$; the idea here is more precisely that when λ_t is increased, the first term tends to increase P_{FA}, whereas there is no corresponding term which increases when λ_f increases.) This greater effectiveness of λ_f in improving system performance did not occur in the situation associated with (5.27), for which $\lambda_f \neq F(\Lambda_f)$. The reason for the difference is that in the case of (5.27), increasing λ_f, $\lambda_f \neq F(\Lambda_f)$ increases the number λ_f out of the available number Λ_f of system frequencies on which each transmitter radiates, and thus increases the mutual interference on these frequencies. By contrast, in the case of (5.36), $\lambda_f = \Lambda_f$ so that increasing λ_f increases the total number of available frequencies on which all transmitters radiate.

The partial differentials of P_{FA} with respect to $(\Delta_t/\bar{T})$ and with respect to λ_f and λ_t will be written to isolate the influence of these parameters.

$$d_{(\Delta_t/\bar{T})} P_{FA} = m\lambda_t \frac{\partial P_{FA}}{\partial(\gamma\Delta_t)} d\left(\frac{\Delta_t}{\bar{T}}\right); \quad \lambda_f = \Lambda_f \tag{5.37}$$

It follows from (5.29) and (5.37) that when the values of all parameters except Δ_t and $\bar{T}$ are constant, decreased pulse width Δ_t or increased modulation efficiency ($\bar{T}$) decrease P_{FA}.

$$d_{(\lambda_f\lambda_t)} P_{FA} = \left(\frac{m\Delta_t}{\bar{T}}\right) \frac{\partial P_{FA}}{\partial(\gamma\Delta_t)} d\lambda_t + \frac{\partial P_{FA}}{\partial(\lambda_f\lambda_t)} d(\lambda_f\lambda_t); \quad \lambda_f = \Lambda_f \tag{5.38}$$

From (5.28), (5.29), and (5.38), it follows that when the values of all parameters except λ_f and λ_t are constant, P_{FA} decreases when,

$$- \frac{\partial P_{FA}}{\partial(\lambda_f \lambda_t)} \, d(\lambda_f \lambda_t) > \left(\frac{m \Delta_t}{\bar{T}}\right) \frac{\partial P_{FA}}{\partial(\gamma \Delta_t)} \, d\lambda_t \; ; \qquad \lambda_f = \Lambda_f \qquad (5.39)$$

that is, when the improvement in performance resulting from the increased number $(\lambda_f \lambda_t)$ of AND gate inputs exceeds the degradation which results from increasing the number λ_t of interference pulses radiated on each frequency of a frame. When $d\lambda_t = 0$, an increase in λ_f always decreases P_{FA}. However, since $\lambda_f = \Lambda_f$, increasing λ_f increases the system bandwidth, and thus the improvement in performance costs bandwidth. With $d\lambda_f = 0$, an increase in λ_t requires no increase in bandwidth, but this increase only decreases P_{FA} when (5.39) is satisfied.

5.5.5 Determination of the Value of the Paramter λ_t which Minimizes P_{FA} when Other Parameters are Fixed. In this section, the value of λ_t is determined which minimizes P_{FA} when the other parameter values are fixed. In a way similar to that described in connection with (5.32),

$$- \frac{\partial P_{FA}}{\partial(\lambda_f \lambda_t)}$$

generally decreases monotonically with increases in λ_t, while

$$\frac{\partial P_{FA}}{\partial(\gamma \Delta_t)}$$

generally decreases monotonically. Thus when all other system parameters are fixed, it follows from (5.36) that increases in λ_t beyond a particular value tend to increase P_{FA}. It follows that there is a value of λ_t which optimizes system performance when the other parameters are fixed. That is, when the bandwidth and the number m of users are fixed, and the system parameters other than λ_t are fixed, there is a value of λ_t which minimizes P_{FA}. One method of finding this minimum is simply to determine P_{FA} for progressively larger values of λ_t until the minimum is found. Alternately, P_{FA} can be minimized by first determining the (generally noninteger) value of λ_t which satisfies (5.40).

$$- \frac{\partial P_{FA}}{\partial(\lambda_f \lambda_t)} \, d(\lambda_f \lambda_t) = \left(\frac{m \Delta_t}{\bar{T}}\right) \frac{\partial P_{FA}}{\partial(\gamma \Delta_t)} \, d\lambda_t \qquad (5.40)$$

As previously described in connection with (5.33), of the two adjacent integer values of λ_t, the value of λ_t which results in a smaller value of P_{FA} is the one which optimizes system performance.

Examples of the application of some of the results of this section to a system which employs clocked binary modulation and a sampling receiver are given in Chapter VI.

5.6 Mutual Interference Reduction

Direct mutual interference is a primary limiting factor in RADA system performance. The mutual interference and its effects

are characterized by the receiver input RF interference pulse rate and by the receiver output error pulse rate. Techniques which reduce the effective interference pulse rate or the error pulse rate tend to improve receiver performance. Using an appropriate receiver implementation, the interference pulse rate is reduced by discriminating against pulses of different amplitude than the signal pulses, using either an amplitude level discriminator or a cumulative amplitude level discriminator in the receiver video stages (Schmitt trigger). Before a signal is detected, the discriminator searches, say, from high to low pulse amplitude levels for properly coded signals. Efficient modulations, modulations which tend to reduce the average rate at which frames are transmitted, reduce the interference pulse rate. Since the voltage corresponding to a voice waveform is near zero a larger fraction of the time, the interference pulse rate can be reduced by using efficient, voice activated modulations which produce a modulated signal only when there is a significant voice input. Extremal Sampling (Refs. 1.11 - 1.18) and "DATEC" modulation (Ref. 14), a modification of delta modulation, are such voice-actuated modulations. Similarly, a squelch circuit will reduce the interference pulse rate when employed with modulations which are not voice-actuated; the squelch circuit must not distort the demodulated signal, however. Station discipline--prohibition of transmitter use except when necessary--also tends to reduce the interference pulse rate.

Techniques which are effective in reducing the demodulator input error pulse rate will now be presented. The post gate (Section 1.6.2) is effective in reducing the demodulator input error pulse rate. In addition, the results of Chapter III show that in typical situations the duration of error pulses will be significantly shorter than that of the message pulses (see Fig. 3.5, a normalized plot of the duration of error pulses); pulse width discrimination is, therefore, effective in reducing the demodulator input (AND gate output) error pulse rate. This discrimination can be achieved by using either a pulse width discriminator, or by using a filter and a threshold circuit. Examples 1d and 2d of Chapter III illustrate the effectiveness of pulse width discrimination in reducing the error pulse rate. Pulse width discrimination can be employed with both ungated receivers and gated receivers.

5.7 Synchronization

Throughout the preceding chapters, it has been assumed that after initial synchronization the receiver continuously maintains time synchronization with the transmitter during each message transmission. This is a realistic assumption for a RADA system, using a modulation method such as delta modulation, in which frames are transmitted during the pauses in voice.

With the clock stabilities anticipated for small, portable transceivers, and for a system in which no frames are transmitted during pauses in voice, the given receiver may have to time-synchronize to its target transmitter after each voice pause. In this case, synchronization will have to be obtained quickly (say in less than . 1 second) to prevent excessive distortion caused by information loss before synchronization is achieved.

CHAPTER VI

OPTIMAL PERFORMANCE OF A RADA SYSTEM EMPLOYING SAMPLING RECEIVERS

6.1 Introduction

The process by which mutual interference among RADA transmissions generates receiver output errors was described and studied analytically in Chapter III. The bandwidth of RADA systems, the effects of differential changes in the values of the system parameters, and the choice of system parameter values to optimize system performance were investigated in Chapter V. In this chapter, some of the results of Chapter V are illustrated in optimizing the performance and determining the bandwidth of a RADA system employing clocked binary modulation and sampling receivers; the receiver output error characteristics of such a system were described in Section 3.4.5. This particular type of system is utilized to illustrate the results of Chapter V for several reasons. The system is of both practical and theoretical interest because its error rate is a lower bound of the error rates of the systems studied in Chapter III, when the same parameter values are used, and when these systems do not employ pulsewidth discrimination or output filtering and thresholding (see Section 5.6). Further, the analytical expression for the error probability of systems employing

clocked binary modulation and sampling receivers is of a simple form which can readily be optimized.

In this chapter then, the system parameter values are chosen analytically to "optimize" system performance; the theoretical system bandwidth which corresponds to a specified false alarm rate is determined; a method of designing a practical optimum system is described; analytical expressions are given for the rate of information transmission for an "optimum" system and for a "practical" optimum system. Examples are included.

6.2 Optimization of the Performance of a RADA System Employing Clocked Binary Modulation and Sampling Receivers

From (3.1) and (3.82), the false alarm rate of a system employing clocked binary modulation and sampling receivers is given by (6.1).

$$P_{SFA} = (1-k)\left(1 - e^{-\gamma\Delta_t}\right)^{\lambda_f \lambda_t} \qquad (6.1)$$

System performance is now "optimized" by choosing the value of the product $\lambda_f \lambda_t$ to minimize the value of P_{SFA} which corresponds to a given value of $\frac{m k \Delta_t}{\Lambda_f T_c}$; this optimization is discussed in general terms in Chapter V in connection with (5.31), (5.32), (5.33), and (5.34). The rationale for fixing $\frac{m k \Delta_t}{\Lambda_f T_c}$ is that the optimum is based on the assumptions of a fixed number, m, of users, a fixed system bandwidth

(proportional to Λ_f/Δ_t), and fixed modulation parameters, or modulation efficiency (T_c/k). The minimum is determined by equating the partial derivative of P_{SFA} with respect to $(\lambda_f\lambda_t)$ to zero. This partial derivative is denoted here by $d_{(\lambda_f\lambda_t)} P_{SFA}/d(\lambda_f\lambda_t)$, and it is the derivative of P_{SFA} which accounts for the direct dependence of $P_{SFA} = P_{SFA}(\gamma\Delta_t, \lambda_f\lambda_t)$ on $(\lambda_f\lambda_t)$ as well as its implicit dependence on $\lambda_f\lambda_t$ through $\gamma\Delta_t = \dfrac{mk\lambda_f\lambda_t\Delta_t}{\Lambda_f T_c}$. From (5.31),

$$\frac{d_{(\lambda_f\lambda_t)} P_{SFA}}{d(\lambda_f\lambda_t)} = (1-k)\left(1 - e^{-\gamma\Delta_t}\right)^{\lambda_f\lambda_t - 1}\left[-e^{-\gamma\Delta_t}\ln e^{-\gamma\Delta_t} + \left(1 - e^{-\gamma\Delta_t}\right)\ln\left(1 - e^{-\gamma\Delta_t}\right)\right] \quad ; \quad \lambda_f \leq \Lambda_f \tag{6.2}$$

This derivative is distinguished from that partial derivative of P_{SFA} with respect to $(\lambda_f\lambda_t)$, $\partial P_{SFA}/\partial(\lambda_f\lambda_t)$, which does not account for the dependence of $(\lambda_f\lambda_t)$ on $(\gamma\Delta_t)$ (Ref. 27). Since the factor $(1-k)\left(1 - e^{-\gamma\Delta_t}\right)^{\lambda_f\lambda_t - 1}$ is always positive, it does not affect the sign of $d_{\lambda_f\lambda_t} P_{SFA}/d(\lambda_f\lambda_t)$, and it is only necessary to examine the bracketed quantity in (6.2) to find minima of P_{SFA}. Making the substitutions

$$e^{-\gamma\Delta_t} = y \tag{6.3}$$

and

$$-\gamma\Delta_t = \ln y \tag{6.4}$$

the bracketed quantity of (6.2) then becomes

$$-y \ln y + (1-y) \ln (1-y) \quad . \tag{6.5}$$

This function is plotted in Fig. 6.1. It is apparent that there is a single minimum of P_{SFA} at $y = .5$. Hence the requirement for a minimum of P_{SFA} is, from (6.3)

$$e^{-\gamma \Delta_t} = .5 \; ; \qquad \lambda_f \leq \Lambda_f \tag{6.6}$$

or, from (6.4)

$$\gamma \Delta_t = .693 \; ; \qquad \lambda_f \leq \Lambda_f \quad . \tag{6.7}$$

The value of the product $\lambda_f \lambda_t$ which minimizes P_{SFA} is, using (1.2),

$$\lambda_f \lambda_t = .693 \, \frac{\Lambda_f T_c}{mk\Delta_t} \; ; \qquad \lambda_f \leq \Lambda_f \tag{6.8a}$$

or, using (5.22)

$$\lambda_f \lambda_t = .541 \, \frac{T_c W_n}{mk} \; ; \qquad \lambda_f \leq \Lambda_f \tag{6.8b}$$

Substituting (6.2) and (6.8a) into (6.1) the minimum value of P_{SFA}, $P_{SFA}(\min)$ under the constraint $mk\Delta_t/\Lambda_f T_c$ = constant is then,

$$\frac{(1-e^{-\gamma\Delta_t})^{-(\lambda_f\lambda_t-1)}}{1-k}\;\frac{d_{(\lambda_f\lambda_t)}\,P_{SFA}}{d(\lambda_f\lambda_t)} = -y\,\ell n\,y + (1-y)\,\ell n\,(1-y)$$

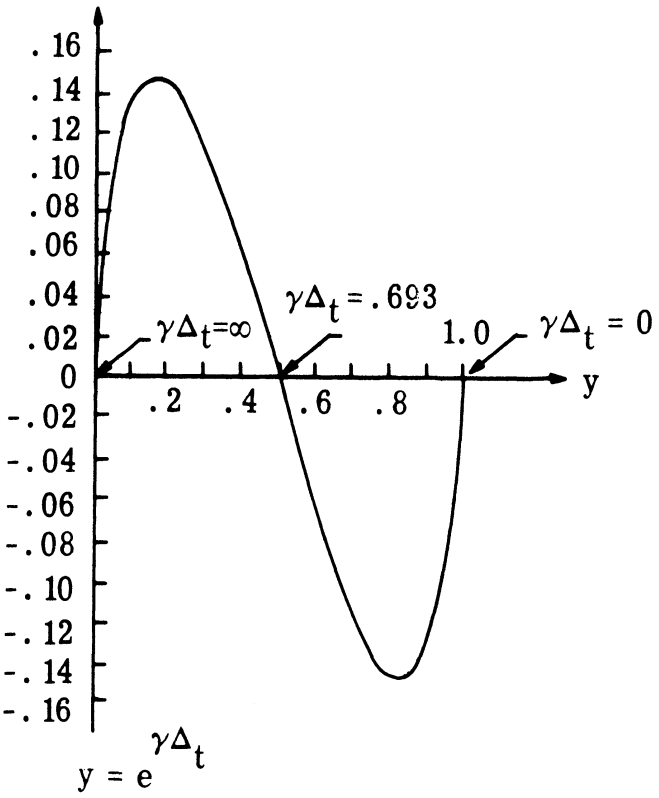

Fig. 6. 1. $-y\,\ell n\,y + (1-y)\,\ell n\,(1-y)$ vs. y.

$$P_{SFA}(\min) = (1-k)\left(1 - e^{-mk\frac{\lambda_f\lambda_t\Delta_t}{\Lambda_f T_c}}\right)^{\lambda_f\lambda_t}$$

$$\lambda_f\lambda_t = \frac{.693\,\Lambda_f T_c}{mk\Delta_t}, \qquad \lambda_f \leq \Lambda_f \tag{6.9a}$$

or,

$$P_{SFA}(\min) = (1-k)(.5)^{.693\frac{\Lambda_f T_c}{mk\Delta_t}}; \qquad (\lambda_f \leq \Lambda_f) \tag{6.9b}$$

or from (6.8b)

$$P_{SFA}(\min) = (1-k)(.5)^{.541\frac{T_c W_n}{mk}}; \qquad (\lambda_f \leq \Lambda_f) \tag{6.9c}$$

It should be remembered that in real systems Λ_f and $\lambda_f\lambda_t$ are integers. If, when the values of the other parameters in (6.9b) are fixed, a specified value of $P_{SFA}(\min)$ determines a noninteger value of Λ_f, then the next larger integer value of Λ_f is used in order not to exceed the specified value of $P_{SFA}(\min)$; that is, substituting the larger, integer value of Λ_f into (6.9b), results in a value of $P_{SFA}(\min)$ which is less than the specified $P_{SFA}(\min)$. The bandwidth W_n for the integer value of Λ_f is greater than that specified for the noninteger Λ_f. In real systems, the product $\lambda_f\lambda_t$ is also an integer. In general, $\lambda_f\lambda_t$ determined

by (6.8a), using the integer value of Λ_f, is not an integer. With the values of all other parameters fixed, it is apparent from Fig. 7.1 that, exclusively, either the high or low integer value of $\lambda_f\lambda_t$ adjacent to the noninteger value of $\lambda_f\lambda_t$ results in the minimum P_{SFA} which can be obtained with an integer value of $\lambda_f\lambda_t$. As mentioned in connection with (5.34), the value of the $\lambda_f\lambda_t$ product chosen in designing a particular system is determined by its practical convenience as well as by the desire to minimize P_{SFA}. If the integer value of $(\lambda_f\lambda_t)$ which minimizes P_{SFA} is impractical, the convenience of the next smaller and next larger integer values is investigated, and so on. For each value of $(\lambda_f\lambda_t)$, P_{SFA} must be examined to determine whether the specified minimum is achieved; if it is not achieved for a particular integer value of $\lambda_f\lambda_t$, then it will not be achieved with the remaining integer values of $(\lambda_f\lambda_t)$ which are also on the same side (less than or greater than) of the noninteger values of $\lambda_f\lambda_t$. If the possible choices of $(\lambda_f\lambda_t)$ which correspond to the initial integer value of Λ_f have been exhausted; then the next larger integer value of Λ_f is selected; the corresponding noninteger value of $\lambda_f\lambda_t$ is determined; and the process of searching for suitable integer values of $\lambda_f\lambda_t$ is repeated. The use of integer values of Λ_f which are larger than the initial integer values requires additional system bandwidth, so that the convenience of various choices of Λ_f and $(\lambda_f\lambda_t)$ must be weighed against the corresponding bandwidth cost.

In the remainder of this chapter, Λ_f and $\lambda_f\lambda_t$ are assumed to be continuous variables to simplify the discussion; determination of the corresponding integer values of Λ_f, λ_f, λ_t which minimize P_{SFA} is apparent in particular cases. The value of $P_{SFA}(\min)$ which corresponds to continuous values of $\lambda_f\lambda_t$ is a lower bound of the value of $P_{SFA}(\min)$ which corresponds to integer values of $\lambda_f\lambda_t$, a lower bound which is attained in those cases when continuous $\lambda_f\lambda_t$ has an integer value. Correspondingly, the information rates defined for continuous $\lambda_f\lambda_t$ are an upper bound.

6.2.1 Optimization of Receiver Performance when λ_f and λ_t are Bounded. Assume that λ_f and λ_t have practical upper bounds, say $\lambda_f \leq \lambda_f'$, $\lambda_t < \lambda_t'$, which are such that

$$\lambda_f'\lambda_t' < .693 \frac{\Lambda_f T_c}{mk\Delta_t} . \tag{6.10}$$

Then it follows from Fig. 6.1 (or from Eq. 5.32) that since P_{SFA} decreases monotonically with $\lambda_f\lambda_t$,

$$\lambda_f\lambda_t < .693 \frac{\Lambda_f T_c}{mk\Delta_t} \tag{6.11}$$

P_{SFA} can be minimized by choosing $\lambda_f = \lambda_f'$, $\lambda_t = \lambda_t'$. Generally, it is more practical to decrease P_{SFA} a given amount by increasing λ_t than by increasing λ_f.

6.2.2 Optimization of Receiver Performance when $\lambda_f = \Lambda_f$.

When $\lambda_f = \Lambda_f$ and Λ_f is permitted to vary, then from (6.8a), (6.12) determines the value of λ_t which minimizes P_{SFA}.

$$\lambda_t = .693 \frac{T_c}{mk\Delta_t} \tag{6.12}$$

From (6.1) and (6.12),

$$P_{SFA}(\min) = (1-k)\left(1 - e^{-\frac{mk\lambda_t\Delta_t}{T_c}}\right)^{\lambda_f\lambda_t} ;$$
$$\lambda_t = \frac{.693\ T_c}{mk\Delta_t} , \qquad \lambda_f = \Lambda_f \tag{6.13a}$$

or,

$$P_{SFA}(\min) = (1-k)(.5)^{\lambda_f\left(\frac{.693\ T_c}{mk\Delta_t}\right)} ; \qquad \lambda_f = \Lambda_f \tag{6.13b}$$

or using (5.22),

$$P_{SFA}(\min) = (1-k)(.5)^{.541\frac{T_c W_n}{mk}} ; \qquad \lambda_f = \Lambda_f \tag{6.13c}$$

It is apparent from a comparison of the functional forms of (6.9a) and (6.13a) that unlike the case where $\lambda_f < \Lambda_f$, P_{SFA} is not symmetric

with respect to $\lambda_f\lambda_t$ when $\lambda_f = \Lambda_f$; when $\lambda_f = \Lambda_f$, P_{SFA} always decreases monotonically with λ_f, and decreases monotonically with λ_t to a minimum at

$$\lambda_t = .693 \frac{T_c}{mk\Delta_t} . \qquad (6.12)$$

The physical basis for the forms of the dependence of P_{SFA} on λ_f and λ_t when $\lambda_f < \Lambda_f$, and when $\lambda_f = \Lambda_f$ is apparent. When $\lambda_f < \Lambda_f$, and Λ_f is fixed, a given fractional increase in λ_f or in λ_t has the same effect --a given fractional increase in the number $\lambda_f\lambda_t$ of AND gate inputs and a given fractional increase in the number $\frac{mk\lambda_f\lambda_t\Delta_t}{\Lambda_f T_c}$ of interference pulses per second on each frequency channel. The first effect tends to decrease P_{SFA}, the second to increase it. When the mutual interference parameter $\gamma\Delta_t < .693$, the decrease is greater than the increase and there is a net reduction in P_{SFA} for increases of λ_f or λ_t (or both). The value of $\lambda_f\lambda_t = .693 \frac{T_c}{mk\Delta_t}$ is the choice of $\lambda_f\lambda_t$ which optimizes system performance. When $\lambda_f = \Lambda_f$ and λ_f varies, a given fractional increase in λ_f increases the number $\lambda_f\lambda_t$ of AND gate inputs, which decreases P_{SFA}; the increase in λ_f also increases the system bandwidth. There is no increase in the number of interference pulses on each frequency channel as there is when $\lambda_f < \Lambda_f$, and Λ_f is fixed. On the other hand, a given fractional increase in λ_t tends to increase the number of gate inputs, decreasing P_{SFA}, and also tends to increase

the number of interference pulses on each channel, increasing P_{SFA}. A given fractional increase in λ_t is therefore less effective than the same fractional increase in λ_f in decreasing P_{SFA}, and will increase P_{SFA} (when $\lambda_t > .693\ T_c/mk\Delta_t$).

Without regard to practical considerations, the optimum RADA receiver is an "adaptive" receiver which increases λ_f and λ_t with decreasing m to satisfy (6.8) or (6.12) at all times.

6.3 Bandwidth of Optimum RADA Systems Employing Clocked Binary Modulation and Sampling Receivers

The bandwidth of an optimum RADA system which employs clocked binary modulation and sampling receivers is readily determined by using the results of Section 6.2. Taking the logarithm of (6.9a) or (6.13c) and rearranging, there results

$$\frac{W_n}{m} = -2.67\ \frac{k}{T_c}\ \ell n \left[\frac{P_{SFA}(\min)}{1-k}\right] ; \qquad \lambda_f \leq \Lambda_f \qquad (6.14)$$

W_n/m is the bandwidth (as defined in Section 5.4) per subscriber of a RADA system which uses the value of $\lambda_f\lambda_t$ which minimizes the false alarm probability. The quantity W_n/m is plotted in Fig. 6.2 in normalized form as a function of $P_{SFA}(\min)/(1-k)$ with k/T_c as a parameter. Thus, for example, assuming $k = .5$, $P_{SFA}(\min) = 10^{-3}$, $T_c = 50$ microseconds, then $W_n/m = 1.66 \times 10^5$ cycles per second per user.

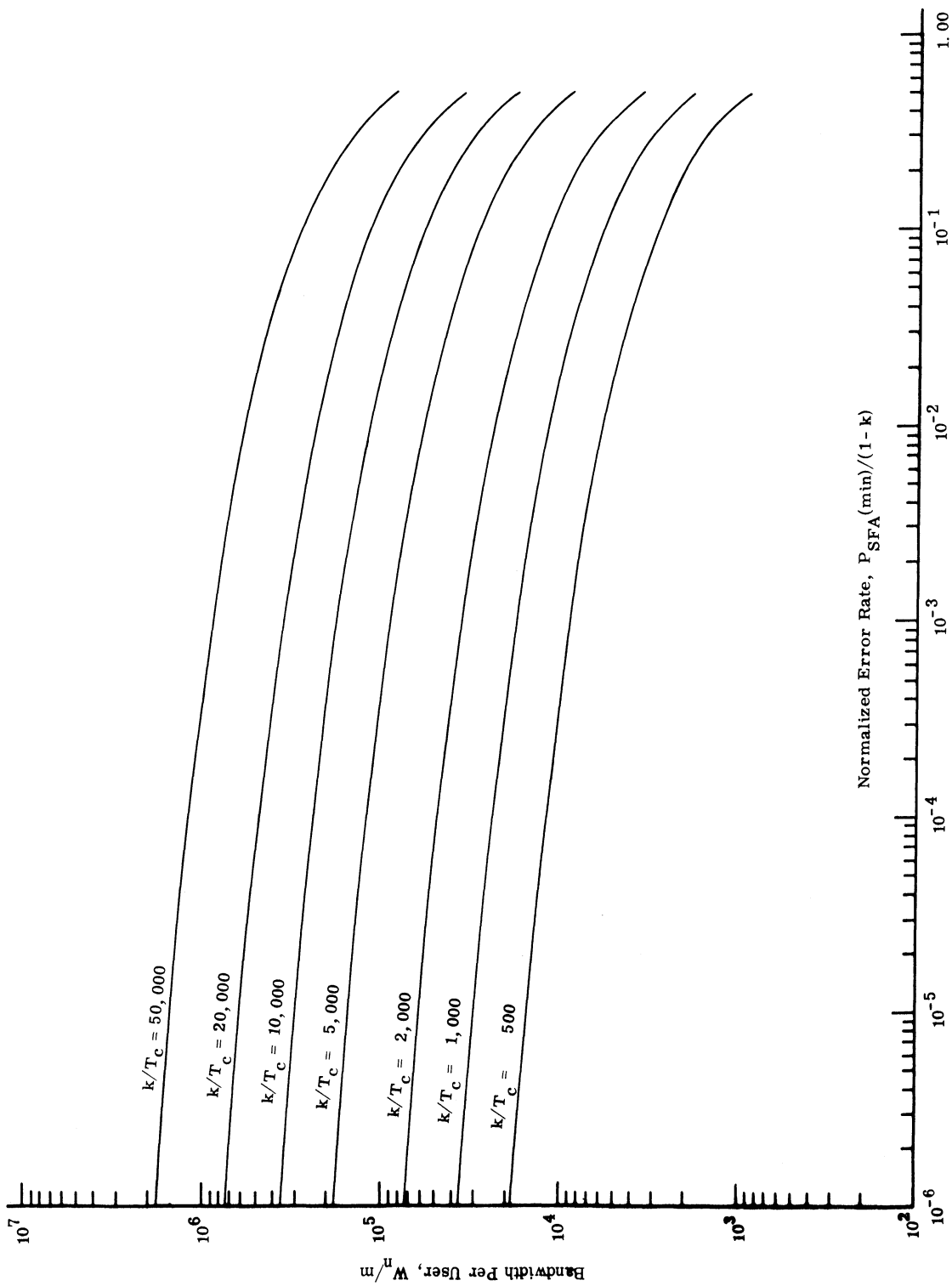

Fig. 6.2. Bandwidth per user, W_n/m, vs. normalized error rate, $P_{SFA}(min)/(1-k)$, for a RADA system employing clocked binary modulation and sampling receivers, and optimal for m users.

Let m in (6. 14) equal Mq_1 where Mq_1 is the design maximum RADA system active subscriber capacity corresponding to a specified false alarm rate $P_{SFA}(\min)$. Then for specified modulation parameters k and T_c the RADA system bandwidth is now given by

$$W_n = -2.67\,(Mq_1)\,\frac{k}{T_c}\,\ell n\left[\frac{P_{SFA}(\min)}{1-k}\right]\;; \qquad \lambda_f \leq \Lambda_f \qquad (6.15)$$

W_n increases linearly with the maximum RADA system subscriber capacity, Mq_1.

6.4 Design of RADA Systems Using a Sampling Receiver

In practical design situations, $P_{SFA}(\min)$, k, T_c, (Mq_1) are typically chosen beforehand. A minimum value of Δ_t is specified by synchronization problems, circuit problems, and propagation effects. The system bandwidth, W_n, is determined from (6. 15). The number Λ_f of system frequencies $\lambda_f\lambda_t$ is determined by (6. 9b) rearranged as (6. 16a) for convenience. The number $(\lambda_f\lambda_t)$ of AND gate inputs is determined from (6. 8a) and (6. 16a).

$$\frac{\Lambda_f\, T_c}{(Mq_1)\,k\,\Delta_t} = -2.08\;\ell n\left[\frac{P_{SFA}(\min)}{1-k}\right]\;; \qquad \lambda_f \leq \Lambda_f \qquad (6.16a)$$

$$\lambda_f\lambda_t = -1.44\;\ell n\left[\frac{P_{SFA}(\min)}{1-k}\right]\;; \qquad \lambda_f \leq \Lambda_f \qquad (6.16b)$$

Equation 6. 16a specifies the optimal noninteger value of Λ_f and, (6. 16b) specifies the optimal noninteger value of the product $\lambda_f\lambda_t$. The decision on what integer values of Λ_f, $\lambda_f(\lambda_f \leq \Lambda_f)$, and λ_t to use is then left to the designer. Generally, if a sufficiently large code vocabulary is available, the choice of large λ_t, small λ_f will reduce system complexity.

It is not practical to change the number $\lambda_f\lambda_t$ of receiver AND gate inputs to match the interference level of the channel at each time instant. Accordingly, a practical design procedure is to design a system (determine Λ_f, λ_f, and λ_t) for a specified maximum design number of active subscribers Mq_1 as was just done using (6. 16). Assume a system has been designed for Mq_1 subscribers, and that the system parameters are then held constant. Let $P_{SFA}(Mq_1, m)$ denote the false alarm probability of a system, minimized with respect to $\lambda_f\lambda_t$ for Mq_1 subscribers, when there are m subscribers using the system. The designed false alarm probability, $P_{SFA}(\min) = P_{SFA}(Mq_1, Mq_1)$.

Substituting (6. 8a) with $m = Mq_1$ into the exponential of (6. 9a), and (6. 8b) into the exponent of the bracketed factor of (6. 9a),

$$P_{SFA}(Mq_1, m) = (1-k)\left(1 - e^{-.693\frac{m}{Mq_1}}\right)^{\frac{.541\, T_c W_n}{Mq_1 k}} \qquad (6.17)$$

It is apparent that when $m < Mq_1$, $P_{SFA}(Mq_1, m)$ is smaller than the design value, and the system will satisfy the designed false alarm specification. That is,

$$P_{SFA}(Mq_1, m) < P_{SFA}(Mq_1, Mq_1); \quad m < Mq_1 \qquad (6.18)$$

When $m > Mq_1$,

$$P_{SFA}(Mq_1, m) > P_{SFA}(Mq_1, Mq_1); \quad m > Mq_1 \qquad (6.19)$$

and the system will exceed the designed false alarm specification. The quantity $P_{SFA}(Mq_1, m)$ is plotted in Fig. 6.3 as a function of m/Mq_1, with $T_c W_n/Mq_1$ and k as parameters. For an example of the use of Fig. 6.3, assume an optimal RADA system having a false alarm probability $P_{SFA}(Mq_1, m) = 10^{-3}$ at its rated number of users. For this system, the value of $T_c W_n/Mq_1$ is determined in Fig. 6.3e from the curve which intersects the abscissa value $m/Mq_1 = 1$, and the ordinate value $P_{SFA}(Mq_1, m) = 10^{-3}$. The interpolated value of $T_c W_n/Mq_1$ equals 8.3. When the system is loaded by half the rated number of users, the false alarm rate is determined from the same curve for an abscissa value $m/Mq_1 = .5$, and is, $P_{SFA}(Mq_1, .5\, Mq_1) = 10^{-5}$.

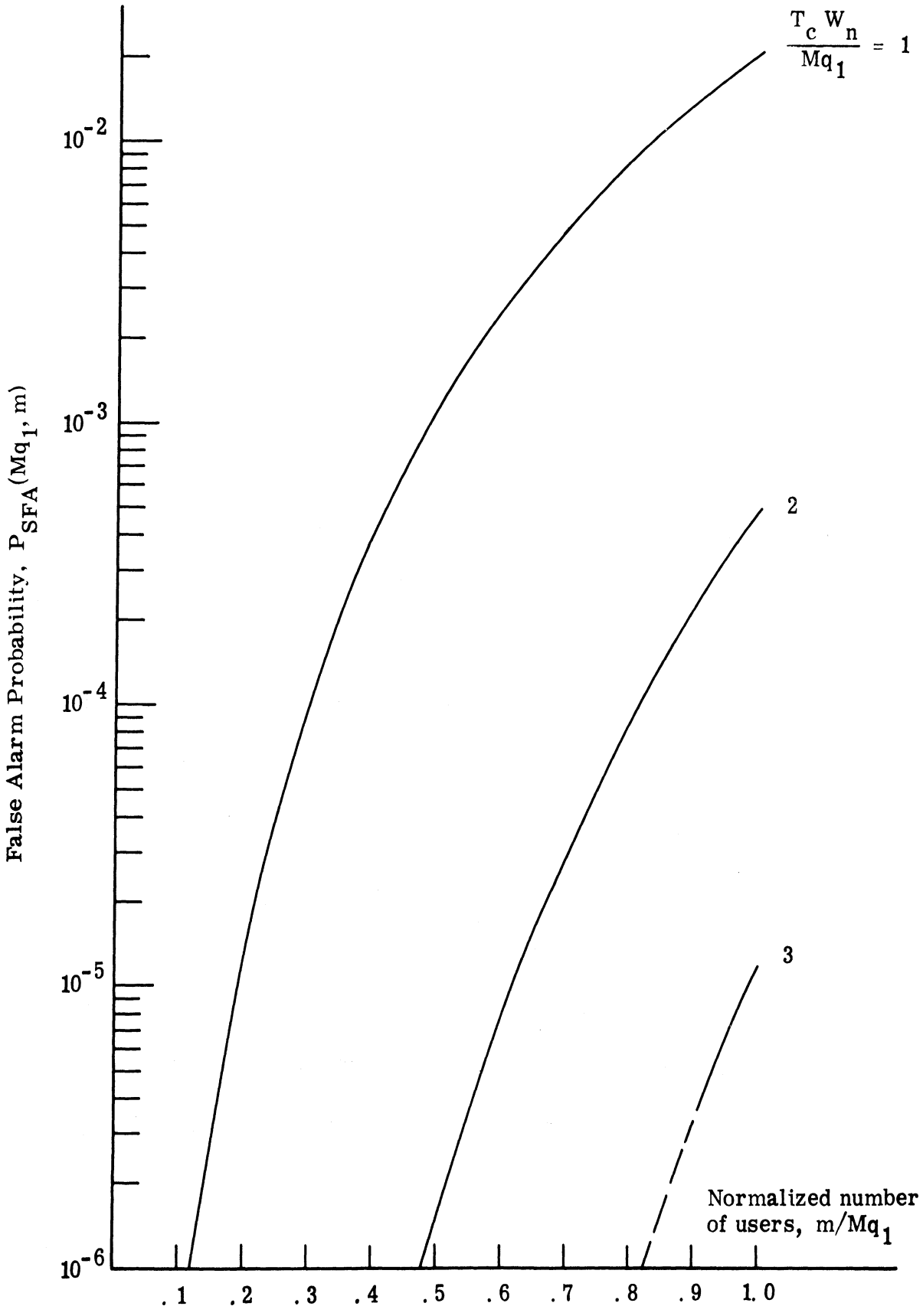

Fig. 6.3(a). False alarm probability, $P_{SFA}(Mq_1, m)$, vs. normalized number of users, m/Mq_1, for an optimal RADA system employing clocked binary modulation and sampling receivers, and designed for Mq_1 users; k = .1.

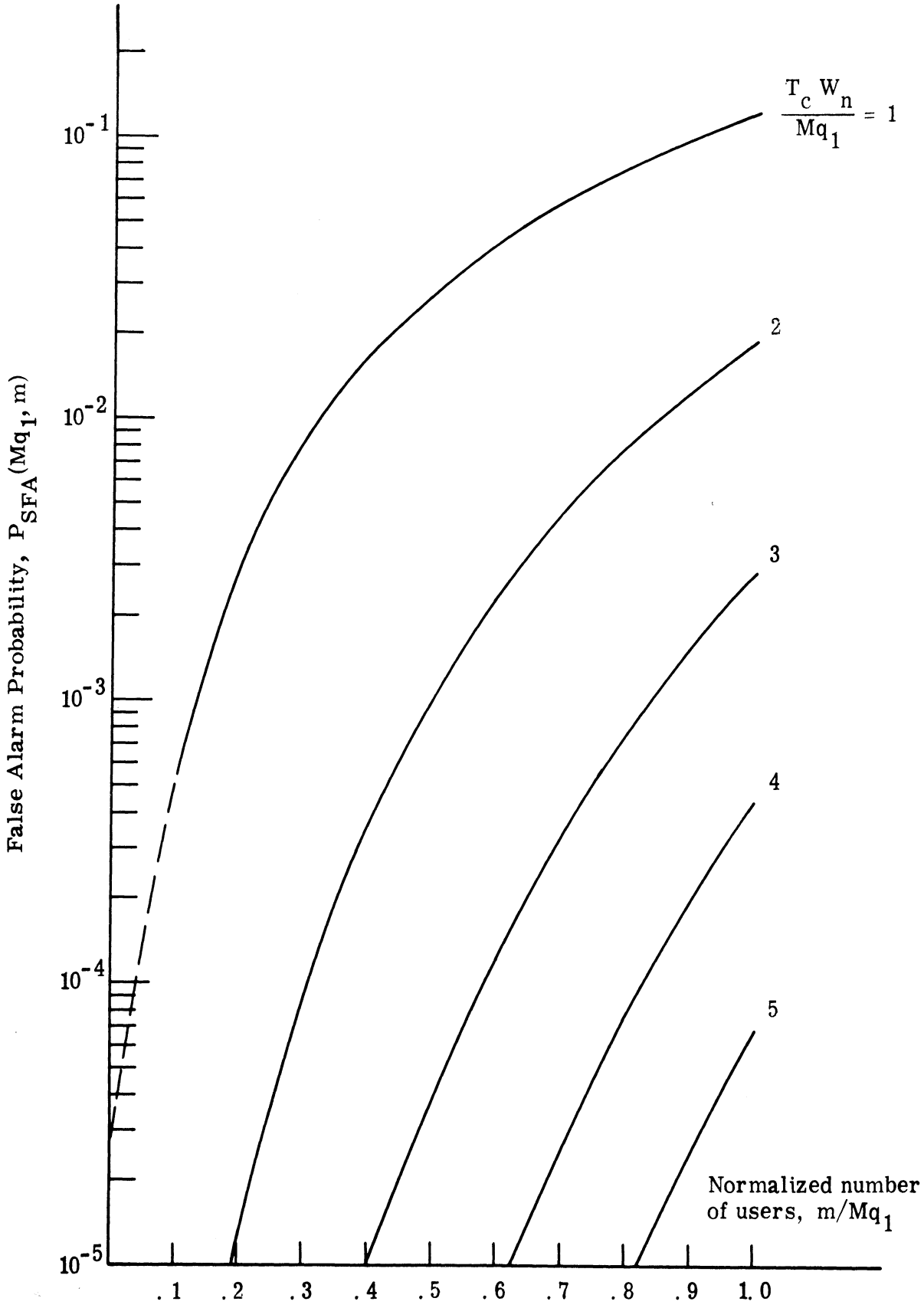

Fig. 6.3(b). False alarm probability, $P_{SFA}(Mq_1, m)$, vs. normalized number of users, m/Mq_1, for an optimal RADA system employing clocked binary modulation and sampling receivers, and designed for Mq_1 users; k = .2.

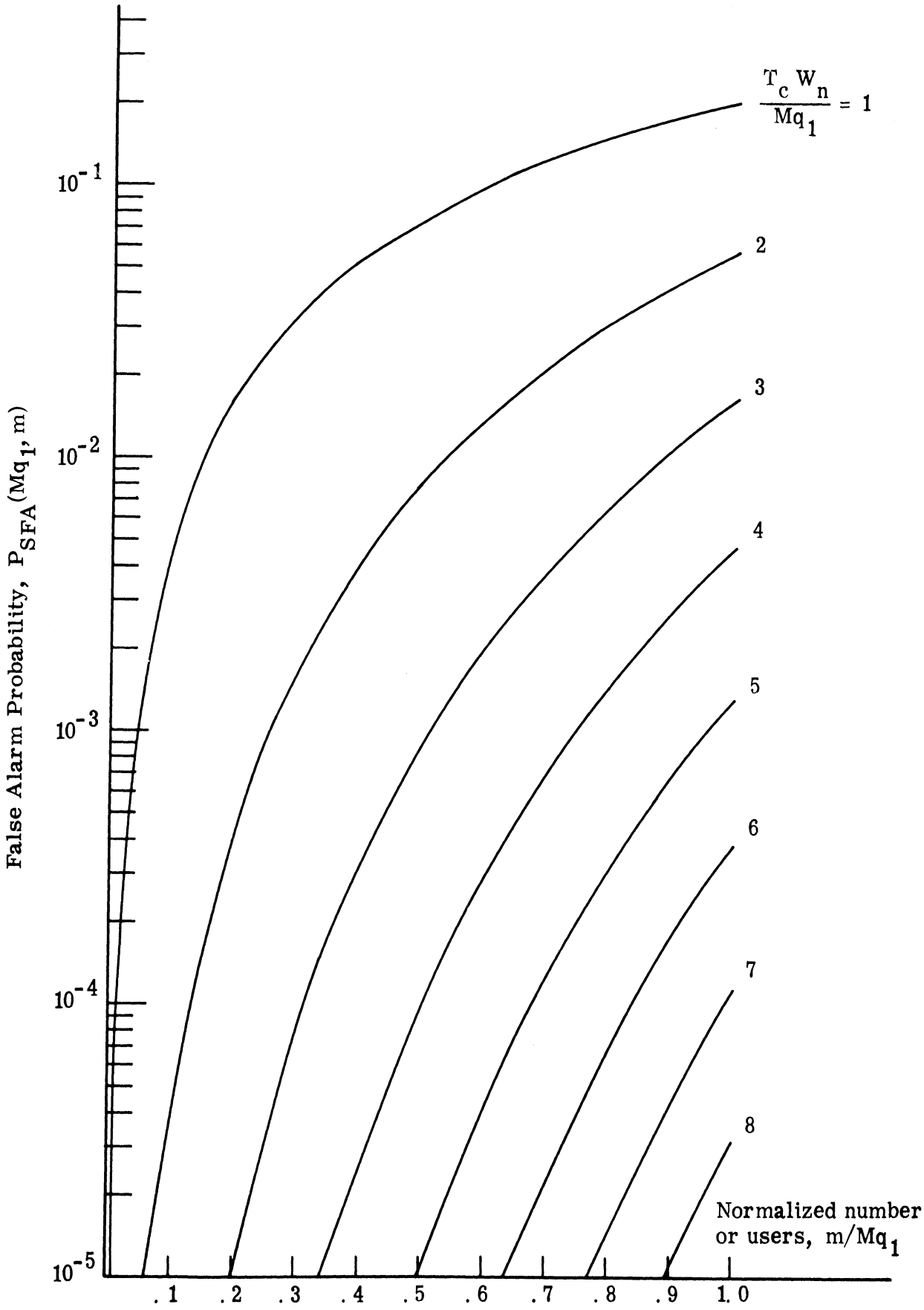

Fig. 6.3(c). False alarm probability, $P_{SFA}(Mq_1, m)$, vs. normalized number of users, m/Mq_1, for an optimal RADA system employing clocked binary modulation and sampling receivers, and designed for Mq_1 users; k = .3.

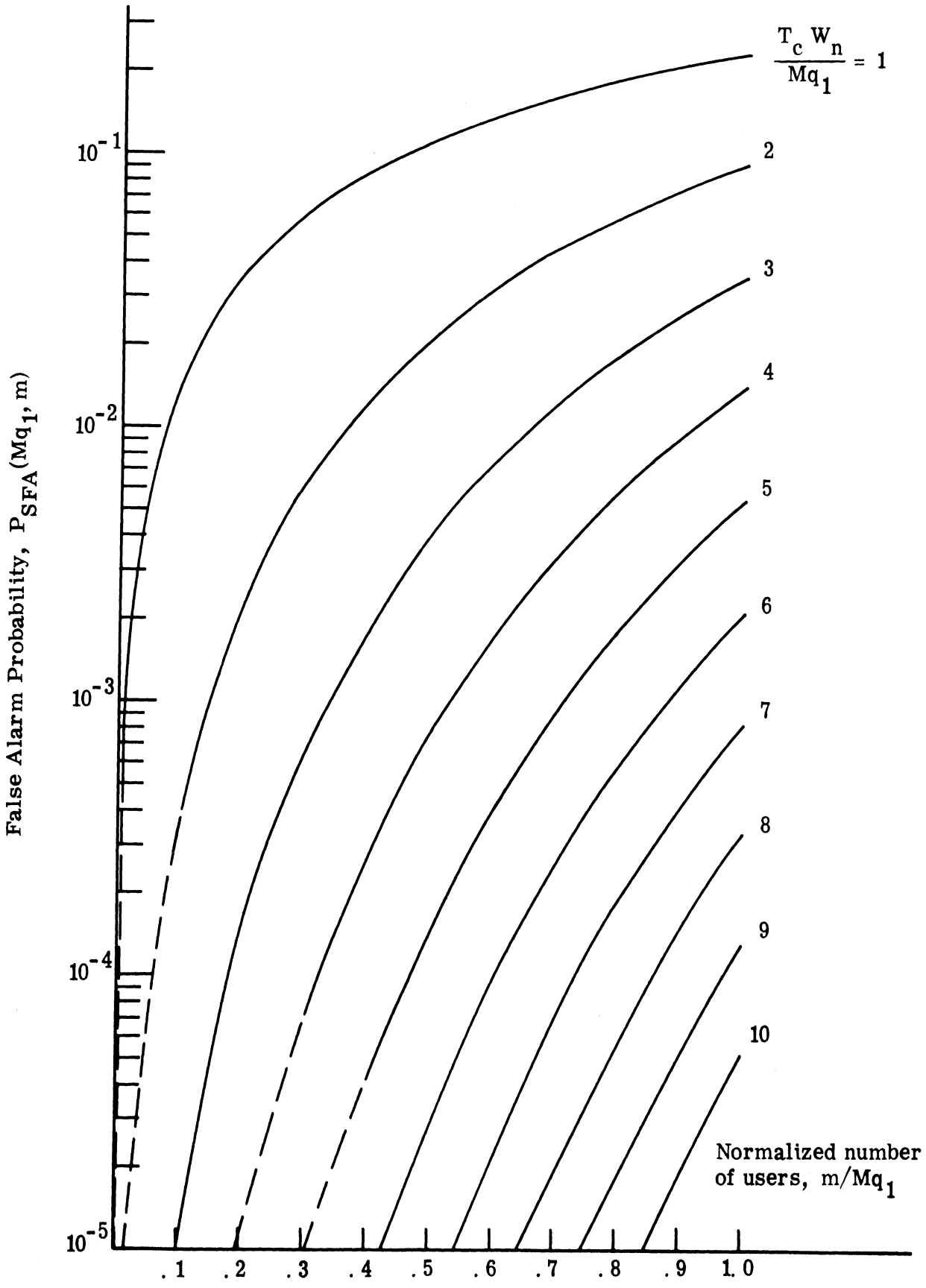

Fig. 6.3(d). False alarm probability, $P_{SFA}(Mq_1, m)$, vs. normalized number of users, m/Mq_1, for an optimal RADA system employing clocked binary modulation and sampling receivers, and designed for Mq_1 users; k = .4.

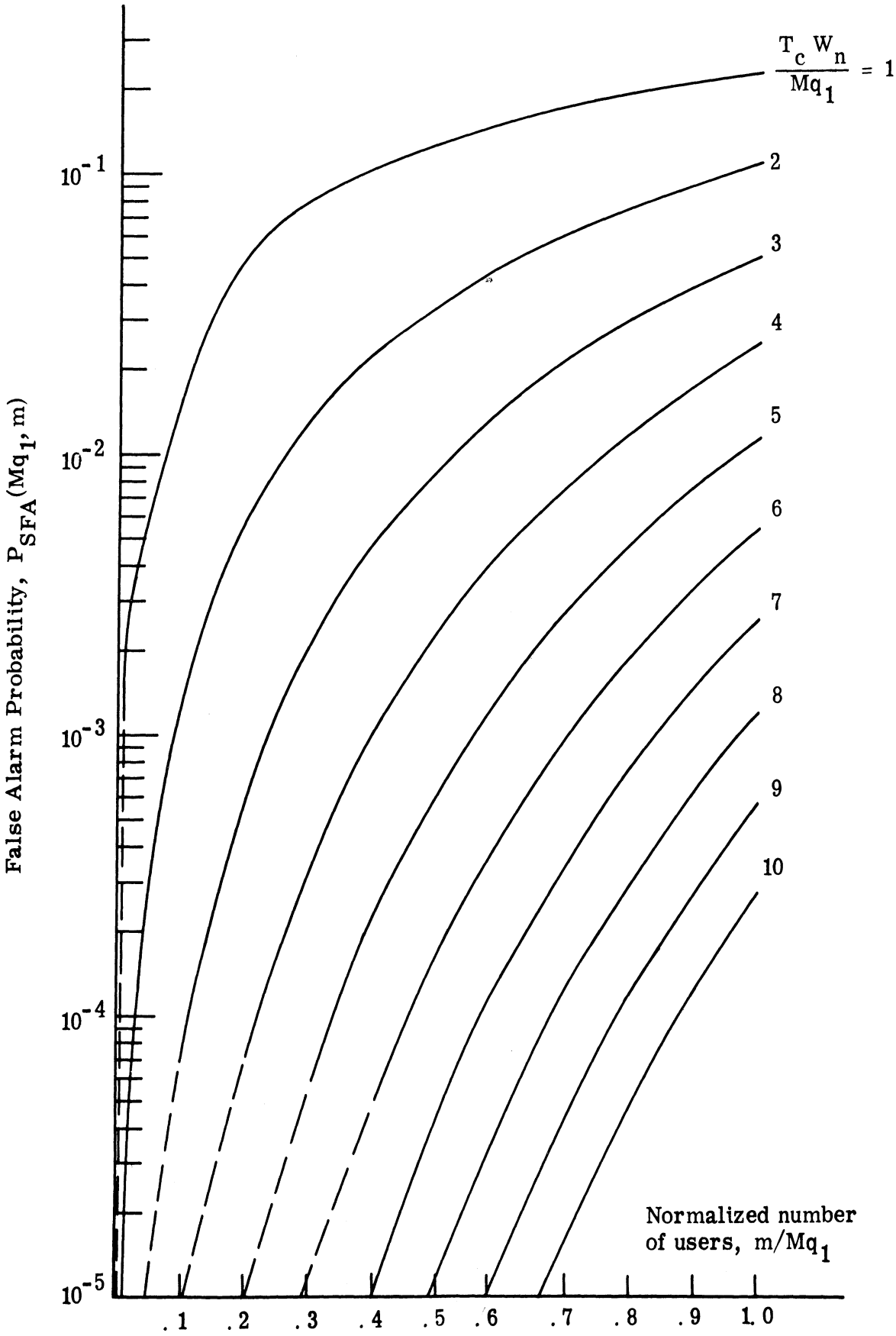

Fig. 6.3(e). False alarm probability, $P_{SFA}(Mq_1, m)$, vs. normalized number of users, m/Mq_1, for an optimal RADA system employing clocked binary modulation and sampling receivers, and designed for Mq_1 users; k = .5.

6.5 Examples of Design of a RADA System Using a Sampling Receiver

Example 1

The parameters to be used in a RADA system are $k = .5$, $T_c =$ 125 microseconds, $P_{SFA} = .1$, $\Delta_t = 1$ microsecond, $Mq_1 = 100$. Determine the bandwidth W_n of the RADA system with sampling receiver and the tradeoff between parameters λ_f, λ_t.

Solution 1

From (6.16a), $\Lambda_f = 1.34$. Use $\Lambda_f = 2$ to obtain the desired value of P_{SFA}. From (6.9b), the corresponding value of $P_{SFA}(\min)$ is

$$P_{SFA}(\min) = 4.6 \times 10^{-2}$$

The bandwidth W_n is, from (6.15) or from Fig. 6.2

$$W_n = 2.58 \times 10^6 \text{ cps}$$

(This compares with $W_n = 1.72 \times 10^6$ cps when $\Lambda_f = 1.34$.) From (6.16b),

$$\lambda_f \lambda_t = 3.57$$

Substituting $\lambda_f \lambda_t = 3$ and $\lambda_f \lambda_t = 4$ into (6.1),

$$\lambda_f \lambda_t = 3 \qquad P_{SFA} = 4.6 \times 10^{-2}$$

$$\lambda_f \lambda_t = 4 \qquad P_{SFA} = 4.6 \times 10^{-2}$$

Systems with $\Lambda_f = 2$, $\lambda_f\lambda_t = 3$ and $\lambda_f\lambda_t = 4$ have the same P_{SFA}, which is less than the specified value $P_{SFA} = .1$. The system for which $\lambda_f = 1$, $\lambda_t = 3$ would be the simplest to construct. However, the address codes of more than 100 subscribers would be highly dependent statistically, which might increase the value of P_{SFA} significantly over the calculated value $P_{SFA} = .046$. The same comments apply, to a lesser extent to a system for which $\lambda_f = 1$, $\lambda_t = 4$. The system with $\lambda_f = 2$, $\lambda_t = 2$ would appear to be the best choice, if it can provide a suitable number of address codes which are relatively independent statistically.

The penalty paid for the use of the co-channel system is a false alarm probability $P_{SFA} = 4.6 \times 10^{-2}$.

The bandwidth $W_n = 2.58 \times 10^6$ cps is the least bandwidth which will provide a value of P_{SFA} less than or equal the specified value $P_{SFA} = .1$ (Mq_1, k, Δ_t, T_c fixed; Λ_f, λ_f, λ_t integers). The result neglects synchronization errors, the effects of statistical dependence of codes, random channel noise, pulse cancellation, multipath effects, cross coupling between frequency channels, effects of the large dynamic range of received signals, and so on. Under ideal conditions, the performance of this system would be approached:

Example 2

Solve Example 1 with $P_{SFA}(\min) = .01$.

Solution 2

From (6. 16a) $\Lambda_f = 3.26$. Use $\Lambda_f = 4$. From (6.9b)

$$P_{SFA}(\min) = 4.15 \times 10^{-3}$$

The bandwidth W_n is, from (6. 15) or from Fig. 6.2

$$W_n = 5.00 \times 10^6 \text{ cps}$$

From (6. 16b)

$$\lambda_f \lambda_t = 6.73 \ .$$

Setting $\lambda_f \lambda_t = 7$ limits the choice to a $\lambda_f = 1$, $\lambda_t = 7$ system, which has practical disadvantages. A choice of $\lambda_f \lambda_t = 6$ or $\lambda_f \lambda_t = 8$ would permit a variety of practical systems which will satisfy the initial P_{SFA} requirement. The tradeoff between λ_f and λ_t would be in the direction of larger λ_f as the number of address codes required increases.

6.6 Information Rate of a RADA System Using Clocked Binary Modulation and a Sampling Receiver

Previous results of this chapter, and the results obtained in Section 3.4.6 will be used in this section to determine the rate at which information is transmitted by a RADA system using clocked binary modulation and a sampling receiver. The rate R per clock period, T_c, at which the information is transmitted is given by (3.98) and (3.99).

$$R = \mathcal{F}[(1 - P_m)(1-k)] - (1-k)\mathcal{F}(P_m) \qquad (3.99)$$

where,

$$\mathcal{F}(P) = -[P \log_2 P + (1-P) \log_2 (1-P)] \qquad (3.98)$$

A RADA system using a sampling receiver with $\lambda_f \lambda_t$ chosen to minimize P_{SFA} can transmit information at a rate R_{max} which can be determined by substituting the value $P_m(\min)$ corresponding to $P_{SFA}(\min)$

$$P_m(\min) = (.5)^{.541 \frac{T_c W_n}{mk}} \quad ; \quad \lambda_f \leq \Lambda_f \qquad (6.20)$$

into (3.98).

$$R_{max} = \mathcal{F}\left\{\left[1 - (.5)^{.541 \frac{T_c W_n}{mk}}\right](1-k)\right\} - (1-k)\mathcal{F}\left[(.5)^{.541 \frac{T_c W_n}{mk}}\right] \quad \lambda_f \leq \Lambda_f \qquad (6.21)$$

The rate R_{max} applies to an "adaptive" type of RADA receiver, one which continuously adjusts λ_f and λ_t to minimize P_{SFA}. The quantity R_{max} can be read from the curves of Fig. 6.4 for $m/Mq_1 = 1$.

For the "practical," nonadaptive receiver described in Section 6.4,

$$R(Mq_1, m) = \mathcal{F}\left\{\left[1 - \left(1 - e^{-.693\,\frac{m}{Mq_1}}\right)^{\frac{.541\,T_c\,W_n}{Mq_1\,k}}\right](1-k)\right\}$$

$$- (1-k)\mathcal{F}\left[\left(1 - e^{-.693\,\frac{m}{Mq_1}}\right)^{\frac{.541\,T_c\,W_n}{Mq_1\,k}}\right] \qquad (6.22)$$

Both (6.21) and (6.22) have been determined for continuous Λ_f and $(\lambda_f \lambda_t)$; the rates R_{max} and $R(Mq_1, m)$ are, therefore, upper bounds on the rates which apply when Λ_f and $(\lambda_f \lambda_t)$ are integers. The method of determining the integer values which optimize system performance has been described in Section 6.2. The rate $R(Mq_1, m)$ is the maximum rate, per clock period, of information transmission by a RADA system having a false alarm probability which is minimized with respect to λ_f and λ_t, when the rated number Mq_1 of users load the system, and when m users are loading the system. This rate is only achieved for the theoretical case in which the transmitted signals are coded in infinitely long binary sequences which are uniquely distinguishable at the receiver. The rate $R(Mq_1, m)$ is plotted in Fig. 6.4 as a function of the normalized number of users, m/Mq_1, with $T_c W_n/Mq_1$ and k as parameters. It is seen in the figures that for a given value of k, the maximum rate equals the entropy of a binary process with probabilities k and (1-k), as expected; thus, for k = .5, the maximum rate is one

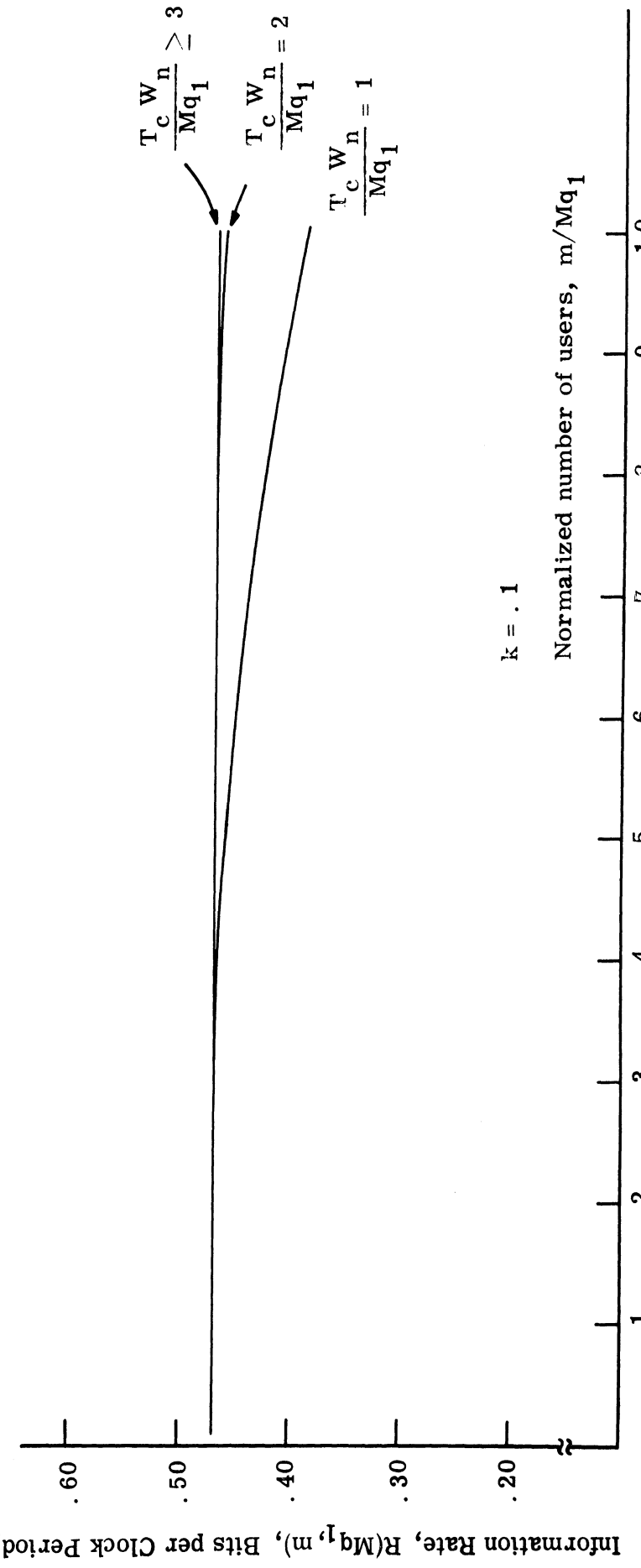

Fig. 6.4(a). Information rate, $R(Mq_1, m)$, vs. normalized number of users m/Mq_1, for an optimal RADA system employing clocked binary modulation and sampling receivers, and designed for Mq_1 users; $k = .1$.

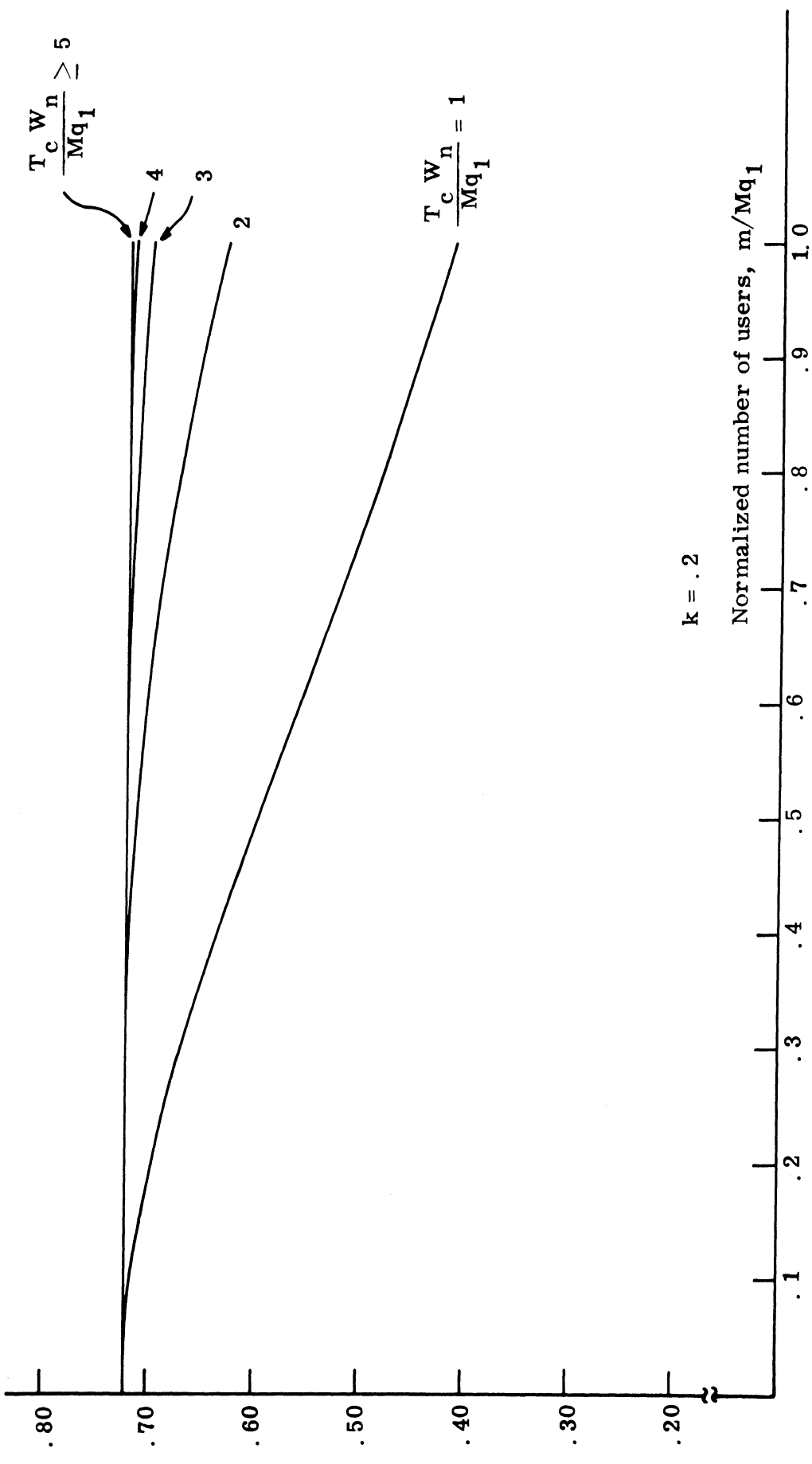

Fig. 6. 4(b). Information rate, $R(Mq_1, m)$, vs. normalized number of users m/Mq_1, for an optimal RADA system employing clocked binary modulation and sampling receivers, and designed for Mq_1 users; k = .2.

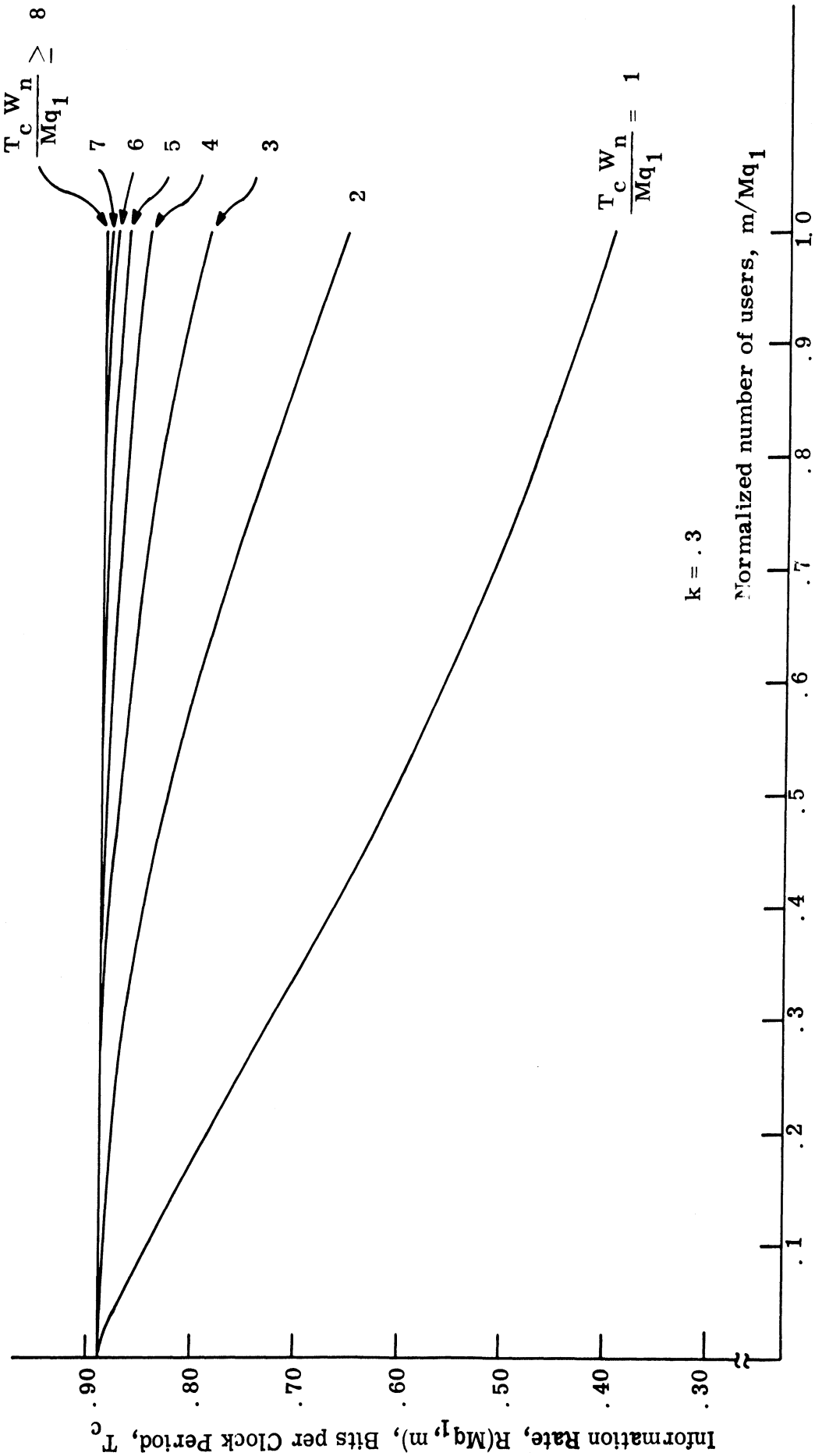

Fig. 6.4(c). Information rate, $R(Mq_1, m)$, vs. normalized number of users m/Mq_1, for an optimal RADA system employing clocked binary modulation and sampling receivers, and designed for Mq_1 users; k = .3.

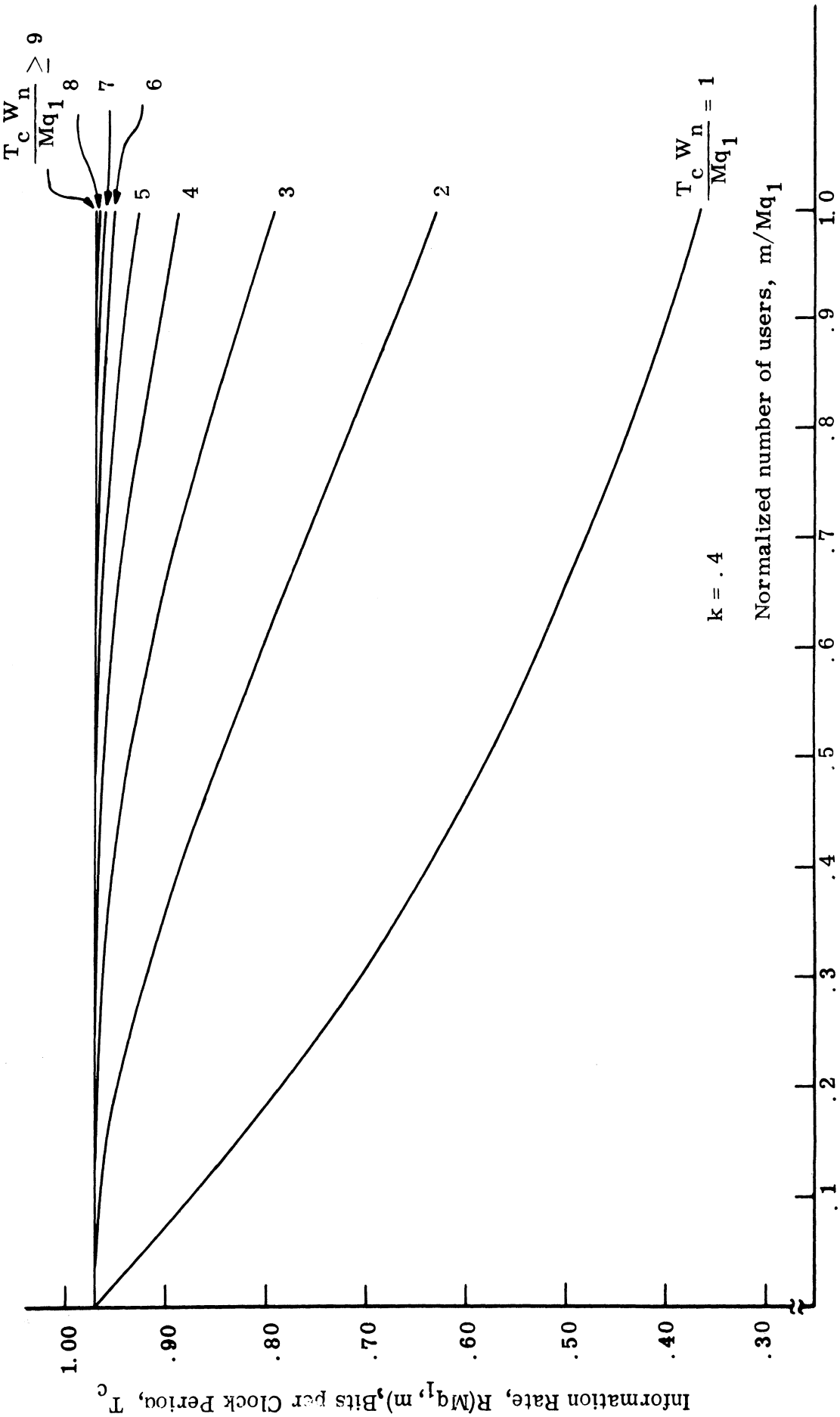

Fig. 6.4(d). Information rate, $R(Mq_1, m)$, vs. normalized number of users m/Mq_1, for an optimal RADA system employing clocked binary modulation and sampling receivers, and designed for Mq_1 users; $k = .4$.

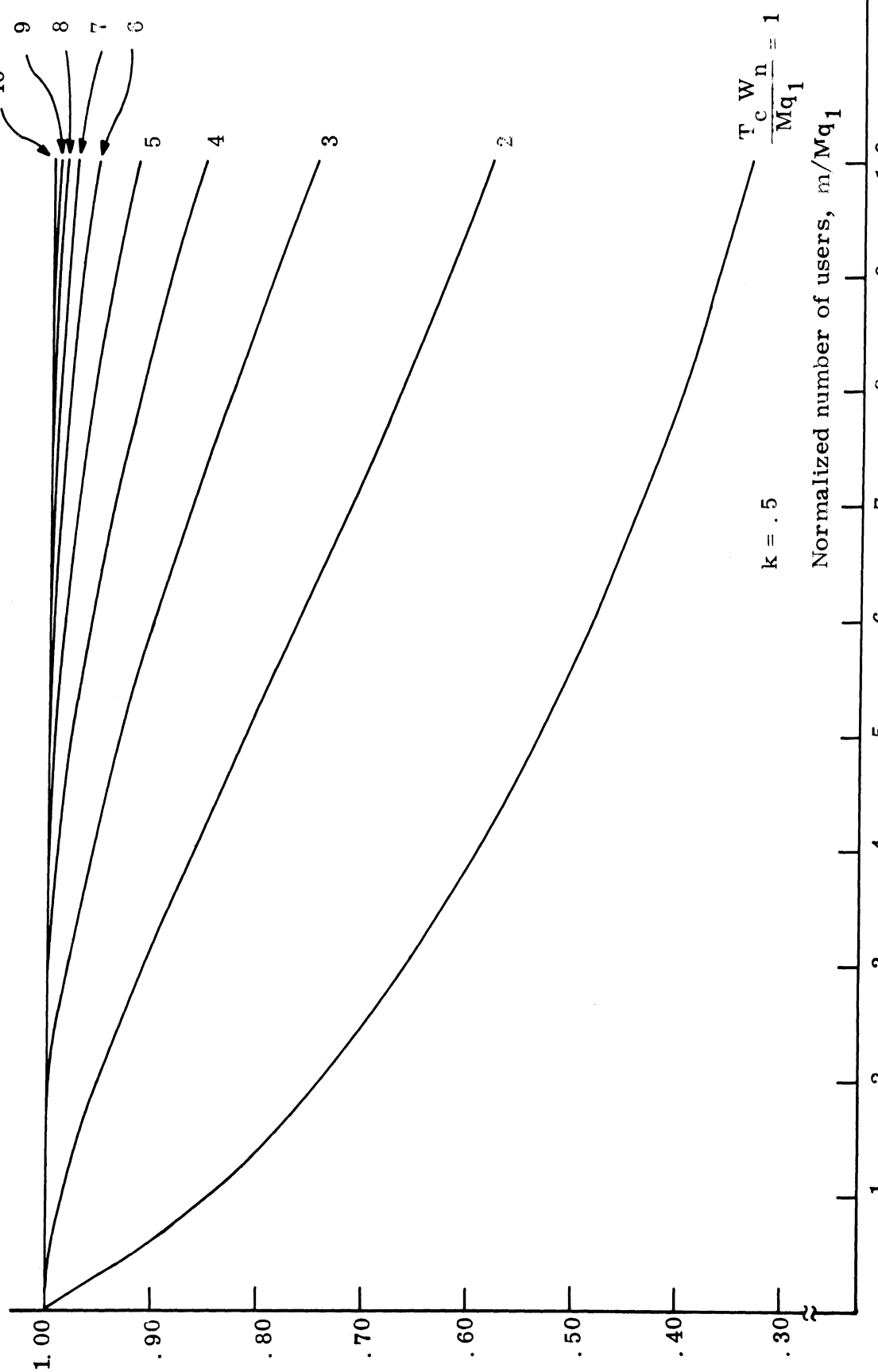

Fig. 6.4(e). Information rate, $R(Mq_1, m)$, vs. normalized number of users m/Mq_1, for an optimal RADA system employing clocked binary modulation and sampling receivers, and designed for Mq_1 users; k = .5.

bit per clock period, T_c. The rate decreases as the number of users increases because of the mutual interference among system users. The information rate decreases at a faster rate for systems having a smaller ratio of bandwidth expansion, $T_c W_n$, per design number of users, Mq_1, which systems are less immune to interference. Consider, again, the example of Section 6.4 for which k = .5 and $T_c W_n/Mq_1 = 8.3$. When loaded at half capacity, $m/Mq_1 = .5$, the rate $R(Mq_1, .5Mq_1) \cong 1$ bit per clock period. At rated capacity, the rate $R(Mq_1, Mq_1) \cong .99$ bits per clock period. The relatively high information capacity of this system is also reflected by the small false alarm probabilities given for the example of Section 6.4; this high capacity results from the use of equiprobable symbols (k = .5) and from the relatively large bandwidth expansion per rated user, $T_c W_n/Mq_1$, which is employed.

CHAPTER VII

CONCLUSIONS AND RECOMMENDATIONS

The studies of this dissertation are focussed upon the central problem of determining and minimizing the effects of mutual interference among RADA systems; isolating those effects which are caused by the power level of interfering signals; and isolating those effects which are caused by erroneous frames produced by these signals.

In analyzing those interference effects which are attributable to the interference power level (Chapter II), it is assumed that when the signal-to-mutual-interference power ratio of a received signal exceeds the reciprocal of the receiver dynamic range, then the signal power exceeds the power of the spurious interference and receiver noise. When this is true the signal is called a useful received signal. In Chapter II, a lower bound is determined for the probability of a useful received signal; this probability is defined over an ensemble of nets with particular net parameter values. This bound is defined in terms of the receiver's dynamic range, the density of packing of transmitters in the net area, and the ratio of the distance separating the given transmitter and target receiver to the minimum distance between transceivers in the net. Because it is a lower bound which is determined for the probability of a useful received signal, the

probability specified by this bound will, in general, be exceeded by nets with the corresponding parameter values. Equivalently, such nets will permit a more dense transceiver packing than specified, and will utilize more bandwidth than is necessary for a net with the particular parameter values.

In studying those interference effects which result from erroneous frames produced by the interfering signals (Chapter III), the error statistics are determined in terms of the actual number of interfering transmitters. It is considered that this result is more meaningful than an error rate obtained by averaging over an assumed distribution of users, particularly since this distribution may vary considerably. For example, the distribution of the number of users in a military communication system will differ considerably, in an emergency situation, from the distribution for ordinary non-emergency operations. Further, the statistics of emergency situations are generally unpredictable from one situation to the next. The number of active transmitters which must be accommodated in the worst case is used in system design for emergencies, rather than the number of transmitters which provides a certain average level of performance in normal operating conditions.

The best measures of system performance (Chapter III) which can be used for a particular system are those measures which correlate most highly with the subjective observations of receiver

output signal quality. For ungated receivers, this would be the error rate or error pulse duty factor. For gated receivers, this would be the false alarm probability.

The general optimization procedures of Chapter V are applicable to all of the performance measures which have been presented here. Since these measures have typically been plotted as a function of $\gamma\Delta_t$ and $\lambda_f\lambda_t$, the optimization is performed in terms of these parameters. The specific optimization which is carried out in Chapter VI is for a system which employs a sampling receiver.

The analytical results of this dissertation are based on a number of assumptions. Relaxation of these assumptions provides a suggestion for reasonable areas of future study. In the RADA system model developed in Chapter III, fixed AND gate input pulsewidths are assumed, whereas in fact the pulsewidths are variable. A realistic, tractable model which accounts for the variation of pulsewidths would constitute a definite advancement in modeling of these systems. Another area of useful endeavor is to determine, using the results of references in this area (Section 1.5.2.2), the size of the RADA code vocabularies which correspond to various system coding parameters (λ_f, Λ_f, λ_t, Λ_t), to specify the number of users which a particular system can accommodate with a specified error rate. Also, it is desirable to investigate the tradeoff between system optimization and vocabulary size; optimization of system performance (by choosing an

optimal value of the product $\lambda_f \lambda_t$) tends to alter the number of available user addresses. Another problem of significance is the determination of a class of pulse modulations (source encodings) of the voice waveform which tend to optimize system performance. Although efforts have been devoted to this problem, as cited in Section 1.5.2.1, a continuous examination of the applicability of newly developed pulse modulations to RADA systems is worthwhile.

APPENDIX

PROTOTYPE RADA SYSTEMS

The general principles of RADA systems were described in Section 1.2; three prototype RADA systems are described in this appendix. Since RADA type systems are still in a state of evolution, the final versions of these systems may be somewhat different than those described here. The systems discussed in this appendix are the Martin RACEP system, the Motorola RADEM system, and the Bendix CAPRI system.

The Martin RACEP System (Random Access and Correlation for Extended Performance) (Refs. 11 - 14, 1.6 - 1.8)

The acronym, RACEP, is used by the Martin Company to classify several items of functionally similar prototype RADA equipment including: the Engineering Model Subscriber Set, the Model 660 Subscriber Set, the Transponder Unit, the Guard Band Monitor Unit, and the Multiple Subscriber Set. Disregarding special features, all of these RACEP prototype units are similar to the Engineering Model Subscriber Set with regard to the general method of transmission and reception of information. Recent characteristics (Ref. 1.8) of this prototype set are described in this appendix. Previous parameter values are indicated in Refs. 1.6 and 1.7. Most recently, the acronym "RADA"

has been applied to a Martin net communications system in which the information is modulated in pulse-position modulation and transmitted in frequency-division multiplex, after searching for a vacant frequency channel (Refs. 1. 19 - 1. 23); RADA techniques are employed for the vacant channel search, and for other supervisory functions. This system is a complex one which is characterized by many special functions, and it is not described in this appendix.

A block diagram of the RACEP prototype transmitter is shown in Fig. A. 1(a), a representative message frame is shown in Fig. A. 1(b), and a block diagram of a prototype receiver in Fig. A. 1(c). The basic principles of RADA system operation were described in Section 1. 2, and they will be recapitulated here for the RACEP system. To address a target receiver, the operator of the given transmitter sets the transmitter delay line taps so that the total delay of each modulator output pulse, in passing through the transmitter and receiver delay lines, is 32 microseconds. That is, the given transmitter addresses the target receiver by choosing the values of delay within the transmitter to complement those within the receiver with respect to the delay line length (32 microseconds). Within the transmitter, the voice input to the transmitter is sampled at an 8 kc rate, and each sample amplitude modulates the position of a pulse. With no voice modulation, the instantaneous modulator output pulse rate is 8000 pps. With voice modulation, the average output rate is 8000 pps, but the instantaneous rate

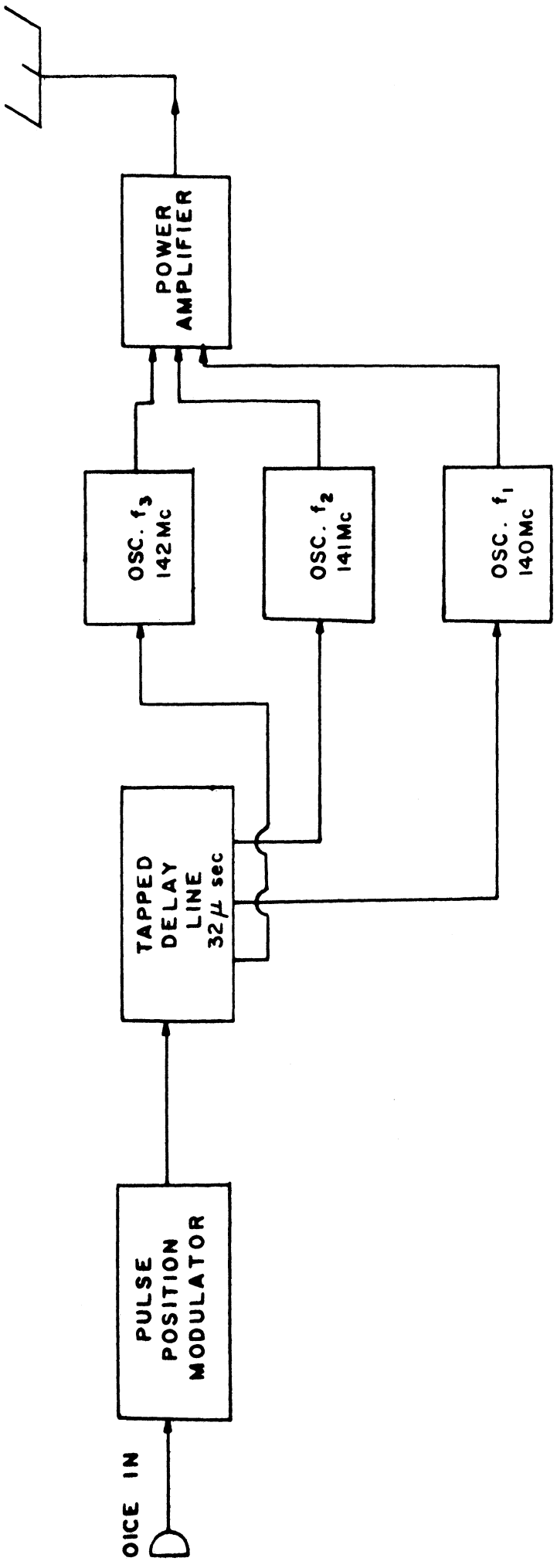

Fig. A. 1(a). Functional Martin RACEP transmitter block diagram.

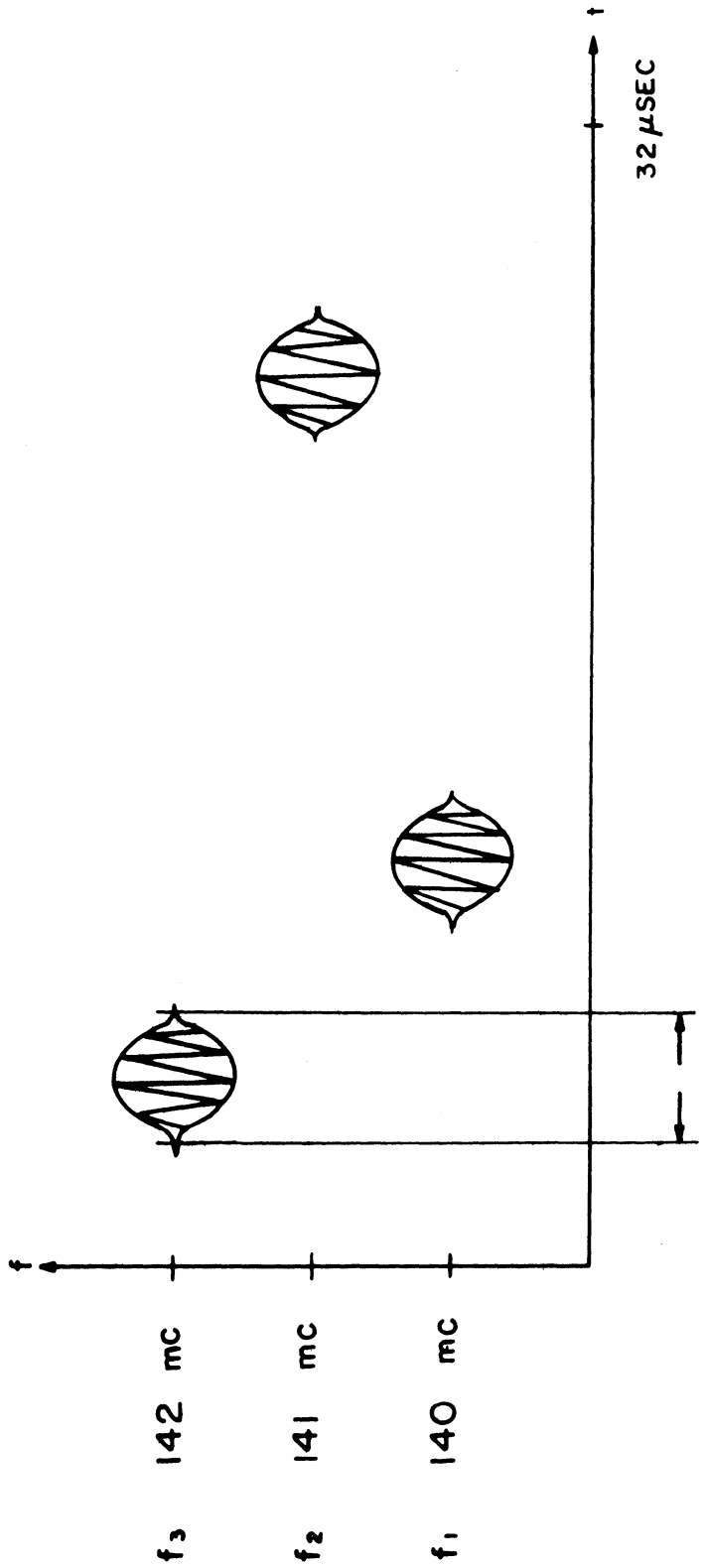

Fig. A. 1(b). Representative transmitted time-frequency code frame for Martin RACEP system.

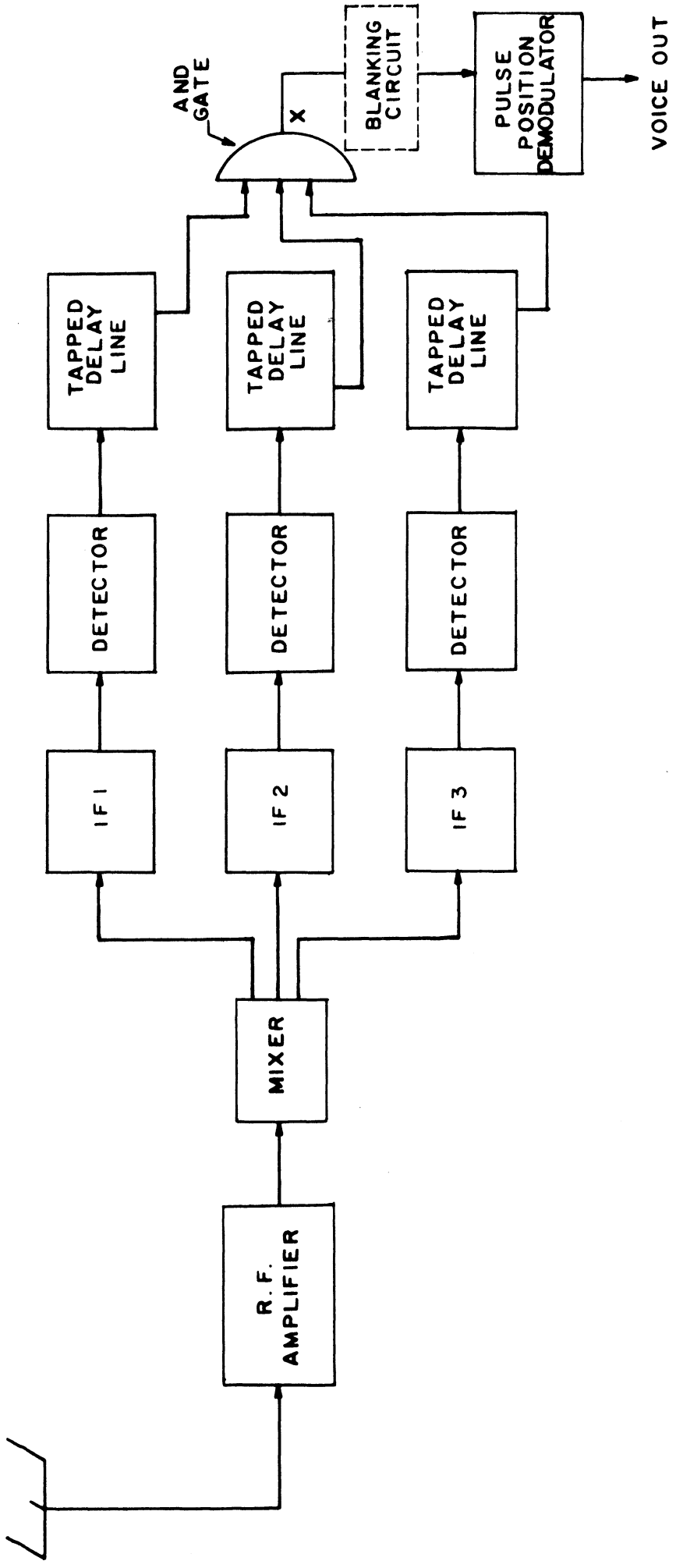

Fig. A. 1(c). Functional Martin RACEP receiver block diagram.

is larger or smaller. The maximum deviation in the position of the modulator output pulses is ± 30 microseconds with respect to the no voice, 8 kc pulse train. Each pulse at the output of the pulse-position modulator generates an addressed group of three pulses (a message frame). At the transmitter output, the frequency and delay of the pulses of the frame are determined by the oscillator frequencies and delay line tap settings. [Fig. A. 1(a) and Fig. A. 1(b)] The delay lines employed in prototype equipment have a total delay of 32 microseconds, and are tapped at 2 microsecond intervals. The duration of the transmitted pulses, measured between the half-voltage points of the pulse envelope, is 1. 5 microseconds. The three pulses of the frame are transmitted on the three carrier frequencies, 140 Mc, 141 Mc, and 142 Mc. Peak pulse power is 1 kw. (Peak pulse power is readily adjustable in the prototypes.)

Within the receiver, the received signal is processed as follows. Pulses on the three RF frequencies are separated in tuned RF stages and then detected. Each detected pulse is then delayed by an amount which complements the transmitter delay; in this way, pulses transmitted in a frame are delayed, and appear at the output of the three receiver delay lines at the same time. These coincident pulses actuate an AND gate, producing an output pulse. In some prototype receivers, this pulse is the direct input to the receiver pulse-position demodulator. In other, more recent RACEP receivers (Ref. 1. 8) the

AND gate output is the input to a "blanking circuit" shown in Fig. A. 1(c). This circuit gates pulses out of the receiver demodulator input which occur less than 80 microseconds after a receiver demodulator input pulse. If this pulse is a message pulse, the blanking circuit gates out the error pulses which occur before the following message pulse. Recent prototype RACEP receivers have an output filter (Ref. 1. 8) which limits the receiver bandwidth to 2000 - 2500 cps. The filter limits the useful receiver output bandwidth from 4 kc (corresponding to a sampling rate of 8 kc) to 2 - 2. 5 kc. Some of the prototypes employ DATEC modulation, a modification of delta modulation which is reportedly a very efficient representation of voice (Ref. 14). Many of the experimental modifications which have been made on prototype RACEP systems are described in Ref. 1. 7. Some of these may have been changed as of the writing of Ref. 1. 8 and are not indicated here. Tables of RACEP parameters are presented in Ref. 1. 6 - 1. 8. Table A. 1 is an abstract from Ref. 1. 8 which indicates the system parameter values.

Features of the RACEP system (Refs. 1. 6 - 1. 8) include ringing circuitry, a "command override" function, a "double function alert," and a "net" mode of operation. The command override function permits sending a message to all RACEP subscribers simultaneously. When the coded command override message is sent, the following occurs:

(1) All transmitters in the command override network except the originating transmitter are temporarily disabled.

	Engineering Model Subscriber Set	Model 660 Subscriber Set	Transponder	Guard Band Monitor Unit	Multiple Subscriber Unit Master
Weight (lbs.)	68	46	78	74	71
Length (in.)	17-11/16	13-1/3	x	x	x
Width (in.)	18-3/4	17-1/4	x	x	x
Height (in.)	12-1/2	10-1/8	x	x	x
Volume (cu. in.)	4146	2329	x	x	x
Average Power (w)	25	x	50	x	75
Peak Power (w)	1000*	x	x	x	x
Bandwidth (Mc)	4	x	x	x	x
Center Frequency (Mc)	141	x	x	x	x
Pulse Width (μsec)	1.5	x	x	x	x
Maximum Pulse Deviation (μsec)	30	x	x	x	x
Primary Input Power	24-32 volts dc	x	x	x	x
Current Drain (amp)	9	x	12	x	12
Maximum Pulse Rate (kpps)	24	x	48	x	72

x Indicates same characteristic as Engineering Model Subscriber Set.

* These parameters are adjustable. The values shown are those found to be convenient at USAEPG (United States Army Electronics Proving Ground).

Table A. 1. RACEP equipment characteristics. **

** Abstract from Ref. 1. 8.

(2) All receivers in the network are automatically set to receive the command override message.

(3) Each transceiver is responsive only to the command override signal until reset by the operator at the completion of the command override signal.

The double function alert permits sending two distinct alert conditions to all stations. When a station receives the coded alert message, the following occurs:

1. One of two lights turns on to indicate the particular alert condition, a buzzer sounds.

2. The same alert signal is retransmitted.

3. A lockout is generated so the signal is accepted and is retransmitted only once.

In the "net" mode, subscribers use the same code for transmission and reception. Duplex-like conversation is possible in the net mode.

Field tests with prototype RACEP equipment indicate that signals received in the presence of 8 - 9 interfering user stations are acceptable (output signal-to-noise ratio greater than 10 db), even with interferers located within 50 feet of the test receiver while the given transmitter was located 16 miles from the test receiver. The results of these tests are explained in detail in Ref. 1. 8.

The Motorola System RADEM (Random Access Delta Modulation)

(Refs. 11 - 13, 15, 1.9, 1.0 and 1.28 through 1.33)

Block diagrams of the RADEM transmitter and receiver are shown in Fig. A.2(a) and Fig. A.2(c). The form of the RADEM time frequency frame is shown in Fig. A.2(b). The block diagrams and time frequency frame show that there are four pulses in a RADEM frame. Actually, prototype RADEM transmitters radiate a single pulse on either three or four of the five RADEM system frequencies. There are 16 possible time positions for each .5 microsecond pulse in a 26 microsecond RADEM frame. Frequencies in the range 150 - 400 Mc are considered for RADEM (Ref. 1.9).

Three differences of RADEM and RACEP are that RADEM uses different parameter values (e.g., transmitted pulsewidth, total number of system frequencies), delta modulation, and digital delay instead of delay lines.

At the transmitter, voice information is coded in single digit two level delta modulation (Fig. A.2a).

By means of the delta modulation, the voice signal is coded into a binary "one" or a binary "zero" in successive 26 microsecond clock intervals, resulting in a 38.4 kc binary pulse train at the modulator output. When the modulator output is a binary "one" in a particular clock interval, a frame such as is shown in Fig. A.2(b) is transmitted in the interval. When the modulator output is a "zero", a frame is

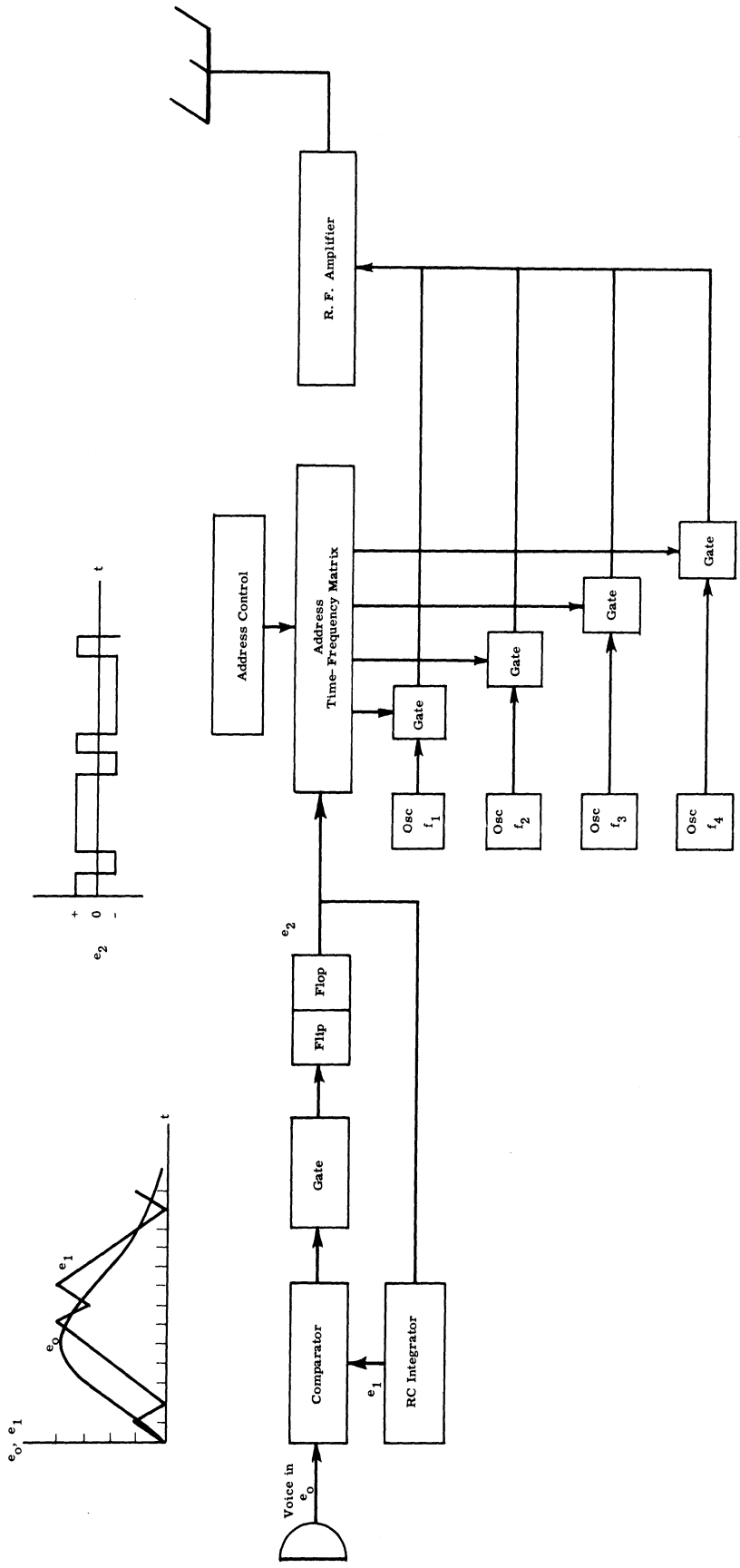

Fig. A.2(a). Motorola RADEM transmitter block diagram.

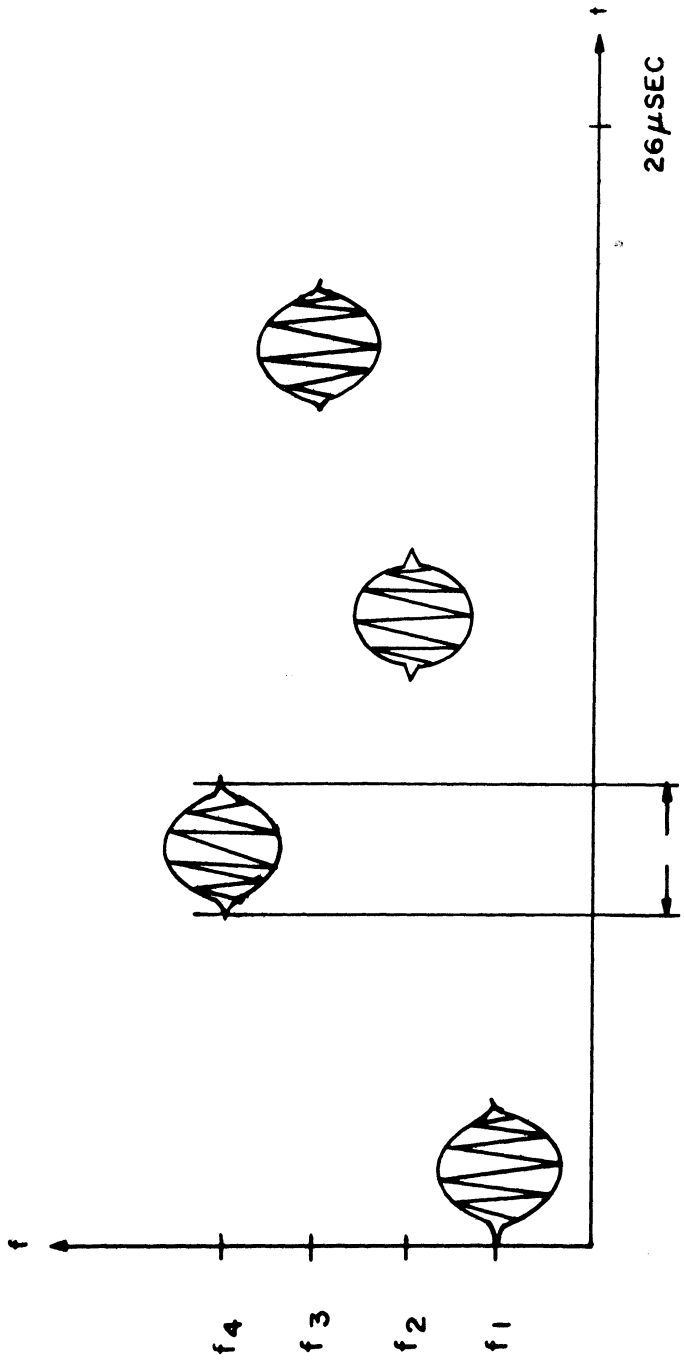

Fig. A.2(b). Representative transmitted time-frequency code frame for Motorola RADEM system.

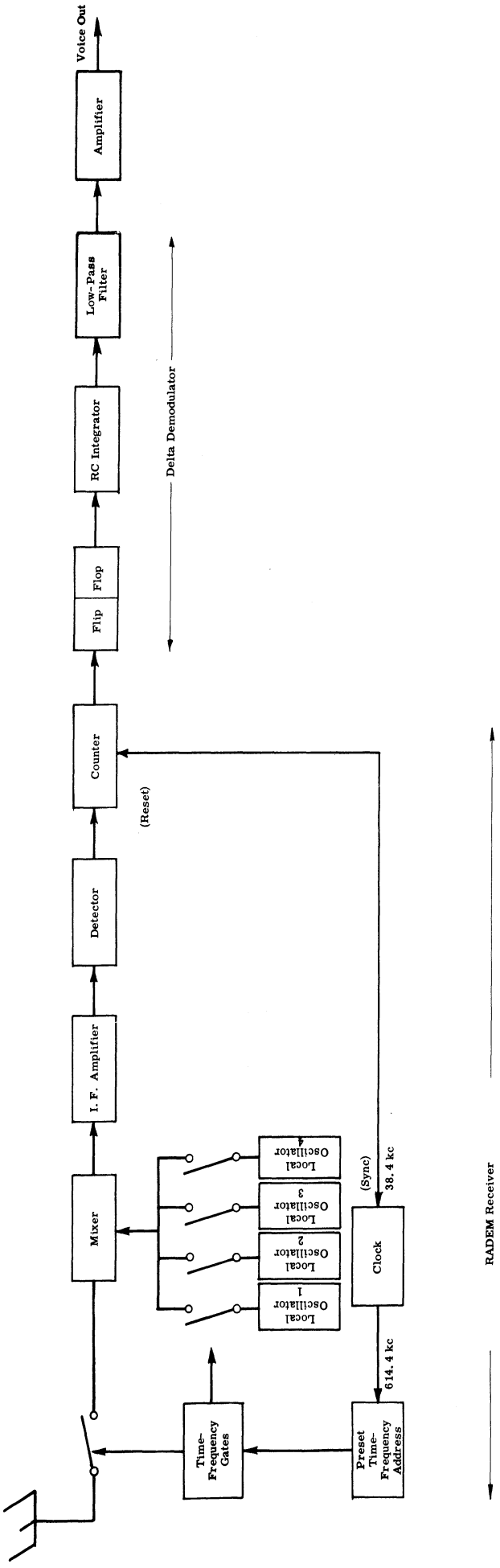

Fig. A.2(c). Motorola RADEM receiver block diagram.

not transmitted. The "Address Control" circuit and the "Address Time-Frequency Matrix" produce pulses which gate the four oscillator output voltages to produce the time frequency code frame. The specific implementation of a RADEM system has not been described in the literature. In the following paragraphs, conjecture is made about the implementation. Depending on the address of the target receiver, each of the pulses which gate the four oscillators must be positioned in one of 16 time slots in a 26 microsecond frame. Each gating pulse is generated in the following manner. In the Address Time-Frequency Matrix, a 614.4 kc (16 x 38.4 kc) clock pulse train is derived from the 38.4 kc clock by multiplying the clock rate by 16. The 614.4 kc clock drives a four-stage counter in the Address Time-Frequency Matrix. The counter counts from one to sixteen in each frame interval, resets, and counts to sixteen in the following frame, and so on. The four stage counter has eight outputs, one pair of outputs from each of the four counter stages. The Address Control circuit is used to connect four counter outputs, one output from each counter, to the inputs of an AND gate. By connecting the AND-gate inputs to the proper set of four counter outputs, a pulse can be generated in any one of the 16 time slots in a frame. A fifth AND-gate input is connected to the modulator output, and modulates the information on the oscillator gating pulse. Thus, a single five input AND gate generates each oscillator gating pulse. Since there are four pulses in a frame, four AND gates in the Address Time-

Frequency Matrix are connected to the counter by the Address Control circuit. The position of each pulse in a frame is conveniently changed by using a 16-position four-pole switch in the Address Control circuit. For each switch position, a different set of four counter outputs is connected to the AND gate input. Thus, by setting four switches in the proper positions, AND gate output pulses are generated in four selected time slots in each frame, and in no other time slots.

A block diagram of the RADEM receiver is shown in Fig. A. 2(c). With the exception that information does not modulate the gating pulses, the Preset Time Frequency Address circuit and the Time Frequency Gates generate four gating pulses in each frame in the same way as the Address Control circuit and the Time-Frequency Matrix generate gating pulses in the RADEM transmitter. The relative timing of the pulses on the four frequencies is fixed, and constitutes the receiver address. Assuming that a correctly coded group of four pulses is present at the receiver input, the gating pulses are used to gate the mixer and the four local oscillator inputs at the proper time to allow detection of the four pulses. It is apparent that the RADEM receiver must be time synchronized with a correctly coded received pulse group if the four pulses are to be detected. Given that the RADEM receiver is synchronized to a received signal, RADEM receiver operation is as follows. At the end of each frame interval, the flip-flop is set to the "one" state if the three stage binary counter contains a four. Otherwise,

the flip-flop is set to the zero state. After a slight delay, the counter is reset to zero. In this way the flip-flop output voltage in each frame interval is modulated with the information received during the preceding frame interval. The flip-flop output voltage is integrated in an RC integrator to produce the RADEM receiver output.

Before a RADEM receiver has synchronized with a properly coded received signal, the clock of the RADEM transceiver in the receive mode is designed to run fast or slow relative to the clock of a RADEM transceiver in the transmit mode. In this way, the times of the opening of the receiver gates precess relative to the epochs of the pulses in a time-frequency code frame. The receiver will always precess to the correct gate timing within a few milliseconds after a properly coded signal appears at the receiver antenna terminals. Once correct phasing is obtained, the receiver clock locks to, and maintains synchronization with the received signal.

Assuming that spurious pulses seldom have the proper amplitude and phase to cancel a pulse in a received, properly coded time-frequency frame, the primary source of interference to a RADEM receiver results from groups of four pulses from different transmitters which happen to arrive at the receiver with the correct time-frequency pattern for detection in a clock interval when no properly coded time-frequency code frame is received. Each such pulse group causes the receiver flip-flop to be set in the wrong state in a 26 microsecond

interval, and results in an error voltage of two quantization levels at the end of the interval.

Analytic work of van de Weg (Ref. 28) describes the signal-to-quantizing-noise ratios to be expected for delta modulation; in Ref. 29, de Jager compares delta modulation with PCM. Generally, delta modulation is a more efficient scheme of encoding voice information than PCM. Particularly, for a 3.5 kc bandwidth voice signal, a 38.4 kc sampling rate, the signal-to-quantizing-noise ratio for delta modulation is 30 db. For comparison, a signal-to-quantizing-noise ratio of 33 db is available with 4 digit PCM, which requires four times as much bandwidth as delta modulation, even in the absence of synchronizing information.

Experimental results given in Ref. 1.10 indicate that a 4.2 percent error rate in delta modulation pulses results in a 20 db signal-to-noise ratio at the delta demodulator output. A 15 percent error rate results in a 13 db signal-to-noise ratio.

The Bendix CAPRI System (Coded Address Private Radio Intercom) (Ref. 1.5)

A block diagram of the CAPRI transmitter is shown in Fig. A.3(a). This block diagram is this writer's implementation of a verbal description given in Ref. 1.5. The transmitter output signal is shown in Fig. A.3(b), a block diagram of the receiver is shown in Fig. A.3(c). The system description given here follows that of Ref. 1.5.

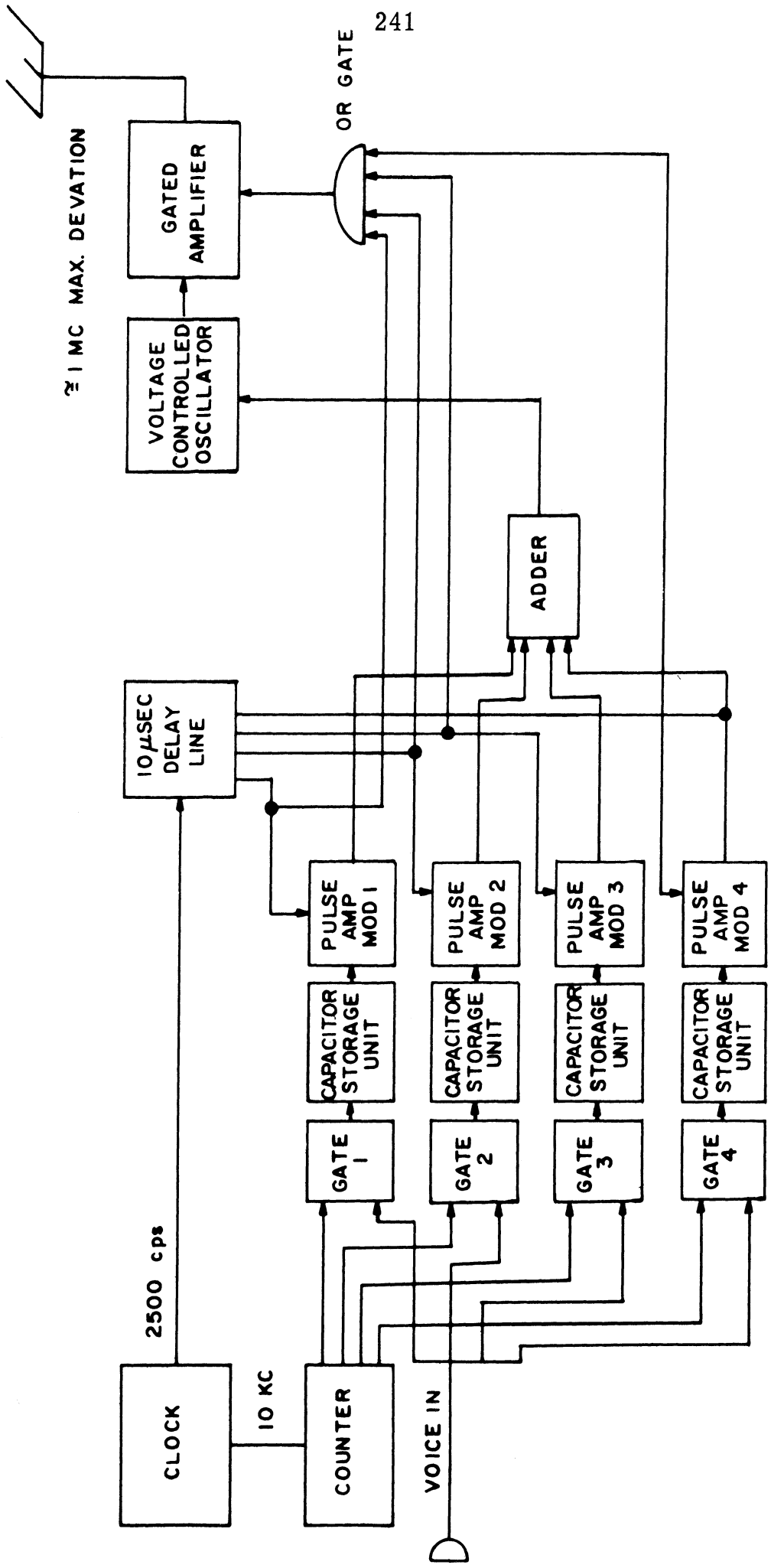

Fig. A. 3(a). Bendix CAPRI transmitter block diagram.

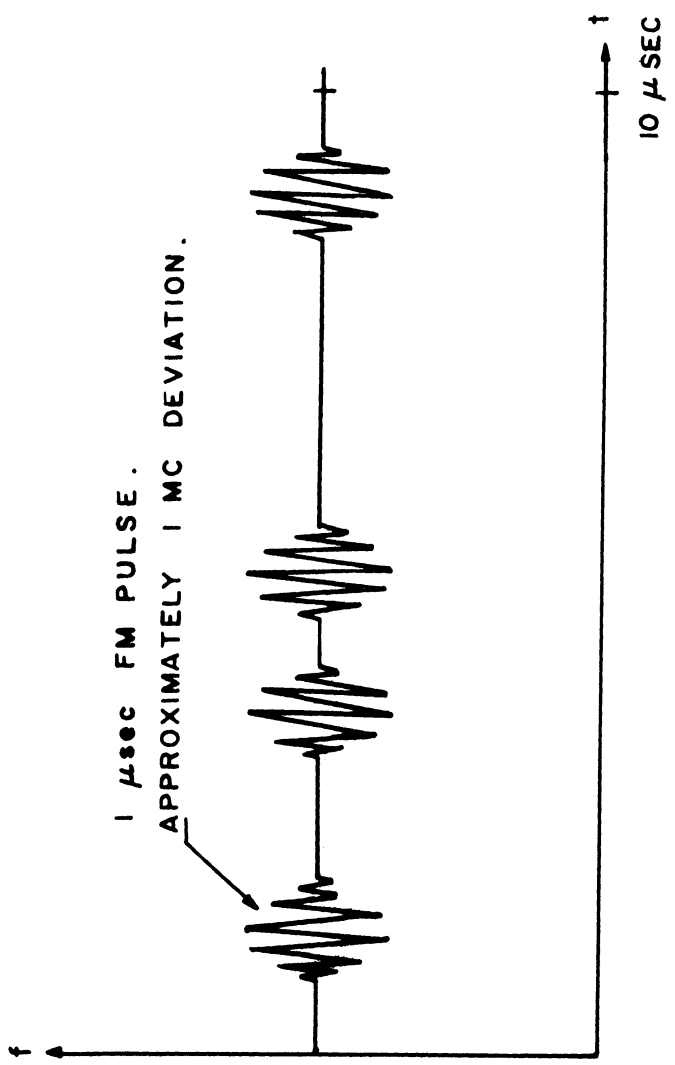

Fig. A. 3(b). Representative transmitted time-frequency code frame for Bendix CAPRI system.

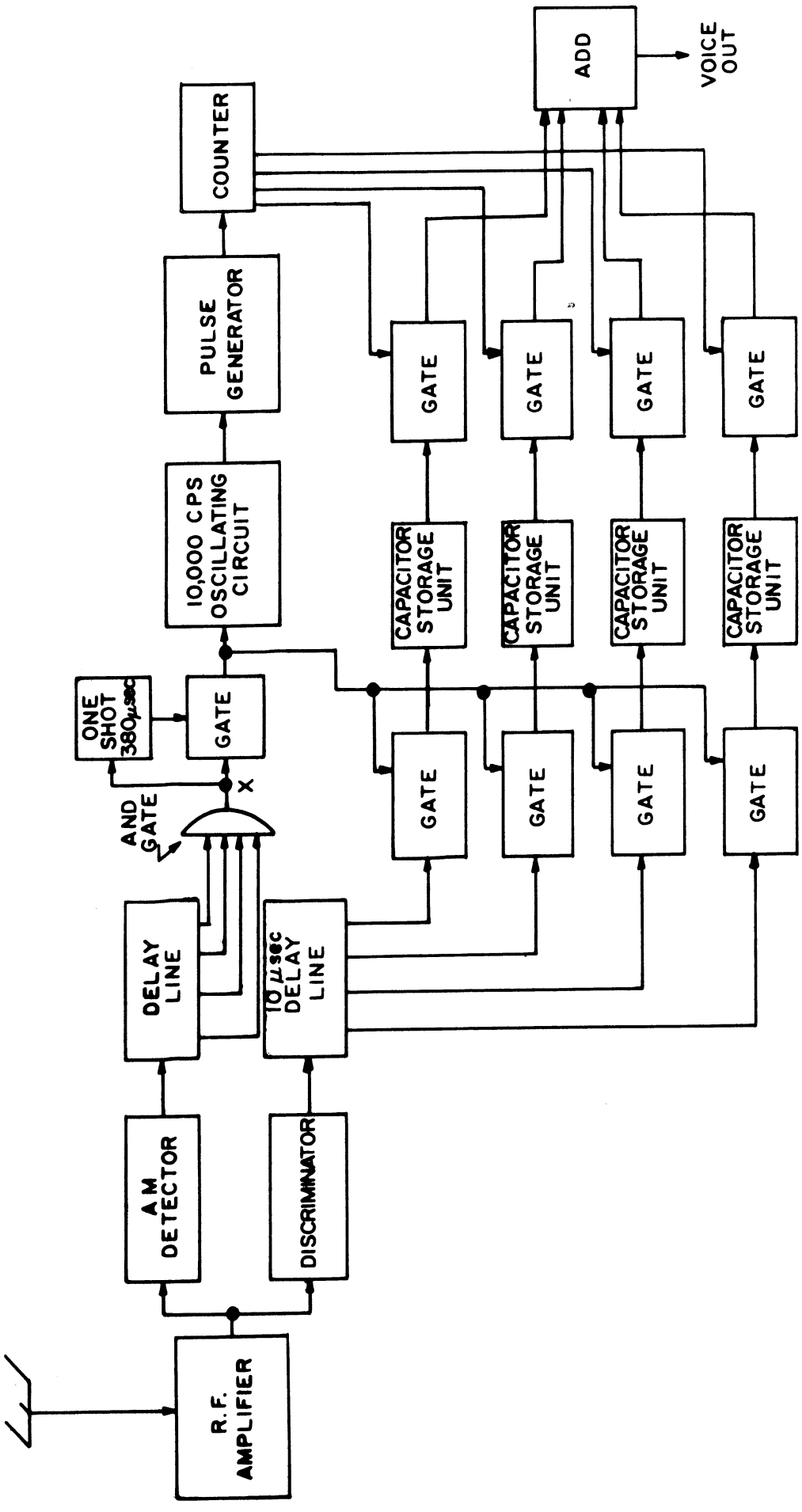

Fig. A. 3(c). Bendix CAPRI receiver block diagram.

To transmit to a given receiver, the transmitter delay line taps are set to match (i.e., complement, modulo the delay line length) those of the receiver. The transmitter delay line is a 10 microsecond line with a tap at each one microsecond delay increment. The transmitted signal is coded by selection of a particular set of four taps.

The transmitter clock generates two trains of one microsecond pulses, with repetition rates of 2500 pps and 10,000 pps. The 10,000 pps pulse train is used to sample the voice information. The samples are stored successively in four capacitor storage units; the fifth sample replaces the first, and so on. After each fourth pulse of the 10,000 pps pulse train, a 1 microsecond, 2500 pps pulse is fed into the ten microsecond delay line. The four pulses at the output taps of the delay line are amplitude-modulated by the voltages stored in the four capacitor storage units. In the implementation described by Bendix, the four pulse-modulator output voltages are added and used to modulate a voltage-controlled oscillator. The oscillator is the input to an amplifier which is gated on by each of the four pulses at the delay line output as in Fig. A.3(a). The gating is not necessary if the voltage-controlled oscillator is designed to produce an output voltage only when there is an input amplitude-modulated pulse. The transmitter time-frequency diagram is shown in Fig. A.3(b).

In the receiver, the signal follows an address path and an information path. In the first, the signal envelope is detected and receives,

in the delay line, the four delays appropriate for the code. The four delay-line outputs drive an AND gate and produce a gate output pulse. Thus the gate output at point x [Fig. A. 3(c)] is a train of 2500 one microsecond pulses per second. The output of the one-shot gate following the AND gate can have no pulses with a spacing of less than 380 microseconds between them. (The spacing between a correct pulse pair is 400 microseconds.) The 2500 pps pulse train is used to obtain a 10,000 pps pulse train which drives a four-stage counter. The four-counter outputs are used to gate voltages, stored on capacitors, which are proportional to the original samples of the signal at the transmitter. The smoothed sum of the samples is the desired output waveform.

The information stored in the capacitors is obtained as follows. The discriminator output is a pulse train with the pulse amplitude corresponding to the original sample amplitudes. These pulses are coded in time. A second delay line in the receiver removes the coding in time; the four signal samples occur at the delay-line taps at the same time that a coincidence pulse is generated by the first AND gate (unless the coincidence pulse is spurious). The coincidence pulse allows the samples to enter the storage units. As was described previously, the voltages in the four storage units are sampled sequentially at a 10 kc rate. The smoothed sum of the samples is the receiver output signal.

LIST OF REFERENCES

1. F. E. Terman, Radio Engineers' Handbook, McGraw-Hill Book Co., Inc., New York, 1943.

2. J. P. Costas, "Poisson, Shannon and the Radio Amateur," Proceedings of the IRE, December 1959 (Section V).

3. C. E. Shannon, The Mathematical Theory of Communication, The University of Illinois Press, Urbana, Illinois, 1949.

4. D. H. Hamsher, "System Concepts for Address Communication Systems," IRE Transactions on Vehicular Communications, Vol. VC-9, No. 3, December 1960, pp. 102-106.

5. D. P. Harris, "Unscheduled Spectrum Sharing in Communication," Convention Record, 5th National Symposium on Global Communications (GLOBECOM), Chicago, Illinois, May 22-24, 1961, pp. 273-276.

6. R. Filipowsky and E. Scherer, "Time Division Multiplex System with Addressed Information Packages," 1957 IRE National Convention Record, Part 8, pp. 132-139.

7. J. M. Kirshner, "Signal Space, Modulation, and Bandwidth," PGMEC Conference, June 1962, pp. 149-153.

8. H. Blasbalg, D. Freeman and R. Keeler, "Random-Access Communications Using Frequency Shifted PN (Pseudo-Noise) Signals," 1964 IEEE International Convention Record, Part 6, New York, New York, March 23-26, 1964, pp. 192-216.

9. C. H. Dawson, "An Introduction to Random-Access, Discrete-Address Systems, 1964 IEEE International Convention Record, Part 6, New York, New York, March 23-26, 1964, pp. 154-158.

10. J. R. Pierce and A. L. Hopper, "Nonsynchronous Time Division with Holding and with Random Sampling," Proceedings of the IRE, September 1952.

11. "Wideband Communications is Army Plan," Electronics, April 5, 1963.

REFERENCES (Cont.)

12. P. J. Klass, "System Offers Private-Line Radio Service, Aviation Week and Space Technology, May 13, 1963.

13. H. E. McGuire, "Combined Coding Increases Spectrum Usage," Electronics, October 26, 1962.

14. S. G. Varsos and B. Norvell, "DATEC - Digital Adaptive Technique for Efficient Communications," Institute of Electrical and Electronics Engineers International Convention, Communication and Modulation Techniques, March 26, 1964.

15. H. Magnuski, "Wideband Channel for Emergency Communication," Eighth National Communication Symposium, Utica, New York, October 1-3, 1962.

16. C. H. Dawson and H. Sklar, "False Addresses in a Random Access System Employing Discrete Time-Frequency Addressing," 1964 IEEE International Convention Record, Part 6, New York, New York, March 23-26, 1964, pp. 217-230.

17. C. C. Diaz and B. R. Norvell, "Selection of a Pulse Modulation Communication System Based on Results of Intelligibility Measurements," 1964 IEEE International Convention Record, Part 6, New York, New York, March 23-26, 1964, pp. 182-191.

18. W. Bedsole and J. Lomax, "Propagation Measurements for a Frequency-Time Coded Pulse Communications System," 1964 IEEE International Convention Record, Part 6, New York, New York, March 23-26, 1964, pp. 170-181.

19. R. W. Heffner, "A Backscatter-Multipath Model for Groundwave Pulse Communications Systems," 1964 IEEE International Convention Record, Part 6, New York, New York, March 23-26, 1964, pp. 159-169.

20. M. V. Mathews, "Extremal Coding for Speech Transmission," IRE Transactions on Information Theory, IT-5, September 1959, pp. 129-136.

21. L. R. Spogen, H. N. Shaver and D. E. Baker, "Speech Processing by the Selective Amplitude Sampling System," The Journal of the Acoustical Society of America, Vol. 32, No. 12, December 1960.

REFERENCES (Cont.)

22. M. J. Wiggins, "Pulse Error Reduction in Pulse Position Modulation Systems," 1955 IEEE International Convention Record, Part 2, New York, New York, March 22-26, 1965, pp. 14-19.

23. B. W. Beals and F. R. Zitzmann, "Simulation for RADAS," IEEE Tenth National Communications Symposium, Utica, New York, October 5-7, 1964, pp. 77-82.

24. M. G. Kendall and A. Stuart, The Advanced Theory of Statistics, Vol. 1: "Distribution Theory," Hafner Publishing Company, New York, 1958, pp. 88-89.

25. P. M. Morse, Queues, Inventories and Maintenance, Publications in Operations Research, No. 1, John Wiley and Sons, Inc., New York, November 1958, Chapter 2, pp. 8-9.

26. W. M. Brown, Analysis of Linear Time Invariant Systems, McGraw-Hill Book Co., Inc., New York, 1963, Chapter 5.

27. I. S. and E. S. Sokolnikoff, Higher Mathematics for Engineers and Physicists, McGraw-Hill Book Co., Inc., New York, 1941, pp. 127-134.

28. H. van de Weg, Quantizing Noise of a Single Integration Delta Modulation System with an N Digit Code, Phillips Research Reports, Vol. 8, Nr 5, October 1953.

29. F. de Jager, Delta Modulation, a Method of PCM Transmission Using the 1 Unit Code, Phillips Research Reports, Vol. 7, Nr 6, December 1952.

30. D. Chesler, "m-ary RADA System," Proceedings of the IEEE, Vol. 53, No. 4, April 1965 (Correspondence).

31. R. C. Sommer, "On the Optimization of Random Access Discrete Address Communications," Proceedings of the IEEE, Vol. 52, No. 10, October 1964 (Correspondence).

32. E. N. Gilbert, "Cyclically Permutable Error-Correcting Codes," IEEE Transactions on Information Theory, Vol. IT-9, No. 3, July 1963.

REFERENCES (Cont.)

33. Einarsson, G., "Time-Frequency Coded Pulse Communication Systems," Ericsson Technics, Vol. 21, No. 2, October, 1965.

34. Cramer, H. Mathematical Methods of Statistics, Princeton University Press, 1957.

35. H. J. Godwin, "On Generalizations of Tchebychef's Inequality," Journal of the American Statistical Association, Vol. 50, No. 271, September 1955, pp. 923-945.

36. Von Mises, R., Mathematical Theory of Probability and Statistics, H. Geiringer (Ed.), Academic Press, New York, 1964.

AUXILIARY LIST OF REFERENCES

1. 1 J. E. Taylor, Asynchronous Multiplexing, General Electric Research Laboratory, Report No. 58-RL-1982, Schenectady, New York, June 1958.

1. 2 L. R. Spogen, Jr., W. H. Reading, III and V. R. Latorre, Parameters of a Non-Synchronous, Random Access, Discrete Address Communications System, University of Arizona, Tucson, Arizona, Final Report, January 1961.

1. 3 F. F. Fulton, Jr., Channel Utilization by Intermittent Transmitters, Technical Report No. 2004-2, Stanford Electronics Laboratories, Stanford University, Stanford, California, May 12, 1961.

1. 4 D. P. Harris, Unscheduled Communication in a Common Frequency Channel, Technical Report, LMSD-895081, Lockheed Aircraft Corp., Sunnyvale, Calif., January 1961.

1. 5 CAPRI Coded Address Private Radio Intercom, Internal Memorandum, BRM 1498A, Bendix Radio Division, The Bendix Corporation, Baltimore 4, Maryland, January 11, 1962.

1. 6 Operating Notes for Signal Corps' Basic RACEP Units, Internal Memorandum, OR 2408, Contract No. DA 36-039 sc-80708, Martin Marietta Corp., Orlando, Florida, March 1962.

1. 7 DDC 291 207, RACEP Prototype Equipment, Final Report AF 19 (604)-8511, Martin Marietta Corp., December 1962.

1. 8 DDC 400 379, Lt. E. J. Woll, Jr., Engineering Evaluation of RACEP Discrete Address Communications Equipment, Final Report for USATECOM, Project No. 6G-3213-01, 15 March 1963.

1. 9 H. Magnuski, "Motorola's Contributions to RADAS Techniques," Motorola Engineering Bulletin, Vol. 11, No. 1, 1963.

1. 10 H. Magnuski, "Motorola's Contributions to Random Access Discrete Address Techniques, Part 2," Motorola Engineering Bulletin, 2nd Issue, 1963.

AUXILIARY LIST OF REFERENCES (Cont.)

1. 11 Final Report, Selective Amplitude Sampling, USAEPG-SIG 960-73, Contract DA-36-039 sc-89146, The Applied Research Laboratory, University of Arizona, Tucson, Arizona, January 1961.

1. 12 L. R. Spogen, Jr., et al., Supplement Number 1 to Selective Amplitude Sampling, USAEPG-SIG 960-73, The Applied Research Laboratory, University of Arizona, Tucson, Arizona, January 1961.

1. 13 Final Report, Investigation of Aperiodic Sampling in Random Access Discrete Address Systems, USAERDAA-ELCT-1-64, Contract DA-36-039 sc-80872, Electronics Department, Fort Huachuca, Arizona, June 1964.

1. 14 Technical Report, Statistics, Quantization and Coding Aspects of the Application of Aperiodic Sampling Techniques to RADA Systems, USAERDAA-ELCT-3-64, Contract DA-36-039 sc-80872, Electronics Department, Fort Huachuca, Arizona, June 1964.

1. 15 Technical Report, Cross Channel Interference Criteria in a RADA System, USAERDAA-ELCT-2-64, Contract DA-36-039 sc-80872, Electronics Department, Fort Huachuca, Arizona, June 1964.

1. 16 Technical Report, Effect of Errors on Speech Intelligibility and Quality, USAERDAA-ELCT-5-64, Contract DA-36-039 sc-80872, Electronics Department, Fort Huachuca, Arizona, June 1964.

1. 17 Technical Report, Simulation Techniques for Aperiodic Sampling Study of RADA Systems, USAERDAA-ELCT-4-64, Contract DA-36-039 sc-80872, Electronics Department, Fort Huachuca, Arizona, June 1964.

1. 18 D. R. Rothschild, et al., Investigation of Asynchronous Time Multiplexing (ATM): Efficient Multiplexing of Multichannel Data and Extremally Sampled Speech Sources, Final Report, Contract No. DA-02-086 AMC-0131(E), Cooley Electronics Laboratory, The University of Michigan, Ann Arbor, Michigan, (in preparation).

1. 19 U. S. Army Division Area Random Access Discrete Address (RADA) Communication System Design Plan, Vol. I: Summary, OR 3758, U. S. Army Electronics Materiel Agency, Contract DA-36-039-AMC-00147(E), Martin Marietta Corp., Martin Company, Orlando, Florida, 21 March 1963 - 20 March 1964.

AUXILIARY LIST OF REFERENCES (Cont.)

1.20 U. S. Army Division Area Random Access Discrete Address (RADA) Communication System Design Plan, Vol. II: Operational Aspects, OR 3758, U. S. Army Electronics Materiel Agency, Contract DA-36-039-AMC-00147(E), Martin Marietta Corp., Martin Company, Orlando, Florida, 21 March 1963 - 20 March 1964.

1.21 U. S. Army Division Area Random Access Discrete Address (RADA) Communication System Design Plan, Vol. III: Technical Aspects, OR 3758, U. S. Army Electronics Materiel Agency, Contract DA-36-039-AMC-00147(E), Martin Marietta Corp., Martin Co., Orlando, Florida, 21 March 1963 - 20 March 1964.

1.22 U. S. Army Division Area Random Access Discrete Address (RADA) Communication System Design Plan, Vol. IVa: Operational Analysis, OR 3758, U. S. Army Electronics Materiel Agency, Contract DA-36-039-AMC-00147(E), Martin Marietta Corporation, Martin Co., Orlando, Florida, 21 March 1963 - 20 March 1964.

1.23 U. S. Army Division Area Random Access Discrete Address (RADA) Communication System Design Plan, Vol. IVb: System Analysis, OR 3758, U. S. Army Electronics Materiel Agency, Contract DA-36-039-AMC-00147(E), Martin Marietta Corporation, Martin Co., Orlando, Florida, 21 March 1963 - 20 March 1964.

1.24 RADAS System Design Plan, Vol. I: Summary, U. S. Army Electronics Materiel Agency, Contract No. DA-36-039-AMC-00141(E), Radio Corporation of America, New York, New York, 12 May 1964.

1.25 RADAS System Design Plan, Vol. II: Operational Aspects, U. S. Army Electronics Materiel Agency, Contract No. DA-36-039-AMC-00141(E), Radio Corporation of America, New York, New York, 12 May 1964.

1.26 RADAS System Design Plan, Vol. III: Technical, U. S. Army Electronics Materiel Agency, Contract No. DA-36-039-AMC-00141(E), Radio Corporation of America, New York, New York, 12 May 1964.

1.27 RADAS System Design Plan, Vol. IV: Supporting Data, U. S. Army Electronics Materiel Agency, Contract No. DA-36-039-AMC-00141(E) Radio Corporation of America, New York, New York, 12 May 1964.

AUXILIARY LIST OF REFERENCES (Cont.)

1.28 RADA System Study Plan, Vol. I: Summary, U. S. Army Electronics Materiel Agency, Contract No. DA-36-039-AMC-00146(E), Motorola, Inc., Chicago, Illinois, May 1964.

1.29 RADA System Study Program, Vol. II: Operational Aspects, U. S. Army Electronics Materiel Agency, Contract No. DA-36-039-AMC-00146(E), Motorola, Inc., Chicago, Illinois, May, 1964.

1.30 RADA System Study Program, Vol. III: Technical, U. S. Army Electronics Materiel Agency, Contract No. DA-36-039-AMC-00146(E), Motorola, Inc., Chicago, Illinois, May 1964.

1.31 RADA System Study Plan, Vol. IVa: Supporting Data Operational U. S. Army Electronics Materiel Agency, Contract No. DA-36-039-AMC-00146(E), Motorola, Inc., Chicago, Illinois, May 1964.

1.32 RADA System Study Plan, Vol. IVb: Supporting Data Technical, U. S. Army Electronics Materiel Agency, Contract No. DA-36-039-AMC-00146(E), Motorola, Inc., Chicago, Illinois, May 1964.

1.33 RADA System Study Plan, Vol. IVc: Supporting Data Appendices, U. S. Army Electronics Materiel Agency, Contract No. DA-36-039-AMC-00146(E), Motorola, Inc., Chicago, Illinois, May 1964.

1.34 J. Kaiser, J. W. Schwartz and J. M. Aein, Multiple Access to a Communications Satellite with a Hard-Limiting Repeater, Vol. I: Modulation Techniques and Their Applications, Report R-108, Institute for Defense Analyses, Research and Engineering Support Division, January 1965.

1.35 J. M. Aein and J. W. Schwartz (eds.), Multiple Access to a Communication Satellite with Hard-Limiting Repeater, Vol. II: Proceedings of the IDA Multiple Access Summer Study, Report R-108, Institute for Defense Analyses, Research and Engineering Support Division, April 1965.

DISTRIBUTION LIST

No. of Copies	
23	Defense Documentation Center Attn: DDC-IRS Cameron Station (Bldg. 5) Alexandria, Virginia 22314
1	Office of Assistant Secretary of Defense (Research and Engineering) Attn: Technical Library, RM 3E1065 Washington, D. C. 20301
1	Bureau of Ships Technical Library Attn: Code 312 Main Navy Building, Room 1528 Washington, D. C. 20325
1	Director U. S. Naval Research Laboratory Attn: Code 2027 Washington, D. C. 20390
1	Commanding Officer and Director U. S. Navy Electronics Laboratory Attn: Library San Diego, California 92101
2	Headquarters, U. S. Air Force Attn: AFCIN Washington, D. C. 20325
1	Rome Air Development Center Attn: EMLAL-1 Griffiss Air Force Base New York 13442
1	Headquarters Strategic Air Command Attn: DOCE Offutt Air Force Base, Nebraska 68113

DISTRIBUTION LIST (Cont.)

No. of Copies	
1	Systems Engineering Group (SEPIR) Wright-Patterson Air Force Base, Ohio 45433
2	Electronic Systems Division (AFSC) Scientific and Technical Info Div (ESTI) L. G. Hanscom Field Bedford, Massachusetts 01731
2	Air Force Cambridge Research Laboratories Attn: CRXL-R L. G. Hanscom Field Bedford, Massachusetts 01731
2	Chief of Research and Development Department of the Army Washington, D. C. 20315
1	Ofc of the Chief of Communications-Electronics Attn: OCC-E Department of the Army Washington, D. C. 20315
2	Commanding General U. S. Army Materiel Command Attn: R&D Directorate Washington, D. C. 20315
2	Redstone Scientific Information Center Redstone Arsenal, Alabama 35809
1	Commanding Officer 52d USASASOC Fort Huachuca, Arizona 85613
1	Commanding General U. S. Army Combat Developments Command Attn: CDCMR-E Fort Belvoir, Virginia 22060

DISTRIBUTION LIST (Cont.)

No. of Copies	
1	Deputy Commander U. S. Army Combat Developments Command Communications-Electronics Agency Fort Huachuca, Arizona 85613
1	Commanding Officer Harry Diamond Laboratories Connecticut Ave. and Van Ness St., N.W. Washington, D. C. 20438
1	USAECOM Commodity Management Office AMSEL-EW Ft. Monmouth, New Jersey
1	Commanding General U. S. Army Electronics Command Attn: AMSEL-RD-LNR Fort Monmouth, New Jersey 07703
1	Commanding Officer U. S. Army Electronics Command R&D Activity White Sands Missile Range, New Mexico 88002
1	Chief, Mountain View Office Electronic Warfare Lab., USAECOM P. O. Box 205 Mountain View, California 94042
2	Commanding General U. S. Army Security Agency Attn: IADEV Arlington Hall Station Arlington, Virginia 22212
1	Commanding General U. S. Army Security Agency Attn: IACON Arlington Hall Station Arlington, Virginia 22212

DISTRIBUTION LIST (Cont.)

No. of Copies	
1	Commanding General U. S. Army Security Agency Combat Development Activity Arlington Hall Station Arlington, Virginia 22212
1	Commanding General U. S. Army Electronics Command Attn: AMSEL-WL-D Fort Monmouth, New Jersey 07703
1	Commanding General U. S. Army Electronics Command Attn: AMSEL-WL-C Fort Monmouth, New Jersey 07703
1	Commanding General U. S. Army Electronics Command Attn: AMSEL-WL-S Fort Monmouth, New Jersey 07703
1	Commanding General U. S. Army Electronics Command Attn: AMSEL-WL-N Fort Monmouth, New Jersey 07703
1	Commanding General U. S. Army Electronics Command Attn: AMSEL-WL-E Fort Monmouth, New Jersey 07703
1	Commanding General U. S. Army Electronics Command Attn: AMSEL-RD-GFR Fort Monmouth, New Jersey 07703
1	Commanding General U. S. Army Electronics Command Attn: AMSEL-NL-E (Mr. Reindl) Fort Monmouth, New Jersey 07703

DISTRIBUTION LIST (Cont.)

No. of Copies	
1	Commanding General U. S. Army Electronics Command Attn: AMSEL-NL-E (Mr. Hecker) Fort Monmouth, New Jersey 07703
1	Commanding General U. S. Army Electronics Command Attn: AMSEL-NL-E (Mr. Tepper) Fort Monmouth, New Jersey 07703
10	Cooley Electronics Laboratory The University of Michigan Ann Arbor, Michigan
1	Stanford Electronics Laboratories Stanford University Stanford, California

Unclassified

Security Classification

DOCUMENT CONTROL DATA - R&D

(Security classification of title, body of abstract and indexing annotation must be entered when the overall report is classified)

1. ORIGINATING ACTIVITY (Corporate author) Cooley Electronics Laboratory The University of Michigan Ann Arbor, Michigan	2a. REPORT SECURITY CLASSIFICATION Unclassified 2b. GROUP N/A

3. REPORT TITLE

A Study of Random Access Discrete Address Communications Systems
Volume I: Study and Analysis

4. DESCRIPTIVE NOTES (Type of report and inclusive dates)

Technical Report No. 167

5. AUTHOR(S) (Last name, first name, initial)

C. Craig Ferris

6. REPORT DATE	7a. TOTAL NO. OF PAGES	7b. NO. OF REFS
October 1965	237	55

8a. CONTRACT OR GRANT NO. DA 36-039 AMC-03733 (E) b. PROJECT NO. 1P0 21101 A042-01-02 c. d.	9a. ORIGINATOR'S REPORT NUMBER(S) 6137-12-T 9b. OTHER REPORT NO(S) (Any other numbers that may be assigned this report) N/A

10. AVAILABILITY/LIMITATION NOTICES

This document is subject to special export controls and each transmittal to foreign governments or foreign nationals may be made only with prior approval of CG, U. S. Army Electronics Command, AMSEL-WL-C

11. SUPPLEMENTARY NOTES	12. SPONSORING MILITARY ACTIVITY
N/A	U. S. Army Electronics Command Fort Monmouth, New Jersey AMSEL-WL-C

13. ABSTRACT

An analytical study is made of RADA (random access discrete address) communications systems. The factors which influence system performance are embodied in mathematical models which are used to determine, analytically, the quantitative effects of these factors on system performance. The investigations include the following. An analytical study of the mutual-interference-power-density at a receiver in a general co-channel RADA net environment is carried out. A determination is made as to the probability that a useful signal is at the receiver. Theoretical expressions for the statistics of the error process on two types of modulation are evaluated. A method is determined of choosing system parameters to minimize receiver output error probability for a given bandwidth. An expression is derived for the information rate of a RADA transmission in terms of the statistics of the error process. Finally, a sampling RADA receiver is proposed for use with clocked binary modulation and optimum parameters are determined for systems using this type of receiver.

DD FORM 1 JAN 64 1473

Unclassified.

Security Classification

14. KEY WORDS	LINK A		LINK B		LINK C	
	ROLE	WT	ROLE	WT	ROLE	WT
Communications Systems Pulse Communication Random access discrete address system						

INSTRUCTIONS

1. ORIGINATING ACTIVITY: Enter the name and address of the contractor, subcontractor, grantee, Department of Defense activity or other organization *(corporate author)* issuing the report.

2*a*. REPORT SECURITY CLASSIFICATION: Enter the overall security classification of the report. Indicate whether "Restricted Data" is included. Marking is to be in accordance with appropriate security regulations.

2*b*. GROUP: Automatic downgrading is specified in DoD Directive 5200.10 and Armed Forces Industrial Manual. Enter the group number. Also, when applicable, show that optional markings have been used for Group 3 and Group 4 as authorized.

3. REPORT TITLE: Enter the complete report title in all capital letters. Titles in all cases should be unclassified. If a meaningful title cannot be selected without classification, show title classification in all capitals in parenthesis immediately following the title.

4. DESCRIPTIVE NOTES: If appropriate, enter the type of report, e.g., interim, progress, summary, annual, or final. Give the inclusive dates when a specific reporting period is covered.

5. AUTHOR(S): Enter the name(s) of author(s) as shown on or in the report. Enter last name, first name, middle initial. If military, show rank and branch of service. The name of the principal author is an absolute minimum requirement.

6. REPORT DATE: Enter the date of the report as day, month, year; or month, year. If more than one date appears on the report, use date of publication.

7*a*. TOTAL NUMBER OF PAGES: The total page count should follow normal pagination procedures, i.e., enter the number of pages containing information.

7*b*. NUMBER OF REFERENCES: Enter the total number of references cited in the report.

8*a*. CONTRACT OR GRANT NUMBER: If appropriate, enter the applicable number of the contract or grant under which the report was written.

8*b*, 8*c*, & 8*d*. PROJECT NUMBER: Enter the appropriate military department identification, such as project number, subproject number, system numbers, task number, etc.

9*a*. ORIGINATOR'S REPORT NUMBER(S): Enter the official report number by which the document will be identified and controlled by the originating activity. This number must be unique to this report.

9*b*. OTHER REPORT NUMBER(S): If the report has been assigned any other report numbers *(either by the originator or by the sponsor)*, also enter this number(s).

10. AVAILABILITY/LIMITATION NOTICES: Enter any limitations on further dissemination of the report, other than those imposed by security classification, using standard statements such as:

(1) "Qualified requesters may obtain copies of this report from DDC."

(2) "Foreign announcement and dissemination of this report by DDC is not authorized."

(3) "U. S. Government agencies may obtain copies of this report directly from DDC. Other qualified DDC users shall request through _____."

(4) "U. S. military agencies may obtain copies of this report directly from DDC. Other qualified users shall request through _____."

(5) "All distribution of this report is controlled. Qualified DDC users shall request through _____."

If the report has been furnished to the Office of Technical Services, Department of Commerce, for sale to the public, indicate this fact and enter the price, if known.

11. SUPPLEMENTARY NOTES: Use for additional explanatory notes.

12. SPONSORING MILITARY ACTIVITY: Enter the name of the departmental project office or laboratory sponsoring *(paying for)* the research and development. Include address.

13. ABSTRACT: Enter an abstract giving a brief and factual summary of the document indicative of the report, even though it may also appear elsewhere in the body of the technical report. If additional space is required, a continuation sheet shall be attached.

It is highly desirable that the abstract of classified reports be unclassified. Each paragraph of the abstract shall end with an indication of the military security classification of the information in the paragraph, represented as *(TS)*, *(S)*, *(C)*, or *(U)*.

There is no limitation on the length of the abstract. However, the suggested length is from 150 to 225 words.

14. KEY WORDS: Key words are technically meaningful terms or short phrases that characterize a report and may be used as index entries for cataloging the report. Key words must be selected so that no security classification is required. Identifiers, such as equipment model designation, trade name, military project code name, geographic location, may be used as key words but will be followed by an indication of technical context. The assignment of links, rules, and weights is optional.